

# Sustainable Air Handling by Evaporation and Adsorption



**Fatemeh Esfandiari Nia**

**January 12, 2011**



# Sustainable Air Handling by Evaporation and Adsorption

Proefschrift

ter verkrijging van de graad van doctor  
aan de Technische Universiteit Delft,  
op gezag van de Rector Magnificus Prof.ir. K.C.A.M.Luyben  
voorzitter van het College voor Promoties  
in het openbaar te verdedigen op woensdag 12 januari 2011 om 10:00 uur

door

Fatemeh ESFANDIARI NIA  
PhD, Sharif University of Technology, Tehran, Iran

Dit proefschrift is goedgekeurd door de promotoren:

Prof. dr. ir.A.H.C. van Paassen†

Prof. dr. ir.B.J. Boersma

Prof. dr. ir.A.H.M. Verkooijen

Samenstelling promotiecommissie:

Rector Magnificus

Prof. dr. ir.A.H.C. van Paassen†

Prof. dr. ir. B.J. Boersma

Prof. dr. ir A.H.M. Verkooijen

Prof. dr. J.L.M. Hensen

Prof. dr. ir. M.H. de Wit

Prof. dr. ir. T.H. van der Meer

Prof. ir. P.G. Luscure

Prof. dr. ir. P.A. Wieringa

voorzitter

Technische Universiteit Delft, promotor

Technische Universiteit Delft, promotor

Technische Universiteit Delft, promotor

Technische Universiteit Eindhoven

Technische Universiteit Eindhoven

Technische Universiteit Twente

Technische Universiteit Delft

Technische Universiteit Delft

This research has been funded by SenterNovem, ROB project 0377-06-03-01-012 and Carrier Holland Heating, WOI and SOK.

Keywords: desiccant, heat mass transfer, modeling, air conditioning, adsorption, evaporation,

Copyright© 2011 by F. Esfandiari Nia and A.H.C. van Paassen

All right reserved

No part of this thesis may be reproduced, stored in a retrieval system, or transmitted, in any form or by any means, without the prior written permission of the authors.

Any use or application of data, methods and/or results etc., published in this book will be at the user's own risk. The authors accept no liability for damages suffered from such use or application.

ISBN 978-90-9025918-5

Printed in the Netherlands

# In Memoriam

## **Dolf van Paassen**

**June 6, 1941 - June 30, 2009**

In the year 2009, we lost professor dr. ir. Dolf van Paassen, the professor of Energy in the Built Environment, and my dear supervisor who valuably and patiently guided me during 5 years of my PhD studies and got me where I am today in this research.

Dolf graduated from the TUDelft as an electrical engineer in 1967. After working for the Shell Laboratory as a research assistant, he joined TUDelft as a faculty in Mechanical Engineering department in 1971. His thesis "Indoor Climate, Outdoor Climate and Energy Consumption" a new approach to the calculation of the effect of the outdoor and indoor climate on the energy consumption in buildings based on methods of statistical analysis was one of the outstanding research studies in this field. From 1985 to 1998 he was Associate Professor, and since 1998 became a Professor of Energy in the Built Environment.

Dolf and his research topics were popular with the students, as always he introduced innovative and practical subjects with industrial applications with emphasis on control techniques in HVAC systems. One of his research interests was to maximize the use of natural resources to achieve comfort in buildings. Dolf valuably guided these projects with his excellent background in Electrical Engineering. In recent years, he had many graduate students in the fields of phase change materials for climate control of buildings, desiccant cooling and dehumidification, heat and cold storage in aquifers, buildings with double façade and conditioning of closed greenhouses. He taught Indoor Climate Control Fundamentals and Indoor Climate Control Design in TUDelft, both very popular courses among students. In 1984, Dolf received the gold medal TVVL, a distinction that once every five years is awarded for his outstanding contributions to the development of installations in buildings. In 1999 he also received the B.J. Max Prize for his studies, publications and lectures, both nationally and internationally on the topic of Climate Technology. He was a member of many technical forums and committees. Until 3 months prior to his death, he was still very active in his professional life. Besides his professional activities, he was very talented in painting and created many beautiful works of art.

Many students like me were very honored and fortunate to have Dolf as our professor. It is hard to think about Dolf without reflecting the love and respect he had for his lovely wife Margriet.

I always remember Dolf as a committed, intelligent, cultured, and kind individual with good sense of humor and generosity. Dear Professor, Dear friend, we miss you greatly but we are comforted by the knowledge that you are now free of pain and in a better place.

Fatemeh E. Nia



# Summary

A considerable fraction of today's energy consumption is due to air-conditioning of buildings, involving both heating and cooling. Energy cost and environmental concerns force designers to find sustainable solutions. Desiccant cooling as a sustainable technology is attractive to be investigated for making different design tools.

The main subject of this research is cooling and dehumidification by a wheel which contains a matrix of sorption material or desiccants such as silica gel. Desiccants adsorb water vapor due to the difference of water vapor pressure between the surrounding air and their surface. To make the system operate continuously, adsorbed water vapor must be driven out of the desiccant material (regeneration) so that it can be dried enough to adsorb water vapor in the next cycle. In combination with a heat exchanger to recover the regeneration heat and an adiabatic humidifier at the end of this process, cooled air can be attained. The rotary dehumidifier/regenerator wheel appears to be the front runner in the current desiccant system development effort.

The main purpose of the research is making the design tools to analyse and to compare any desiccant cooling system with traditional and conventional air handling units.

In this thesis, heat and mass transfer are modelled in different components of sustainable air handling systems based on adsorption and evaporation. The sustainable components considered in this thesis range from indirect evaporative coolers to desiccant wheel. Also the traditional air cooler is modelled in order to compare its performance with that of the sustainable components. All models are simulated by the simulation code Simulink (Matlab) with the advantage that any system can be analysed just by linking the inputs and outputs of the various models.

Because there is a lack of knowledge about the performance of desiccant wheels, significant attention is paid to validate the heat and mass transfer model. Test facilities were set up in a climate room to investigate the model of desiccant wheel. In general, the accuracy of the models is acceptable within a margin error of practical applications.

The validated physical models are used to simulate various air conditioning systems in order to analyze them with respect to capacity, energy consumption, and environmental aspects. In addition, simplified equations are developed for dehumidifier wheels in order to reduce simulation time for year round analyses. With these equations a hybrid evaporative cooling system with desiccant wheel as an auxiliary system is simulated for a reference year and for two different climates (extreme and moderate). The energy costs and carbon dioxide (CO<sub>2</sub>) emissions are calculated for the different systems in the different climates.

Year round simulations show that desiccant air conditioning systems are only advantageous when a free source of thermal energy is available for regeneration. If this is not the case, then it can be made advantageous by a hybrid system with desiccant in operation only during peak hours.

The validated simplified models of air cooler and desiccant wheels are implemented in the computer program Enerk. It can be used to analyse and to compare any desiccant system with traditional and conventional air handling units. From a practical point of view it can be considered as the end product of this research.



# Samenvatting

## Sustainable Air Handling by Evaporation and Adsorption

De noodzaak duurzaam te ontwerpen dwingt ontwerpers naar duurzame oplossingen te zoeken. Koeling door middel van droging (desiccant cooling) is er één van.

Het kernpunt van dit onderzoeksproject is de koeling en ontvochtiging van een wiel dat bestaat uit een matrix van adsorptiemateriaal (desiccant) dat vocht kan opnemen. Het systeem wordt continue gemaakt door het vocht er weer uit te drijven met een zeer warme luchtstroom (regenereren), zodat het voldoende gedroogd is om in de volgende cyclus weer vocht op te nemen. In combinatie met een warmtewisselaar die de regeneratiewarmte terugwint en een adiabatische bevochtiger aan het eind van het proces kan men gekoelde lucht realiseren.

Alle modellen zijn gesimuleerd met het simulatie programma Simulink (Matlab). Dit heeft het voordeel dat allerlei systemen gesimuleerd kunnen worden door het koppelen van de juiste in- en uitgangen van de deelmodellen. Om de computertijd acceptabel te houden zijn sterk vereenvoudigde modellen afgeleid uit de uitgebreidere fysische modellen.

In dit proefschrift wordt het warmte en vochttransport in de verschillende componenten van het duurzame koelsysteem beschreven en in fysische modellen omgezet. Deze componenten variëren van een indirecte verdampingskoeler tot een desiccant wiel. Ook van de traditionele luchtkoeler is een model gemaakt om de desiccant koeling te kunnen vergelijken met de traditionele vorm van koelen.

De modellen zijn zoveel mogelijk met experimenten gevalideerd. In het algemeen zijn de nauwkeurigheden voldoende om de verschillende koelsystemen te vergelijken op basis van capaciteit, energiegebruik en milieu aspecten (CO<sub>2</sub> emissie).

Het draaiende ontvochtigings/regenerator wiel blijkt het essentiële onderdeel in het totale systeem en vanwege de gebrekkige kennis hierover is hieraan de meeste aandacht besteed.

Simulaties op jaarbasis laten zien dat airconditioning systemen met vochtadsorptiewielen voordelen bieden als er een bron met gratis thermische energie met temperaturen tussen de 60 en 90 °C beschikbaar is of als het desiccant wiel alleen ingezet wordt tijdens piekuren. Een andere mogelijkheid is het toepassen van een hybride systeem (keuze tussen conventioneel en gas gedreven desiccant koeling tijdens piekuren. Is er restwarmte beschikbaar dan kan de CO<sub>2</sub> emissie sterk gereduceerd worden. Bovendien wordt de behoefte aan elektriciteit tijdens zomerse piekuren altijd sterk verlaagd, hetgeen de kans op oververhit koelwater voor de centrales vermindert.

Het simulatieprogramma van het desiccant koelsysteem is in het gebruikersvriendelijke computer programma Enerk ingebouwd, zodat nu een vergelijk met allerlei luchtbehandelingsystemen mogelijk is geworden.

## TABLE OF CONTENTS

<b>1. INTRODUCTION.....</b>	<b>1</b>
1.1. <i>Evaporative cooling and Desiccant Wheels .....</i>	<i>1</i>
1.2. <i>Energy Recovery Systems .....</i>	<i>2</i>
1.3. <i>Future energy development and Energy Conservation .....</i>	<i>2</i>
1.4. <i>Outline and overview of this thesis.....</i>	<i>4</i>
References.....	6
<b>2. ADVANCED INDIRECT EVAPORATIVE COOLER .....</b>	<b>7</b>
Introduction .....	7
2.1. <i>The process.....</i>	<i>9</i>
2.2. <i>Mathematical model of the wet heat exchanger .....</i>	<i>12</i>
2.3. <i>Simulink Model.....</i>	<i>14</i>
2.4. <i>Sensitivity analysis .....</i>	<i>17</i>
2.5. <i>Model solutions and comparison with test results.....</i>	<i>19</i>
2.5.1.    Laboratory Cooler.....	19
2.5.2.    Demonstration Unit .....	20
2.5.3.    Carrier Holland heating tests .....	22
2.6. <i>Summary and conclusion.....</i>	<i>24</i>
NOMENCLATURE.....	25
References.....	26
<b>3. AIR COOLER.....</b>	<b>27</b>
Introduction .....	27
3.1. <i>Heat and mass transfer modeling.....</i>	<i>28</i>
3.1.1.    Heat transfer coefficients .....	34
3.1.1.1.    Water side, glycol Effect.....	34
3.1.1.2.    Air side.....	34
3.2. <i>Experimental study.....</i>	<i>37</i>
3.3. <i>Results .....</i>	<i>40</i>
3.4. <i>Graphical model using Mollier diagram.....</i>	<i>42</i>
3.4.1.    Linear curve approximation.....	43
Second order curve approximation .....	44
3.5. <i>Summary and conclusions .....</i>	<i>45</i>
NOMENCLATURE.....	45
References.....	47
<b>4. DESICCANT WHEELS.....</b>	<b>49</b>
Introduction .....	49

4.1.	<i>Basic concepts</i> .....	52
4.1.1.	Desiccant Wheels .....	52
4.1.2.	Mechanical vs. Desiccant Dehumidifiers .....	53
4.1.3.	Performance of Desiccant Dehumidifiers .....	54
4.1.4.	Process Air Temperature Rise .....	55
4.1.5.	Post-Cooling .....	55
4.1.6.	Open-cycle solid desiccant systems.....	56
4.1.7.	Adsorption Fundamentals .....	58
4.1.7.1.	Porous Adsorbents .....	58
4.1.7.2.	Adsorption Equilibrium .....	59
4.1.7.3.	Equilibrium Relations .....	59
4.1.7.4.	Potential Theory of Adsorption.....	64
4.1.7.5.	Adsorption hysteresis.....	64
4.1.7.6.	Diffusion in porous particles.....	65
4.2.	<i>Literature review</i> .....	66
4.2.1.	Computational Background .....	66
4.2.2.	Experimental Background .....	67
4.2.3.	Open-cycle solid desiccant systems.....	67
4.3.	<i>Governing equations</i> .....	68
4.3.1.	Simulation Platform and Subsystems .....	74
4.3.2.	Evaluation of the coefficients and step sizes for Dehumidifier .....	74
4.4.	<i>The behavior of solutions</i> .....	76
4.4.1.	Model solutions for different wheel speeds and regeneration air temperatures .....	76
4.4.2.	Outlet adsorption-side humidity profiles and optimum speed of wheel .....	78
4.4.3.	Steady periodic solutions and stability .....	81
4.4.4.	Effects of wall thickness on the heat and mass transfers in desiccant wheels for air dehumidifier and enthalpy wheel .....	84
4.4.5.	Desiccant wheels in low and high speeds for different conditions of inlet air and sorption matrix .....	86
4.4.6.	Sensitivity of the individual parameters .....	87
4.5.	<i>The correlations for outlet air conditions for a desiccant wheel as dehumidifier</i> .....	90
4.5.1.	Correlations .....	90
4.5.2.	Accuracy of Correlations .....	93
4.5.3.	The effect of errors in correlations on the results of simulation of a typical cooling cycle for supply air conditions .....	95
4.5.4.	Sensitivity Studies and Control Variables .....	96
4.6.	<i>Analytical approach</i> .....	98
4.6.1.	The basic equations of heat and mass transfer .....	98
4.6.2.	The approach and solutions .....	100
4.6.3.	The investigation of the simplified assumptions .....	102
4.6.4.	Example .....	104
4.7.	<i>Dimensionless groups</i> .....	106
4.8.	<i>Summary and conclusions</i> .....	110
	<i>NOMENCLATURE</i> .....	112
	<i>References</i> .....	114
<b>5.</b>	<b>MODEL VALIDATION.....</b>	<b>119</b>
	<i>Introduction</i> .....	119
5.1.	<i>Model validation by available test results for an enthalpy wheel</i> .....	119
5.1.1.	The principle information .....	119

5.1.2.	The Experimental Measurements in Different Air Conditions and Wheel Speeds and Comparison with the Model Solutions.....	120
5.1.3.	Adsorption Isotherm Curve .....	121
5.1.4.	Dependency of Efficiency curves on the speed of rotation in different air conditions .....	123
5.2.	<i>Experimental studies for dehumidifier wheel DRI.....</i>	<i>125</i>
5.2.1.	Objective.....	125
5.2.2.	Test Set Up to study Dehumidifier Wheel .....	125
5.2.3.	Experiments .....	128
5.2.4.	Experimental results .....	128
5.2.5.	Test set up to study of Enthalpy Wheel .....	134
5.3.	<i>Summary and conclusion of experimental studies.....</i>	<i>137</i>
	<i>References.....</i>	<i>139</i>
<b>6.</b>	<b>DESICCANT COOLING SYSTEMS .....</b>	<b>141</b>
	<i>Introduction .....</i>	<i>141</i>
6.1.	<i>Modeling of desiccant cooling systems.....</i>	<i>142</i>
6.1.1.	Modeling for Desiccant Wheel.....	144
6.1.2.	Modeling of wet heat exchanger for heat recovery unit .....	144
6.1.3.	Computer Simulation.....	146
6.1.4.	Results of Simulation.....	146
6.1.5.	Desiccant cooling system with three wheels .....	149
6.2.	<i>The sensitivity analysis for control strategy .....</i>	<i>151</i>
6.3.	<i>Year round simulation and control of a hybrid air-conditioning system.....</i>	<i>153</i>
6.4.	<i>Results of yearly simulation.....</i>	<i>156</i>
6.5.	<i>Summary and conclusion.....</i>	<i>165</i>
	<i>NOMENCLATURE.....</i>	<i>167</i>
	<i>References.....</i>	<i>168</i>
<b>7.</b>	<b>CONCLUSIONS AND FUTURE WORK .....</b>	<b>171</b>
7.1.	<i>Conclusions .....</i>	<i>171</i>
7.2.	<i>Future Work .....</i>	<i>174</i>
	<b>Appendix A: Practical Application of Results of This Thesis .....</b>	<b>177</b>
	<b>Appendix B: K-factors for One Row in Air Cooler .....</b>	<b>181</b>
	<b>Acknowledgements .....</b>	<b>183</b>
	<b>Curriculum Vitae .....</b>	<b>185</b>
	<b>Publication list related to this thesis.....</b>	<b>187</b>



# 1. INTRODUCTION

## 1.1. Evaporative cooling and Desiccant Wheels

Evaporative cooling is one of the most traditional and one of the most energy-efficient methods of cooling a home. It has been regarded as environmentally "safe", since the process typically uses no ozone-depleting chemicals, and demands one-fourth as much energy as refrigeration during the peak cooling months of the year. <sup>[1]</sup> In dry climates, evaporative cooling can be used to inexpensively cool large homes.

The drop in temperature depends on how much water the air can absorb (a function of relative humidity), how evenly the pad media is wetted, and how long the air is exposed to the pad (a factor of turbulence, wetness, and speed of air movement), the evaporability of the water, and the ability of the building to "vent" warmer exhaust air back to the outside.

Direct evaporative cooling adds moisture to the air. Therefore, in humid climates, or during the late summer rainy season in the desert it is not efficient and practical. The other main drawback is the limitation of lowest temperature to wet bulb temperature and therefore not practical for humid climates. The other problem of evaporative coolers is possible appearing of Legionella. Indirect evaporative cooling system eliminates the problem of Legionella in the supply air flow, but it is even less efficient than direct system. An advanced indirect evaporative cooler has been introduced to increase the performance of the indirect evaporative cooler and to reach lower temperatures (even below the Wet Bulb temperature). This has been modeled and studied in this thesis.

One of the solutions to application of evaporative systems in warm humid climates is use of the desiccant dehumidifier wheel. In conjunction with evaporative coolers it can significantly reduce air conditioning operating costs since the energy required to power a desiccant cooling system is small provided that regeneration heat required to drive out the moisture such as solar and waste heat are available.

Advantages of using desiccant cooling systems include the following: (1) very small electrical energy is consumed and the sources for the regenerating thermal energy can be diverse ; (2) a desiccant system is likely to eliminate or reduce the use of ozone depleting CFCs (depending on whether desiccant cooling is used in conjunction with evaporative coolers or vapor compression systems, respectively); (3) control of humidity can be achieved better when compared to those cases employing vapor compression systems since sensible and latent cooling occur separately; (4) improvement in indoor air quality is likely to occur due to normally high ventilation and fresh air flow rates being

employed; and (5) desiccant systems have the capability of removing airborne pollutants.<sup>[2-4]</sup>

## 1.2. Energy Recovery Systems

Ventilation of buildings to provide fresh air and remove contaminants has always been important for people. After the energy crisis, the ventilation rate was considerably decreased to save energy consumption needed to condition the air according to the available standards. But there was a considerable increase in indoor air quality problems resulting from high concentration of air contaminants. Therefore, the standards were revised to include higher outdoor ventilation air flow rates to attain acceptable indoor air quality.<sup>[3]</sup> In addition, it was needed to control humidity between 40 to 60%. According to Fanger's model comfort is guaranteed for a sitting person in an air velocity lower than 0.1 m/s and an indoor temperature of 24°C.<sup>[5, 6]</sup> For all air systems, usually applied in combination with desiccant cooling systems, this means that the supply air temperature should be between 15.5 and 18.5 °C.

ISO 7730-1984 Moderate thermal environment specifies the comfort zone for buildings space conditions.<sup>[7]</sup> These standards for outdoor ventilation rates as well as comfort conditions are hardly satisfied by the conventional air conditioning systems used for the buildings in hot humid climates. According to the American Society of Heating, Refrigerating and Air-Conditioning Engineers (ASHRAE<sup>[8]</sup>) 20 to 40% of thermal load is needed to condition ventilation air for commercial buildings, and it can be even increased in universities or hospitals and all the buildings which need 100% fresh air.<sup>[9]</sup>

Energy Recovery systems such as desiccant wheels could prepare a large fraction of the heating and cooling load for ventilation as well as humidity control of supply air in the buildings. Therefore, it decreases the amount of energy required to condition an air stream that is ventilated into a building by using rotary regenerators that allow the system to recover energy from the exhaust air stream which is then disposed into the environment.<sup>[7]</sup> Typically rotary regenerators are used where high ventilation rates are required because of the relatively high initial cost of the equipment has to be recaptured by significant energy savings. In the Netherlands they had to be applied to fulfill the energy requirements (Energy Performance Coefficient).<sup>[10]</sup> Desiccant wheels are attractive rotary regenerators that have been used in either cooling and dehumidification, or heating and humidification processes.

## 1.3. Future energy development and Energy Conservation

A considerable fraction of today's energy consumption is due to air-conditioning of buildings, which involves cooling as well as heating. Since energy costs and environmental concerns are also increasing, the task of designing efficient air-conditioning systems is increasingly important.



It is possible that the world is heading towards a global energy crisis due to a decline in the availability of cheap oil, and recommending to decrease our dependency on fossil fuel consumption. This has led to increasing interest in alternate power/fuel research such as solar energy and geothermal energy, as well as increasing interest in the concept of Energy Conservation.

Energy Conservation is an important component of energy policy. In general, energy conservation reduces the energy consumption and energy demand, and thus offsets the growth in energy supply needed to keep up with population growth. This reduces the rise in energy costs, and can lower the need for new power plants, and energy imports. The reduced energy demand can provide more flexibility in choosing the most preferred methods of energy production.

Reducing emissions and implementing energy conservation measures are important parts of lessening climate change effects. It facilitates the replacement of non-renewable resources with renewable energy and is often the most economical solution to energy storage as well as a more environmentally benign alternative to increased energy production.

New technologies may make better use of already available energy through improved efficiency such as insulation by using heat exchangers; it is possible to recover some of the energy in waste warm water and air, for example, preheating the incoming fresh water. New power plants may become more efficient with technology like cogeneration. New designs for buildings may incorporate techniques like passive solar systems.

The concept of introducing a mandatory and comprehensive European energy policy was approved at the meeting of the European Council on October 27, 2005 in London.

As a result of the decision to develop a common energy policy, the first proposals, Energy for a Changing World were published by the European Commission, following a consultation process on January 10, 2007. It is claimed that they will lead to a “post-industrial revolution”, or a low-carbon economy, in the European Union, as well as increased competition in the energy markets.<sup>[11]</sup>

Key proposals<sup>[11]</sup> include:

- A cut of at least 20% in CO<sub>2</sub> emissions from all primary energy sources by 2020 (compared to 1990 levels), while pushing for an international agreement to succeed the Kyoto Protocol aimed at achieving a 30% cut by all developed nations by 2020.
- A cut of up to 50% in carbon emissions from primary energy sources by 2050, compared to 1990 levels.
- The development of a European Strategic Energy Technology Plan to develop technologies in areas including renewable energy, energy conservation, low-energy buildings.

Desiccant cooling technology with the possibility of using waste heat and solar thermal energy for regeneration is one of the technologies that saves energy and can serve as a suitable alternative for energy conservation purposes. Based on these conclusions and remarks, in this study the CO<sub>2</sub> emission and energy costs have been investigated for a comparison between a reference system and a typical cooling system using desiccant technology.

## 1.4. Outline and overview of this thesis

The objective of this thesis is to model and simulate sustainable cooling systems needed for air conditioning. These tools should lead to better designs. Moreover, their yearly energy consumption should be optimized and compared by year round simulations. Desiccant wheels are the key component of these systems<sup>[12]</sup> and the most important and complicated for modeling. See chapter 4 of this thesis for a detailed discussion. The main goals are to:

- Develop the models of evaporative cooling components ranging from direct to indirect and numerical model for adsorption and coupled heat and mass transfer in the desiccant wheels.
- Validate the models with experimental data from laboratory and companies as well as published papers on experimental studies in this field.
- Use the validated model to make simplified equations to calculate outlet air conditions from desiccant wheels.
- Develop an analytical approach to make average of steady state solutions for model to be used in rough calculations for system design.
- Make simplified models for simulation of different components of sustainable air conditioning cycles with evaporation and adsorption.
- Conduct yearly simulation of a typical hybrid desiccant cooler with simplified models and comparison with conventional chillers for a typical office building.
- Use and to apply the study results in the programs such as Enerk and VABI.

In the first part of this study (chapter 2) a regenerative indirect evaporative cooler that can reduce the air temperature lower than wet bulb and close to the dew point named Static Cooler, has been studied. The simulation of heat and mass transfer in the system has been carried out and compared with the experimental data of different companies.

In chapter 3 an air cooler, as an auxiliary system of a hybrid desiccant cooling system, has been modeled and validated experimentally. The condensation is an important phenomenon that has been considered in the modeling. The experiments for validation of air cooler model have been discussed in the same chapter. In addition, the results of this study have led us to develop a design tool using the Mollier diagram. Desiccant cooling cycles have been compared with traditional ones using the air cooler.

In chapter 4, heat and mass transfer and adsorption have been modeled in a desiccant wheel. The model solutions have been studied and compared with the published experimental and validated numerical studies for both sorption and enthalpy wheels. The dimensionless groups as well as simplified equations have been derived for dehumidifier so that it can be used in long term simulation of different cycles of desiccant wheels. An approximate approach that uses a number of simplified assumptions to give analytically averaged solutions of basic equations has been described in this chapter. Although the results have lower accuracy when compared to the physical numerical models and simplified correlations, the analytical approach can still be considered a proper model for year round simulation of the cycles including desiccant wheels with less limited conditions of application. In addition, some practical questions concerning design and performance of these wheels, their speeds, and the solid thickness of sorption matrix have been evaluated by the models.

In chapter 5, the results of experimental studies of desiccant wheels using an experimental set up in the climate room in TU Delft have been described. In addition, the comparison of model solutions with some measurements of previous tests, prepared by Carrier Holland Heating, has been carried out and discussed in this chapter.

The use of graphical computer tool of Simulink that can be easily connected to the building models and the models of other components is an attractive method to test various control strategies. This thesis is focused on air handling by desiccant cooling; therefore, the building is not considered in detail. It is assumed that the installation had to deliver the specified air supply conditions at specific outside conditions. Consequently, the air handling is applied in a constant air system for ventilation purposes. After heating and cooling to compensate the building cooling load is not considered in the analyses. This approach is in agreement with the accepted procedures applied in the communication between consultancies and manufactures. The key control parameters can be easily and quickly modified for year round simulation.

In chapter 6, having made different Simulink models for different air conditioning cycles with physical model, various systems have been studied and the most important conclusions and results have been discussed. Furthermore, a year round simulation of a desiccant cooling system assisted by a water chiller (hybrid system) has been developed. It has been shown that the performance of desiccant air conditioning systems highly depends on the operating parameters of the desiccant wheel.

This study has been conducted for a warm climate (Beijing) and a moderate climate (The Netherlands) with various supply temperatures and cooling capacities. The required regeneration heat for the desiccant cooling system has been minimized by choosing proper values of regeneration temperature. The desiccant control strategy influences the system performance by selecting the optimum speed of wheel. The control strategy will allow the regeneration temperature to vary in proportion to the cooling load in order to obtain the desired supply air temperature. In addition, the appropriate selection of wet heat exchanger has been considered in the control algorithm.

A summary of the main conclusions of this thesis has been presented in chapter 7. Finally, the future work or the main questions that can be addressed when referring to these results and major area of future research have been discussed in the last chapter.

## References

1. Karpiscak Martin M. ,Babcock Thomas M., France Glenn W. , Zauderer Jeffrey Hopf, Susan B. Foster, Kenneth E., Evaporative Cooler Water Use in Phoenix, Journal AWWA , Vol. 90, Issue. 4, April, 121-130, 1990.
2. D.G.Waugaman, A.Kini, C.F.Kettleborough, A Review of Desiccant Cooling Systems, J.of Energy Resources Technology, 115, 1-8, 1993.
3. Steich G., Performance of Rotary Enthalpy Exchangers, M.S. Thesis in Mechanical Engineering, University of Wisconsin-Madison, 1994.
4. Dauo K., Wang R.Z., Xia Z.Z., Desiccant Cooling air conditioning: a review, Renewable and sustainable energy reviews, 10, 55-77, 2006.
5. ASHRAE, Standard 62-1989, American Society of Heating, Refrigerating and Air-Conditioning Engineers, Atlanta, GA, 1989.
6. An Energy Policy for Europe, Communication from the Commission to the European Council and the European Parliament, Brussels 10.1.2007.
7. Hausen H., Wärmeübergang im Gegenstrom, Gleichstrom und Kreuzstrom, Springer Verlag, 1. Auflage, Berlin, 1950.
8. ASHRAE, Fundamentals Handbook, Atlanta: American Society of Heating, Refrigerating and Air-Conditioning Engineers, Inc, 1997.
9. Carey Simenson, Heat And Moisture Transfer in Energy Wheels, PhD thesis, university of Saskatchewan, Canada, 1998.
10. A.H.C.van Paassen, Indoor Climate Control Fundamentals (Dutch version), TUDelft, ET, 2004.
11. Andrew Rettman, EU sticks out neck in global climate change battle, EU Observer 09/03/07, <http://euobserver.com/9/23665>.
12. Maclain-cross I.L., High Performance Adiabatic Desiccant Open-Cooling Cycles, ASME J. of Solar Energy Engineering, 107, P.102-104, 1985.

## 2. ADVANCED INDIRECT EVAPORATIVE COOLER

### Introduction

In recent years evaporative cooling system has been an attractive alternative for conventional air conditioning systems. It has been because of the energy cost, the environmental impact, the greenhouse effect of CO<sub>2</sub> emissions and the destruction of the ozone layer due to the increased emission of coolants.

Evaporative cooling systems can be classified in two categories of direct and indirect systems. Direct evaporative systems are based on spraying water directly in the air flow. The air follows an adiabatic trajectory in the psychrometric diagram. Its main drawback is the limitation of lowest temperature to wet bulb temperature and possible appearing of Legionella, bacteria pneumophilia. Although this will not happen while the system is operating in its typical range of 20 °C and below, but when the installation is switched off and water in the reservoir is not properly drained away then these conditions could lead to formation of these bacteria and their explosive growth. By treating the water and preventing formation of stagnant water in the system this potential problem can be avoided.

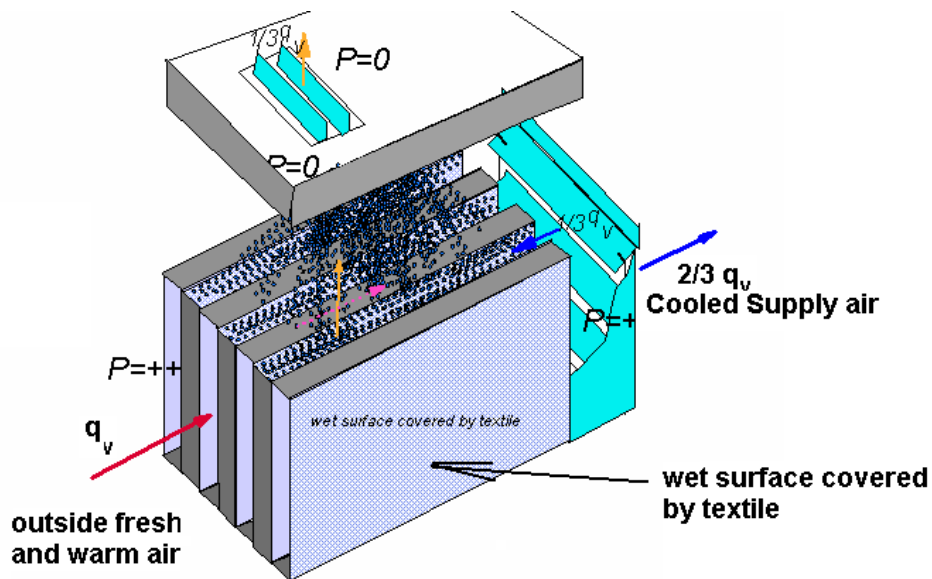


*Figure 2.1. A schematic of Static Cooler*

Indirect evaporative cooling is based on the cooling effect of water evaporation but not directly in the air flow. They are separated by means of a non porous wall. The heat transfer in this process occurs between the air and the water cooled in a cooling tower. Although this system eliminates the problem of Legionella in the supply air flow, it is less efficient than the direct system.

There are various cooling systems that can be considered as an advanced indirect evaporative cooler. One such system is the Static Dew Point Cooling system.<sup>[1]</sup> To increase the performance of the indirect adiabatic cooler and to reach lower temperatures (even below the Wet Bulb temperature), the Static Dew Point Cooler has been developed as shown in figures 2.1 and 2.2. It is a system mostly used for larger air quantities (4000m<sup>3</sup>/h and more), without a discharge fan, without a circulation pump, without a water collector and without a purging device. Therefore, the name “Static Dew Point Cooler” has chosen for a system with almost no maintenance involved.<sup>[1]</sup> The process takes place in a heat exchanger made of synthetic material.

At the end of the heat exchanger, approximately one third of this cooled air is re-routed as process air. The process is a counter flow process and along the external surface of the heat exchanger plates, covered with an absorbent (hygroscopic layer). Evaporation of the existing moist in this layer, indirectly takes place, using energy from the primary air, flowing on the other side of the plate wall. The absolute humidity of the air-to-be-cooled remains unchanged during the cooling process. The process air discharges the evaporated moisture towards the open air and can not enter the conditioned room.

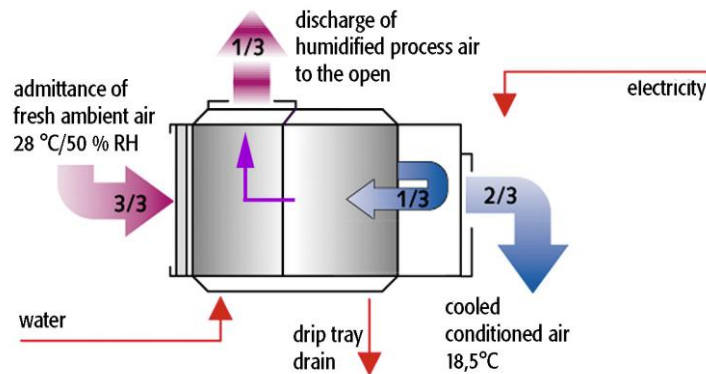


**Figure 2.2.** The principle of operation<sup>[1]</sup>

Static Dew Point Cooling characterizes itself by almost no maintenance costs. This, and the low energy consumption, contributes greatly to the fact that the total running costs are considerably lower than those of a traditional air conditioning installation. The only moving part in Static Dew Point Cooler is the fan at air inlet. The system has been developed for moderate and warm climates, like in most European countries. In this thesis this advanced cooling system is selected to demonstrate how

knowledge about mass and heat transfer can be used to answer various engineering questions.

The most important question about this cooler was: could air temperatures be reached below the Wet Bulb temperature? How does the air temperature approach the dew point?

## **2.1. The process**

The process takes place in a heat exchanger made of a synthetic material. At the end of the heat exchanger, approximately one third of this cooled air is re-routed as process air. The process is in counter flow and along the external surface of the heat exchanger plates covered with an absorbent (hygroscopic layer).

Evaporation of the existing moist in this layer, indirectly takes place, using energy from the primary air flowing on the other side of the plate wall.

The absolute humidity of the air-to-be-cooled remains unchanged during the cooling process. If the air is cooled until the point where condensation will occur, the Dew Point temperature is reached. (Mollier diagram for moist air: figure 2.3).

Evaporation of the existing moisture in the absorbent layer cools the primary air "indirectly" The amount of kJ taken from the primary air is equal to the amount of kJ necessary for evaporation of the moisture and warming the process air.

The process air discharges the evaporated moisture towards the open air and can not enter the conditioned room. In the explanatory Mollier diagram (figure 2.3, point 1). primary air of 28°C/50% Relative Humidity (11.8 gr humidity /kg air) is admitted and cooled down to 18.5°C.

At the end of the heat exchanger, approximately one third of this cooled air (point 2: 18.5°C/87% Relative Humidity) is re-routed and becomes process air. At this point the process air enters the wetted process area. This almost adiabatic process ( $h = \text{constant}$ : 47 kJ/kg) picks up moisture until it reaches 95% Relative Humidity (figure 2.3, point 3: 17.8°C/95% Relative Humidity).

From there the process air stops reacting adiabatically and starts picking up moisture and heat along the wetted outer surface of the heat exchanger plates, until it leaves toward the ambient (at 26.5°C/92% Relative Humidity).

This adiabatic process and the use of only one fan, makes this type of cooling so unique but on the other hand it can not be used as balanced ventilation with heat recovery.

This chapter presents the results of modeling and simulation of this advanced evaporative cooler named Static Cooler. The thermal model has been generated to answer the questions. In addition, an analytical model based on previous studies <sup>[3]</sup> in the

literature has been developed and solved in Excel. The solutions of these two models are very close to each other with a 0.4 to 4% difference in supply temperature.

The Excel program is unable to deliver the process air temperature and humidity, but it shows to be a very quick and appropriate tool for designing the static cooler. This simplified model in Excel is not presented here and the interested reader for additional information is referred to that article [3].

The model solutions have been compared with different test results of measurements performed by Re/genT<sup>[2]</sup> and Carrier Holland Heating.

The tests in Re/genT have been executed on two different configurations of coolers, a laboratory cooler installed in the Re/genT laboratory and the other is Demonstration unit. The coolers tested in Re/Gent as well as the units tested in Carrier Holland Heating, have been evaluated by simulation results using the given dimensions and the characteristics.



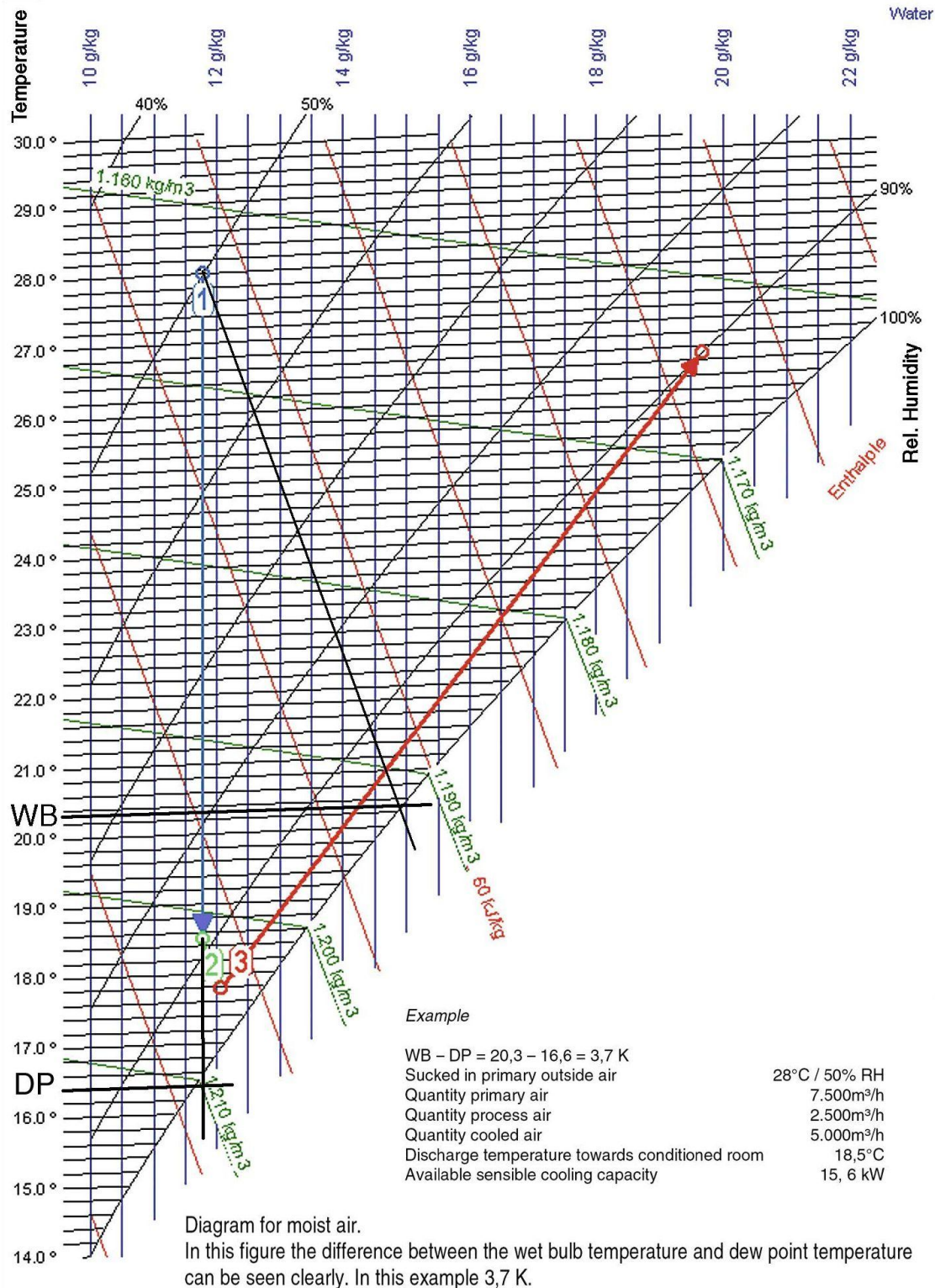
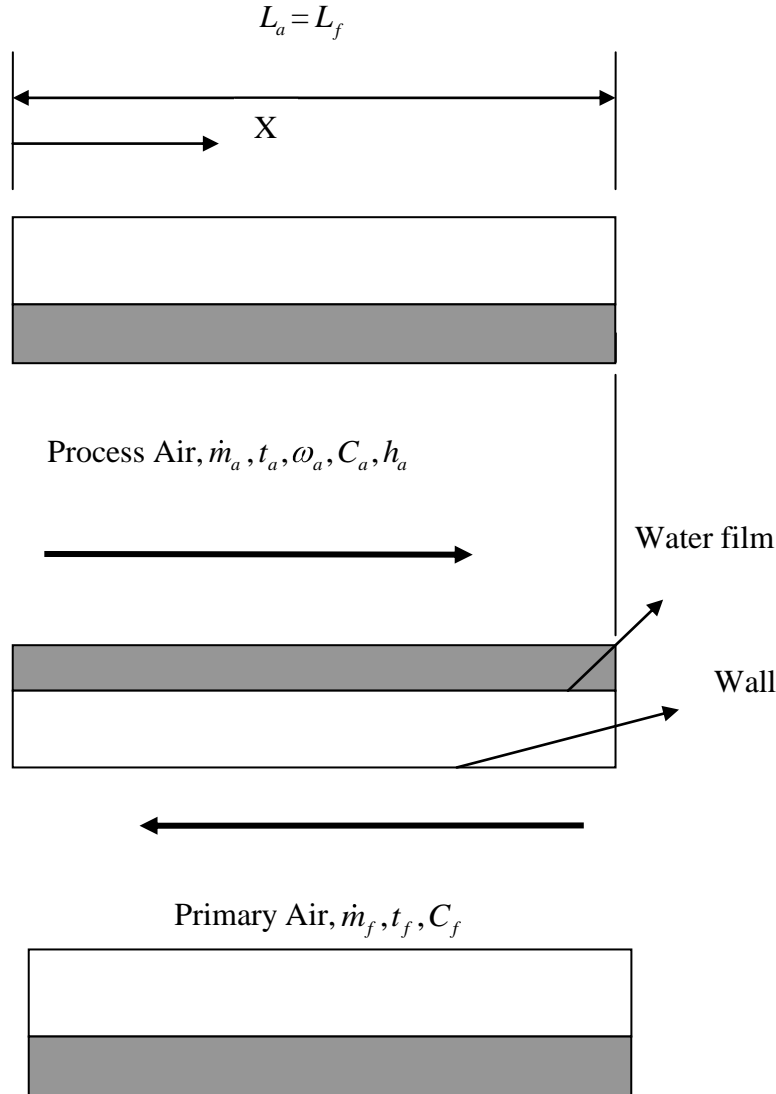


Figure 2.3. The Mollier diagram for moist air<sup>[1]</sup>

## 2.2. Mathematical model of the wet heat exchanger

In this part a wet surface heat exchanger has been represented by a mathematical model <sup>[3]</sup> that consists of a set of differential equations which has been solved using Matlab Simulink. The solutions of simulation for Static Cooler have been compared with the test results of measurements.

The model structure is shown schematically in figure 2.4



**Figure 2.4.** Structure of mathematical model of wet surface heat exchanger

The analysis of a wet heat exchanger is based on following assumptions:

- 1- Thermal and moisture diffusivity in the flow directions for both air stream and walls has been neglected.
- 2- Heat transfer to the surrounding has been neglected.
- 3- The passage walls are impervious to mass transfer.
- 4- Pressures and mass flow rates are constant and uniform for both air streams.
- 5- All the thermophysical properties and heat and mass transfer coefficients are constant.
- 6- The passage geometry is uniform throughout the heat exchanger.
- 7- The Lewis number for air is equal to one.
- 8- The specific enthalpy of moist air has been written as:

$$H_a = C_a(t + 273.15) + \omega_a H_g \quad (2.1)$$

- 9- The evaporating water film is stationary and continuously replenished at its surface with water at the same temperature.
- 10- The moisture content of the air in the equilibrium with the water surface is a function of the water surface temperature according to <sup>[4]</sup> :

$$\omega_w = \frac{10^{+6} e^{\frac{-5295}{273.15+t_w}}}{\left[ 1 - 1.61 \times 10^{+6} e^{\frac{-5295}{273.15+t_w}} \right]} \quad (2.2)$$

Conservation of energy in the primary air stream:

$$C_f \dot{m}_f L_f \frac{\partial t_f}{\partial (L_a - x)} = UA(t_w - t_f) \quad (2.3)$$

That U is the overall heat transfer coefficient between water surface and primary air ( $Wm^{-2}K^{-1}$ ):

$$\frac{1}{U} = \frac{1}{h_f} + \frac{a_p}{k_p} + \frac{a_w}{k_w} \quad (2.4)$$

For conservation of energy and water at the air-water interface:

$$h_a A(t_a - t_w) + h_D A H_{fg}(\omega_a - \omega_w) + UA(t_f - t_w) = 0 \quad (2.5)$$

In wet heat exchangers, such as Static Cooler, heat is transferred between a primary air stream and a moist air stream through a water film on the moist air side of the heat transfer surface. For conservation of water vapor in the humid or process air stream:

$$\dot{m}_a L_a \frac{\partial \omega_a}{\partial x} = h_D A(\omega_w - \omega_a) \quad (2.6)$$

For conservation of energy in the humid air stream:

$$\dot{m}_a L_a \frac{\partial H_a}{\partial x} = h_a A(t_w - t_a) + h_D H_g A(\omega_w - \omega_a) \quad (2.7)$$

Inlet primary air temperature and the inlet process air temperature and moisture content are known and constant.

In addition, the Lewis relation is satisfied, that is

$$h_D = \frac{h_a}{C_a} \quad (2.8)$$

For calculation, the Nusselt number given in the literature for flat plate's cross section geometry and uniform heat flow can be used: [5]

$$Nu = 8.235 \quad (2.9)$$

And

$$St = \frac{Nu}{Re \times Pr} \quad (2.10)$$

For parallel plates Reynolds number is given by:

$$Re = 2\dot{m}_a(1 + \omega_a)b_a / A_c \mu \quad (2.11)$$

Therefore heat transfer coefficient can be calculated as:

$$h_a = St C_a \dot{m}_a / A_c \quad (2.12)$$

### 2.3. Simulink Model

The model used in this simulation has been build up based on a main framework for each element shown in figure 2.5. That can be regarded as an interaction of five main subsystems. Figure 2.6 is the block diagram of simulation model, which was developed using Matlab Simulink. Each subsystem is composed of a series of more intricate subsystems. The calculation blocks are storing the response of an output.

Therefore the subsystem to calculate outlet primary air temperature can be written as:

$$\dot{m}_f C_f (t_{fi} - t_{fo}) + UA(t_w - t_{fo}) = 0 \quad (2.13)$$

or:

$$t_{fo} = \frac{\dot{m}_f C_f}{\dot{m}_f C_f + UA} t_{fi} + \frac{UA}{\dot{m}_f C_f + UA} t_w \quad (2.14)$$

The subsystem to calculate the outlet process air enthalpy is according to:

$$\dot{m}_a(H_{ai} - H_{ao}) + h_a A(t_w - t_a) + h_D H_{fg} A(\omega_w - \omega_a) = 0 \quad (2.15)$$

Therefore

$$H_{ao} = H_{ai} + \frac{h_a A}{\dot{m}_a}(t_w - t_a) + \frac{h_D H_{fg} A}{\dot{m}_a}(\omega_w - \omega_a) \quad (2.16)$$

For the moist content of outlet process air:

$$\dot{m}_a(\omega_{ai} - \omega_{ao}) + h_D A(\omega_w - \omega_a) = 0 \quad (2.17)$$

$$\omega_{ao} = \frac{\dot{m}_a}{\dot{m}_a + h_a A} \omega_{ai} + \frac{h_D A}{\dot{m}_a + h_a A} \omega_w \quad (2.18)$$

For water temperature, the subsystem can be derived from the conservation of energy and water at the air-water interface:

$$t_w = \frac{h_a}{h_a + U} t_a + \frac{h_D H_{fg}}{h_a + U} (\omega_a - \omega_w) + \frac{U}{h_a + U} t_f \quad (2.19)$$

That  $\omega_w$  is the moist content of air in saturation layer close to water layer with same temperature of water film. Each subsystem in figure 2.6 contains other subsystem to calculate all the necessary parameters.

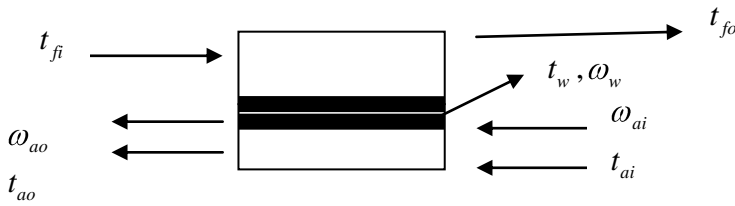


**Figure 2.5.** Schematic of discretization of one of the channels for Simulink code

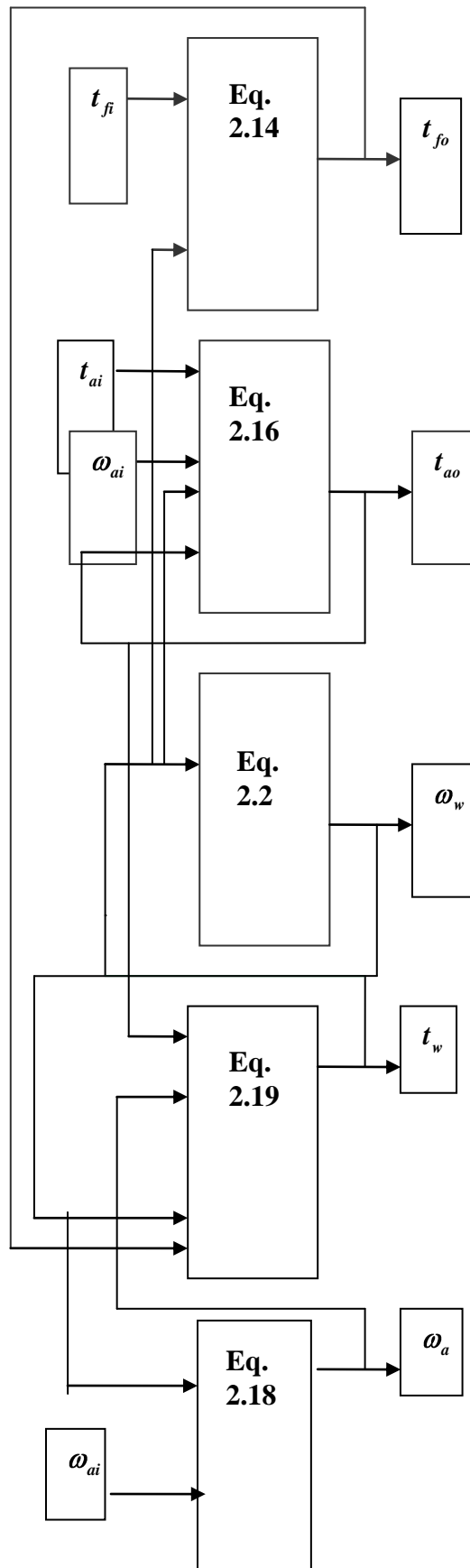


**Figure 2.6.** Simulink representation of the model

## 2.4. Sensitivity analysis

Figures 2.7 and 2.8 show how the different dimensions of the static cooler can affect the cooling performance of the system for a typical outside condition of 31°C and 41.3 % relative humidity and 1.84 kg/s air flow rate.

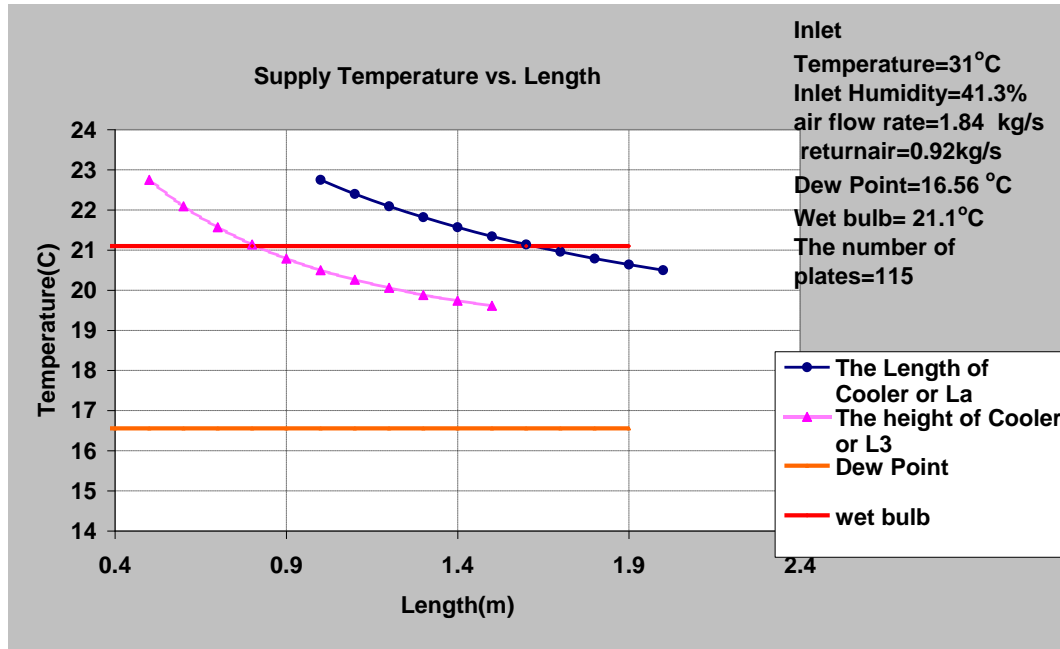


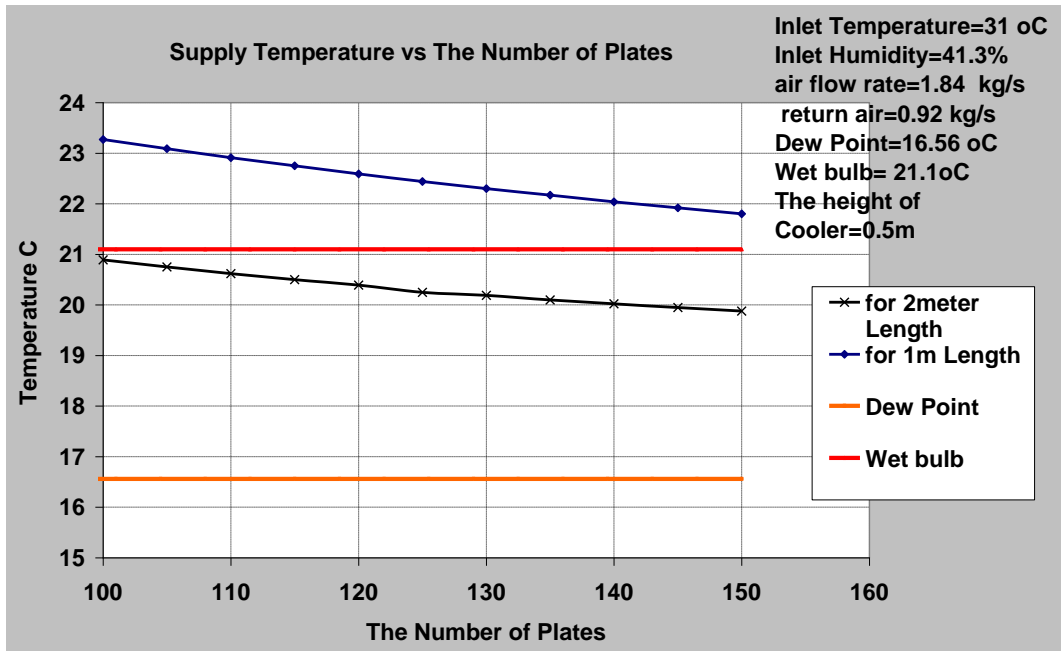
**Figure 2.7.** The effect of dimension of cooler on the cooling performance

According to this sensitivity study for constant volume of air, the bigger cooler can have the better performance. The length of  $L_a$  in these figures is the dimension in flow direction, the length of  $L_3$  in figures is the height of cooler.

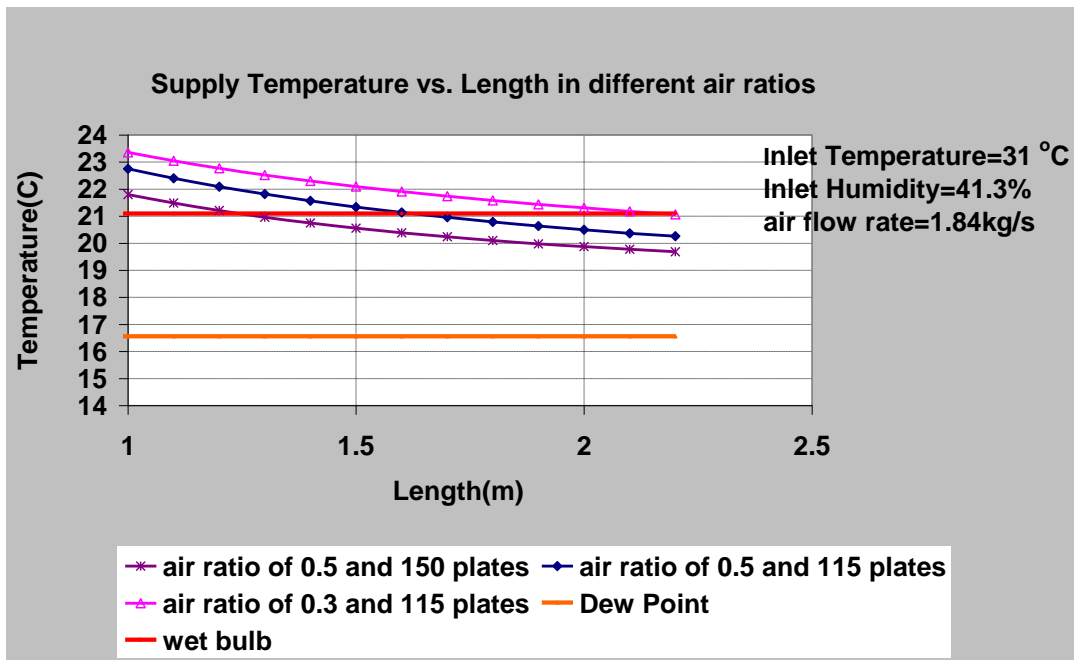
Figure 2.8 shows how the cooling performance changes with increasing the number of plates. The increase in the number of plates with constant air flow rate leads to lower air speeds and it makes reducing in supply air temperature.

Figure 2.9 shows the effect of different configuration for cooler and air ratios on the cooling performance of static cooler regarding dew point and wet bulb temperature. The profiles have been demonstrated for different ratios of primary air, process air and different number of plates as a function of cooler length of  $L_a$ .

As shown in these figures with an appropriate design the supply temperature can reach below wet bulb temperature but still far from dew point.



*Figure 2.8. The effect of number of plates on cooling performance*



*Figure 2.9. The effect of cooler length on cooling performance regarding dew point and wet bulb temperatures for different air ratios and different number of plates*



## 2.5. Model solutions and comparison with test results

### 2.5.1. Laboratory Cooler

The picture and dimensions of this cooler are shown in figures 2.10 and 2.11. For laboratory cooler with the characteristics as follows the test results and simulation solutions can be compared according to table 2.1.

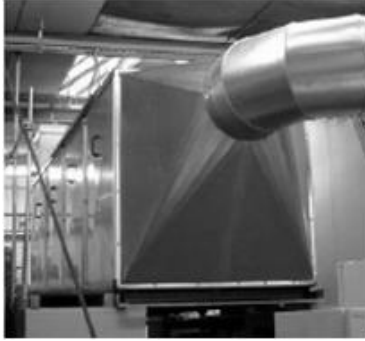


*Figure 2.10. Laboratory cooler <sup>[2]</sup>*

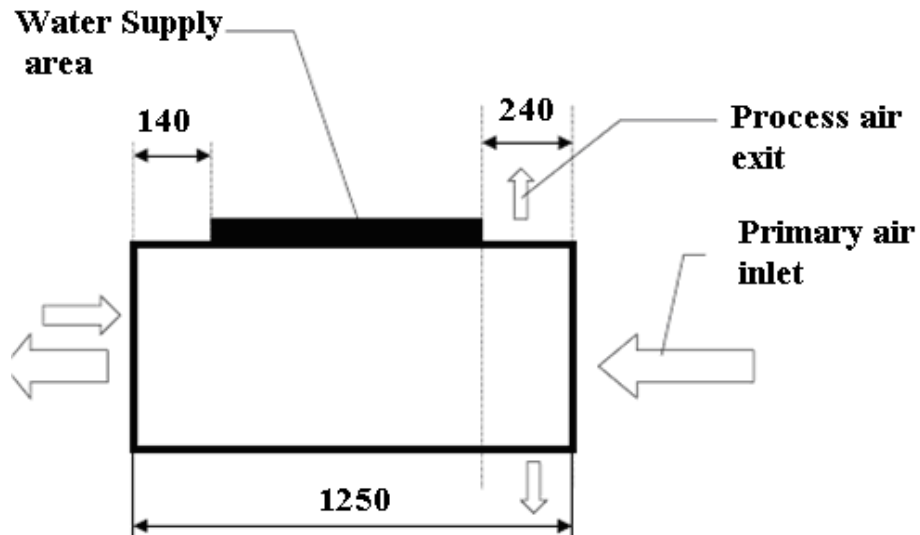


*Figure 2.11. The dimensions of Laboratory Cooler <sup>[2]</sup>*

The number of elements for simulation solutions given in table 2.1 is 50 and primary and process air flows are various as given in this table. Figure 2.12 shows the dimension and passage cross section for these coolers.

$$L_a = L_f = 1250 - 140 - 240 = 870mm$$

$$L_2 = 360mm$$

$$L_3 = 1000\text{mm}$$

$$b_f = b_a = 3\text{mm}$$

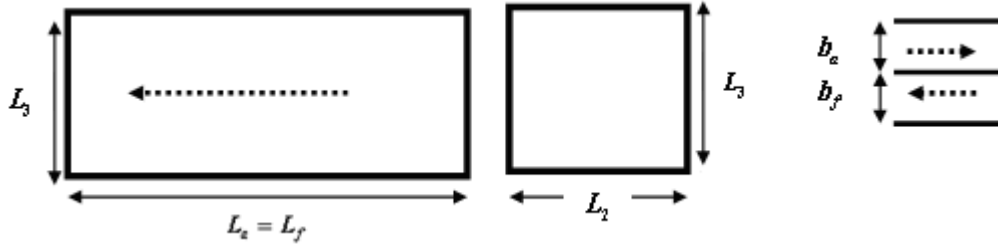


**Figure 2.12.** The characteristic of dimensions and passage cross section of coolers

### 2.5.2. Demonstration Unit

For Demonstration unit tests which the characteristics of the cooler given as follows the test results and simulation solutions can be compared according to table 2.2.

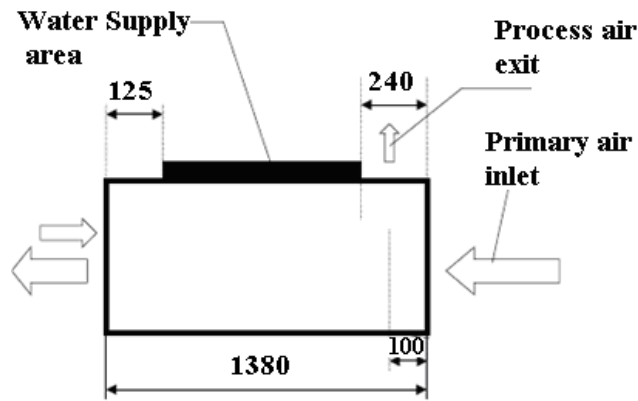


**Figure 2.13.** The dimensions of Demonstration unit <sup>[2]</sup>

$$L_a = L_f = 1380 - 125 - 240 = 1015\text{mm}$$

$$L_2 = 500\text{mm}$$

$$L_3 = 425\text{mm}$$

$$b_f = b_a = 3\text{mm}$$

The number of elements for simulation solutions given in table 2.2 is 50 and primary and process air flows are various given in the table.

The last rows in the tables show the amount of error in the results according to energy conservation equation:

$$\dot{m}_f C_f (t_{fi} - t_{fo}) = \dot{m}_a (H_{o\text{-process air}} - H_{i\text{-process air}}) \quad (2.20)$$

**Table 2.1.** The comparison between test results and simulation results for Laboratory cooler tests

Primary flow: kg/s	1.95	2.23	0.7	1.97	1.96	0.63	0.63	1.9
Process flow :kg/s	1.02	0.79	0.2	0.83	.83	.23	.23	1.04
Inlet air Temperature: °C	21.9	21.7	19.4	20.4	21.5	21.2	20.9	27.5
Inlet air temperature after fan: °C	23.2	23.2	20.2	21.8	22.8	22	22.7	26.8
Humidity %	34.5	33.9	44.1	43.1	38.8	40.7	37.3	40.4
Absolute Humidity: g/kg	6.1	6	6.5	7	6.7	6.7	6.4	8.9
Dew Point: °C	6.8	6.6	7.6	8.7	8.2	8.1	7.4	12.3
Wet bulb temperature: °C	13.9	13.8	13	14.1	14.3	14	13.9	17.6
Enthalpy: kJ/kg	38.85	38.6	36.81	39.71	39.97	39.15	39.1	49.65
Air temperature above fan: °C	16.1	17.4	15.2	15.3	15.6	15	16.7	19.9
Simulation result for temperature: °C	14.89	15.8	12.26	15.34	15.56	12.29	12.88	18.89

The comparison between test results and simulation results for Demonstration unit tests as well as Laboratory Cooler has been given in tables 2.1 and 2.2. The outlet air temperatures, measured and also calculated by simulation always are higher than dew point temperature for both units. For Laboratory unit the measured outlet air temperature always is higher than wet bulb temperature but in a few conditions could reach to wet bulb or lower. For simulation of Demonstration unit there are a few points which results are lower than wet bulb temperatures. However, with these configurations simulation results never can reach to dew points. The simulation results confirm the comment that

the plates have not been wetted properly and uniform during test measurements. Any improvement to the performance of the system can be investigated easily and quickly according to selection of appropriate dimension and configuration of the system and the characteristics of air flow rate and the appropriate selection of ratio of process and primary airs. It has typically been shown in figures 2.7-9 that how the changes in the design and configuration of system and air ratios can affect on the air temperature.

**Table 2.2.** The comparison between test results and simulation results for Demonstration unit tests

Primary flow kg/s	0.31	0.3	0.32	0.42	0.29	0.33
Process kg/s	0.16	0.12	0.12	0.17	0.14	0.014
Inlet air Temperature °C	21.3	21.2	24.5	24.3	25.3	24
Inlet air Temperature after fan °C	22.4	22.2	25	25.5	26.1	25.4
Humidity %	43.81	44.34	40.45	39.75	40.7	34.62
Absolute Humidity g/kg	7.4	7.4	8	8.1	8.6	7
Dew Point °C	9.5	9.5	10.65	10.83	11.72	8.69
Wet bulb temperature	14.79	14.72	16.28	16.54	17.17	15.54
Enthalpy kJ/kg	41.34	41.13	45.52	46.28	48.17	43.38
Air temperature above fan °C	15.94	17.12	13.57	16.22	16.53	12.93
Simulation result for temperature °C	12.38	12.56	14.19	14.77	14.72	12.8
Balance, simulation%	0.0017	0.0007	0.0047	0.0016	0.0129	0.0023

The error for simulation is resulting from the difference between the discretized equations in Simulink and the equations of energy and water conservations. The increase of the number of discretized elements increases the accuracy, but will reduce the speed of simulation due to the increase of the calculation time.

### 2.5.3. Carrier Holland heating tests

The dimension of the unit tested by Carrier HH, shown in figure 2.14 has been given as:

$$L_a = L_t = 1250 \text{ equivalent to } 1000 + 0.75 \times 250 = 1190 \text{ mm}$$

$$L_2 = 1000 \text{ mm}$$

$$L_3 = 500 \text{ mm}$$

$$b_f = 4 \text{ mm}$$

$$b_a = 3 \text{ mm}$$

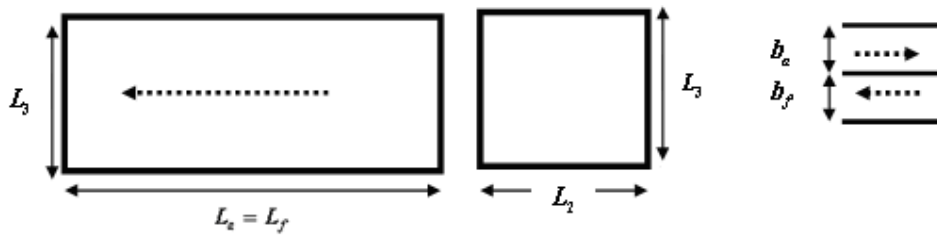


**Figure 2.14.** The dimension of the unit tested by Carrier HH

**Table 2.3.** Table of the comparison between test results and simulation results for Carrier unit tests

$\dot{m}_f$ kg/s	$\dot{m}_a$ kg/s	$t_i$ °C	RV %	$t_o$ °C	Humidity g/kg	Wet bulb Temperature °C	$\frac{\dot{m}_a}{\dot{m}_f}$	Dew Point Temperature °C	Simulation Results for outlet air Temperature °C
1.8	0.64	29.7	50.4	23.7	13.24	21.8	0.34	18.3	21.99
1.8	0.64	31.4	39.2	22.6	11.31	21	0.34	15.87	21.19
1.48	0.51	29.2	49.2	23	12.54	21.2	0.34	17.46	20.88
1.49	0.51	29.2	71.4	25.8	18.37	24.9	0.34	23.49	24.82
1.847	0.64	27.8	34.5	21	8.05	17.3	0.34	19.52	17.93
1.84	0.65	25.9	67.9	22.5	14.31	21.4	0.35	21.46	21.63
1.84	0.65	25.6	49.1	20.3	10.1	18.3	0.35	14.14	18.65
1.84	0.65	25.2	33.9	18.2	6.77	15.3	0.35	8.2	16.01
1.84	0.65	28.9	32.9	20.3	8.18	17.7	0.35	10.99	18.4
1.84	0.65	27.4	51.4	21.7	11.78	20	0.35	16.5	20.8
1.84	0.65	29.6	69.1	25.8	18.18	25	0.35	23.33	25.7
1.84	0.62	29.8	49.9	23.8	13.18	21.8	0.33	18.24	22.77
1.82	0.62	29.6	50.5	23.8	13.19	21.7	0.34	18.24	22.7
1.84	0.62	29.7	50.5	24.2	13.26	21.8	0.33	18.34	22.83
1.84	0.62	25.7	31.8	19.9	6.54	15.2	0.33	7.7	15.66
1.85	0.62	25.5	31.8	19	6.46	15.1	0.33	7.52	15.49
1.85	0.62	25.6	50.1	20.7	10.31	18.4	0.33	14.45	19.04
1.84	0.62	29.4	32.6	22.7	8.35	18	0.33	11.29	18.94
1.84	0.62	29.5	70.4	26.6	18.43	25.1	0.33	23.55	25.83
1.84	0.62	27.8	50.2	22.8	11.78	20.2	0.33	16.5	21.04
1.84	0.62	27.4	33	20.6	7.51	16.7	0.33	9.73	17.33
1.72	0.57	18.6	63.2	16.3	8.46	14.3	0.33	11.48	14.29
1.84	0.62	25.7	68.7	22.9	14.31	21.4	0.33	19.52	21.92
1.84	0.62	31.1	41.3	24.4	11.72	21.2	0.33	16.42	22.33

Since only 1000 mm of the cooler length is in counter flow conditions and the rest or 250 mm is in cross flow condition, regarding the ratio of efficiency for cross flow and counter flow the efficient length of this part has been calculated and in equation 2.28 has been considered. As it has been shown in table 2.3, the comparison between test results and simulation results for Carrier unit tests show that simulation results are always lower than measured values. This finding is reasonable since the faults in manufacturing of the glued tissue sheets of the heat exchanger may happen easily and the cooler will fail to achieve

lower temperatures as the model predicts. In addition, even the results of simulation are higher than wet bulb temperatures.

## **2.6. Summary and conclusion**

- The modeling and simulation in this chapter is according to differential equations of heat and mass transfer between moist air and water film in process air side. The equations are based on heat balance in the primary air stream and heat and mass balance at the air-water interface in the process air stream.
- The user friendly and flexible programming environment of Simulink provides an excellent significantly to study and modeling the Static Cooler.
- The simulation results of primary air temperature and process air temperature and absolute humidity has been compared with the average value of experimental measurements in different places according to Re/gent report as well as Carrier Holland Heating measurements.
- Any type of improvement of the performance of the system can be investigated easily and fast according to selection of appropriate dimension and configuration of the system and the characteristics of air flow rate and the appropriate selection of ratio of process and primary airs.
- The comparison between the reported test results and modeling and simulation results show ability and significant potential to improve Static Cooler performance to deliver temperatures lower than wet bulb temperature.
- The simulation results confirm the comment that the plates have not been wetted properly and uniform during test measurements.
- The results show that for present configuration of dimension and characteristics the unit is not able to deliver the desired temperature but with some changes in design it could be possible to approach to the desired point that is below wet bulb temperature.

## NOMENCLATURE

a	Thickness ( $m$ )
A	Surface area, associated with U or heat transfer coefficient ( $m^2$ )
$A_c$	Minimum air flow area ( $m^2$ )
b	Air passage size ( $m$ )
C	Specific heat capacity ( $J kg^{-1} K^{-1}$ )
h	Heat transfer coefficient ( $W m^{-2} K^{-1}$ )
$h_D$	Mass transfer coefficient ( $kg m^{-2} s^{-1}$ )
H	Specific enthalpy ( $J kg^{-1}$ )
$H_{fg}$	Latent heat of vaporization of water ( $J kg^{-1}$ )
$H_g$	Water vapor enthalpy ( $J kg^{-1}$ )
k	Thermal conductivity ( $W m^{-1} K^{-1}$ )
L	Air passage length in flow direction ( $m$ )
$\dot{m}$	Mass flow rate ( $kg s^{-1}$ )
Nu	Nusselt number (dimensionless)
Pr	Prandtl number (dimensionless)
Re	Reynolds number (dimensionless)
RV	Relative Humidity (%)
St	Stanton number (dimensionless)
t	Temperature ( $^{\circ}C$ )
U	Overall heat transfer coefficient ( $W m^{-2} K^{-1}$ )
x	Distance from air inlet ( $m$ )

## Greek letters

$\mu$	Dynamic viscosity ( $Pa.s$ )
$\omega$	Humidity ( $kg kg^{-1}$ )

## Subscripts

a	process air
f	primary air
g	Gas
i	Inlet
o	Outlet
p	Plate
w	water film

**References**

1. P.G.H. Uges, Air conditioning using R718(water) as refrigerant, StatiqCooling BV, Po.box 10269, NL-7301 GG Apeldoorn, The Netherlands, Fax.; +31 (0)55 3664504, E-mail: [dauw.cooling@planet.nl](mailto:dauw.cooling@planet.nl).
2. P.Beks, Test results of measurements on two dew point coolers, Re/gent B. V. Lage Dijk 22, 5705 BZ Helond, the Netherlands.
3. I.L. Maclain-cross, P.J. Banks, A general theory of wet surface heat exchangers and its application to regenerative cooling, ASME J. of Heat Transfer, 103, p.579-585, 1981.
4. L.Z. Zhang, J.L. Niu, Performance comparisons of desiccant wheels for air dehumidification and enthalpy recovery, Applied Thermal Engineering, 22, 1347–1367, 2002.
5. Frank P. Incropera, David P. Dewitt, Theodore L. Bergman, and Adrienne S. Lavine, Fundamentals of Heat and Mass Transfer, 6th Edition, Wiley, 2007.



### 3. AIR COOLER

“Reprinted with permission from the American Society of Mechanical Engineers, ASME”

#### Introduction

Air coolers, as fin-and-tube heat exchangers, have engineering applications in air-conditioning apparatuses. One of their applications is in hybrid desiccant air conditioning systems in which the air cooler is one of the components. In addition, a reliable air cooler model fed by cold water from chillers is needed to compare advanced evaporative air conditioning systems to traditional coolers.

There are a large number of studies in this field. Kays and London <sup>[1]</sup> have introduced various types of heat transfer surfaces. However, the estimation of convective heat transfer coefficients is important to design a high-performance heat exchanger. The local heat transfer coefficients on the outer surface of tubes, in shell-and-tube heat exchangers with a staggered tube arrangement, have been visualized and determined from heat transfer measurements by Li and Kottke. <sup>[2]</sup> These coefficients are transformed to mass transfer coefficients by employing the analogy between heat and mass transfer. An experimental study of local heat transfer coefficients, in a staggered tube array with plate fins, was investigated by Murray et al. <sup>[3]</sup> The results indicate that most positions on the tubes and on the fins record an increase in heat transfer with decreasing fin spacing, although there is an optimal spacing value below which local heat transfer coefficients decrease. Ay, et al., <sup>[4]</sup> performed an experimental study using an infrared thermovision to monitor temperature distribution over a plate-fin surface inside the plate finned-tube heat exchangers. They demonstrate that the averaged heat transfer coefficient of staggered configuration is 14–32% higher than that of in-lined configuration.

Experimental results for the convective coefficient distribution in both the inside and conical end zones of the extended surface in a finned pipe are presented for three different flow velocities in a paper by Mariscal, et al. <sup>[5]</sup> Bourgiou, et al. <sup>[6]</sup> used the film method, which takes the influence of mass transfer on the thermal calculation into account. They developed a model to simulate the heat transfers by condensation of the humid air on finned-tubes bundles.

They concluded that the knowledge of the fin portion, which works in a wet regime, is very important for the heat transfer rate calculation. In a wet regime, the effective heat transfer coefficient of the gas phase and the apparent heat transfer coefficient with condensation grow proportionally with the condensation flow rate. According to Bourgiou, et al., the apparent heat transfer coefficient with condensation can exceed the value of the heat transfer coefficient of the gas phase by 10 times.

This statement could not be explained and was not compatible with our experimental studies. There was a large difference between our experimental data and this result. The modeling of heat and mass transfer in an air cooler described in this chapter was validated by a set of experiments in the laboratory with an air cooler of eight rows. An analysis of the experimental results shows that a correction of the heat transfer coefficient and also a correction of the correlation between heat and mass transfer are needed. This validated model is used to construct a graphical model for transients in the Mollier diagram. Due to its simplicity, it requires low computing times and it, therefore, proves to be extremely useful for year round simulation studies. The model is based on the approach of Green.<sup>[7]</sup>

### 3.1. Heat and mass transfer modeling

The configuration of the air cooler is shown in figure 3.1. It consists of in-line coils with extended surfaces with continuous flat plate fins. The individual tubes in a coil are interconnected to form the required serpentine arrangement of multi-pass tubes circuits by use of return bends, where the water flow is distributed. Therefore, the laminar flow will be temporarily turbulent (walk in effect) in the beginning of the next tube.

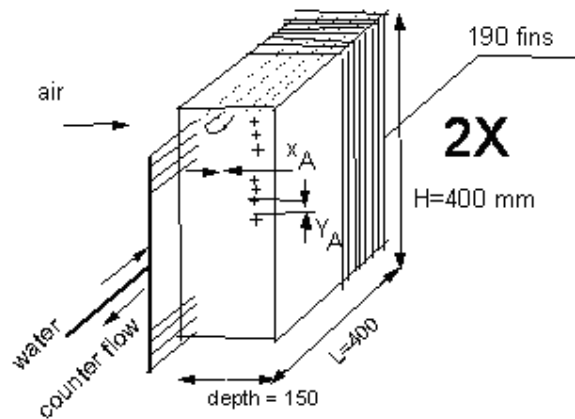


**Figure 3.1.** Configuration of air cooler for experiments, two units are connected in series, thus  $2 \times 4 = 8$  rows

Fouling aspects that may have a big impact on the performance are not considered. A scale factor is applied by adding an extra heat resistance.

The configuration of the coil such as fin spacing, tube spacing, types of fins as well as the amount of condensation on the coils and fins and the degree of surface cleanliness determine the point at which moisture will be condensed on the coil.

The heat and mass balance is written for an element and the resulting equations are integrated over one discrete element  $dl$ . To simplify the process of solving the equations, the saturation curve is linearised.

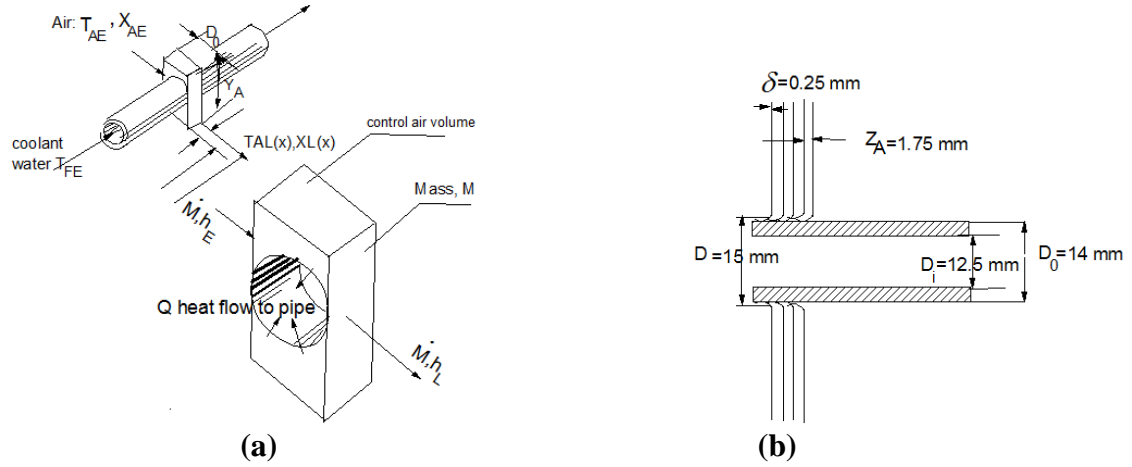


**Figure 3.2.** (a) discretization of a row of serpentine coils (b) fins and tube configuration

The cooler has been constructed with equivalent layers so that only one horizontal layer is considered. In this layer the coils are situated as a kind of serpentine of various rows. The coils are subdivided in rows and each row is subdivided in elements with thickness  $dl$ .

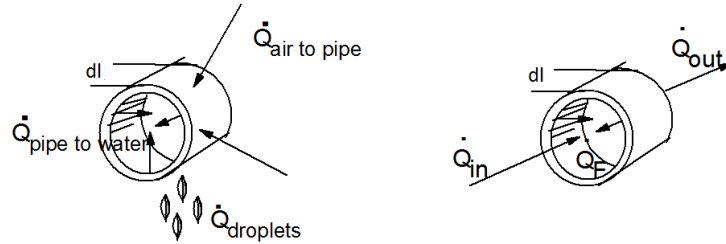


**Figure 3.3.** Representation of sensible and latent heat flows for an element

The mass balance is ignored when the coil surface temperature is higher than the dew point of the passing air.

The sensible heat to cool down the air by coil is written as follows:

$Q_{\text{sensible, air} \rightarrow \text{coil}} = \text{Heat need to cool the air flow}$

$$H_{AA} \pi D_0 dl \cdot K_{opp} \eta (\bar{T}_A - T_C) = C_A \dot{M}_A (T_{AE} - T_{AL}) \quad (3.1)$$

This gives:

$$T_{AL} - T_{AE} + C_I (\bar{T}_A - T_C) = 0 \quad (3.2)$$

With:

$$C_I = H_{AA} \pi D_0 \cdot K_{opp} \eta / (\rho_A V_A Y_A C_A) \quad (3.3)$$

For latent heat:  $\dot{Q}_{latent,air \rightarrow coil} = \text{Heat released by condensation}$

$$H_m \pi D_0 dl \cdot K_{opp} (\bar{X} - X_s) \cdot R \cdot \eta = R \cdot (X_E - X_L) \cdot \dot{M}_A \quad (3.4)$$

$$X_L - X_E + C_2 (\bar{X} - X_s) = 0 \quad (3.5)$$

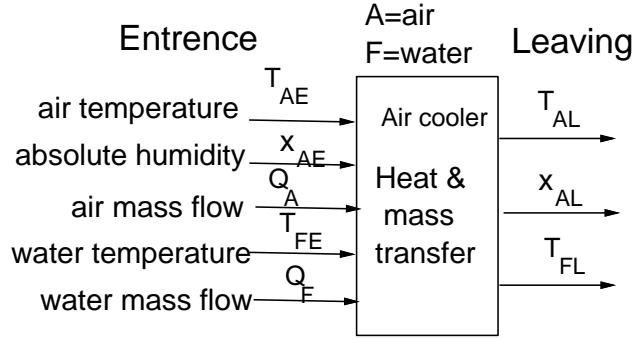


**Figure 3.4.** Inputs / outputs of an air cooler model

With:

$$C_2 = H_m \pi D_0 \cdot K_{opp} \cdot \eta / (\rho_A V_A Y_A) \quad (3.6)$$

$$\dot{Q}_{air \rightarrow coil} = \dot{Q}_{coil \rightarrow water} - \dot{Q}_{droplets} \quad (3.7)$$

$$\dot{Q}_{air \rightarrow coil} = H_{AA} \pi D_0 \eta K_{opp} dl (\bar{T}_A - T_C) - H_D \pi D_0 \eta K_{opp} dl (\bar{X} - X_s) R \cdot \sigma \quad (3.8)$$

$$\text{with: } \sigma = 0 \text{ when } \bar{X} \leq X_s \quad \text{dry} \quad (3.9)$$

$$\sigma = 1 \text{ when } \bar{X} > X_s \quad \text{wet}$$

$$\dot{Q}_{coil \rightarrow water} = H_F \pi D_i dl (T_C - T_F) \quad (3.10)$$

$D_i$  = diameter inside tubes

$T_F$  = temperature cooling water at place l.

$$\dot{Q}_{droplets} = H_D \pi D_0 dl \cdot K_{opp} \eta (\bar{X} - X_s) C_{water} T_{droplet} \quad (3.11)$$

It is assumed that:  $T_{droplet} = T_C$

If the cooler surface is dry, then:

$$\bar{X} = X_S \text{ and } X_L = X_E \quad (3.12)$$

This gives:

$$-B_2(\bar{T}_A - T_C) - B_7(\bar{X} - X_S) + B_3(T_C - T_F) = 0 \quad (3.13)$$

In case the cooler is dry:

$$B_7 = 0 \quad (3.14)$$

In this model, ideal analogy between heat and mass transfer is assumed, resulting in  $Le = 1$ :

$$H_m = \frac{H_A}{Le \ C_p} \quad (3.15)$$

Considering fin efficiency:

$$H_A = H_{AA} \cdot \eta \quad (3.16)$$

For the cooling water

$\dot{Q}_{\text{coil} \rightarrow \text{water}}$  = increase in heat content of water

$$H_F \pi D_i dl \cdot (T_C - T_F) = \dot{M}_F C_F (T_{F,E} - T_{F,L}) \quad (3.17)$$

$$\frac{dT_F}{dl} + \frac{H_F \pi D_i}{\dot{M}_F C_F} (T_F - T_C) = 0 \quad (3.18)$$

$$\frac{dT_F}{dl} + C_3 (T_F - T_C) \quad (3.19)$$

$$\frac{\partial T_F}{\partial \xi} + B_1 (T_F - T_C) = 0 \quad (3.20)$$

With  $\xi = \frac{l}{L}$

The saturation curve is made linear around the working point  $(X_R, T_R)$  by:

$$X_S = X_R + TG_R (T_C - T_R) \quad (3.21)$$

$$X_S = TG_R \cdot T_C + REF \quad (3.22)$$

In the reference working point:

$$T_R = 9^\circ\text{C} \text{ and } X_R = 7.26 \times 10^{-3} \text{ kg/kg}$$

$$REF = X_R - TG_R \cdot T_R \quad (3.23)$$

$$TG_R = 5.3 \times 10^{-4} \text{ and } REF = 0.002395$$

$$T_A = 0.5(T_{AE} + T_{AL}) \quad (3.24)$$

$$X_A = 0.5(X_E + X_L) \quad (3.25)$$

There are 5 equations (3.2; 3.5; 3.13; 3.20; 3.22) with 5 unknown variables  $T_{AL}$ ,  $X_{AL}$ ,  $T_C$ ,  $X_S$ , and  $T_{FL}$ .

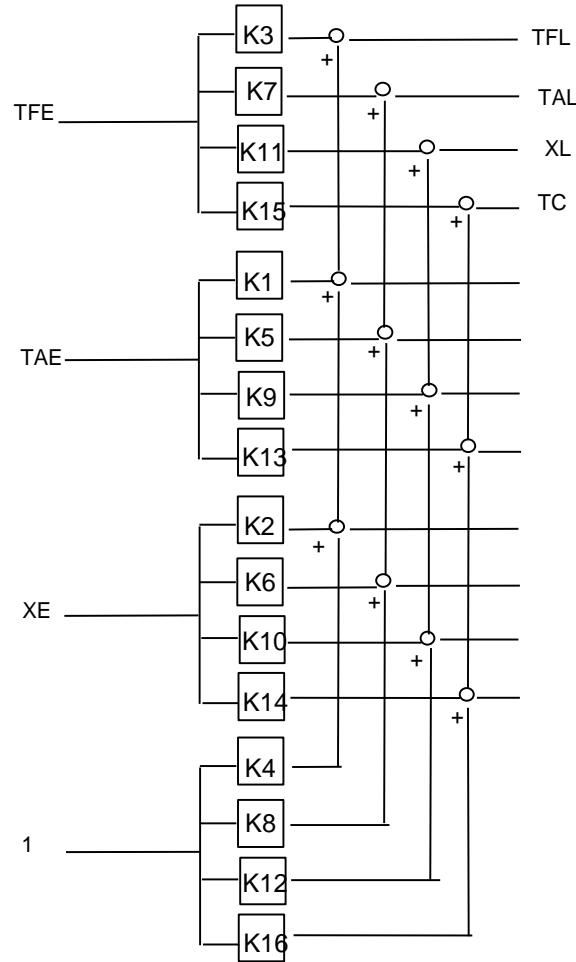


**Figure 3.5.** *K-factors relate input and outputs of one row*

The equations of a slice  $dl/L$  are integrated from place  $l$  to the end value  $L$  analytically. The unknown variables are expressed according to the known ones, which results in the following set of equations:

$$T_{FL} = K_1 T_{AE} + K_2 X_E + K_3 T_{FE} + K_4 \quad (3.26)$$

$$T_{AL} = K_5 T_{AE} + K_6 X_E + K_7 T_{FE} + K_8 \quad (3.27)$$

$$X_L = K_9 T_{AE} + K_{10} X_E + K_{11} T_{FE} + K_{12} \quad (3.28)$$

$$T_C = K_{13} T_{AE} + K_{14} X_E + K_{15} T_{FE} + K_{16} \quad (3.29)$$

Coefficients of K have been given in Appendix C.

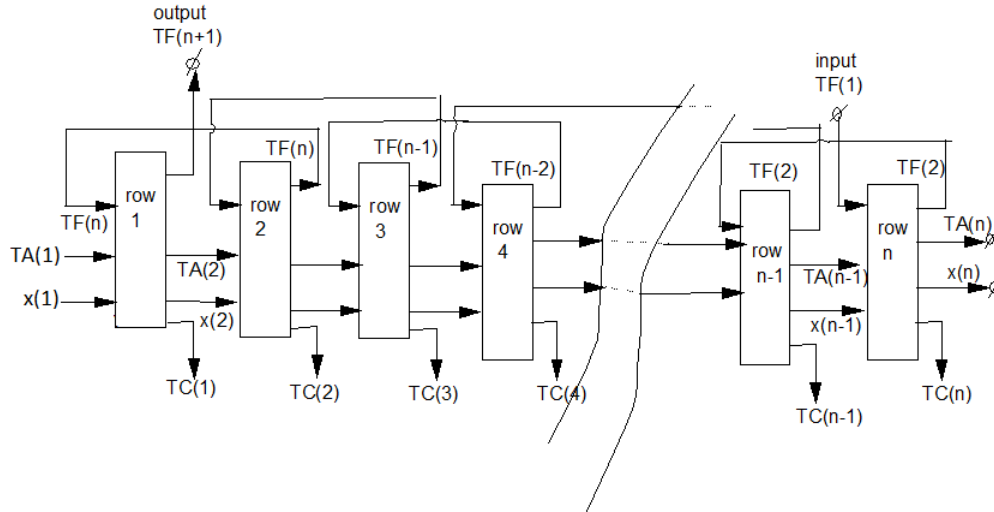


**Figure 3.6.** Connection of rows in reality and in the model

A coil can now be described by a set of linear equations.

The coefficients K are complex equations of physical properties and dimensions of the air cooler. Moreover, they are different for a dry and wet row. K-factors are dependent on the surface conditions of the coil and fins.

The set of values is different for a dry or wet coil and are given in the appendix.

In the simulation, each row should be tested on dry or wet conditions and the appropriate set of equations have to be selected.

The combined set of equations of all coils can be solved based on the linear equations,

Detection dry / wet coil surface i

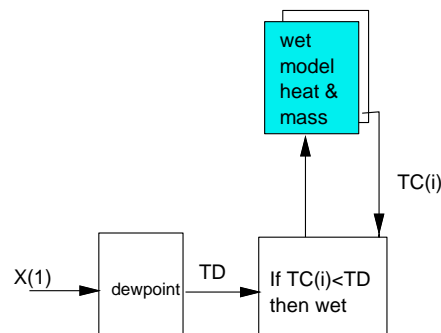


**Figure 3.7.** Detection of dry or wet conditions on the coil surfaces

correlating the input and outputs of one coil. The simulation can be appropriately done by means of Excel or Simulink, as indicated in figure 3.6.

For each row, it should be detected whether the fin and coil surface temperature is above or below the dew point of the passing air. If it is lower, condensation occurs and all the coefficients that are connected with condensation will be considered equal to zero. This selection criterion is schematically shown in figure 3.7.

### 3.1.1. Heat transfer coefficients

#### 3.1.1.1. Water side, glycol Effect

Considering the glycol in cold water, the coefficients were calculated. 50% glycol was used in the experiments. Following formula is used:

$$\rho_F = 1000 + \frac{FGL\%}{50} 65 \quad (3.30)$$

$$\lambda_F = (0.6 - \frac{FGL\%}{50} 0.18) \cdot 10^{-3} \quad (3.31)$$

$$C_F = 4.22 - \frac{FGL\%}{50} 0.96 \quad (3.32)$$

$$\mu_F = (1 + \frac{FGL\%}{50} 4.45) \cdot 10^{-3} \quad (3.33)$$

$$\nu_F = \mu_F / \rho_F \quad (3.34)$$

$$H_F = \frac{\lambda_F}{D_i} Nu \quad (3.35)$$

Considering walk-in effect, it can be written as:

$$Nu = 1.36 (P_e \frac{D_i}{L'})^{0.4} \quad (3.36)$$

$$L' = L - 0.025 \cdot R_e \cdot D_i \text{ for } R_e < 1000$$

$$\text{else } L' = L - 0.025 \cdot 1000 \cdot D_i \quad (3.37)$$

$$P_e = R_e \cdot P_r = \frac{\nu_F D_i \rho_F c_{pF}}{\lambda_F} \quad (3.38)$$

$$R_e = \frac{\nu_F D_i \rho_F}{\mu_F} \quad (3.39)$$

$$P_r = \frac{c_F \mu_F}{\lambda_F} \quad (3.40)$$

In figure 3.8 the effect of the addition of Glycol and the walk-in effect are shown.

#### 3.1.1.2. Air side

The following formula was used to calculate the coefficient in the air side:



$$H_{AA} = \frac{\lambda_A}{D_{eq}} Nu \quad (3.41)$$

$$Nu = 2.7 \left( Pe' \frac{D_{eq}}{D} \right)^{0.4} \text{ for } Nu > 2.2 \quad (3.42)$$

$$Nu = 2.26 \left( Pe' \frac{D_{eq}}{D} \right)^{0.4} \text{ for } Nu < 2.2 \quad (3.43)$$

$$D_{eq} = \frac{4 \cdot AA \cdot D}{A_{tot}} \quad (3.44)$$

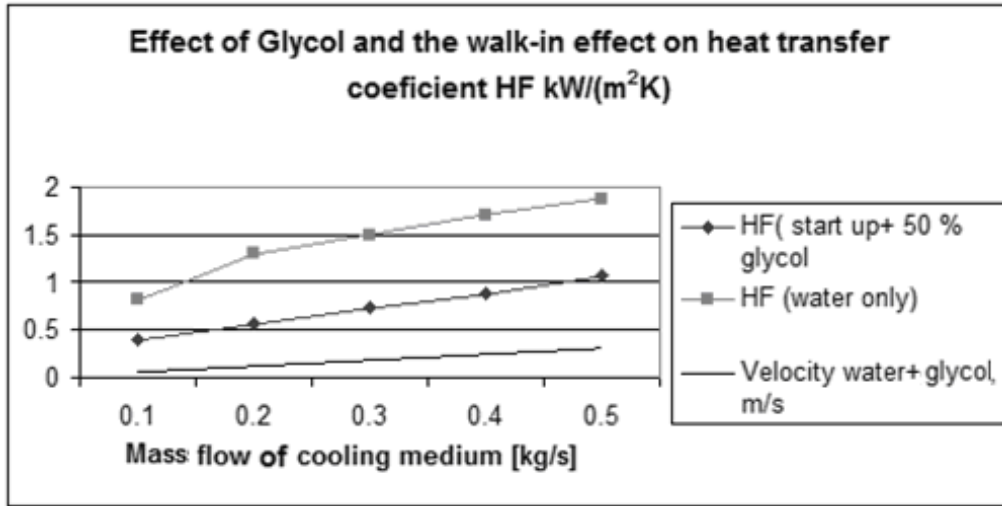


**Figure 3.8.** The effect of Glycol and walk in effect on the heat transfer coefficient  $H_F$ , the walked-in effect is caused by the increased turbulence due to the coil bends (start-up from turbulence to laminar flow)

The tubes are extended by fins which have different temperatures in those parts that are further away from the tubes. The gradient in temperature should be taken into account as well as the gradient in the enthalpy of the saturated air close to the fins. This can be done by the introduction of the fin efficiency. For a wet surface, it is defined as follows:

$$\eta_{f, wet} = \frac{h - \bar{h}_s}{h - h_s} \quad (3.45)$$

$\bar{h}_s$  is the enthalpy of air in the boundary layer of the total surface and  $h_s$  is the enthalpy of air in the location of the tube.

What decreases the heat transfer is a kind of compensation factor. If the fin temperature is equal to that of the tubes:

$$H_A = H_{AA} \left( \frac{A_{tube}}{A_{tot}} + \frac{A_{fin}}{A_{tot}} \cdot \eta_{f, wet} \right) \quad (3.46)$$

Also for a dry fin, the temperature gradient of the fin as demonstrated in figure 3.10 should be taken into account. According to Mac Adams and Hufschmidt <sup>[8]</sup> the fin efficiency can be written as:

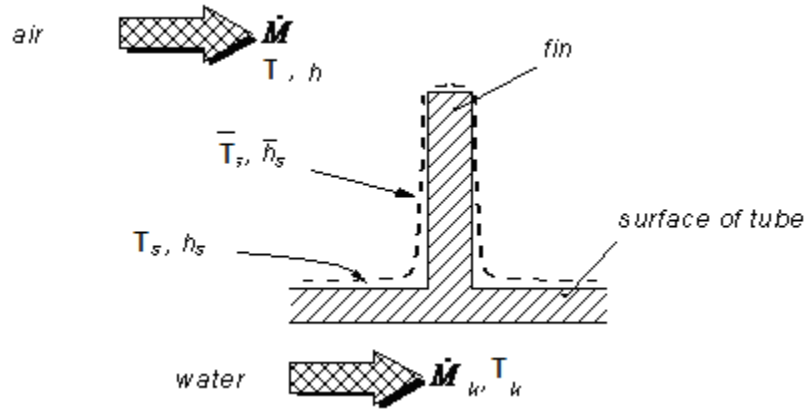


**Figure 3.9.** The temperature gradient and also the enthalpy gradient of the saturated air close to the fins

$$\eta_{dry} = \frac{T - \bar{T}_{fin}}{T - T_b} = \frac{Tgh(f.l)}{f.l} \quad (3.47)$$

In which:

$$f = \sqrt{\frac{2\bar{H}_{AA}}{\lambda_{fin} \cdot \delta}} \quad (3.48)$$

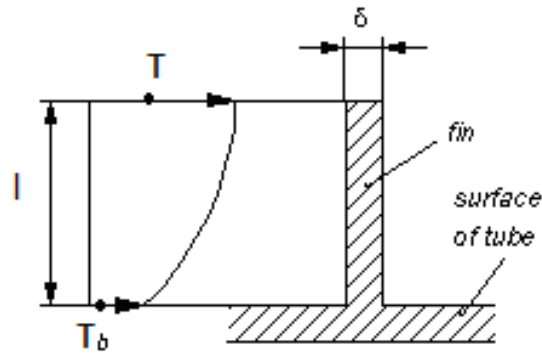


**Figure 3.10.** The temperature gradient of the fin

In the condensation state, the heat transfer is dependent on the parameter "f":

$$f = (R_{fi} - R_o) \sqrt{\frac{\bar{H}_{AA}}{(1 - R.B)\lambda_{fin} \cdot y_b}} \quad (3.49)$$

The declination line between air temperature of 20 and 15°C is written as follows:

$$B = \frac{dX}{dh} = \frac{(14.7 - 10.7) \times 10^{-3}}{57.2 - 41.9} = 0.261 \times 10^{-3} \quad (3.50)$$

The relation between " $f$ " and the fin efficiency is given in figure3.11.

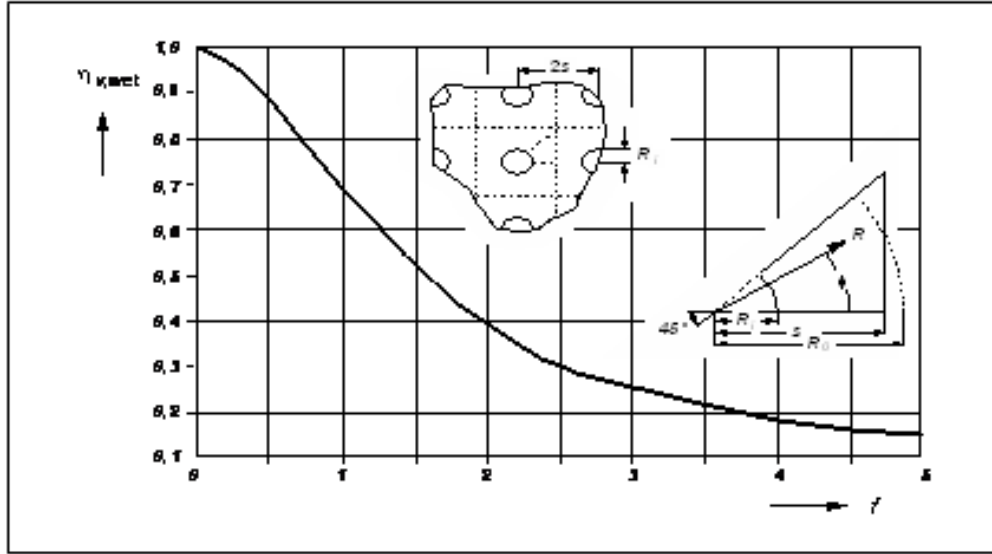


**Figure 3.11.** Fin efficiency at different geometries ( $\eta_{f, wet} = 0.075f^2 + 0.505f + 1.055$ ; if  $0.75 < f < 3$ )

### 3.2. Experimental study

In order to validate the model, a set of experiments was done in the laboratory with an air cooler of 8 rows. <sup>[11]</sup> The cooler dimensions were as follows: depth 0.3 m, height 0.4 m, and width 0.4 m. The cooler had been built by means of 12 levels of coils mounted as serpentine on top of each other. The serpentine swings consisted of 8 rows. Each of the rows was provided by 190 fins, with a mutual distance of 1.75 mm.

The coils in the 12 levels had mutual supply and discharge. The air flowed in the direction of the serpentine swing (parallel-flow) or in the opposite direction (counter-flow). Because of the small temperature difference between the air and the cooling water, preference is given to counter flow.

The cooling fluid consisted of 50% glycol and 50% water. For the fluids in the coils, reliable heat transfer coefficients were available and were the same as the ones used in the model.

For the heat transfer coefficient in the air side it was more difficult to find the relevant values, because the fin configuration of passages of the air were less well defined and

therefore more difficult to standardize in dimensionless equations. The following procedure was applied to find the proper values of heat transfer coefficients.

First, the entire overall heat transfer coefficient  $U$  was derived from the experiments. It can be written in a function of the heat transfer coefficients on the water and air side ( $H_F$ ,  $H_A$ ).

We were then able to calculate  $H_A$  from the known values of  $U$  and  $H_F$ , resulting in the following equation:

$$Nu = 2.7 \left( Pe' \frac{D_{eq}}{D} \right)^{0.4} \text{ for } Nu > 2.2 \quad (3.51)$$

$$Nu = 2.26 \left( Pe' \frac{D_{eq}}{D} \right)^{0.4} \text{ for } Nu < 2.2 \quad (3.52)$$



For a wet cooler, it was shown that it is necessary to reduce the heat transfer coefficients substantially to get a good agreement with the measurements.

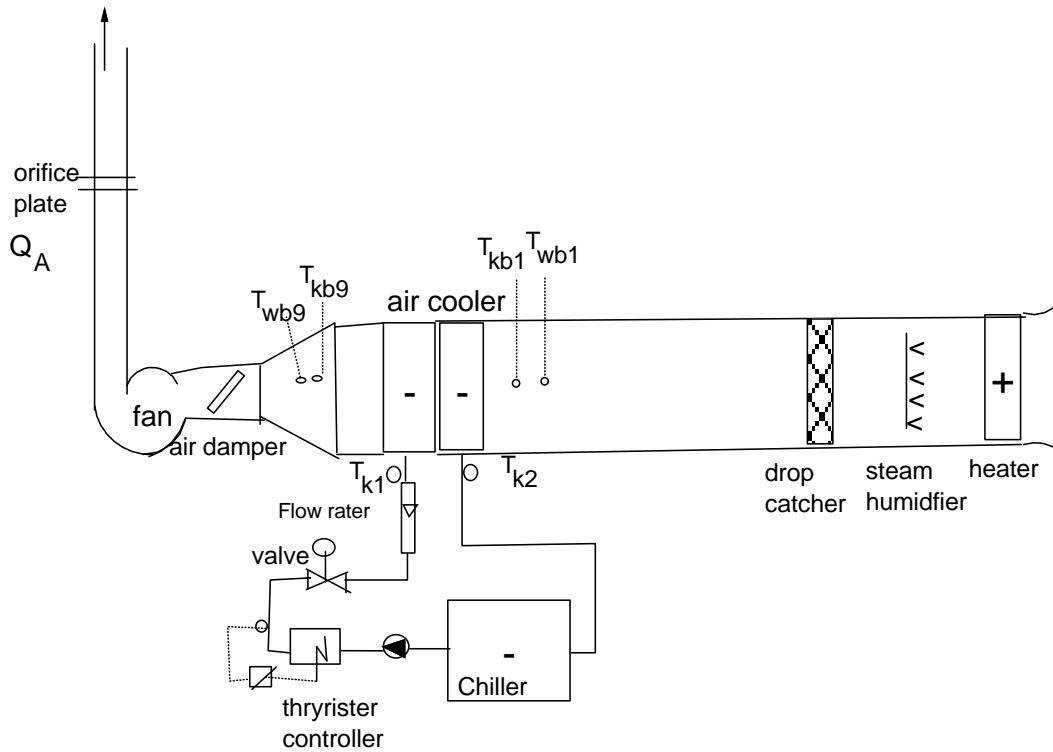


**Figure 3.13.** The schematic of the experimental setup

**Table 3.1.** Input and output values of air and water conditions, measured and calculated by the physical model. No adaptation on the heat transfer coefficients

no	TAE	XE*1000	QA	input		output measured			output calculated (model)		
				TFE	QFE	TAL	XAL/1000	TFL	TAL	XAL/1000	TFL
1	31,4	14,8	0,48	8,1	0,49	18,6	13,4	13,4	18,24446	11,9063	14,67736
2	30,3	18,4	0,46	8,2	0,52	20,8	15,4	13,9	19,21854	12,87466	15,47047
3	26,1	10,9	0,48	4,9	0,49	14,3	10	9,3	13,53258	9,069992	10,2944
4	25,8	19,9	0,48	5,7	0,49	19,4	14,3	12,1	18,1035	12,52114	14,12226
5	21,7	10,2	0,48	4,9	0,49	12,8	9,2	8,7	11,95097	8,430059	9,306475
6	21,8	15,6	0,47	4,7	0,49	15,8	11,4	9,8	14,3542	10,27259	11,15229
7	30,9	14,4	0,47	8,2	0,33	19,9	13,9	15	19,3153	12,46683	16,04906
8	30,3	18,9	0,46	7,9	0,33	21,8	16,5	15,8	21,59124	14,40194	17,27563
9	26,4	10,9	0,48	5,7	0,33	15,3	10,6	11,5	15,21329	9,885684	12,29562
10	26,1	20,6	0,46	5,8	0,33	20,7	15,5	14,4	20,49201	14,08377	16,04483
11	21,6	10,1	0,48	4,8	0,33	13,6	9,7	9,8	12,88099	8,907337	10,35043
12	22	16	0,47	5,1	0,33	17	12,3	12	16,47822	11,43136	13,12878
13	30,9	13	0,48	8,4	0,16	20,4	13,1	19	20,65525	12,76412	19,84273
14	29,9	19,3	0,46	7,8	0,16	23,3	18	20,1	23,70277	16,83359	20,36316
15	26	20,1	0,46	5,3	0,16	21,7	16,6	18,4	22,96784	15,96737	18,85904
16	21,9	10,6	0,48	5,2	0,16	15,4	10,4	13,5	15,0315	10,06176	13,75433
17	22,4	16,3	0,47	4,9	0,16	18,6	13,5	15,6	19,27988	13,05072	16,5344
18	30,2	9,3	0,48	7,5	0,66	14,8	9,3	10,8	13,21922	8,610904	11,8476
19	31,3	14,7	0,48	8	0,65	17,6	12,7	12,3	16,70437	10,98192	13,75746
20	29,8	18,2	0,46	9,1	0,66	19,9	14,6	13,8	17,98127	12,011	15,36953
21	26,3	10,6	0,48	5,1	0,65	13,9	9,6	8	12,23846	8,377195	9,688568
22	21,6	10,1	0,48	4,9	0,67	12,4	8,9	7,9	10,7956	7,763466	8,625655
23	21,9	16,1	0,47	4,9	0,67	15,4	11	9,3	12,84435	9,522602	10,63432
24	25,9	17,4	0,47	6,1	0,65	17,5	12,4	10,6	15,25393	10,70753	12,52377

The air cooler was tested for 24 different inlet air conditions and air and water flows given in table 3.1. In figure 3.12 the test facility is shown, while Figure 3.13 displays the schematic. The inlet air conditions could be changed over a wide range (for temperature 21 to 31°C and for humidity 9 to 21 g/kg).

A series of data were observed in the measurement of the air flow, water flow, inlet and outlet temperatures and humidity, all of which are given in table 3.1.

Using the measured data as input for the model, the validation could be carried out. The measurements of outlet air and water conditions are given in table 3.1. It shows the model solutions regarding the measured inlet conditions. The differences between the model and the measurements were calculated. The deviations are rather big, with an average value of 1 K and 1 g/kg (see figure 3.14).

### 3.3. Results

The experimental data and the comparison with model solutions showed that the heat transfer coefficient itself and the correlation between heat and mass transfer had to be adapted.

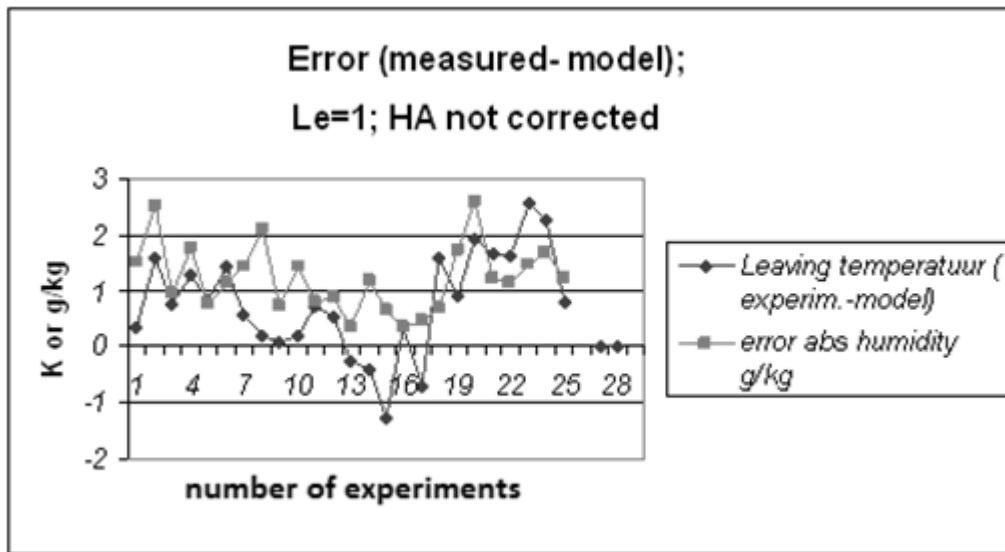


**Figure 3.14.** Deviation between model and humidity of the leaving air flow, heat and mass transfer were used, as mentioned in the text describing the model of the air cooler

Acceptable results were obtained when the heat transfer coefficient of air was divided by a factor  $F_A$  and Lewis number  $Le$ , corrected by multiplying by a factor  $F_D$ .

The heat transfer decreased with an increase in dehumidification and the same was found from the coupling of heat and mass transfer.

In part load the fins were not completely wet. This means that the analogy between sensible and latent heat only partly exists. In the model, this fact was not taken into account. A pipe was assumed to be either wet or dry.

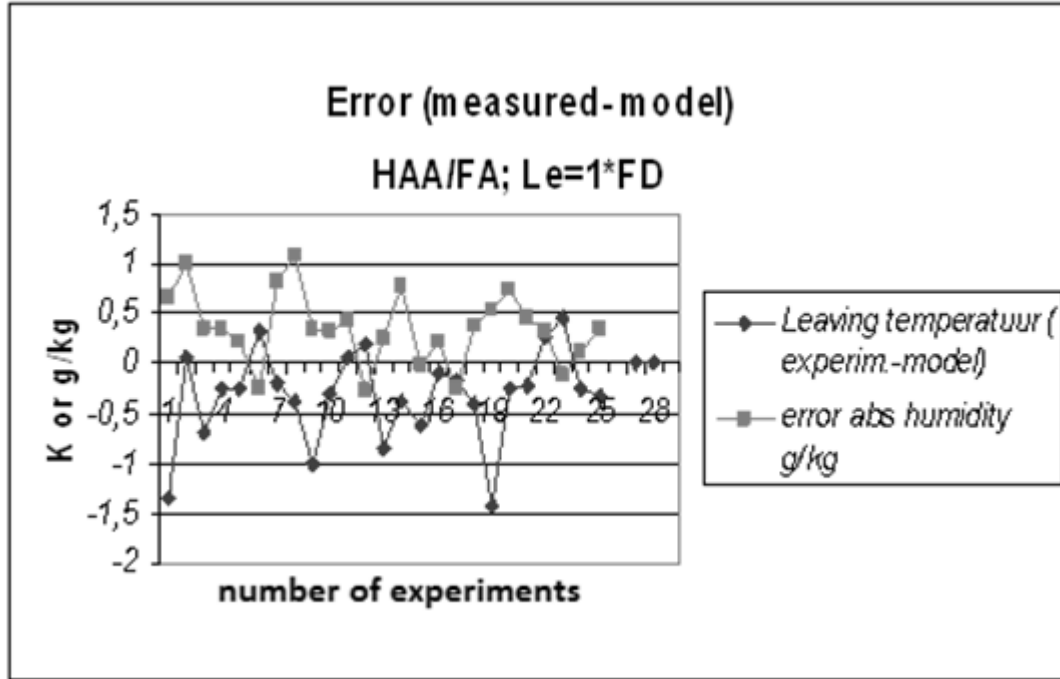


**Figure 3.15.** Deviation between model and humidity of the leaving air flow considering the corrections

To overcome this problem, the  $L_e$  factor was multiplied by a factor that, in turn is dependent on the degree of dehumidification. In that way, the higher the dehumidification was the smaller the mass transfer coefficient  $H_D$  became. This was in agreement with the experiments of Thiel in 1971.<sup>[10]</sup>

The factors were calculated as follows.

Correction Factor  $F_A$  for convective heat transfer:

$$F_A = 0.3 \Delta x + 1.5; \quad \text{Used as: } \frac{H_{AA}}{F_A}. \quad (3.53)$$

That  $\Delta x$  is in gr/kg and the correction factor  $F_D$  for latent heat transfer:

$$F_D = -0.2 \Delta x + 2; \quad \text{Used as: } L_e^* = F_D \cdot L_e. \quad (3.54)$$

Using these corrections the agreement between the model and the measurements is satisfactory (Figure 3.15).

### 3.4. Graphical model using Mollier diagram

A model that gives information of an ideal controlled air cooler has been developed. This means that the desired value of the outlet air temperature delivers the corresponding absolute humidity or enthalpy of the outlet air. Graphically the curve in the Mollier diagram is given that represent the changes of air condition after cooling. The intersection point with the isotherm of the desired temperature gives then the absolute humidity or enthalpy of the outlet air.

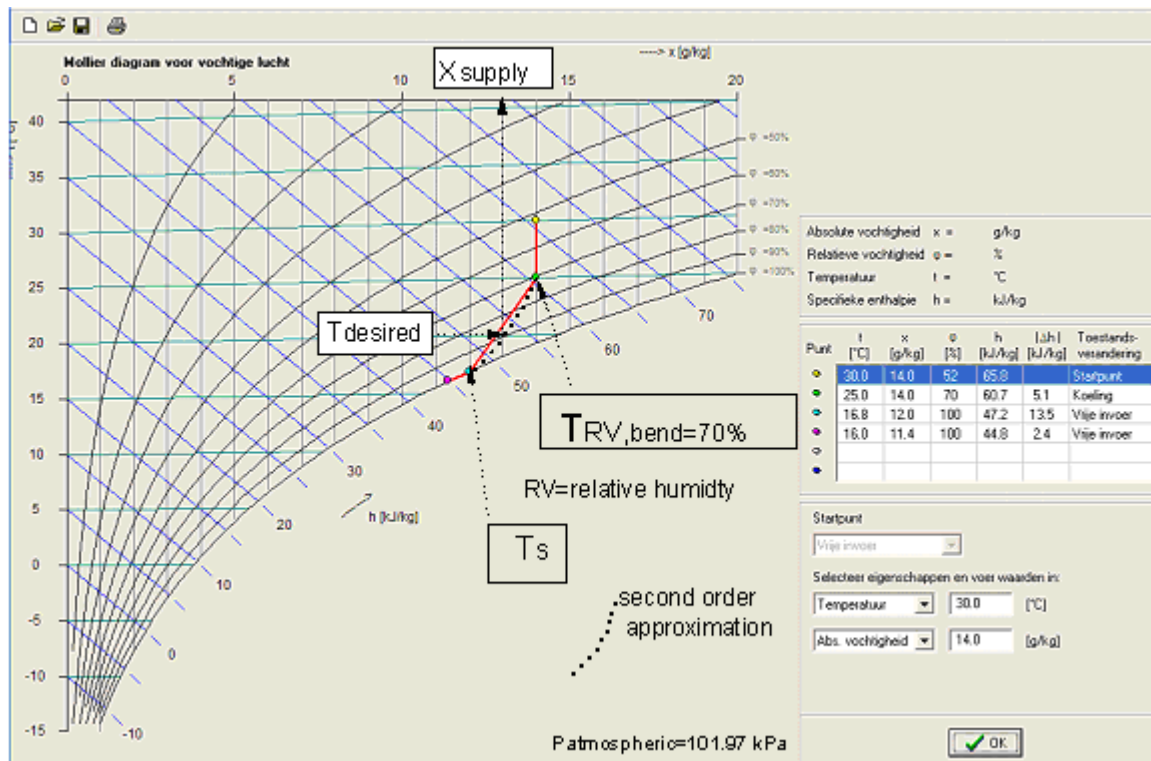


**Figure 3.16.** A master controller dictates a set point for the supply temperature. Then the resulting humidity is found by the intersection of the isotherm of the demand temperature and the cooling curve. For example in figure 3.16 the cooled air is leaving the cooler with the desired temperature  $T_{desired}$  and the resulting absolute humidity  $X_{supply}$

This approach makes modeling quite simple and accurate. This information is needed to define the extra energy for dehumidification. During a part of the year the humid air is dried automatically by condensation when it had to be cool down to deliver supply air with the desired temperature. Consequently, it can only be used for the calculation of year round energy consumption; not for the design of the cooler.

With the detailed physical model it can be demonstrated that the change of air conditions during the cooling process pursue definite courses similar with those drawn in the diagram of figure 3.16. This course can be characterized with the following set of rules:



- Air is cooled down without condensation until the relative humidity is 70% (in the figure indicated by  $T_{RV}=70\%$ )
- From that point condensation occurs and the change of air condition follows a nonlinear curve until the absolute humidity is reduced by 2 g/kg. From that point, indicated by  $T_s$ , the air is saturated and follows the saturation line.
- Applying these rules, equations can be derived that describe the cooling process in the Mollier diagram. With these data the energy required for cooling and dehumidification can be calculated.

As demonstrated in figure 3.16 it works as follows: A master controller dictates a set point for the supply temperature. Then the resulting humidity is found by the intersection of the isotherm of the demand temperature and the cooling curve.

### 3.4.1. Linear curve approximation

The point at which the cooler becomes wet is given by:

$$T_{\phi bend} = 17.6 \cdot \ln\left(\frac{0.2}{0.813} + \frac{P_d}{0.813 \cdot \phi_{bend}}\right) \quad (3.55)$$

With  $P_d = \frac{101.33 X_E}{0.622 + X_E}$

This point is called “bend”, indicating the condition at which condensation starts. A good approximation of that point is the intersection between the lines of constant humidity  $X_E$  (equal to that of the inlet air) and  $\phi_{bend} = 0.7$ .

The curve between bend and saturation conditions is approximated by a linear line:

$$\begin{aligned} T &= aX + b \\ a &= \frac{T_s - T_{\phi bend}}{X_s - X_E} \\ b &= T_s - aX_s \end{aligned} \quad (3.56)$$

The saturated end condition of the air can be calculated as:

$$T_s = 17.6 \cdot \ln\left(\frac{0.2}{0.813} + \frac{P_d^*}{0.813 \cdot \phi_{bend}}\right) \quad (3.57)$$

With  $\phi_{bend} = 1$

And  $P_d^* = \frac{101.33 X_s}{0.622 + X_s}$  with  $X_s = X_E - \Delta X$  and  $\Delta X = 0.002$

The procedure is as follows:

If  $T_{desired} > T_{pbend}$  then

$$X_L = X_E \text{ and } T_L = T_{desired}$$

If  $T_{desired} < T_s$  then

$$T_L = T_{desired} \text{ (desired temperature of air after leaving the air cooler)}$$

$$X_L = \frac{0.622 P_{ds}}{101.33 - P_{ds}} \text{ with } P_{ds} = 0.813 e^{(T_{desired}/17.6)} - 0.2$$

Else

$$T_L = T_{desired}$$

$$X_L = \frac{1}{a}(T_{desired} - b)$$

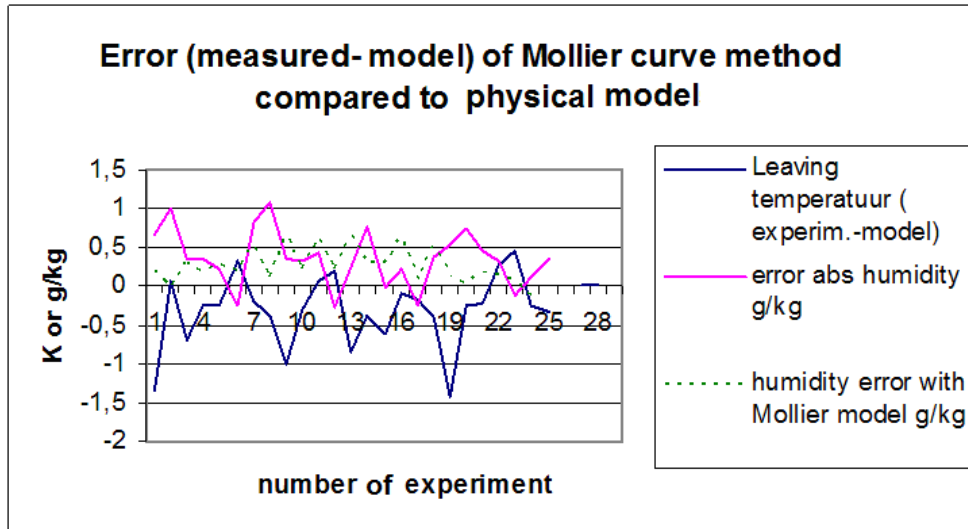


**Figure 3.17.** The errors of graphical model are compared with that of the physical model

## Second order curve approximation

$$T = aX^2 + bX + C$$

The 3rd point to calculate the coefficients of a,b and c is chosen as:

$$T_{s,80} = \frac{1}{3}T_{80} + \frac{2}{3}T_s$$

$$X_{s,80} = X_E - 0.5\Delta X$$

$$a = \frac{T_{80} - T_s - 2T_{80} + 2T_{s,80}}{X_E^2 - (X_E - \Delta X)^2 + 2(X_E - 0.5\Delta X)^2 - 2X_E^2} \quad b = \frac{2}{\Delta X}[T_{80} - T_{s,80} - a\{X_E^2 - (X_E - 0.5\Delta X)^2\}]$$

$$c = T_s - a(X_E - \Delta X)^2 - b(X_E - \Delta X)$$

$$X_L = \frac{-b + \sqrt{b^2 - 4a(c - T_{desired})}}{2a}$$

In figure 3.17 the errors of this model are compared with that of the physical model. The result given in figure above shows that Mollier curve method is even better.

### 3.5. Summary and conclusions

An air cooler, as a finned-tube heat exchanger, was modeled and simulated. In addition, the air cooler was studied experimentally. The experimental set up was made and the measurements were carried out for 24 different input conditions of air and cold water. The results show that corrections for the overall heat transfer coefficient and also for the Lewis number are necessary because of condensation.

The correction factors compensate for the simplified assumptions regarding the wet surface of fins and the analogy between heat and mass transfer. Furthermore, the correction factors depend on the dehumidification quantity.

The corrected model was implemented in the studies of advanced evaporative air conditioning systems, where it was used to construct a graphical model based on rules for transients in the Mollier diagram. Preliminary calculations show that it is very accurate and useful for the simulation of controlled air handling systems and a detailed model was presented in this chapter.

### NOMENCLATURE

A	Surface area ( $m^2$ )
AA	Total front surface of the fins and pipes ( $m^2$ )
$A_f$	Single sided surface of one fin plate ( $m^2$ )
B	Declination of saturation line given by Eq.3.50 ( $kg\ kJ^{-1}$ )
C	Specific heat ( $J\ kg^{-1}\ K^{-1}$ )
dl	Thickness slice of control element, also indicated by dx ( $m$ )
D	Diameter coil ( $m$ )
f	Parameter regarding condensation in Eq.3.47
F	Correction factor given by Eqs.3.49, 3.50
h	Enthalpy ( $kJ\ kg^{-1}$ )
H	Heat transfer coefficient ( $W\ m^{-2}\ K^{-1}$ )
$H_m$	Mass transfer coefficient ( $kg\ m^{-2}\ s^{-1}$ )
$K_{opp}$	Correction factor presenting the increase in the constant surface by fins
l	Length of fin ( $m$ )
L	Length of a tube ( $m$ )
Le	Lewis number
M	Mass ( $kg$ )
$\dot{M}$	Mass flow rate ( $kg\ s^{-1}$ )
n	Number of pipes through one plate
Nu	Nusselt Number

$P_d$	Partial pressure of water vapor ( Pa )
$Pe$	Peclet Number
$Pe^*$	Pe with “walk in effect” involved
$Pr$	Prandtl number
$Q_A$	Air mass flow rate ( $kg\ s^{-1}$ )
$\dot{Q}$	Heat flow ( $J\ s^{-1}$ )
$R$	Evaporation heat ( $J\ kg^{-1}\ m^{-2}$ )
$Re$	Reynolds number
$R_{fi}$	The fictitious fin diameter ( $m$ )[10]
$R_o$	Outside diameter of the tubes ( $m$ )
$T$	Temperature ( $^{\circ}C$ )
$\bar{T}$	Average Temperature( $^{\circ}C$ )
$T_b$	Base temperature( $^{\circ}C$ )
$T_D$	Dew point temperature ( $^{\circ}C$ )
$T_{GR}$	Linearization factor for saturation curve given by Eq.3.21
$T_R$	Reference working point temperature ( $^{\circ}C$ )
$V$	Velocity ( $m\ s^{-1}$ )
$x$	Distance between rows as shown in the figures 3.1( $m$ )
$X$	Humidity ratio ( $kg\ kg^{-1}$ )
$\bar{X}$	Average Humidity ratio ( $kg\ kg^{-1}$ )
$X_R$	Reference working point humidity ( $kg\ kg^{-1}$ )
$y_b$	Half of the fin thickness ( $m$ )
$Y$	Distance between coils ( $m$ )
$Z_A$	Distance between fins ( $m$ )

### **Greek letters**

$\delta$	Fin thickness ( $m$ )
$\xi$	Normalization factor
$\eta$	Fin efficiency
$\lambda$	Thermal conductivity ( $W\ m^{-1}\ K^{-1}$ )
$\mu$	Dynamic viscosity ( $kg\ s^{-1}\ m^{-1}$ )
$\nu$	Kinematic viscosity ( $m^2\ s^{-1}$ )
$\rho$	Density ( $kg\ m^{-3}$ )
$\sigma$	Constant equal to 1 if there is condensation otherwise it is equal to zero

### **Subscripts**

A	air
C	coil and fin surface
eq	equivalent
E	inlet
F	cooling water (Fluid)

i	inside
k	water ( in figures 3.9 and 3.13 )
k <sub>b</sub>	air ( in figure 3.13 )
L	leaving
o	outside
s	saturation
tot	total
wb	wet bulb

### **Acronyms**

FGI%    fraction of Glycol

### **References**

1. W.M. Kays, A.L. London, Compact Heat Exchangers, third ed., McGraw-Hill, New York, 1984.
2. H. Li, V. Kottke, Visualization and determination of local heat transfer coefficients in shell-and-tube heat exchangers for staggered tube arrangement by mass transfer measurements, Exp. Ther. , Fluid Sci., 17 (3) 210–216, 1998.
3. D.B. Murray, B. McMahon, D. Hanley, Local heat transfer coefficients in a finned tubular heat exchanger using liquid crystal thermography, Int. J. Heat Exchangers (1), 31–48, 2000.
4. H. Ay, J.Y. Jang, J. Yeh, Local heat transfer measurements of plate finned-tube heat exchangers by infrared thermography, Int. J. Heat Mass Transfer 45 (20) 4069–4078, 2002.
5. I. Carvajal-Mariscal, F. Sanchez-Silva, M. Toledo-Velazquez, V.A. Pronin, Experimental study on the local convective coefficient distribution on a pipe surface with inclined fins, Exp. Ther. , Fluid Sci. 25 (5), 293–299, 2001.
6. C. Bougriou, R.Bessaih, Determination of apparent heat transfer coefficient by condensation in an industrial finned-tube heat exchanger: prediction, Applied Thermal Engineering, 25, 1863-1870, 2005.
7. Green, Chandra, Shebar S., Water cooling and dehumidifying coil, ASHRAE, N. 2141, 1970.
8. Mc Adams W.H., 1954, Heat transmission, Mc Graw-Hill Publishing Company LTD., New York, London, Toronto page 271, 1954.

9. Lammers J.M. , Analyse van een luchtkoeler in deellast, Internal report Werktuigbouw ST 127, TU Delft, 1975.
10. Thiel G., Die Auslegung von Gas Dampf-Gemisch-Kühlern bei Niedrigen Dampf Partialdrücken am Beispiel des Teuchtluftkühlers, Dissertation, Technische Hochschule, Aachen, 1971.
11. F.Esfandiari Nia, Dolf van Paassen, Determination of heat and mass transfer coefficients by condensation in an air cooler, Proceedings of FEDSM2007,5th Joint ASME/JSME Fluids Engineering Conference, July 30-August 2, San Diego, California, USA, 2007.

# 4. DESICCANT WHEELS

“Reprinted with permission from the journal of Energy & Buildings and the American Society of Mechanical Engineers, ASME”

## Introduction

Conventional cooling systems have two disadvantages. One is high energy costs and the other is environmental impacts. Therefore, some researchers have looked back to the techniques of evaporative cooling that was mostly replaced by conventional chillers. However, this system has its own problems. The main disadvantage is its inefficiency in very humid climates. One solution is to dehumidify the incoming air by forcing it through a desiccant so that the evaporative cooler can operate efficiently on a dry air stream.

Commercially available desiccants include silica gel, activated alumina, natural and synthetic zeolites, titanium silicate, lithium chloride, and synthetic polymers. They adsorb water vapor due the difference of water vapor pressure between the surrounding air and the desiccant surface. In order for the system to operate continuously, adsorbed water vapor must be driven out of the desiccant material (regeneration) so that it can be dried enough to adsorb water vapor in the next cycle.

The rotary dehumidifier/regenerator wheel appears to be the front runner in the current desiccant system development effort.<sup>[1]</sup> The Desiccant wheel, coupled with the traditional air conditioning system, eliminates the need for overcooling and reheating. These desiccant cooling systems are energy efficient, cost effective (provided that solar heat or waste heat from cogeneration installations are available) and environmentally safe. They are used either individually or as an auxiliary system with conventional air conditioning. In these systems, a desiccant removes moisture from the air, which releases adsorption heat and increases the air temperature. The dry air is cooled using either evaporative cooling or a sensible heat recovery system (used to recover heat from the exhaust air). The adsorbed moisture in the desiccant is then removed using thermal energy supplied by natural gas, electricity, waste heat, or solar energy.

Another important application of desiccant wheels that makes them more attractive for industries and researchers is their application as an energy or enthalpy wheel. A significant fraction of today's energy consumption is due to air-conditioning of buildings, which involves both heating and cooling. For example, more than one fifth of the total energy needs in the United States is used for this purpose according to Corradini and Mitchell.<sup>[2]</sup> Recent requirements for clean air in offices, hospitals, restaurants and other public buildings have resulted in a recommendation by the American Society of Heating, Refrigerating and Air-Conditioning Engineers (ASHRAE)<sup>[3]</sup> to increase outdoor

air ventilation. Since energy costs and environmental concerns are also increasing, the task of designing efficient air-conditioning systems is of growing importance. Thermal comfort is determined by both the temperature and the humidity of the air (ASHRAE).<sup>[4]</sup> For this reason, air-conditioning operations involve both heat and mass transfer mechanisms. These operations are either cooling and dehumidifying or heating and humidifying.

It is possible to decrease the amount of energy required to condition an air stream that is ventilated into a building by using rotary regenerators. They allow recovery of energy from the exhaust air stream which is then disposed into the environment.<sup>[2,5]</sup> Typically, rotary regenerators are used in commercial buildings, where high ventilation rates are required, rather than in residential buildings, because the relatively high initial cost of this equipment has to be recaptured by significant energy savings.

Heat exchangers, when combined with mass transfer, have somehow more complex characteristics than devices that transfer only sensible energy. As a result, there is no simple design methodology available for regenerative rotary energy wheels which transfer both sensible heat and water vapor. Despite the lack of accepted design methods or effectiveness correlations, energy wheels are rapidly being introduced into HVAC designs because they can reduce cooling and heating loads in buildings. Energy wheels can also decrease HVAC systems operating and capital costs.

Rotary heat exchangers can transfer moisture as well as heat. Three different designs are usual in the market: <sup>[6]</sup>

- Condensation wheel

The storage mass consists of smooth, untreated metal (mostly aluminum), transferring moisture only when condensation occurs on the warm air side and part of this is taken up by the cold air. The occurrence of condensation causes an increase in pressure drop. Condensation may be carried along with the air flow.

- Hygroscopic wheel (manufacturers call it enthalpy wheel)

The metallic storage mass has a capillary surface structure due to chemical treatment (pickling). Therefore (to a certain degree) moisture is transferred by sorption, i.e. without condensation. Depending on the air conditions, condensation may also occur.

- Sorption wheel (in scientific nomenclature it is also called enthalpy wheel. although it is not the same type of wheel as Hygroscopic wheel). Here the storage mass has a surface that transmits moisture by pure sorption, i.e. without condensation.

In conclusion, energy costs, and other concerns such as the green house affect due to CO<sub>2</sub> emissions emphasize the necessity of application evaporative air conditioning system



such as desiccant technology. In addition, the reduction of peak load of the power stations and the environmental impact such as the destruction ozone layer due to emission of CFC increase attraction to introduce the alternatives such as desiccant cooling technology based on evaporative cooling systems to conventional chillers.

Kang and Maclain-Cross showed that the dehumidifier is the key component of a desiccant cooling system and the cooling coefficient of performance (COP) can be significantly improved by improving the performance of this component. [7]

The main purpose of this chapter is to investigate heat and mass transfer phenomena in desiccant wheels as the most important component of an evaporative air conditioning system. This model needs to be connected to the other building models to simulate and study the performance of different air conditioning systems.

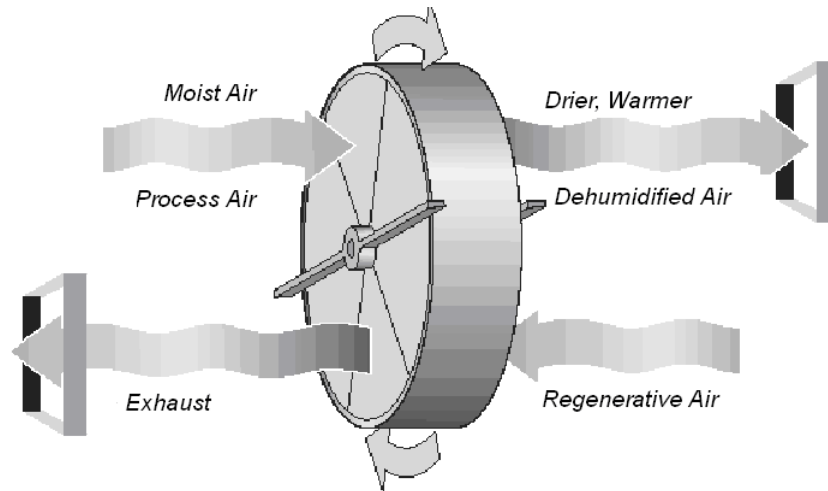


**Figure 4.1.** Air Dehumidifier Wheel <sup>[22]</sup>

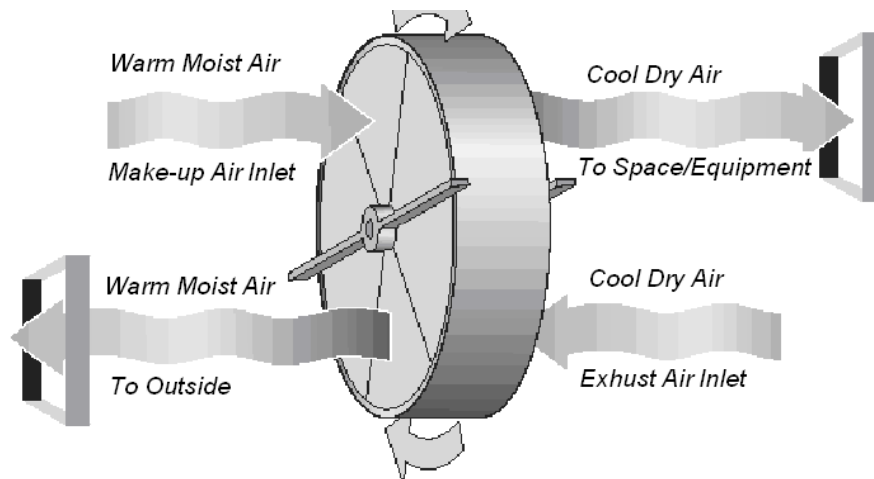


**Figure 4.2.** Enthalpy Recovery Wheel <sup>[22]</sup>

## 4.1. Basic concepts

### 4.1.1. Desiccant Wheels

Desiccant wheels have been widely used for air humidity treatment: dehumidification<sup>[7-12]</sup> and enthalpy recovery.<sup>[12-19]</sup>

In the first case (Figure 4.1), process air is dried after it flows through the wheel, which rotates continuously between the process air and a hot regenerative air stream. The dried air can either be used directly or be employed to make cooling following further psychometric processes known as desiccant cooling.

In the latter case (Figure 4.2), the desiccant wheel rotates between the outside fresh air (supply air) and the exhaust air from room.

Heat and humidity would be recovered from the exhaust in winter (Figure 4.3) and excess heat and moisture would be transferred to the exhaust to cool and dehumidify the process air in the summer (Figure 4.4). However, due to different operating conditions, heat and moisture transfer behaves quite differently in the wheels. The wheel speed is in a range of 10-20 revolution per minute for this type of wheels.

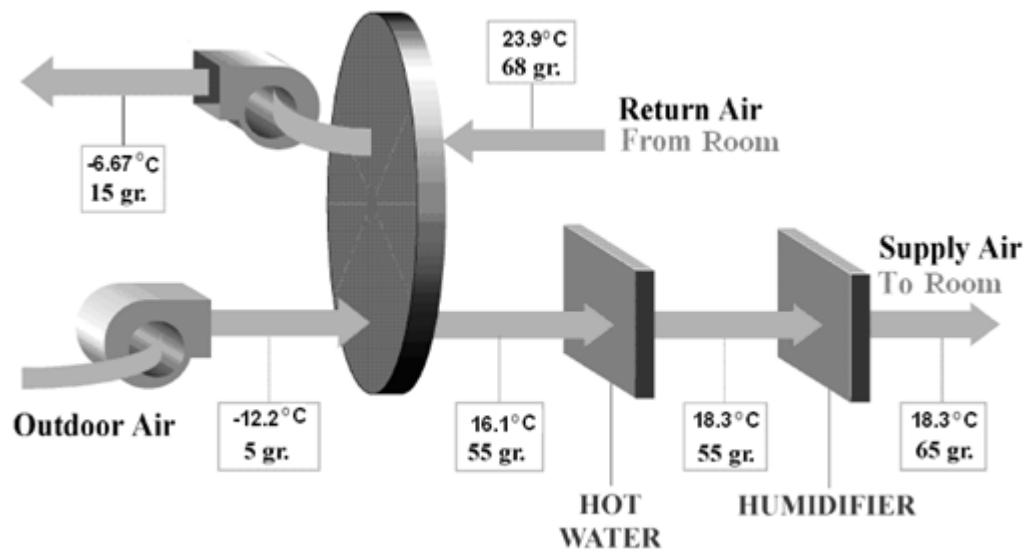


**Figure 4.3.** An Example of Heating Mode Application of Enthalpy Wheel<sup>[21]</sup>

Dry air can be produced in two ways. Air can be cooled to force some of its moisture to condense, or water vapor can be attracted out of the air stream by a desiccant. Both processes are shown in figure 4.5.

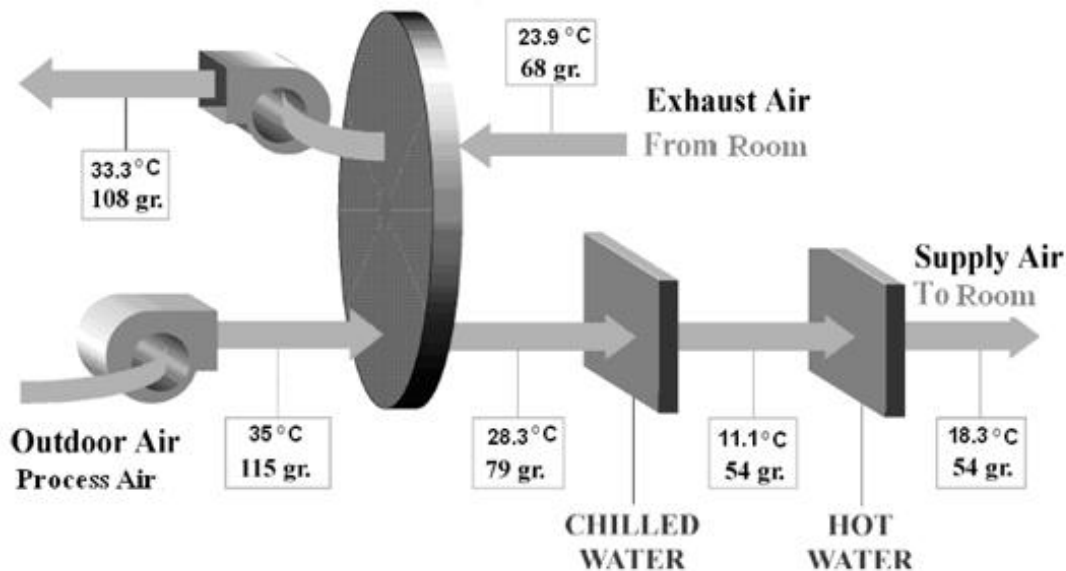


*Figure 4.4. Cooling Mode <sup>[21]</sup>*

#### 4.1.2. Mechanical vs. Desiccant Dehumidifiers

Mechanical dehumidifiers use the cooling principle. They chill air below its dew point, and then reheat that air with excess heat recovered from the initial cooling process. The equipment uses electrical power. Desiccant dehumidifiers attract moisture from the air through a difference in vapor pressures. As air is dehumidified in a desiccant unit, its latent heat (moisture) is converted to sensible heat (temperature). Air leaving a desiccant unit is hot, and must be cooled through a heat exchanger.

The process is powered largely by heat. Mechanical dehumidifiers are the more widely-used technology, especially in residential buildings. Units for commercial buildings have much higher capacity than units used in residences. Mechanical dehumidifiers are very energy-efficient compared to other methods of removing moisture from air. They have strong advantages at higher humidity control levels or where cooling is needed in addition to dehumidification. Also, the technology is nearly identical to cooling equipment and is therefore familiar to most field service technicians.

Desiccant dehumidifiers have been used more widely in industrial applications than in commercial buildings. However, their use has expanded into commercial buildings where there is a benefit to lower-than-usual humidity, such as supermarkets, and ice rinks. They have also been used in ventilation of large buildings like schools, theaters and restaurants. <sup>[17]</sup> Desiccants use much more energy than mechanical dehumidifiers. On the other hand, most of the energy requirement is for regeneration heat. They can use waste heat, from distributed power generation and from natural gas, all of which are very inexpensive during summer seasons. They gain advantages as the

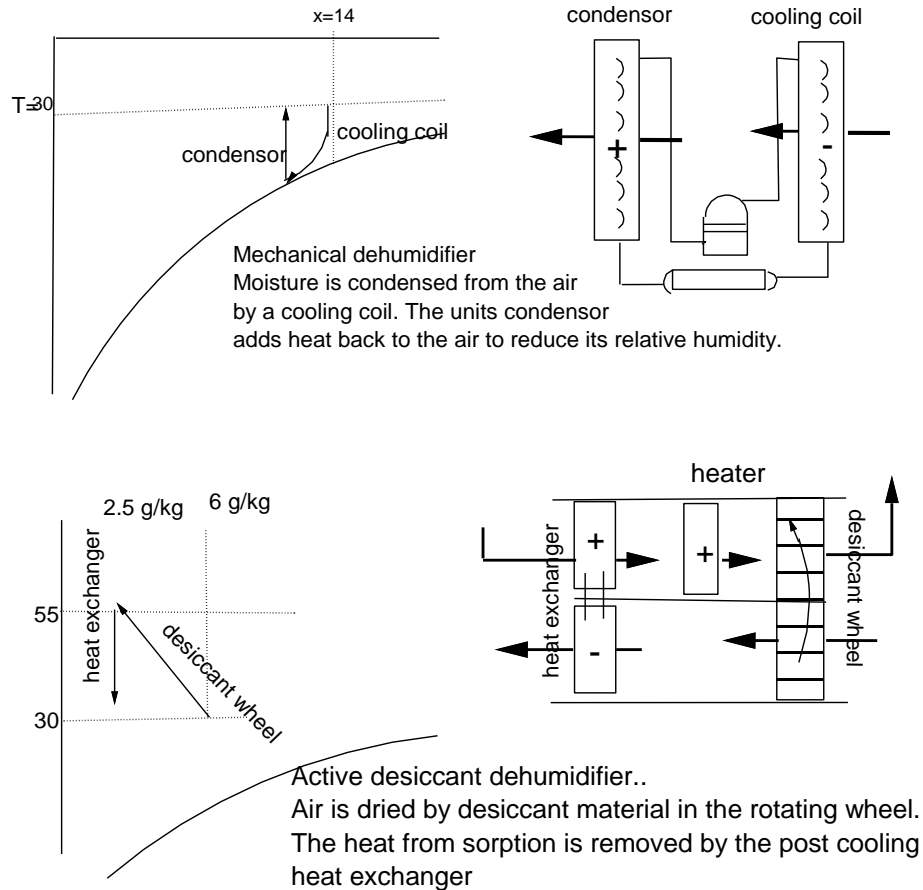


**Figure 4.5.** Dry air can be produced in two ways. Air can be cooled to force some of its moisture to condense, or water vapor can be extracted out of the air stream by a desiccant <sup>[22]</sup>

required dew point goes down to levels where mechanical dehumidification begins to freeze its condensed moisture, or at project locations with low-cost heat and high-cost power. In recent years, owners have benefited from vigorous competition between mechanical and desiccant dehumidifiers in commercial buildings. Both technologies have been successfully applied to many buildings.

A benefit that recently comes up is the peak saving of power plants at hot summer period when cooling problems of power plants occur due to higher demands for electricity due to air conditioning. This results in high tariffs of electricity and makes desiccant cooling cycles more attractive.

#### 4.1.3. Performance of Desiccant Dehumidifiers

The amount of moisture removed by a desiccant dehumidifier depends on many factors such as the depth of the wheel, its rotational speed and the specific sorption

characteristics of the desiccant. But in commercial practice, these variables are fixed by the manufacturer to provide the designer with a simpler device. To predict performance, the HVAC designer only needs to define the temperature, humidity ratio and volume of the entering process air, the size of the unit and the temperature of the reactivation air. These variables interact to produce the desired process outlet moisture levels. It can be seen that the moisture content of process air leaving the unit depends on the inlet conditions:<sup>[22]</sup>

- The *drier* the air entering, the drier it will leave the unit.
- The *cooler* the air entering, the drier it will leave.
- The *hotter* the *regeneration or reactivation air*, the drier the process air will become.
- The *slower* the *process air velocity*, the drier the air will become.

#### 4.1.4. Process Air Temperature Rise

Dehumidification produces the reverse effect of evaporation. As moisture is *removed* from the air, it *releases* the heat that was used to evaporate it originally. The amount of heat depends on the amount of water removed from the air. More dehumidification releases more heat.

In addition to dehumidification heat, a bit more heat can be carried into the process air by the desiccant wheel as it rotates out of the hot reactivation sector. That “carryover” heat usually accounts for less than 10% of the total temperature rise. The exact amount depends on the wheels, rotational speed, the mass of the wheel, and the temperature of the reactivation air. In many equipment designs, the carryover heat is eliminated entirely by a purge sector located between the reactivation and process air and back into the reactivation air where it can be reused to dry the desiccant.

Figures 4.5 and 4.6 show one example of typical moisture removal and temperature rise through a desiccant unit. The exact values will be specific to each manufacturer’s hardware. But regardless of the cleverness of the equipment design, the temperature rise must be *at least* as much as the heat released by the dehumidification process. With a Mollier or Psychrometric chart, the designer can quickly estimate the minimum leaving air temperature as long as he knows the inlet temperature and moisture along with the outlet moisture.

#### 4.1.5. Post-Cooling

Desiccant equipment manufacturers use many methods to remove excess heat, including:

- Air-to-air heat exchanger
- Indirect or direct evaporative cooling
- Vapor-compression cooling

These alternatives are listed in increasing order of cost and cooling power. Often, the desiccant equipment includes only a small amount of post-cooling. The HVAC system designer uses cooling capacity located elsewhere in the system to remove any heat remaining from desiccant dehumidification.

This strategy makes use of the fact that moisture loads are at their peak during the early morning and evening, when the sensible heat loads on the building are relatively low. The surplus cooling capacity available at those times removes heat produced by dehumidification, eliminating the need to add more equipment and cost to the desiccant subsystem.

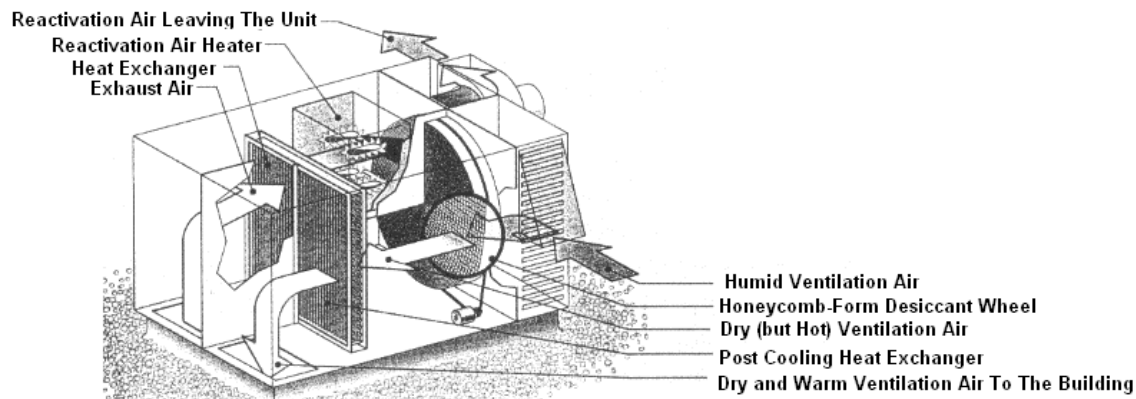


**Figure 4.6.** Desiccant Dehumidifier for Ventilation Air<sup>[22]</sup>

Figure 4.7 shows an example of the simplest form of post cooling. An air-to-air heat exchanger is mounted downstream of the desiccant wheel to cool the hot, dry process air. On the other side of the heat exchanger, relatively cool building exhaust air carries the excess heat out of the building. Often the exhaust air is evaporatively cooled *before* it enters the heat exchanger to provide a greater cooling effect for the process air. Exhaust air provides post cooling at the lowest operating cost. But in many buildings the exhaust outlet cannot be located near the supply air inlet. Then outdoor air is used on the other side of the heat exchanger. In that case, indirect evaporative cooling becomes even more helpful, since the outdoor air is not as cool as exhaust air from the building.

The unit shown in figure 4.7 is typical of desiccant dehumidifiers that dehumidify ventilation air for low-rise commercial buildings where packaged rooftop units are the primary HVAC equipment. When a building has a cooling tower, the desiccant system can use tower water for post cooling, replacing the heat exchanger shown in figure 4.7.

#### 4.1.6. Open-cycle solid desiccant systems

The most studied desiccant cooling cycle is Pennington or ventilation cycle.<sup>[23]</sup> It takes ambient air into a rotating desiccant dehumidifier where moisture is adsorbed. (Figure 4.7)

The temperature increases because of the energy released during the adsorption process. The air then sensibly and evaporatively is cooled and introduced into the conditioned space. The air leaving the room is also first evaporatively cooled, then passed through the sensible heat exchanger where it recovers heat of adsorption from the supply air. Next it is heated with low grade thermal energy and the hot air is used to regenerate the desiccant. COP values of about 0.8-1.0 are commonly predicted for this cycle. This means the cooling is realized with the same amount of low grade heat. An early variation of this cycle was the “recirculation” cycle (Figure 4.8).

The difference is that the air from the conditioned space is recirculated through the dehumidifier and other components. Ambient air is used for regeneration and then exhausted to the atmosphere. COP values of 0.8 and less are commonly predicted for this cycle. The definition of the thermal COP varies and there are two definitions. Some investigators use the space cooling load divided by the thermal energy required to regenerate the desiccant. Others use the heat removed from the process air stream divided by the thermal energy required to regenerate the desiccant.

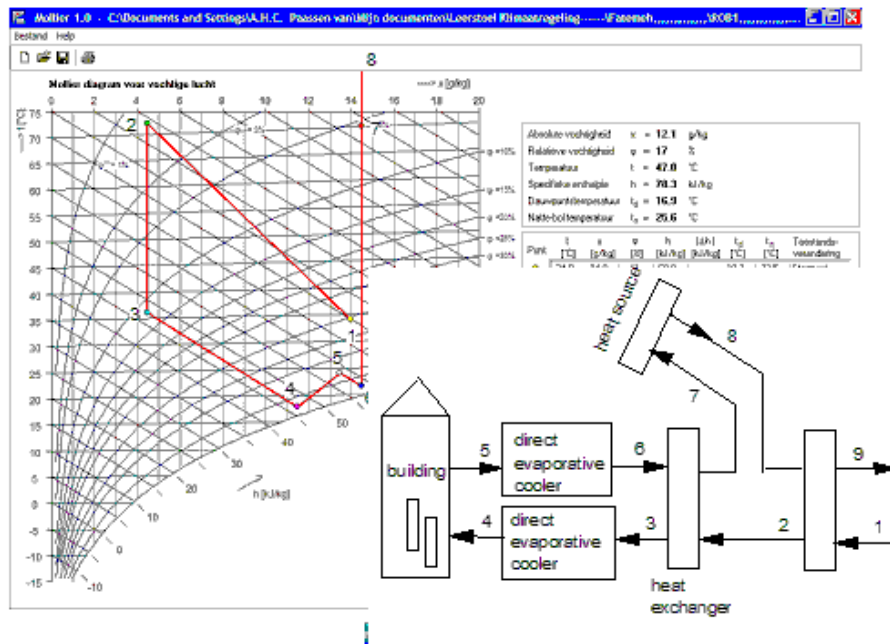
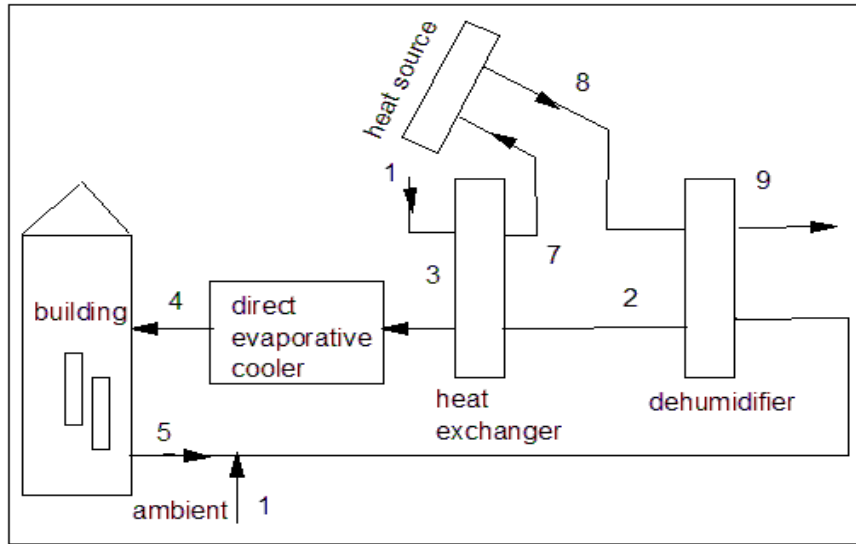


Figure 4.7. Ventilation cycle<sup>[23]</sup>



*Figure 4.8. Recirculation cycle<sup>[23]</sup>*

#### 4.1.7. Adsorption Fundamentals

##### 4.1.7.1. Porous Adsorbents

Physical adsorption is caused mainly by van der Waals force and electrostatic force between adsorbate molecules and the atoms which compose the adsorbent surface. Thus adsorbents are characterized first by properties such as surface area and polarity. Van der Waals force is a weak form of intermolecular attraction between one molecule and a neighboring molecule. All molecules experience intermolecular attractions, although in some cases those attractions are very weak. Even in a gas like hydrogen,  $H_2$ , if the molecules are slowed down by cooling the gas, the attractions are large enough for the molecules to stick together eventually to form a liquid and then a solid.

A large specific area is preferable for providing large adsorption capacity, but the creation of a large internal surface in a limited volume inevitably gives rise to large numbers of small sized pores between adsorption surfaces. The size of micropore determines the accessibility of adsorbate molecules to the adsorption surface so the pore size distribution of micropore is another important property for characterizing adsorptivity of adsorbents.<sup>[2, 23]</sup>

Also some adsorbents have larger pores in addition to micropores which result from granulation of fine powders or fine crystals into pellets or originate in the texture of raw materials. These pores called macropores are several micropores in size. Macropores function as diffusion paths of adsorbate molecules from outside the granule to the micropores in fine powders and crystals. Adsorbents containing macropores and micropores are often said to have “bi-dispersed” pore structures.<sup>[2, 25]</sup>



Surface polarity corresponds to affinity with polar substances such as water. Silica gel and Zeolites are examples of adsorbents of this type. On the other hand nonpolar adsorbents like polymer adsorbents have more affinity with oil than water.<sup>[26]</sup>

#### 4.1.7.2. Adsorption Equilibrium

In practical operations, maximum capacity of adsorbent cannot be fully utilized because of mass transfer effects involved in actual fluid-solid contacting processes. In order to estimate practical or dynamic adsorption capacity, however, it is essential, first of all, to have information on adsorption equilibrium. Then kinetic analyses are conducted based on rate processes depending on types of contacting processes. The most typical of the rate steps in solid adsorbents is the intraparticle diffusion. When adsorbed molecules are mobile on the surface of the adsorbent, diffusion due to migration of the adsorbed molecules is called *surface* or intraparticle diffusion.

Since adsorption equilibrium is the most fundamental property, a number of studies have been conducted to determine the amount of species adsorbed under a given set of conditions (concentration and temperature). There are many empirical and theoretical approaches to find the maximum adsorption capacity of desiccant as a function of the air relative humidity and temperature.<sup>[27-43]</sup>

#### 4.1.7.3. Equilibrium Relations

When an adsorbent is in contact with the surrounding fluid of a certain composition, adsorption takes place and after a sufficiently long time, the adsorbent and the surrounding fluid reach equilibrium. The relation between the amount adsorbed and the concentration in the fluid phase at a constant temperature is called *Adsorption Isothermal* at that temperature.

Adsorption isotherms are described in many mathematical forms, some of which are based on a simplified physical picture of adsorption and desorption, while others are purely empirical and intended to correlate the experimental data in simple equations with two or at most three empirical parameters.

The simplest model of adsorption on a surface is that in which localized adsorption takes place on an energetically uniform surface without any interaction between adsorbed molecules. This model is called *Langmuir Isotherm* and the equation is:<sup>[44]</sup>

$$W = C \frac{P}{1 + CP} \quad (4.1)$$

To understand the mathematical methods for the calculation of adsorption isotherms like Eq. (4.1), a few basic parameters are defined and explained in the following way:

$$W = \frac{\text{Number of surface sites occupied by adsorbate } [Ns]}{\text{Total number of substrate adsorption sites } [N]} \quad (4.2)$$

$N$  is often numerically equivalent to the total number of surface atoms of the substrate. The number of surface sites occupied by adsorbate molecules  $N_s$  at equilibrium at a particular temperature depends on the gas pressure,  $P$ .

The dependence of  $w$  on  $P$  at constant temperature is defined as adsorption isotherm.

Henry law is a linear approximation to derive the adsorption isotherms. The approach is true for only low values of pressure. Therefore it can be written as a linear function in the following way:

$$P = \text{constant} \times W$$

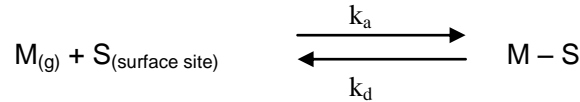
However it is not necessary that the whole isotherm to be linear, it is possible to apply it only to a part of isotherm.

When the isotherms are not linear it is possible to use Langmuir adsorption isotherm or BET method; in this case *Langmuir adsorption isotherm* is needed to be analyzed.

In fact, the Langmuir adsorption isotherm is used to interpret the equilibrium adsorption behavior of a number of systems and in determining the total surface area,  $S_A$ , of solid surfaces. But the Langmuir isotherm needs some simplifications that don't change significantly the result of the situation. The simplifications to bearing in mind are:

1. The surface of the adsorbent is uniform, that is, all the adsorption sites are equal and may be occupied by only one molecule of adsorbate.
2. A dynamic equilibrium exists between the gas (pressure  $P$ ) and the adsorbed layer at constant temperature.
3. Adsorbate molecules from the gas phase are continually colliding with the surface. If the impact is against a vacant adsorption site, a bond between the surface and the molecule is formed. Otherwise, if the impact is against a filled site, the molecule is reflected back into the gas phase.
4. Once adsorbed, the molecules are localized and the enthalpy of adsorption per site remains constant irrespective of coverage.

There is a dynamic equilibrium:



$k_a$  = constant of adsorption

$k_d$  = constant of desorption

So it is possible to write:

$$\text{Rate of adsorption} = k_a P (1-W)$$

$$\text{Rate of desorption} = k_d W$$

$$k_a P (1-W) = k_d W \quad \text{In equilibrium} \quad (4.3)$$

With this equation (4.3) and the equation (4.2)

$$W = \frac{N_s}{N} = \frac{CP}{1 + CP}$$

That  $C = \frac{k_a}{k_d}$

It is important pay attention to three special situations:

A) When the pressure approaches zero, the expression (4.1) can be written as:

$$\frac{CP}{1 + CP} = 0$$

B) If the pressure, as expected, is so low:

$$KP \ll 1$$

$$W = \frac{CP}{1 + [small\ number]} \cong CP$$

$W$  has linear dependence on  $P$ , that is *Henry's law*

C) If the pressure increases to infinity then:

$$\frac{CP}{1 + CP} = 1 = W$$

This equation gives us the condition when all adsorption sites are filled with adsorbate, there is a complete monolayer.

High values of  $C$  imply that a strong bond is formed between the adsorbate and the substrate, if values of  $C$  are low implies that the bond is weak. Figure 4.9 explains the influence of  $C$  on  $W$ .

It is possible to perform an analogous development to find the equation in case of dissociative adsorption:

The above equation is modified when interaction between adsorbing molecules are taken into account. And when adsorbed molecules are free to move on the adsorbent surface, the Langmuir equation is modified to:

$$P = \frac{1}{C} \frac{W}{(1-W)} \exp\left(\frac{W}{1-W}\right) \quad (4.4)$$

Another typical example of the isotherms frequently employed is the *Freunlich* type equation:<sup>[45]</sup>

$$W = k_F P^{(1/n_F)} \quad (4.5)$$

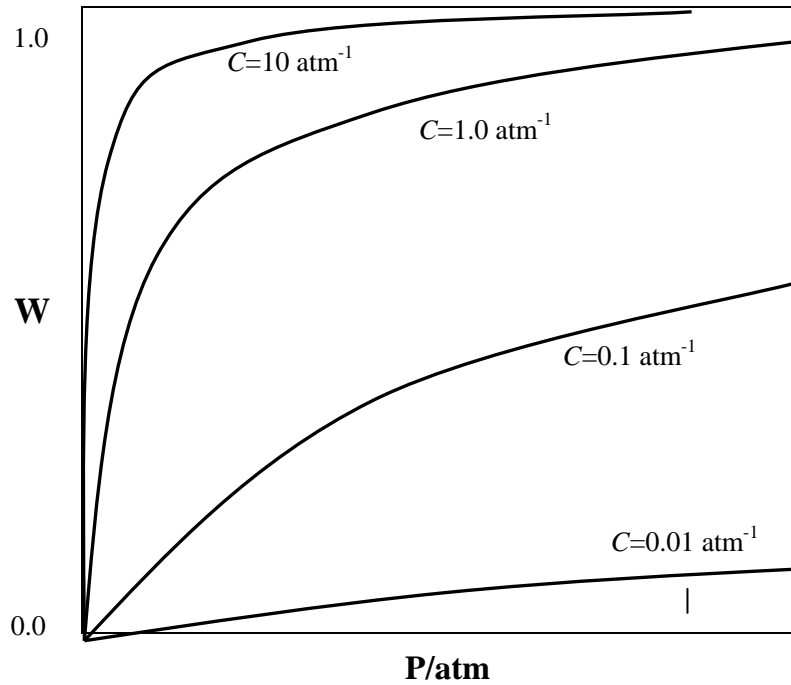


**Figure 4.9.** The influence of  $C$  on  $W$

$k_F$  and  $n_F$  are empirical constants that are different for different desiccants.

This equation is often considered to be an empirical equation. It is possible to interpret this equation theoretically in terms of adsorption on an energetically heterogeneous surface.<sup>[46]</sup>

The International Union of Pure and Applied Chemistry (Sing<sup>[46]</sup>) has accepted a classification of 6 different adsorption isotherms. Representative shapes for these types are shown in figure 4.10. Type I isotherms are characteristic for micro-porous adsorbents. The adsorption-desorption loop is reversible and the water uptake governed by the filling of the internal pore volume rather than the coverage of the internal surface area. The vapor molecules within the pores are subjected to a continuous force field generated by the surrounding surfaces. Examples of this important class of adsorbents are various types of charcoal and silica gel. (Van den Bulck<sup>[47]</sup>)

Adsorbents that are characterized by type III isotherms are non-porous or macro-porous solids like polymers, graphitized carbon or silica aero gels. The intermolecular

forces between the adsorptive molecules are much greater than the forces between the adsorbent and the adsorptive.

As it will be shown in the following sections, the polymer desiccant investigated in this study is characterized by such a type III isotherm.

The type II isotherm is characteristic for non-porous surfaces, macro-porous adsorbents and some compacted powders. The B.E.T. theory, named after its developers Brunauer, Emmett and Teller, is accepted as the standard to predict the adsorption/desorption process for this kind of isotherms. Examples for materials with type II isotherms are graphitized carbon, and compact powders of silica.

Hysteresis is characteristic for type IV and type V isotherms. This phenomenon is traditionally explained by the occurrence of capillary condensation within ink-bottle type pores and it is most often observed for meso-porous adsorbents. The intermolecular forces for the type IV isotherm are similar to those for type I and II isotherms. The adsorption of water vapor on low density silica gel is an example for type IV. The type V isotherms are similar in nature to type III, except that the average pore size is smaller. Examples are the adsorptions of organic vapors on meso-porous adsorbents.

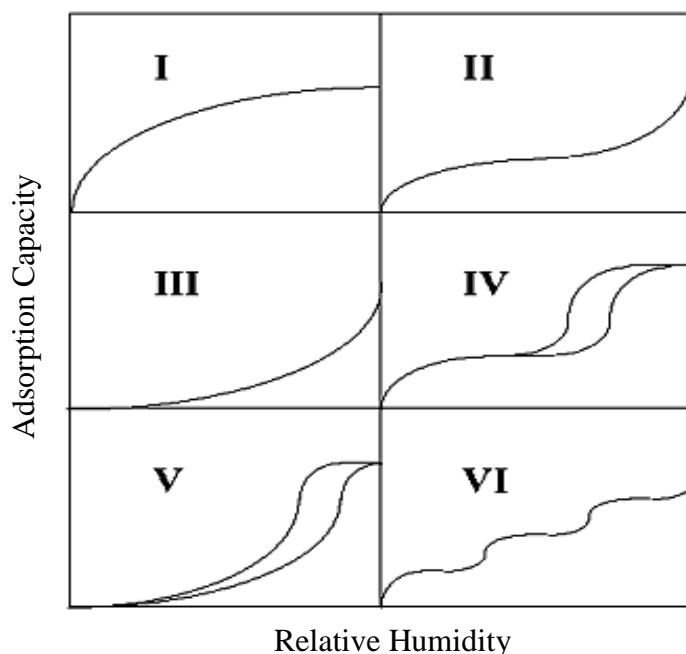


**Figure 4.10.** Classification of Adsorption Isotherms Accepted by the International Union of Pure and Applied Chemistry<sup>[46]</sup>

Type VI isotherms illustrate the stepwise adsorption in multi layers on a non-porous surface or a macro-porous adsorbent, and is similar to the type II isotherm. Each step represents the coverage of a subsequent monolayer. This type of adsorption is fairly rare, i.e., the adsorption of argon or krypton on graphitized carbon at cryogenic temperatures. As it can be observed in figure 4.10 the type I has the best capacity for adsorption without showing hysteresis.

#### 4.1.7.4. Potential Theory of Adsorption

The adsorption capacity of a desiccant material is not only dependent on the relative humidity of the surrounding air but also on its temperature. Thus, the relation of capacity to both temperature and relative humidity must be known in order to determine the performance of a rotary enthalpy exchanger. It is convenient to find a function that involves both of these parameters and allows prediction of the desiccant adsorption capacity at any given temperature-humidity combination.

Such a function is given by the Polanyi theory which was first introduced by Polanyi <sup>[41]</sup> and further developed by Dubinin. <sup>[42]</sup>

Polanyi introduced the so-called adsorption potential,  $A$ , and assumed that the adsorption capacity of an adsorbent  $W$  is a function of  $A$  only:

$$A = RT \ln\left(\frac{P_s}{P_v}\right) \quad (4.6)$$

$$W = f(A) \quad (4.7)$$

$P_v$  represents the actual vapor pressure and  $P_s$  the saturation pressure at the corresponding temperature therefore  $\frac{P_v}{P_s}$  represents relative humidity. Using the definition of  $A$

(Equation 4.6), the Polanyi assumption and the Clausius-Clapeyron equation for the differential heat of adsorption, it can be shown that the adsorption potential  $A$  is the difference in Gibbs free energy between the adsorbed phase and the saturated liquid phase of the adsorptive at the same temperature. (Van den Bulck <sup>[47]</sup>)

The advantage of this theory is that the adsorption capacity  $W_m$  is reduced to a function of only one variable and therefore the entire temperature and humidity ranges can be shown in one characteristic curve. Dubinin <sup>[42]</sup> examined experimental adsorption equilibrium data for many systems and showed that this characteristic curve can often be approximated by the equation:

$$W_m = W_0 \exp\left(-\left(\frac{A}{E_0}\right)^n\right) \quad (4.8)$$

Where  $W_0$  is the total micro-pore volume and  $E_0$  is the characteristic energy of adsorption. Since this equation has been shown to apply only to homogeneous systems of pores, a more complex equation, referred to as the Dubinin-Polstyanov equation <sup>[42]</sup>, is often used to calculate the adsorption capacity of an adsorbent:

$$W_m = W_{0,1} \exp\left[-\left(\frac{A}{E_{0,1}}\right)^{n_1}\right] + W_{0,2} \exp\left[-\left(\frac{A}{E_{0,2}}\right)^{n_2}\right] \quad (4.9)$$

#### 4.1.7.5. Adsorption hysteresis

Hysteresis appearing in the multilayer range of physisorption isotherms is usually associated with capillary condensation in mesopore structures. In case of silica gel it especially is difficult to interpret. In the past it was attributed to a difference in

mechanism between condensation and evaporation process occurring in pores with narrow necks and wide bodies (often referred to as “ink bottle” pores), but it is now recognized that it is a simplification of that happens. Anyway there are a lot of shapes of hysteresis loops and they have often been identified with specific pore structures, figure 4.11 shows the different types of hysteresis loops:

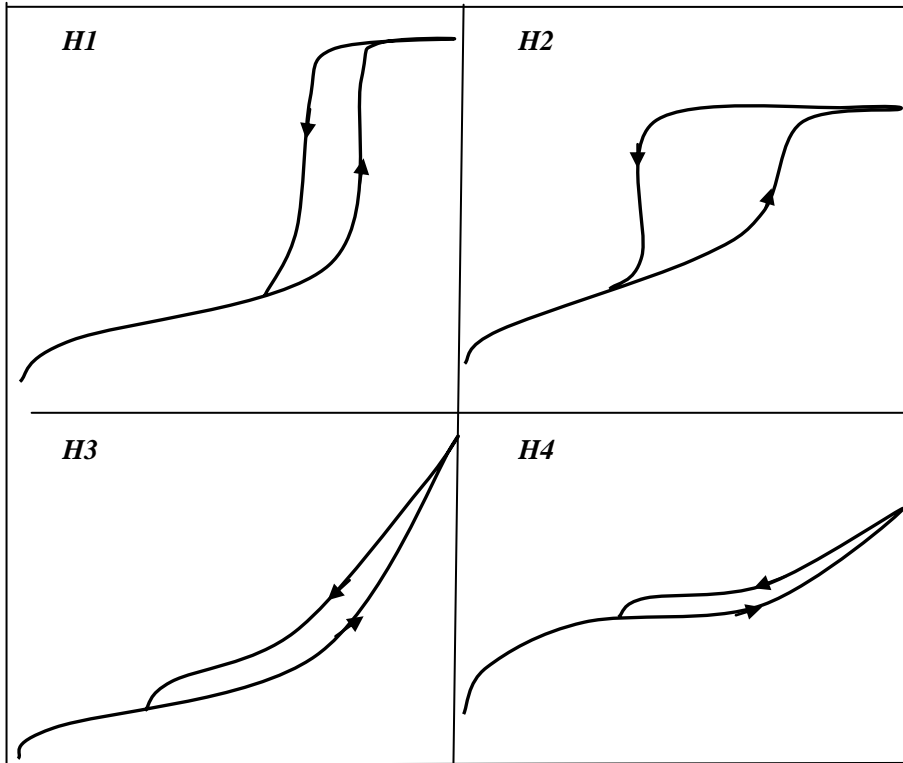


**Figure 4.11.** The different types of hysteresis loops<sup>[46]</sup>

Type **H1** is observed with porous materials known, like agglomerates or compacts of approximately uniform spheres in fairly regular array that have narrow distributions of pore size.

Type **H2** is associated with some corpuscular systems, but in these cases the distribution of pore size and shape is not well defined. This case is so difficult to interpret.

Type **H3** is observed with aggregates of plate-like particles giving rise to slit-shaped pores which does not exhibit any limiting adsorption at high  $p/p_0$ .

Type **H4** appears with narrow slit-like pores, and indicates microporosity.<sup>[46]</sup>

#### 4.1.7.6. Diffusion in porous particles

Most of the adsorbents commercially used are porous particles. For large adsorption capacity, large surface area is preferable; as a result large numbers of fine pores, as fine as possible, are needed. Adsorbate molecules come from outside adsorbent

particles and diffuse into the particle to fully utilize the adsorption sites. Depending on the structure of adsorbent, several different types of diffusion mechanisms become dominant and sometimes two or three of them compete or cooperate. The dominant mechanism also depends on a combination of adsorbate and adsorbent and adsorption conditions such as temperature and concentration range.

When the total pressure is very low or pore diameter is small, mean free path of a gas molecule, becomes smaller than the pore diameter. In this case *Knudsen* diffusion or pore diffusion takes place in the macropore. When adsorbed molecules are mobile on the surface of the adsorbent, diffusion due to migration of the adsorbed molecules may contribute more than pore diffusion to intraparticle diffusion. This type of diffusion is called *surface* diffusion.<sup>[44]</sup>

## 4.2. Literature review

### 4.2.1. Computational Background

Kang and Maclain-Cross<sup>[48]</sup> showed that the dehumidifier is the key component of a desiccant cooling system and the cooling COP can be significantly improved by improving the performance of this component. Detailed models of the heat and mass transfer processes that occur in a dehumidifier can be used to judge the potential benefits of various materials and matrix geometries. Optimization of performance in terms of flow-rate ratios, rotational speeds, and the desiccant /matrix thermodynamic properties is also easily accomplished with these models.

Available evaluations of the performance of the adsorptive dehumidifier have been based mainly on computer simulations. Important among the analytical methods were the “Analogy Theory” by Banks,<sup>[49-53]</sup> the “Finite Difference Method” by Maclain-Cross<sup>[54]</sup> the “Pseudo-Steady State Model” by Barlow and Worek<sup>[57,58]</sup> “Finite Difference Method for crossed cooled Dehumidifiers”. A series of papers evaluated the performance of the system with coupled heat and mass transfer in terms of characteristic potentials  $F_1, F_2$  and characteristic specific capacity  $\gamma$ ,<sup>[49-53]</sup> and an optimization study from viewpoint of the regeneration energy in terms of the capacitance rate parameters  $\Gamma_1, \Gamma_2$  by solving the conservation equations for an equilibrium dehumidifier using wave analysis that includes the effects of “shocks”.<sup>[57, 58]</sup>

MOSHMX<sup>[54]</sup>, a computer program utilizing finite differences, was based on a detailed numerical analysis and extrapolation to a zero-grid size using four carefully chosen grid sizes. MOSHMX was used to study the effect of isotherm shape, maximum water content, heat of adsorption, regenerative matrix thermal capacitance, matrix moisture diffusivity, and adsorption hysteresis on dehumidifier performance. MOSHMX has been used extensively to model dehumidifier operations like transient performance, purging, and desiccant property effects. Finite difference techniques have been used by many researchers to obtain detailed models of dehumidifiers. The program DESSIM<sup>[59]</sup> was developed where the matrix was discretized and each node was treated as a counter flow heat and mass exchanger in which both the mass and heat transfer were assumed to be uncoupled. ET/DESSIM is a model developed based on the DESSIM program.<sup>[59]</sup>



This code incorporated several improvements over the DESSIM program. DCSSMX is a code which in the approach of MOSHMX for solving the heat and mass transfer in a dehumidifier node has been added to the ET/DESSIM program and is more accurate than ET/DESSIM and is widely accepted and used for modeling solid rotary dehumidifiers.<sup>[59]</sup> These codes have been validated, with varying degrees of accuracy, by experimental data. Recently MOSHMX has been modified to model the performance of a silica gel / zeolite, layered desiccant dehumidifier. A ventilation cycle using this dehumidifier performs slightly better than a cycle with a silica gel dehumidifier.

Simonson and Besant<sup>[18, 62]</sup> derived the fundamental dimensionless groups for air-to-air energy wheels from the governing non-linear and coupled heat and mass equations and developed effectiveness correlations for energy wheels using computational data.

#### 4.2.2. Experimental Background

As it mentioned earlier, the most available evaluations of the performance of the adsorptive dehumidifier have been based mainly on computer simulations. Except for the experimental analyses to investigate validity of the foregoing computational models, there are few papers about experimental investigation of rotary humidity regenerators. Neti and wolf<sup>[13]</sup> have compared two different theories; the method of characteristic and a numerical approach. They have reported that the method of characteristic appears to be good for only a small range of conditions, generally for low values of specific capacities. The numerical approach appears to predict the trends well, though sometimes with large errors.

Kodama<sup>[13]</sup> proposed an experimental prediction to estimate the optimal rotation speed and the performance of a rotary adsorber, in which simultaneous enthalpy and humidity changes are dealt with separately by visualizing changes of state of product or exhaust air on a psychrometric chart.

Chuah<sup>[1]</sup> studied an investigation of transient mass transfer in a parallel passage dehumidifier with a thin layer of silica gel on the passage walls. A two-film resistance model was used to approximate the overall transfer resistance between the process air and the solid desiccant. It was found that the two-film model agrees with the experimental results within the experimental accuracy. Popescu<sup>[61]</sup> studied experimentally a 1M desiccant for its capability for simultaneous removal of moisture and some selected pollutants from air.

#### 4.2.3. Open-cycle solid desiccant systems

Moisture removal is achieved in a conventional vapor-compression system by condensation. In high –humidity regions this method could be very inefficient since it usually involves reheating the air after dehumidification. Vapor compression systems are efficient in sensible cooling, whereas desiccant dehumidifiers are efficient in handling latent loads. Hybrid systems, which integrate desiccant dehumidifiers with conventional cooling systems, are proven to provide substantial energy savings.<sup>[62-69]</sup>

Maclaine-Cross <sup>[49]</sup> proposed a system called the Simplified Advanced Solid Desiccant cycle which gave COP values of above 2. He found that energy costs were halved using this hybrid system. His system consisted of a regenerative dehumidifier, a heat exchanger, an evaporative cooler and heating coils and fans, to provide the latent and part of the sensible load, as well as a gas engine-driven chiller which is also used to take up the remaining sensible load. This also suggests that desiccant cooling systems may prove to be competitive with conventional systems when the desiccant units are commercially available. Solar energy prototypes were also built by private companies in 1982, but this early attempt was discouraged by the lack of good analytical methods for the prediction of the performance of regenerative dehumidifiers.

The methods available then were able to predict performance at rotational speeds so low that the whole matrix was in equilibrium with the process and regenerative air streams. Since then, a number of analytical methods have been developed in order to understand and analyze the performance of desiccant dehumidifiers and the desiccant cooling systems.

### 4.3. Governing equations

The dehumidifier is a rotating cylindrical wheel of length  $L$  and radius  $R$  with small channels which walls are adhered with an adsorbent such as silica gel. For simplicity it is divided into two equal sections: the adsorbing section and the regeneration section (desorption of water vapor).

The regeneration and adsorption air streams are in a counter flow arrangement. The schematic of a balanced rotary dehumidifier is illustrated in figure 4.12 and the analysis is based on the following assumptions:

- 1-Axial heat conduction and water vapor diffusion in the air are negligible.
- 2-Axial molecular diffusion within the desiccant is negligible.
- 3-There are no radial temperature or moisture content gradients in the matrix.
- 4- Hysteresis in the sorption isotherm for the desiccant coating is neglected and the heat of sorption is assumed constant.
- 5- The channels that make up the wheel are identical with constant heat and mass transfer surface areas.
- 6- The matrix thermal and moisture properties (support material\desiccant and adsorbed water) are constant.

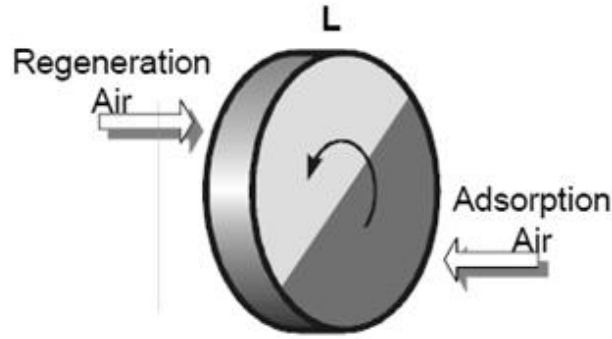


**Figure 4.12.** Desiccant wheel

- 7- The channels are considered adiabatic and impermeable.
- 8- The mass and heat transfer coefficients are constant.
- 9- The adsorption heat per kilogram of adsorbed water is constant.
- 10- The carry over between two air flows is neglected.

Based on the above assumptions, the model used in this analysis is transient and one-dimensional.

One of the channels is divided into to a number of equal step discrete elements or channels as shown in figure 4.13.

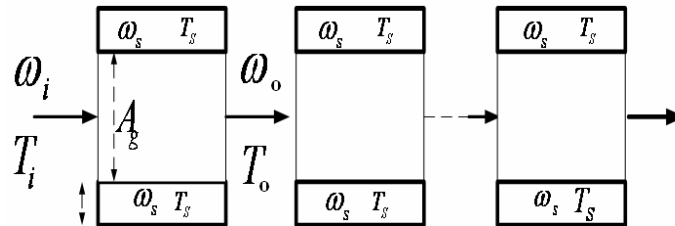


**Figure 4.13.** The schematic of discretization of one of the channels for Simulink code

For each discretized channel that identified in Simulink model as a framework with inlet conditions for air and storing outputs and initial condition for solid, as shown in figure 4.14, the energy and mass conservation equations can be written as follows. Mass transfer equation for the air stream:

$$\frac{d(\rho_g \frac{\rho_v}{\rho_g} A_g L)}{dt} = U_g A_g \rho_g (\omega_i - \omega_o) + h_m A_c (\omega_s - \omega) \quad (4.10)$$

$$\begin{aligned}\frac{d\omega}{dt} &= \frac{U_g}{L}(\omega_i - \omega_o) + \frac{h_m A_c}{\rho_g A_g L}(\omega_s - \omega) \\ &= C_1(\omega_i - \omega_o) + C_2(\omega_s - \omega)\end{aligned}\quad (4.11)$$

Where:

$$\omega = \frac{\rho_v}{\rho_g} \quad (4.12)$$

$$\frac{A_c}{A_g} = \frac{2L}{D_h/2} \quad (4.13)$$

$$C_1 = \frac{U_g}{L} \quad (4.14)$$

$$C_2 = \frac{h_m A_c}{\rho_g L A_g} \quad (4.15)$$

Heat transfer equation for the air stream:

$$\frac{d(\rho_g A_g L C_g T_g)}{dt} = \rho_g U_g A_g C_g (T_{gi} - T_{go}) + h A_c (T_s - T_g) \quad (4.16)$$

$$\frac{dT_g}{dt} = C_1(T_{gi} - T_{go}) + C_3(T_s - T_g) \quad (4.17)$$

$$C_3 = \frac{h A_c}{\rho_g L A_g C_g} \quad (4.18)$$

$$C_3 = Le C_2 \quad (4.19)$$

Mass transfer equation for solid desiccant layer:

$$\frac{d(\rho_d w A_d L)}{dt} = h_m A_c (\omega - \omega_s) \quad (4.20)$$

Where  $w$ , is the water content of desiccant material:

$$\frac{\rho_{vd}}{\rho_d} = w \quad (4.21)$$

So:

$$\frac{dw}{dt} = \frac{h_m A_c}{\rho_d A_d L} (\omega - \omega_s) \quad (4.22)$$

For having the equations according to the variables  $\omega_s, T_s, \omega, T$ , It can be written as:

$$dw = \frac{\partial w}{\partial \phi} \frac{\partial \phi}{\partial \omega_s} d\omega_s + \left( \frac{\partial w}{\partial \phi} \frac{\partial \phi}{\partial T_s} + \frac{\partial w}{\partial T_s} \right) dT_s \quad (4.23)$$

or:

$$dw = SI(\omega_s, T_s) d\omega_s + S2(\omega_s, T_s) dT_s \quad (4.24)$$

$$SI(\omega_s, T_s) = \frac{\partial w}{\partial \phi} \frac{\partial \phi}{\partial \omega_s} \quad (4.25)$$

$$S2(\omega_s, T_s) = \left( \frac{\partial w}{\partial \phi} \frac{\partial \phi}{\partial T_s} + \frac{\partial w}{\partial T_s} \right)$$

So mass transfer equation for desiccant layer will become:

$$\begin{aligned} \frac{d\omega_s}{dt} &= - \frac{S2(\omega_s, T_s)}{SI(\omega_s, T_s)} \frac{dT_s}{dt} + \frac{h_m A_c}{\rho_d A_d L SI(\omega_s, T_s)} (\omega - \omega_s) = \\ &= - \frac{S2(\omega_s, T_s)}{SI(\omega_s, T_s)} \frac{dT_s}{dt} + \frac{C_4}{SI(\omega_s, T_s)} (\omega - \omega_s) \end{aligned} \quad (4.26)$$

Where:

$$C_4 = \frac{h_m A_c}{\rho_d L A_d} \quad (4.27)$$

$$\frac{A_c}{A_d} = \frac{4D_h L}{((D_h + d_t)^2 + D_h^2)} \quad (4.28)$$

$$h_m = \frac{h}{C_g Le} \quad (4.29)$$

And  $Le$  is Lewis number that here is assumed equal one for air stream.

Heat transfer for solid desiccant layer:

$$\frac{d(\rho_d A_d L C_d T_s)}{dt} = q_{st} \rho_d A_d L \frac{dw}{dt} + h A_c (T_g - T_s) \quad (4.30)$$

$$\frac{dT_s}{dt} = \frac{h_m A_c q_{st}}{\rho_d A_d L C_d} (\omega - \omega_s) + \frac{h A_c}{C_d \rho_d A_d L} (T_g - T_s) \quad (4.31)$$

$$\frac{dT_s}{dt} = C_4 C_5 (\omega - \omega_s) + C_6 (T_g - T_s) \quad (4.32)$$

$$C_5 = \frac{q_{st}}{C_d} \quad (4.33)$$

$$C_6 = \frac{h}{C_d \rho_d L} \frac{A_c}{A_d} \quad (4.34)$$

Relative humidity and saturation pressure can be calculated by <sup>[68]</sup>:

$$\phi = \frac{\omega_s P_0}{(0.622 + \omega_s) P_s} \quad (4.35)$$

$$P_s = 10^6 P_0 \exp\left(\frac{-5294}{T}\right) \frac{(1 + 1.61\omega_s)}{(0.622 + \omega_s)} \quad (4.36)$$

For first channel (element) in Adsorption period the initial conditions are known as:

$$T_{gi} = T_{Process \text{ air inlet}} = T_{g,initial} \quad (4.37)$$

$$\omega_{gi} = \omega_{process \text{ air inlet}} \quad (4.38)$$

$$\omega_{si} = \omega_{s \text{ initial}} \quad \text{in } T_{gi} \quad (4.39)$$

$$T_{s,initial} = T_{g,Process \text{ air inlet}} \quad (4.40)$$

And initial conditions for regeneration period:

$$T_{gi} = T_{Re \text{ generation air inlet}} \quad (4.41)$$

$$\omega_{gi} = \omega_{Re \text{ generation air Inlet}} \quad (4.42)$$

$$\omega_{si} = \omega_{s \text{ initial}} \quad \text{in } T_{gi} \quad (4.43)$$

$$T_{s,initial} = T_{g,process \text{ air inlet}} \quad (4.44)$$

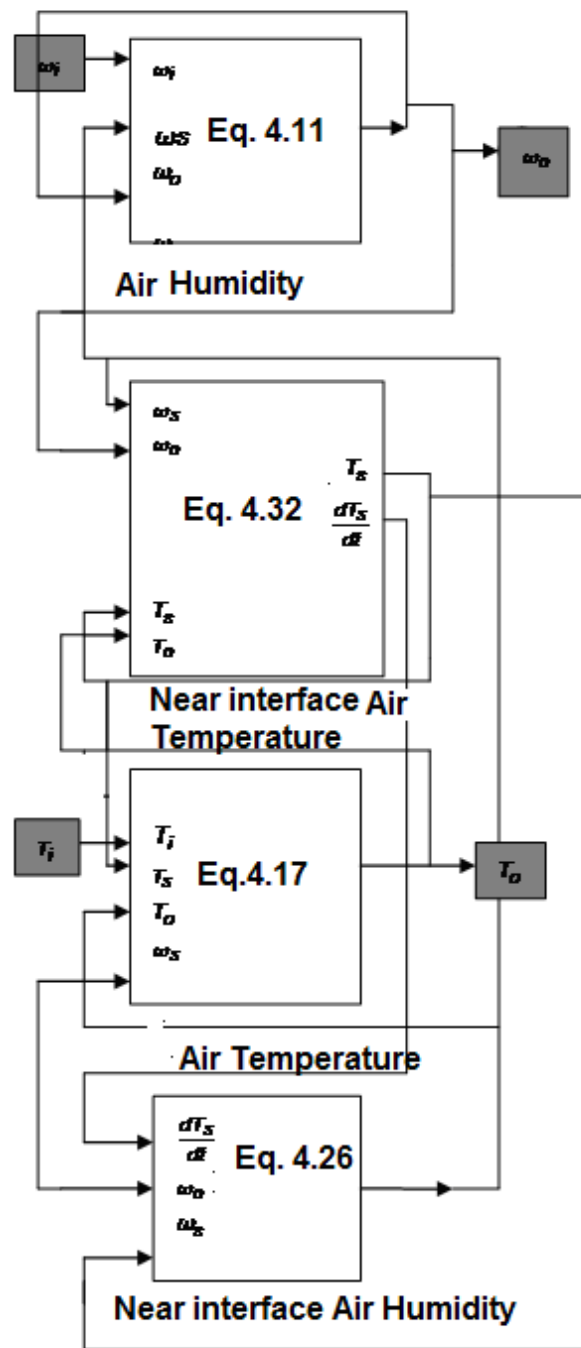


Figure 4.14. Simulink representation of the model

### 4.3.1. Simulation Platform and Subsystems

The model used in this simulation has been build up based on a main framework for each element shown in figure 4.13. It can be regarded as an interaction of four main subsystems shown in figure 4.14. The block diagram shows the set up of the simulation. Each subsystem is composed of a series of other, more detailed, subsystems. The calculation blocks are storing the response of an output. For simulation of the rotation of the wheel between two counter flow adsorption and regeneration air flow, the convenient user defined functions regarding the time step of revolution has been built up and is jointed to the main framework for each element . There are a number of techniques to solve the derived differential equations. The selected scheme of solutions in MATLAB for initial value problems is Runge-Kutta methods with variable time steps.

The output conditions of an individual channel can be considered as average values for each section of the wheel. The time step and the time each channel of wheel passes through the air stream can be considered to evaluate of the output conditions in different wheel angels. A subsystem has been made and connected to the main framework to calculate the average value of outlet air conditions profiles for both air streams. Therefore, the model can be easily connected to the other building models. Since the stable situation can be achieved after 5 revolutions for dehumidifier, the running time for computer is 5 times more than the step time for each revolution. In addition, using a few sub programming in Matlab the time calculation to produce a big number of the desiccant wheel solutions has been provided. This improvement was especially helpful if the simulation needed to be run many times to produce a certain amount of results. For example, in producing simplified equations, 3000 data were produced in 3 working days from simulation. These large numbers of results are necessary to be used in optimization routine to make simplified equations.

### 4.3.2. Evaluation of the coefficients and step sizes for Dehumidifier

Regarding the derived nonlinear equations of combined mass and heat transfer we have many coefficients that are functions of  $T_{air}, \omega_{air}$  that can be considered constant with considering the average values of them. It improves the accuracy and reduces the calculation time. Some of the coefficients are functions of  $T_s, \omega_s$  .

The present model was validated by comparing the simulated results with the published experimental values. <sup>[10]</sup> The adsorption capacity of a desiccant material is not only dependent on the relative humidity of the surrounding air but also on its temperature. Thus, the relation of capacity to both temperature and relative humidity must be known. It is convenient to find a function that involves both of these parameters and allows prediction of the desiccant adsorption capacity at any given Temperature-humidity combination. A correlation for silica gel given in the literature <sup>[2]</sup> is:



$$W = 0.106 \exp \left[ -\left( \frac{A}{8590} \right)^2 \right] + 0.242 \exp \left[ -\left( \frac{A}{3140} \right)^2 \right] \quad (4.45)$$

$$A = -R T \ln \phi \quad (4.46)$$

So for Eq. (4.45) it can be written:

$$S_1(\omega_s, T_s) = \left[ \begin{array}{l} (2.9E-9) \times A \times \frac{RT_s}{\phi} \exp \left[ -\left( \frac{A}{8590} \right)^2 \right] + \\ (4.9E-8) \times A \times \frac{RT_s}{\phi} \exp \left[ -\left( \frac{A}{3140} \right)^2 \right] \end{array} \right] \times \left[ \frac{0.622 P_0}{(0.622 + \omega_s)^2 P_s} \right] \quad (4.47)$$

$$S_2(\omega_s, T_s) = -$$

$$\left[ \begin{array}{l} (2.9E-9) \times A \times \frac{RT_s}{\phi} \exp \left[ -\left( \frac{A}{8590} \right)^2 \right] + \\ (4.9E-8) \times A \times \frac{RT_s}{\phi} \exp \left[ -\left( \frac{A}{3140} \right)^2 \right] \end{array} \right] \times \frac{5294\phi}{T_s^2} \quad (4.48)$$

$$+ \left[ \begin{array}{l} (2.9E-9) \times A \times R \ln \phi \exp \left[ -\left( \frac{A}{8590} \right)^2 \right] + \\ (4.9E-8) \times A \times R \ln \phi \exp \left[ -\left( \frac{A}{3140} \right)^2 \right] \end{array} \right]$$

In the experimental study, <sup>[8]</sup> desiccant wheel has been used as a dehumidifier and the wheel has 20 cm width and the silica gel wall thickness is 0.2 mm. the pitch of the honeycomb shaped rotor used for experiments has been 3.2 x 1.8 mm. The heat of adsorption is calculated between 2100-2300 kJ/kg. The air velocity 2 m/s for air flow in both adsorption and regeneration periods have been reported. The important parameter in the modeling of the desiccant wheels is rotational speed or the *Time step* which can be determined regarding the time passed during each revolution of the wheel. As a simplifying assumption, the wheel in this modeling is considered a *balanced* wheel with two equal cross area and air flow rate for each part. Therefore the *Time step* is two times more than the time needed for one complete matrix rotation. For desiccant dehumidifier wheel, the rotational speeds are in the range 1-30 Revolution per Hour (RPh). The number of time elements is determined by the maximum time of running the program and the time increments that are variable from 0.001 to 0.1 seconds. The number of the elements is 50 for 0.2 meter length of the wheel.

The heat transfer coefficient is calculated by a correlation for forced convection in internal flows. As stated by Bejan, <sup>[68]</sup> the Nusselt number is approximately between 3.63

and 4.364 for this laminar flow arrangement and the hydraulic diameter of the hexagonal passes is estimated to be  $2.25 \times 10^{-3}$  m. The heat transfer coefficient becomes:

$$h = \frac{Nu \cdot k_{air}}{D_h} = 46.7 \frac{W}{m^2 \cdot ^\circ K} \quad (4.49)$$

## 4.4. The behavior of solutions

### 4.4.1. Model solutions for different wheel speeds and regeneration air temperatures

Figure 4.15 shows the solutions of Simulink modeling for the same conditions of temperature and humidity for process and regeneration side but in the different rotational speeds of the wheel as the speed values are shown above the outlet points of the wheel in that figure for both the regeneration and the adsorption sections. The solutions have been given in table 4.1. The inlet process air has 2 m/s velocity, 30°C temperature, 8 gr/kg dry air absolute humidity, and the inlet regeneration air has the same velocity, absolute humidity, but temperature of 80°C.

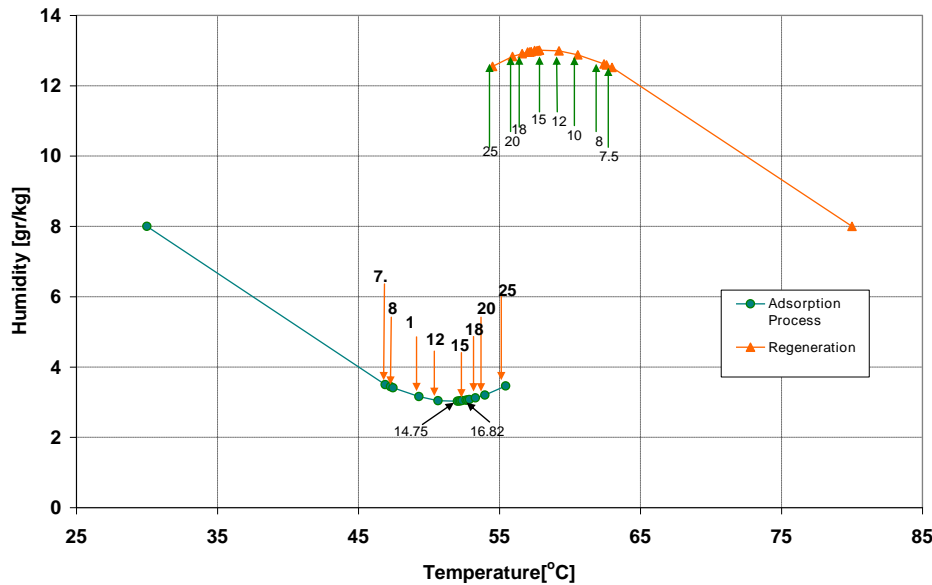


**Figure 4.15.** Variation of the state of outlet air with increasing rotational speed of wheel for both Adsorption and Regeneration

The optimum rotational speed of the wheel with Simulink solutions is 15.5 Rph (revolutions per hour). The rotational speed of a rotary desiccant dehumidifier is inversely proportional to the sorption time. The rotational speed of a rotary desiccant dehumidifier is optimum when the average outlet humidity ratio of the process air flow is the minimum. A rotary desiccant dehumidifier operates in a manner such that the moisture absorbed during the adsorption process must be desorbed during the regeneration process, so when the average outlet humidity ratio in the adsorption stream is optimized, the average outlet humidity ratio of the regeneration stream is maximized.

In other words, the adsorption and regeneration processes will be optimum at the same rotational speed. According to the published studies <sup>[10]</sup> the behavior of the Simulink solutions can be estimate. Figure 4.16 shows the prediction of the optimal rotation speed at various regeneration temperatures and compares the accuracy of the Simulink solutions with an experimental work <sup>[8]</sup> according to actual values which experimentally have been measured in that work. As it can be seen in figure 4.16 the model can predict the optimum speed of the wheel with very close accuracy in most conditions.

Using this model is advantageous because it treats the non-constant coefficients as constant in different temperature and humidity therefore it reduces the calculation time.

In addition, the model has very high degree of accuracy for the temperatures and humidities of the outlet air in different conditions.

**Table 4.1.** The model solutions for different wheel speeds and for both regeneration process as well as adsorption process, the inlet air conditions are 30 °C temperature and 8 gr/kg absolute humidity for adsorption process and 80 °C temperature and 8 gr/kg absolute humidity for regeneration process

Wheel speed [RpH]	Outlet Humidity of Adsorption proce [gr/kg]	Outlet Temerature of Adsorption proce [oC]	Outlet Humidity of Regeneration prc [gr/kg]	Outlet Temerature of Regeneration prc [oC]
7.5	3.5	46.9	12.52	62.98
7.82	3.44	47.27	12.59	62.6
8	3.41	47.45	12.62	62.42
10	3.16	49.29	12.88	60.56
12	3.04	50.64	12.99	59.22
14.75	3.03	52.03	13.01	57.83
15	3.032	52.14	13	57.74
15.25	3.038	52.24	12.99	57.64
15.52	3.045	52.35	13	57.49
16.22	3.057	52.64	12.97	57.24
16.51	3.063	52.76	12.96	57.14
16.82	3.076	52.87	12.96	57
18	3.12	53.3	12.91	56.61
20	3.2	53.97	12.83	55.92
25	3.46	55.44	12.55	54.51

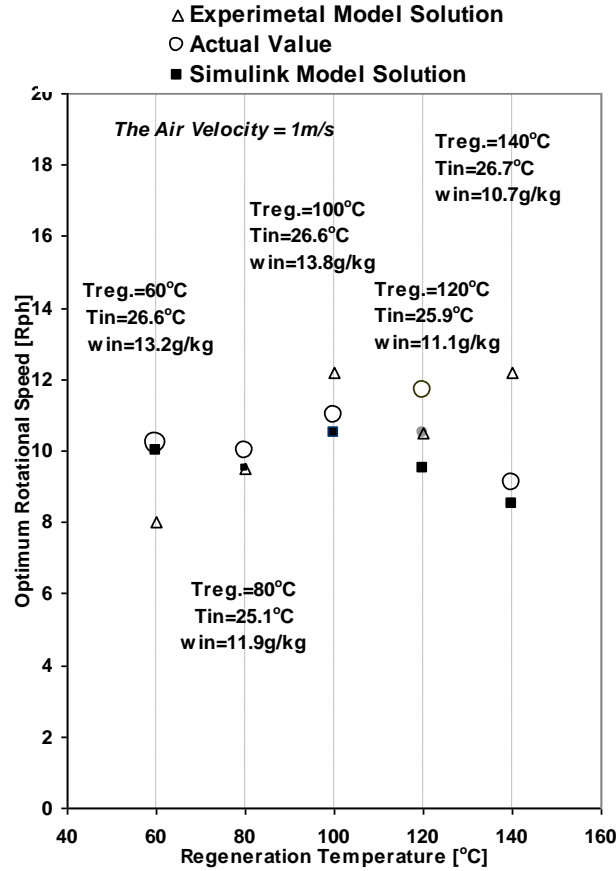


**Figure 4.16.** Prediction of the optimal rotational speed at various regeneration temperatures

#### 4.4.2. Outlet adsorption-side humidity profiles and optimum speed of wheel

The rotational speed of a rotary desiccant dehumidifier is inversely proportional to the sorption time. The rotational speed of a rotary desiccant dehumidifier is optimum when the average outlet humidity ratio of the process air flow is at minimum. A rotary desiccant dehumidifier operates such that the moisture absorbed during the adsorption process must be desorbed during the regeneration process, so when the average outlet humidity ratio in the adsorption stream is optimized, and the average outlet humidity ratio of the regeneration stream is maximized. In the other words, the adsorption and regeneration processes will be optimum at the same rotational speed. According to the published studies <sup>[69, 70]</sup> the behavior of the Simulink model output can be estimated.

When a desiccant wheel rotates much faster than the optimum speed, the adsorption and regeneration processes are too short, which results in poor performance.

Also, when the rotational speed is low, the adsorption and regeneration processes are too long and less effective.

The outlet humidity ratio profiles on the adsorption side are shown in figures 4.17 - 4.19. In figure 4.17 the outlet humidity profile at a faster rotational speed than optimum speed (when the adsorption time is insufficient), is plotted versus the wheel angle. This profile shows that the outlet humidity ratio at the last point, or at an angle of 180, is less than the average value. This means that at the end of adsorption process, the desiccant wheel can still efficiently dehumidify the air stream.

Therefore, the rotational speed should be lower to allow more adsorption time. In figure 4.19 the outlet humidity profile is at slower speeds than optimum rotational speed. In this case the outlet humidity at the end of adsorption is larger than the average value; this implies that the last portion of the adsorption process is inefficient. The rotational speed of the desiccant wheel should increase to ignore this last ineffective portion of the adsorption process. Therefore, to improve dehumidification performance, the rotational speed should be in between the cases illustrated in figures 4.17 and 4.19. As shown in figure 4.18, at the optimum rotational speed, the outlet humidity ratio at the end of the adsorption process, or at an angle of 180, is equal to the average value. This result <sup>[69, 70]</sup> is used in investigating the optimum rotational speeds of desiccant wheel, as the most important design parameter of the wheel, when operating conditions change.

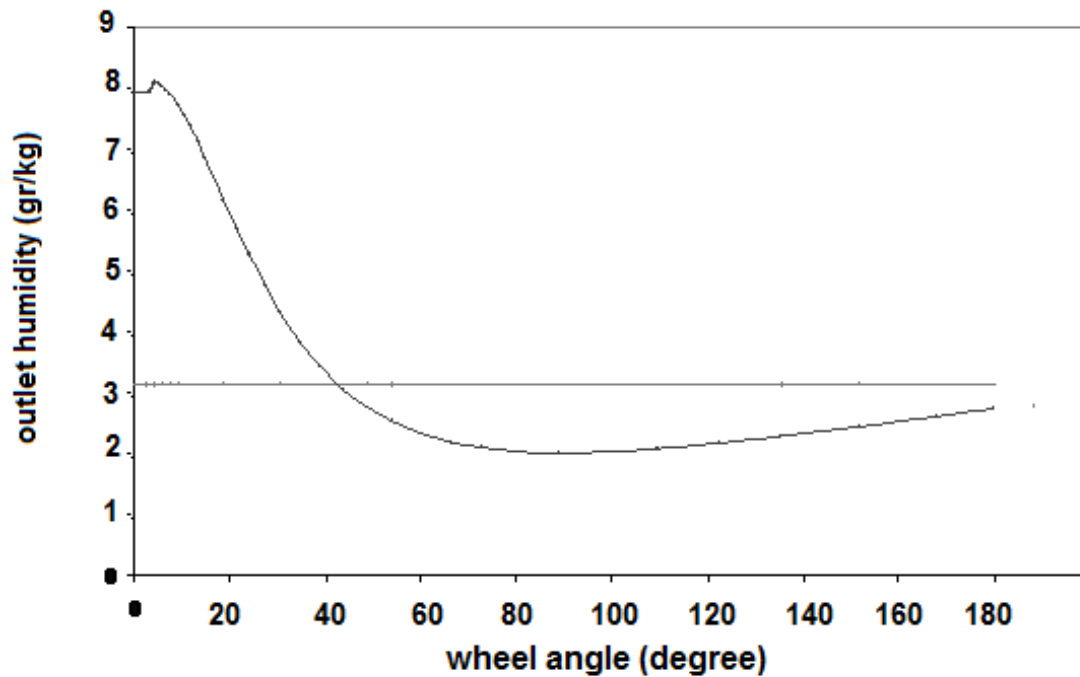


*Figure 4.17. A Simulation solution for adsorption-side outlet humidity ratio profile for wheel at 25Rph*

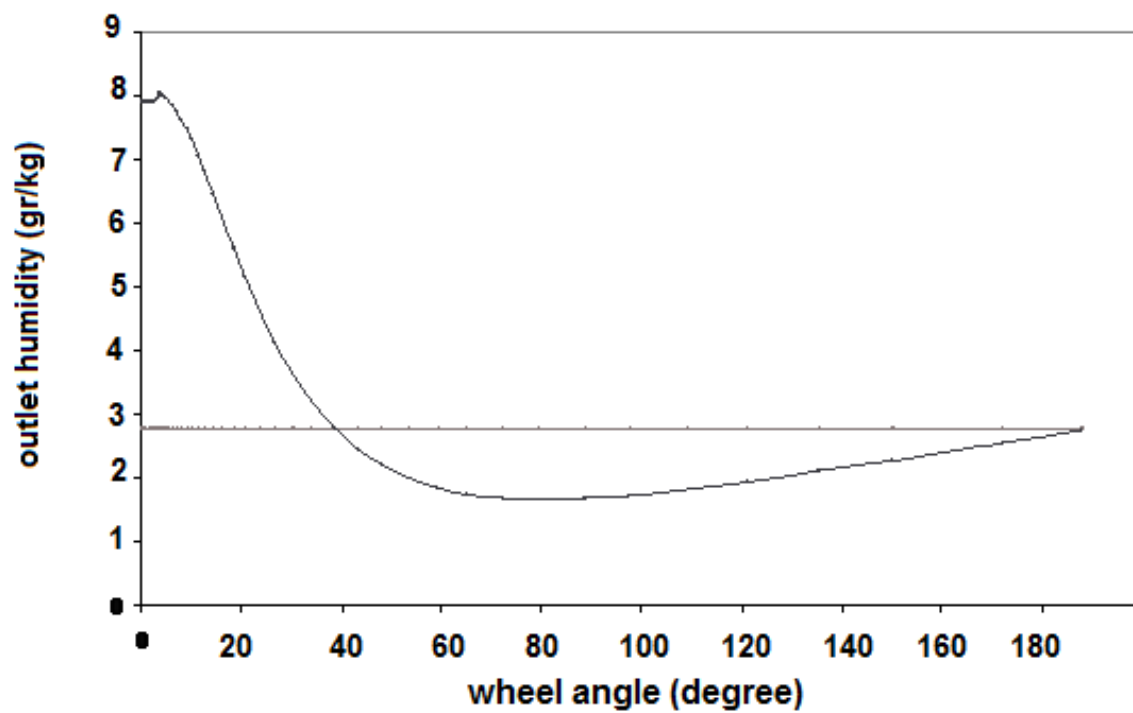


Figure 4.18. Adsorption-side outlet humidity ratio profiles for wheel at 15.5 Rph

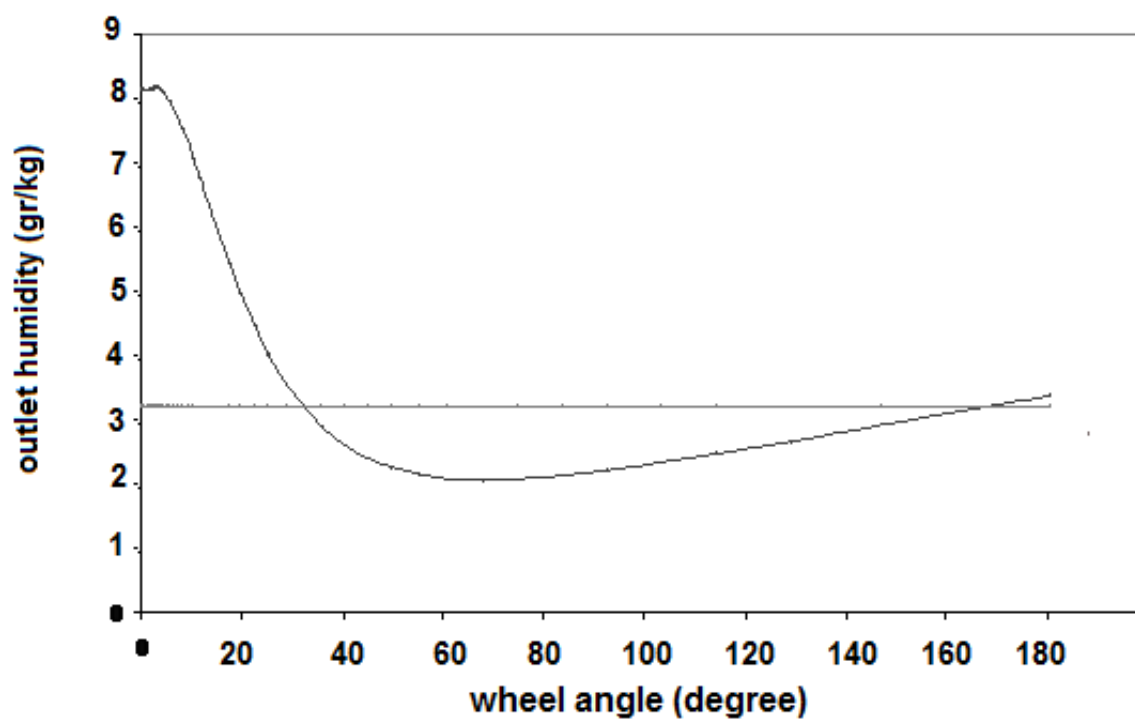


Figure 4.19. Adsorption-side outlet humidity ratio profile for wheel at 12 Rph

#### 4.4.3. Steady periodic solutions and stability

As it was shown in previous parts of this chapter, the model solutions are the outlet air humidity and temperature from wheel in different parts or angles of a wheel for both adsorption process and regeneration process. It has been assumed that the outlet airs for all air channels in a definite angle or degree of the wheel have same temperatures and humidities. Therefore the average of outlet air conditions profiles need to be calculated. It has been observed that if the desiccant wheel is operating as a dehumidifier, the solutions before the first five revolutions still are not stable. In the other terms, the solver is going through trial and error process to find the best initial conditions of saturated air for desiccant layer.

It takes five cycles for the solvers find the right initial values and therefore the stable solutions can be calculated by averaging of outlet air profile for different angles of the wheel. A subroutine has been developed and connected to the Simulink solutions calculating the average of the profile.

The average air temperature and humidity calculated by this subroutine have been shown in figures 4.20 and 4.21 for humidity and temperature of outlet airs, respectively. The inlet air conditions for adsorption are 30°C and 8 gr/kg and 80°C and 8gr/kg for regeneration air. The wheel speed is 15 revolutions per hour that is equal to 240 seconds time step for each revolution. As it can be observed in these figures after the fifth revolution the average of the outlet air conditions profiles are constant and there is stability in the solutions. Therefore, the model connected to the building models and other models needs the calculation time of the maximum five revolutions to produce stable input for the other models.

For a desiccant wheel as an enthalpy wheel, which operates in higher speeds of the range of 10-20 revolutions per minute, the step time for each revolution is equal with typical values of 1-3 seconds. This short time steps for each revolution means that the time steps to discretize the basic equations are in the range of 0.01 second. The results of model solutions given in figures 4.22 and 4.23 show that solvers need more revolutions (regarding typical time step of 2 seconds for each revolution, almost after 200 revolutions) to find right initial values to calculate stable solutions.

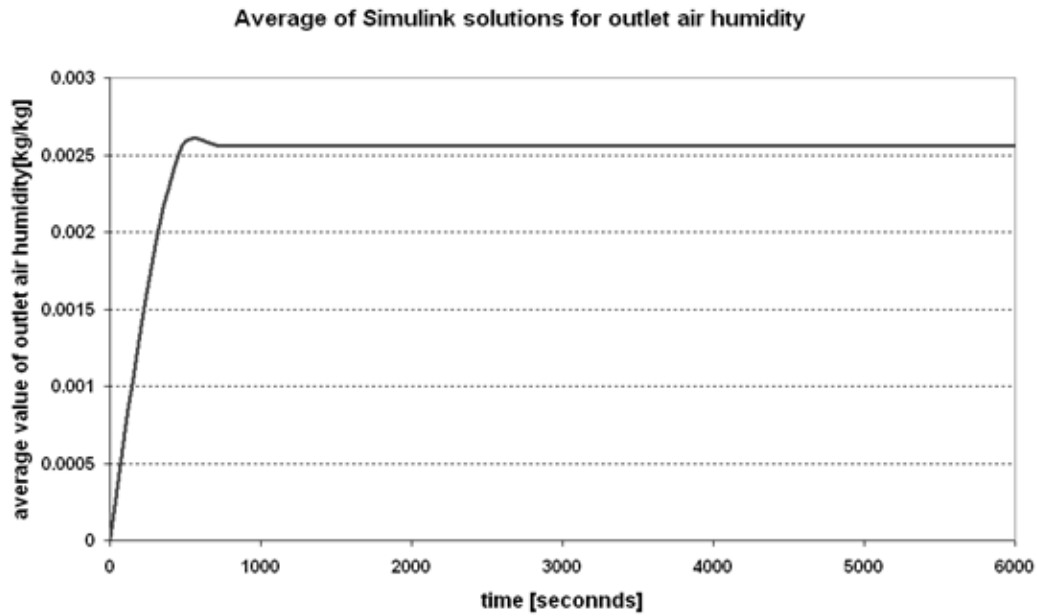


*Figure 4.20. Average of Simulink solutions for outlet air humidity of a desiccant wheel as a dehumidifier (desiccant thickness is 0.14 mm)*

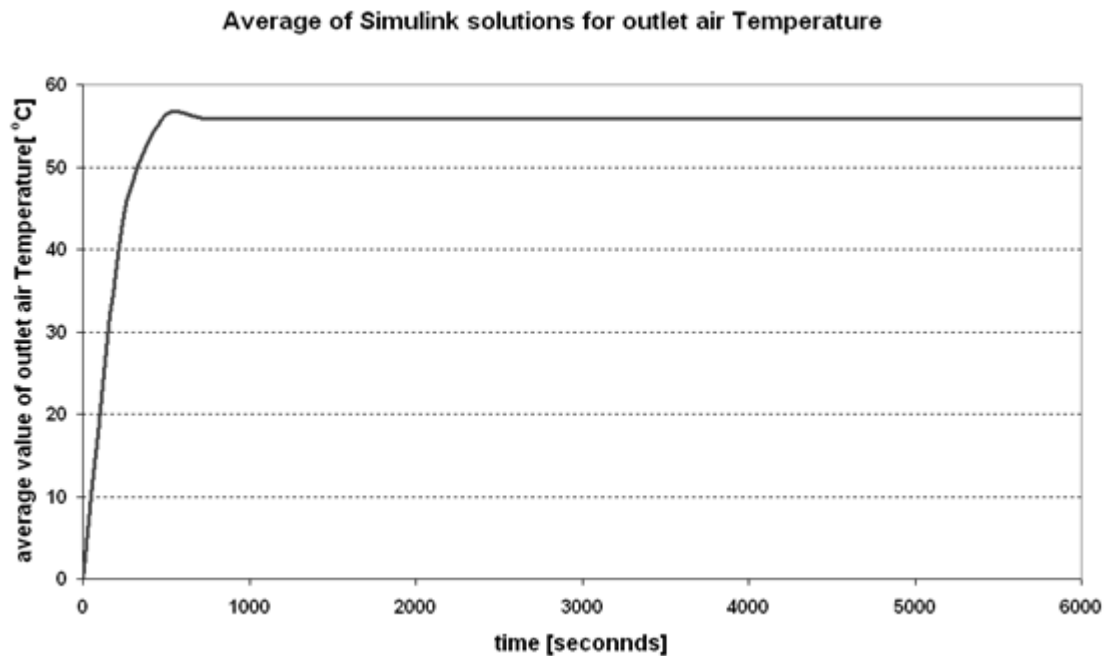


*Figure 4.21. The Average of Simulink solutions for outlet air temperature of a desiccant wheel as dehumidifier. The time step for time discretization is 0.1 seconds*



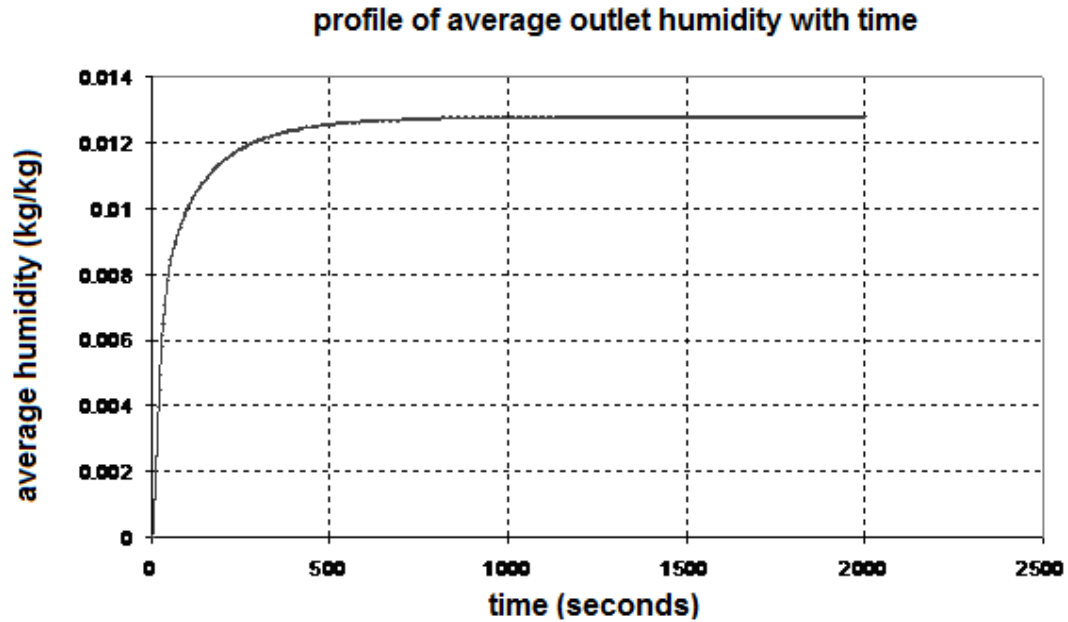


**Figure 4.22.** The Average of Simulink solutions for outlet air humidity of an enthalpy wheel (desiccant thickness is 0.019mm). The wheel speed is 30 revolutions per minute that is equal to 1 second for each revolution. The time step for time discretization is 0.01 seconds

As it has been shown in these figures, after almost 500 seconds the stable solutions of model for average of outlet air conditions of an enthalpy wheel can be expected. Considering the time step for a revolution, which is 3 seconds for a wheel with the speed of 20 revolutions per minute; a long calculation time can be resulted.

As the time discretization for numerical solutions needs time steps of 0.01 seconds, a very high memory is needed to produce the matrix of physical parameters in time steps of 0.01 seconds. Therefore, unfortunately the model for wheel as an enthalpy wheel is not practically useful to be connected to the other building models for long term simulations. Consequently, the simplified and faster models are derived from the physical model.

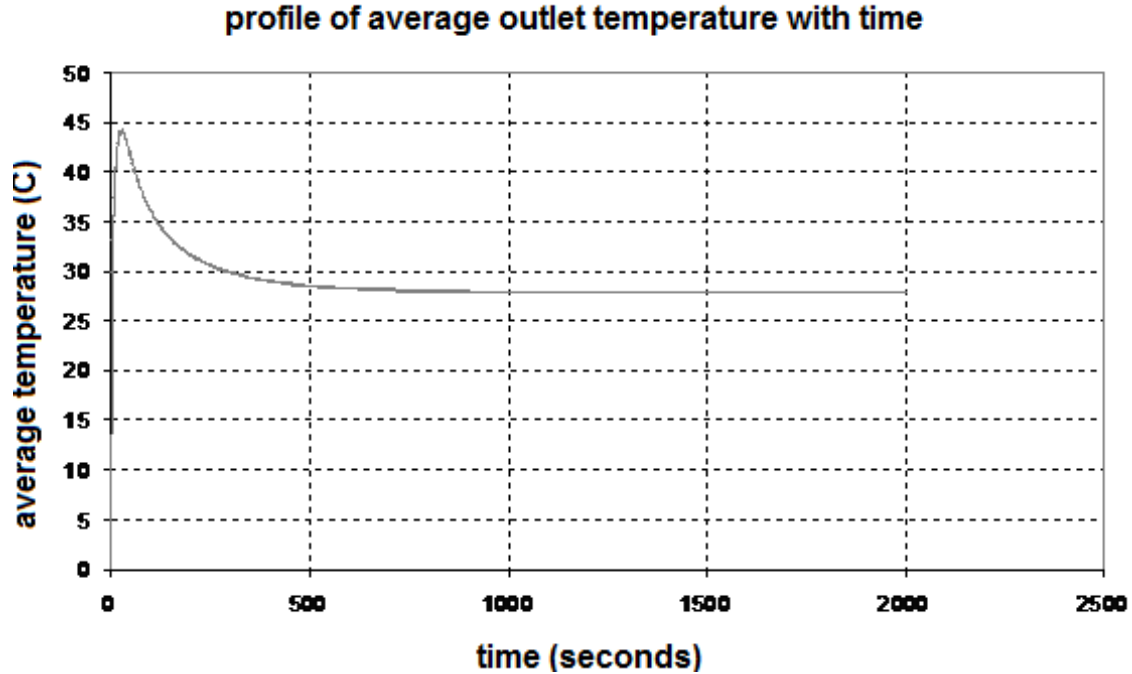


*Figure 4.23. The Average of Simulink solutions for outlet air humidity of an enthalpy wheel*

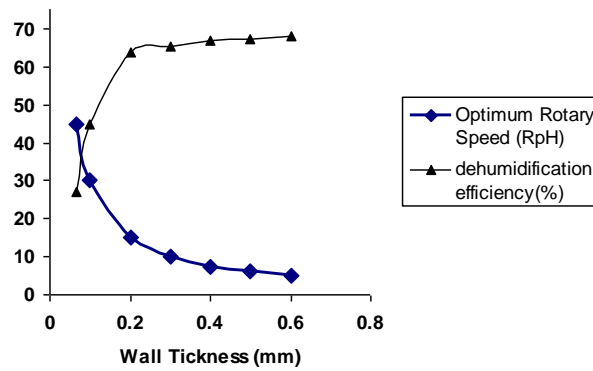
#### 4.4.4. Effects of wall thickness on the heat and mass transfers in desiccant wheels for air dehumidifier and enthalpy wheel

Figure 4.24 shows the optimum rotary speeds (Rph or Revolution per hour) with wall thickness of  $0-3\delta$  where  $\delta$  is a typical optimum thickness for such a wheel in dehumidification. The number of channels in the wheel is kept constant; therefore, the weight of wheel increases with increasing thickness. The resulting values of the dehumidifying efficiency in this figure show that the optimum speed for air dehumidifier decreases as the wall thickness increases.

Therefore, a slower rotating wheel is preferred for wheels with thick channel walls to effectively use the available desiccant material. When the wheel is for air dehumidification, dehumidification efficiency is defined as:

$$\varepsilon_d = \frac{\omega_{inlet} - \omega_{outlet}}{\omega_{inlet}} \quad (4.50)$$

Figure 4.25 shows the optimum rotary speeds for enthalpy recovery. The wheel usually reaches the highest sensible effectiveness and latent effectiveness simultaneously at the same optimum speed. Similar to air dehumidifier, the optimum speed decreases as the wall thickness in the wheel increases.



**Figure 4.24.** Optimum rotary speed for air dehumidification and the corresponding dehumidification efficiency with various wall thicknesses. The number of channels is fixed.

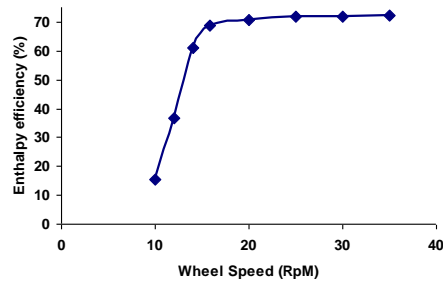


**Figure 4.25.** The enthalpy efficiency of the Wheel for different wheel speed

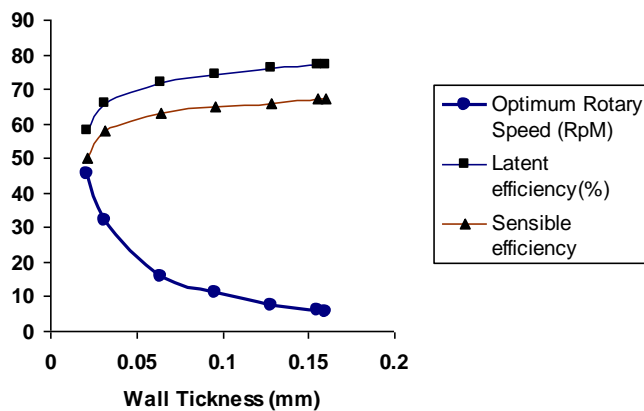


**Figure 4.26.** Optimum rotary speed for enthalpy recovery and the corresponding sensible and latent effectiveness with various wall thicknesses. The number of channels is fixed

The efficiencies are defined as following way and have been shown in figure 4.26:

$$\varepsilon_{st} = \frac{\dot{m} (T_{outlet} - T_{inlet})}{\dot{m}_{min} (T_{Supplyinlet} - T_{Exhaustinlet})} \quad (4.51)$$

$$(4.52)$$

#### 4.4.5. Desiccant wheels in low and high speeds for different conditions of inlet air and sorption matrix

As it was explained in the introduction of this chapter the most important difference between desiccant wheels as dehumidifier and enthalpy recovery is the wheel speed. It is very important to check whether a desiccant wheel can be used with both applications in an air conditioning cycle. On the other hand, it is desirable if wheel can be used as a dehumidifier in the speeds typically 10-20 revolutions per hour in summer and increasing the wheel speed to a typical range of 10-20 revolutions per minute as a heat and moisture recovery in winter applications in the same air conditioning system. Desiccant wheels as dehumidifier need a matrix with solid layer thicker than thickness in enthalpy recovery wheels. A typical thickness of solid layer for a dehumidifier matrix is 0.14 mm comparing with 0.019 mm thickness for desiccant layer in a commercial enthalpy wheel. Table 4.2 gives the model solutions for a desiccant wheel with thick matrix of silica gel or 0.14 mm for different air and wheel conditions.

The inlet air conditions for enthalpy wheel, given in the first row, are 35°C temperature and 20 gr/kg absolute humidity for supply air and 25°C temperature and 10 gr/kg humidity for exhaust air. The outlet air conditions for a wheel with 15 Rpm speed have been shown in table 4.2. A desiccant wheel with thick layer matrix practically can work as efficient as an enthalpy wheel and even better. As it has been shown in this table, dehumidifier wheel can provide 28.77 °C and 11.94 gr/kg air while an enthalpy wheel with same conditions but with thin solid layer under the same wheel speed can produce 28.5°C and 12.2 gr/kg. The outlet air conditions for the same wheel used as a dehumidifier has been shown in the second row. The inlet air conditions are 30°C temperature and 8gr/kg absolute humidity for adsorption air, and 90°C temperature and 8 gr/kg humidity for regeneration air. The outlet air conditions for a wheel with 15 Rph speed have been shown in this table. A desiccant wheel with a thin layer of solid desiccant, with a typical thickness of 0.02mm used as enthalpy wheels, can not be function as dehumidifier although the wheel rotates in low speeds common for dehumidification applications.

**Table 4.2.** The outlet air conditions for a desiccant wheel with thick layer of solid in the matrix. The thickness of the solid layer is 0.14 mm.

Dehumidifier		inlet air conditions		outlet air conditions		return air conditions	
N	V	T(°C)	X(g/kg)	T(°C)	X(g/kg)	T(°C)	X(g/kg)
30Rpm	2m/s	35	20	28.77	11.94	25	10
15Rph	2m/s	30	8	55.9	2.56	90	8

#### 4.4.6. Sensitivity of the individual parameters

In this section the effect and the importance of the individual parameters such as mass flow rate or air velocity, wheel speed, diameter of air passages, desiccant thickness and inlet conditions of air temperature and humidity for process air stream as well as inlet air temperature of regeneration stream on the outlet air conditions and dehumidification effectiveness will be examined. The evaluation is carried out for a dehumidifier wheel with silica gel as desiccant material and the sorption curve used in the simulation is a correlation for silica gel using different isotherm functions given in the literature <sup>[8,2]</sup> or :

$$W = 0.348\phi^{1/1.5} \quad (4.53)$$

The dehumidifier effectiveness is defined as given in Equation 4.50. The initial conditions of humidity for inlet air affects on the effectiveness and outlet temperature as it has been shown in Figures 4.27a and b, 4.28a and b. For the dehumidifier the inlet airs for both process air and regeneration air have the same absolute humidity, but different temperatures. Figure 4.27 b shows that the dehumidifier effectiveness decreases with increasing the inlet air temperature.

A simple linear function can be proposed to show the variation of outlet air temperature with inlet air temperature. As shown in Fig 4.28b, outlet air temperature increases with inlet air temperature. The wheel speed is one of the most important parameters in the dehumidification process itself and in many other applications. The dehumidification effectiveness for a desiccant wheel depends on the regeneration temperature as indicated in figure 4.27c. Figure 4.28c shows the increase of outlet air temperature with regeneration air temperature. Regarding modeling and the mass transfer equations in this chapter, the moisture diffusion in solid layer has been neglected. As mentioned before in this section, for constant wall thickness in the solutions here (0.2 mm) there is limitation in selecting the range for the size of air passages. This simplification is not an appropriate assumption when the gap or air passage diameter is small or the thickness is large <sup>[71]</sup>. Therefore, for constant air passage gap for the solutions here (2.33 mm) there is a limitation in selecting the range for size of wall thickness. Figures 27d and 28d show the effect of solid layer thickness on outlet air temperature and humidity efficiency. The variation of outlet air conditions with mass flow rate is considerably high and it can be regarded as an important parameter for design purposes.

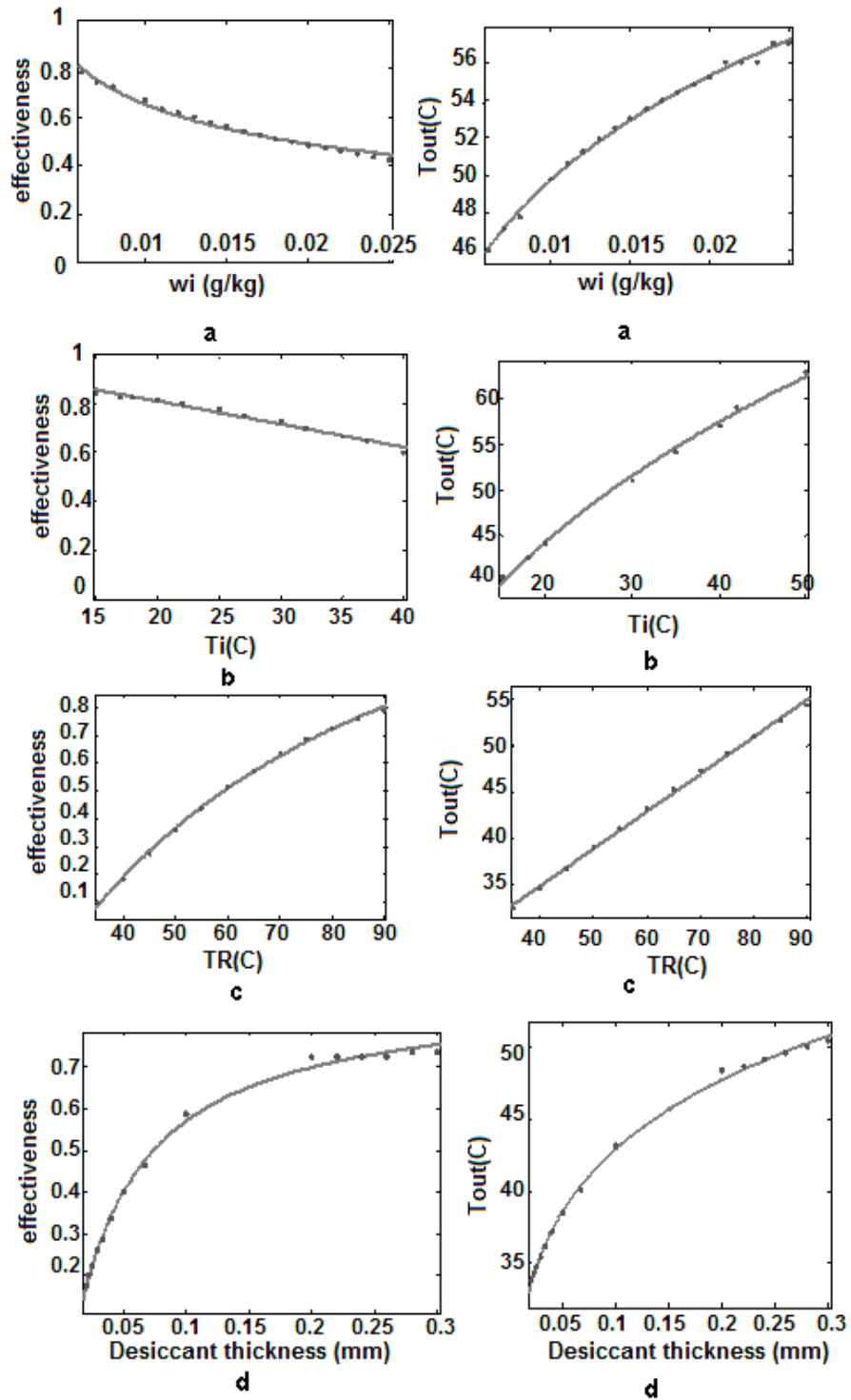
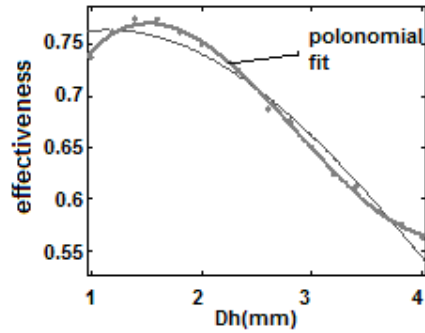
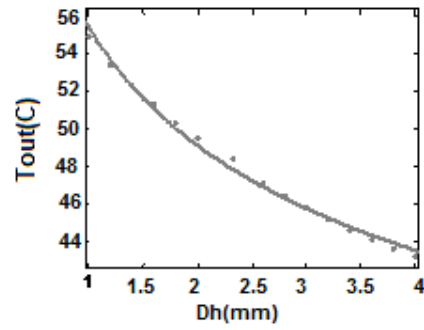


**Figure 4.27.** Sensitivity of the individual parameters for humidity effectiveness

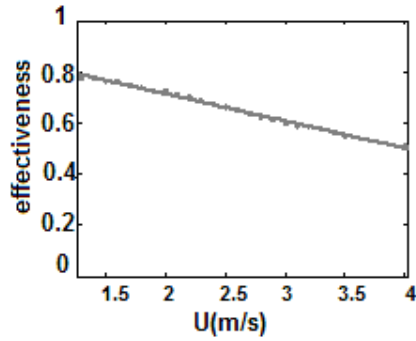
**Figure 4.28.** Sensitivity of the individual parameters for outlet air temperature



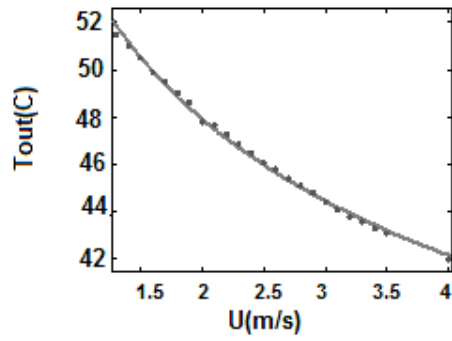
e



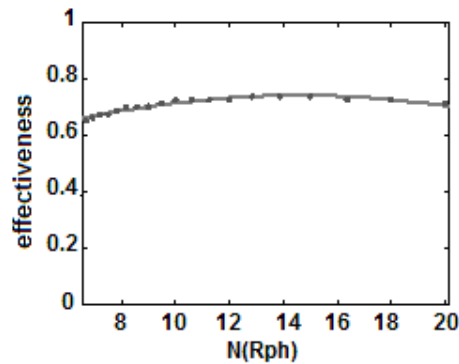
e



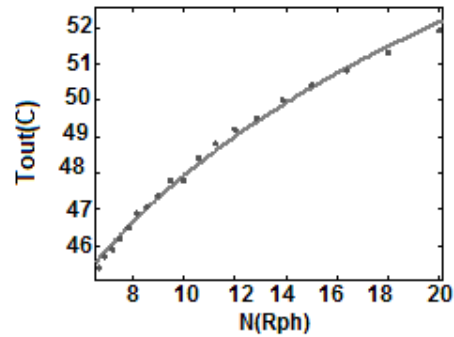
f



f



g



g

Figure 4.27. (Continued)

Figure 4.28. (Continued)

According to the simulation data, the effect of air passages on the wheel effectiveness and outlet temperature are shown in figures 4.27e and 4.28e. The simulation data for different mass flow rates based on different air velocities are shown in figure 4.27f, and 4.28f. The results in figure 4.27g and 4.28g suggest that the wheel speed affects the effectiveness and outlet air temperature and considerably impacts the outlet air relative humidity and enthalpy. These profiles have been produced from simulation of a wheel with the following characteristics: layer thickness of 0.2 mm, 2.25 mm hydraulic diameter of air channels, wheel depth of 20 cm, optimum speed of 15 Rph, air

temperature of 30°C, humidity of 8 gr/kg for inlet air, temperature of 90°C with the same humidity for regeneration air.

#### **4.5. The correlations for outlet air conditions for a desiccant wheel as dehumidifier**

To simulate an air conditioning cycle with a desiccant wheel as a component the physical model is needed to be connected to the other models made for the other components such as heat exchangers and humidifier and building models. The subroutine program is needed to provide for averaging of outlet air conditions of the wheel. However, using averaging subprogram, the computer calculation time to produce stable conditions was long. The model requires certain reiterations to find the best initial conditions of saturated air in the desiccant layers.

After almost 5 cycles the program can find the best initial conditions and stable solutions for outlet air condition. But because of moving averaging method the stable conditions are achieved after a long time that is not practical when simulating the cycle for longer time periods of input data. The solution was to reduce the first four cycles.

The improvised program reduces the primary solutions in iteration processes and gives the stable conditions as output in the 5<sup>th</sup> cycle. It takes almost 2 minutes of calculation time for each input data of outside air conditions.

Although this improvised model is able to produce steady state conditions in acceptable calculation time and can be connected to the other building models, the memory needed to simulate a typical air conditioning cycle for a whole year is still very high.

This problem can be solved by making simplified equations to produce outlet air conditions according to inlet air conditions and the wheel speed. The improved Simulink model is able to produce a large number of solutions in a short time. Therefore 3000 data could be produced in 3 working days. The range of input data was 15°C to 35 °C for air temperatures and 4 gr/kg to 16 gr/kg for air humidity.

##### **4.5.1. Correlations**

With these input conditions, 3000 solutions of the model were produced according to different wheel speed of 10 to 18 revolutions per hour. In addition, the range of air speed was from 0.5 to 3.5 m/s. The regeneration temperature was chosen from 35-90 °C.

Having produced data, an optimization routine in Matlab can produce different mathematical functions to correlate these data in simple equations for outlet air conditions of temperature and humidity. The range of variation of these conditions is fairly vast. In addition, the nonlinear behavior and complexity of the system for the



variations of different parameters required a comprehensive study on sensitivity of model.

Having studied the sensitivity of solutions and evaluating the behavior of model solutions for air conditions in the Mollier diagram, two variables needed to correlate different physical properties to outlet air conditions have been chosen. These variables are:

$$\frac{\Delta T}{\Delta X} \text{ and } \frac{\Delta T}{T_R}.$$

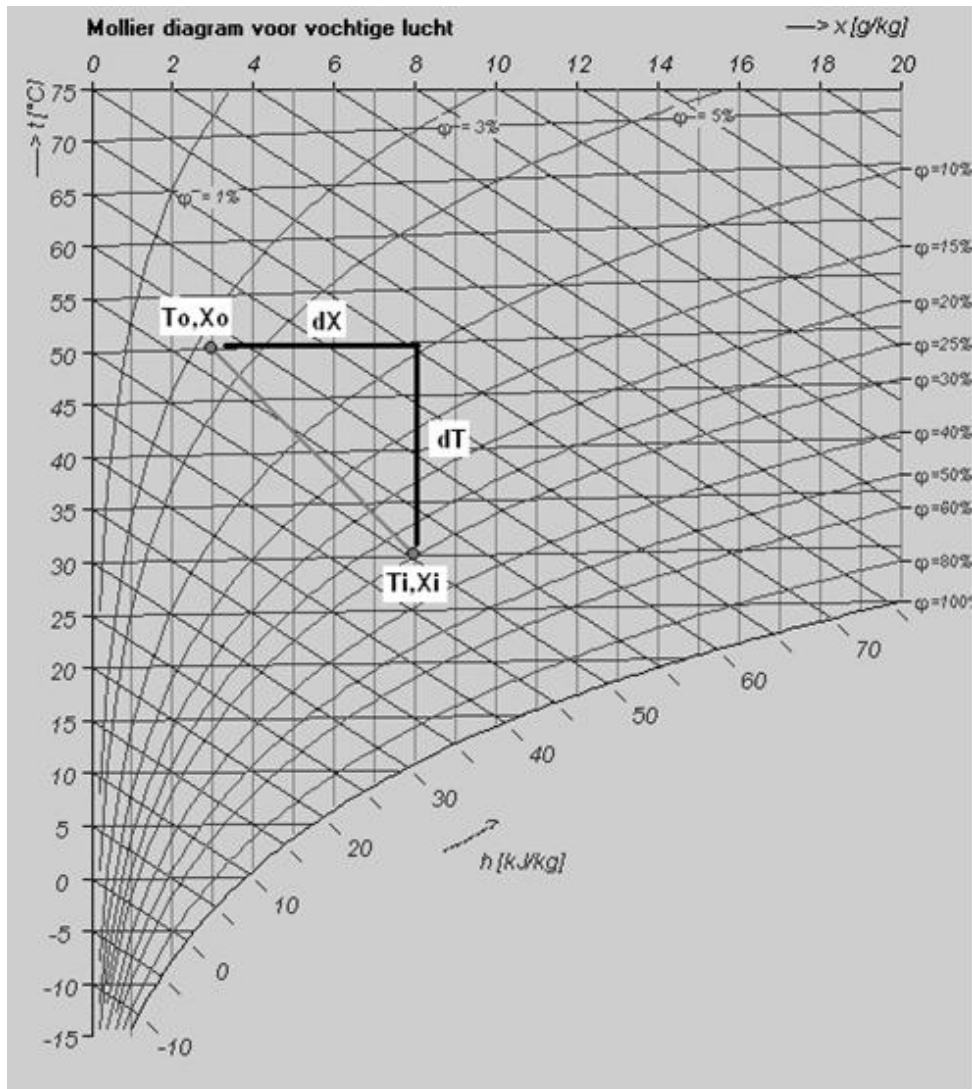


**Figure 4.29.** The meaning of selected function on the Mollier diagram

The first variable is variations of air temperature divided by the variations of air humidity after passing the wheel. This variable can be better understood on the Mollier diagram as shown in figure 4.29. Adsorption is a constant enthalpy phenomenon, however, the enthalpy of air after passing through rotating wheel, between hot and process air stream, changes only by sensible heat exchange between the two air streams. As it can be observed in this figure,  $\frac{\Delta T}{\Delta X}$  is related to the slope of the line connecting inlet and outlet air conditions in the Mollier diagram. Sensitivity analyses show that this variable changes very slowly for a known range of conditions and is almost constant in that area.

This fact helps relating the linear functions that correlate different parameters to each other. For the 3000 data produced by simulation, this function was calculated and different area was selected to make different correlations according to the range of variations of this variable. Fortunately, the variable for practical range of the air and wheel conditions that is fairly large is not changing a lot and remains almost constant. In addition, sensitivity analysis showed that the regeneration temperature  $T_R$  has a significant effect on the variations of outlet air conditions; therefore, the other variable  $\frac{\Delta T}{T_R}$  has been selected as an appropriate function to make the second correlation.

Following this methodology and considering the range and amounts of these two variables for the 3000 data, produced by the physical model, different area was designated for optimization routine in Matlab. More than 1500 data in the range were given by equations (4.54) to (4.58) and the simplified equations have been developed.

$$\text{inlet air temperature: } 15^\circ C \leq T_i \leq 35^\circ C \quad (4.54)$$

$$\text{inlet air humidity for both air streams: } 5 \text{ gr/kg} \leq X_i, X_R \leq 12 \text{ gr/kg} \quad (4.55)$$

$$\text{inlet air speed: } 1.5 \text{ m/s} \leq V \leq 3.5 \text{ m/s} \quad (4.56)$$

$$\text{WheelSpeed: } 10 \text{ RpH} \leq N \leq 18 \text{ RpH} \quad (4.57)$$

$$\text{Regeneration air temperature: } 60^\circ C \leq T_R \leq 90^\circ C \quad (4.58)$$

The correlation created in Matlab will be more accurate when used for the data with the more number of frequencies and less accurate when used for the data with less frequency in the list of generated data. Therefore, the large numbers of data was chosen in the most practical area based on weather data and design conditions of wheel and air speed.

The correlations are:

$$\left| \frac{\Delta T}{\Delta X} \right| = 0.0723N - 0.286V - 0.0401X_R - 0.178X_i + 0.0225T_R + 0.0077T_i + 3.7833 \quad (4.59)$$

$$\frac{\Delta T}{T_R} = -0.0053T_i - 0.0527V + 0.0041N - 0.003X_R + 0.0127X_i + 0.001T_R + 0.3042 \quad (4.60)$$

Therefore the outlet air humidity and temperature can be calculated by:

$$T_{out} = T_{in} + T_R \frac{\Delta T}{T_R} \quad (4.61)$$

$$X_{out} = X_{in} - \frac{T_{out} - T_{in}}{\left| \frac{\Delta T}{\Delta X} \right|} \quad (4.62)$$

In these equations  $X_R$  and  $X_i$  are the air humidity of regeneration air and inlet air, respectively expressed in gr/kg dry air;  $V$  and  $N$  are air velocity and wheel rotational speed expressed in m/s and revolution per hour, respectively; and  $T_R$  and  $T_i$  are regeneration and inlet air temperatures expressed in °C, respectively.

#### 4.5.2. Accuracy of Correlations

Figures 4.30 and 4.31 show a comparison between the air conditions calculated using the correlations and the air conditions calculated by the simulation model.

In figure 4.30 the outlet air temperature has been calculated from the correlation for almost 1500 data with  $\pm 2.8\%$  error when comparing the simulation results for the inlet air and the wheel speed in the range given by equations (4.54) to (4.58).

Figure 4.31 shows a similar comparison but for air humidity with  $\pm 8.5\%$  error. The definition of error is based on a reference value that is an average of all conditions.

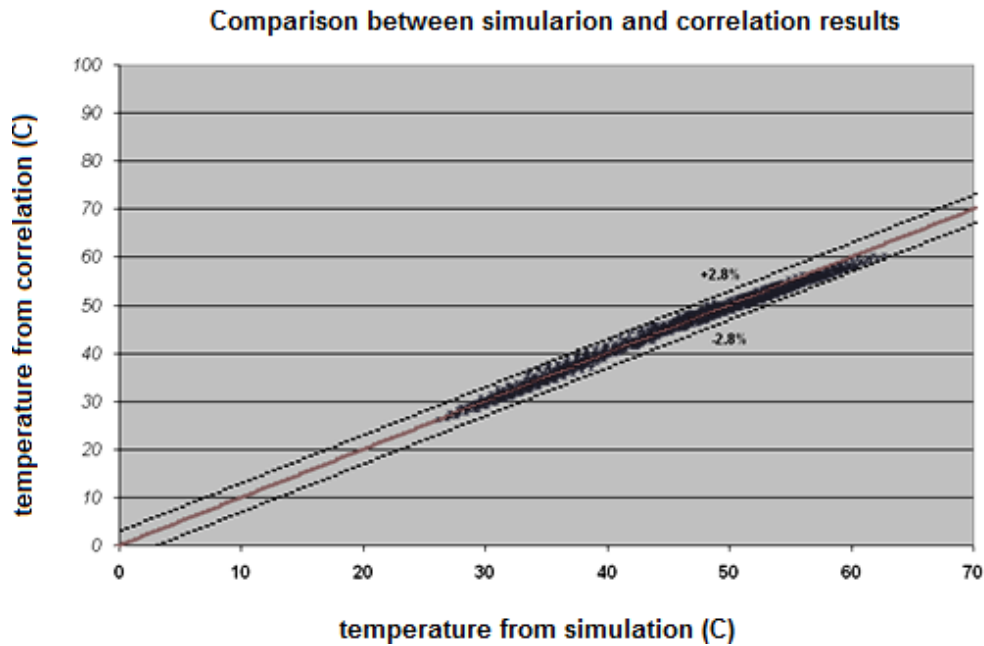


**Figure 4.30.** The comparison between simulation solutions and the results of the correlations given by equations (4.59) and (4.60) for air temperatures

The frequency of the errors for these 1500 data has been shown by the histogram in figure 4.32. The optimization routine in Matlab can calculate the coefficients in equations (4.59) and (4.60) more accurately for area with higher frequency.

Therefore, the data are chosen in the most practical area according to the weather data are shown in figure 4.33. The different areas on the diagram have been categorized according to cooling load and probability. The highest cooling load has been calculated for area 11. Areas 12, 7, 4,5,9,3, and 13 were next, respectively. For cooling load this selection highly depends on the orientation of the building and the type of solar shading.

The areas with the error more than 8.5% are related to the data in the boundaries of the range given by equations (4.54) to (4.58). For this reason the frequency for the lower errors is larger in figure 4.32.

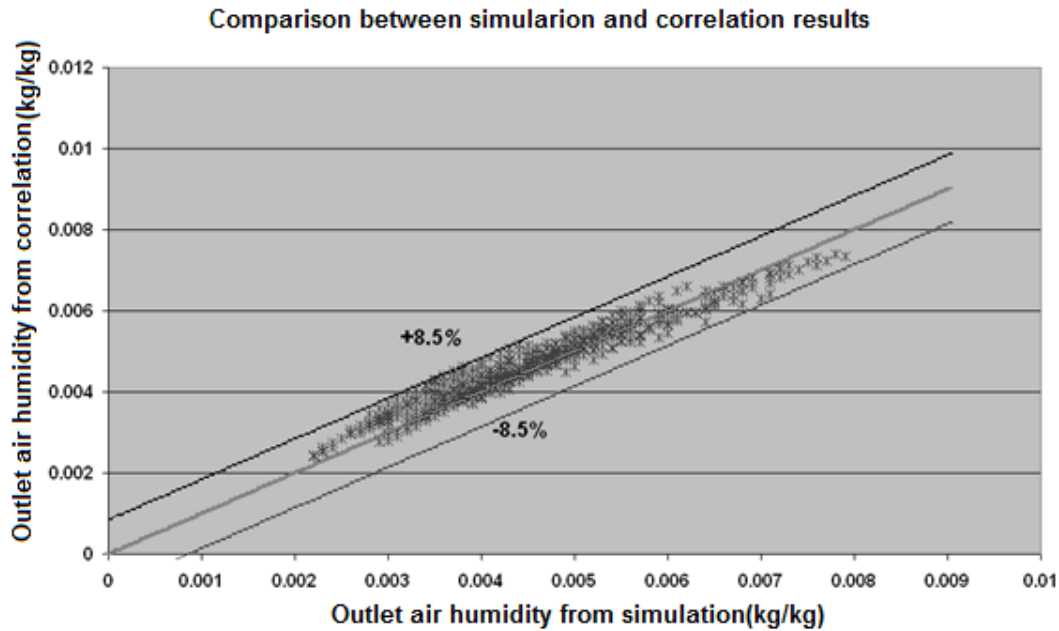


**Figure 4.31.** The comparison between simulation and the correlations

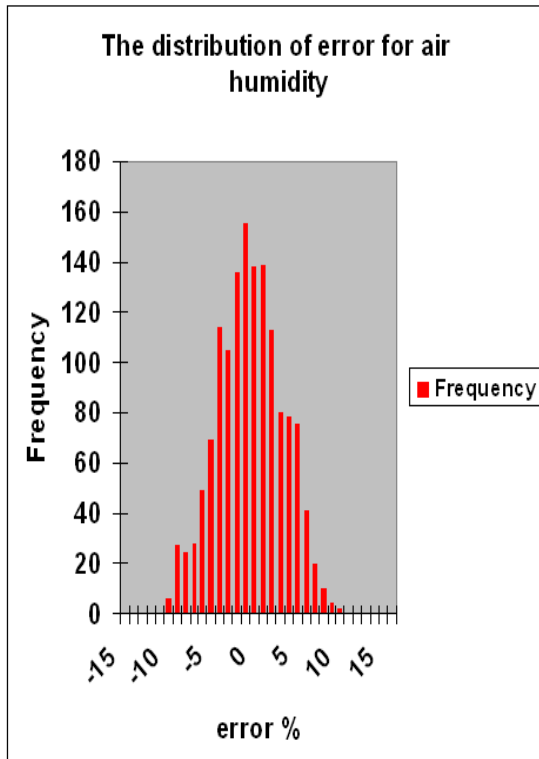


**Figure 4.32.** The frequency of error of results of air humidity given by the correlations

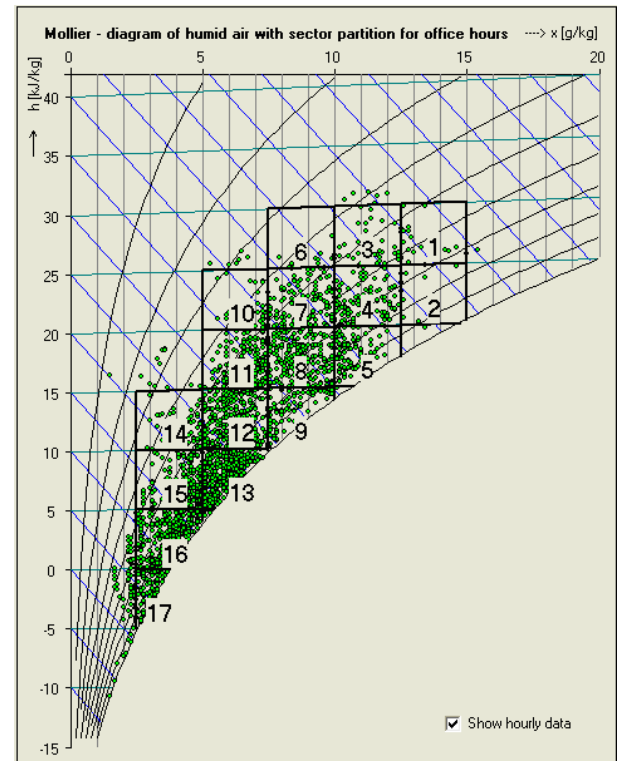


**Figure 4.33.** The weather data or air conditions that happen in Holland during a year (the reference year 1964) on the Mollier diagram

#### 4.5.3. The effect of errors in correlations on the results of simulation of a typical cooling cycle for supply air conditions

Figure 4.34 shows the variation of air conditions on the Mollier diagram for a simple desiccant cooling cycle. The air with the conditions shown as A1 passes from desiccant wheel and dried and heated up to the point B1. Then after a heat exchanger with 72% efficiency it will be cooled down to C1, and with a simple evaporative cooler it reaches to the conditions shown as D1 in the Mollier diagram. The points C2 and D2 are the air conditions if the air after passing the desiccant wheel is in B2. This means that a maximum error of 20% to calculate air humidity of B has resulted in 7% error for supply air temperature of D. These typical results indicate that the error in calculation of the supply air in a desiccant wheel system is reduced by 3 times when compared to the error in the calculation of the air conditions after the wheel.

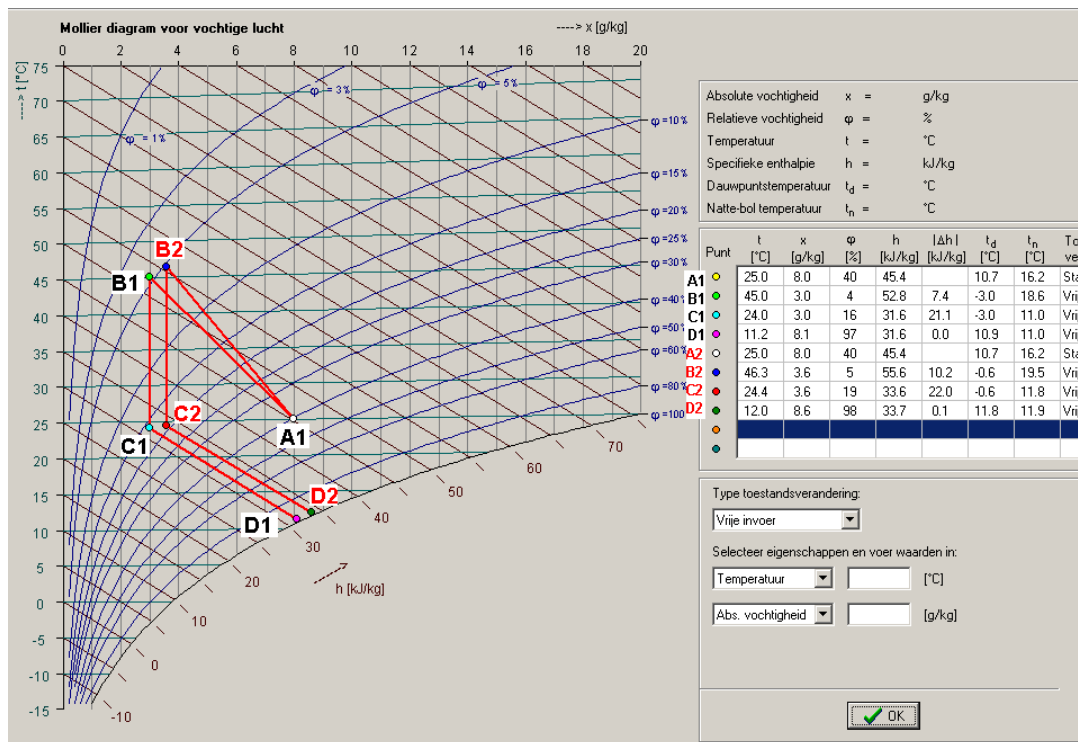


**Figure 4.34.** The figures of B1, C1, D1 show the air condition on the Mollier diagram in different parts of a cooling cycle while B2, C2, D2 show them if they have been calculated with maximum error for humidity and temperature

#### 4.5.4. Sensitivity Studies and Control Variables

The simplified equations or correlations to calculate outlet air conditions given in the previous parts of this chapter have been presented according to inlet air conditions for both air streams as well as the most important parameters.

These parameters are wheel speed and air velocity. In figures 4.35 and 4.36 the sensitivity of model solutions for outlet air conditions of temperature and humidity as a function of different physical parameters have been shown.

The data are for a typical air condition of 30°C and 8gr/kg for adsorption air and 80°C and same humidity for regeneration. The air velocity and wheel speed are 2 m/s and 15 Rph, respectively. In addition, these normalized profiles can help to recognize the most important parameters for controlling the desiccant cooling systems. Regeneration temperature is the most effective variable for controlling these systems.

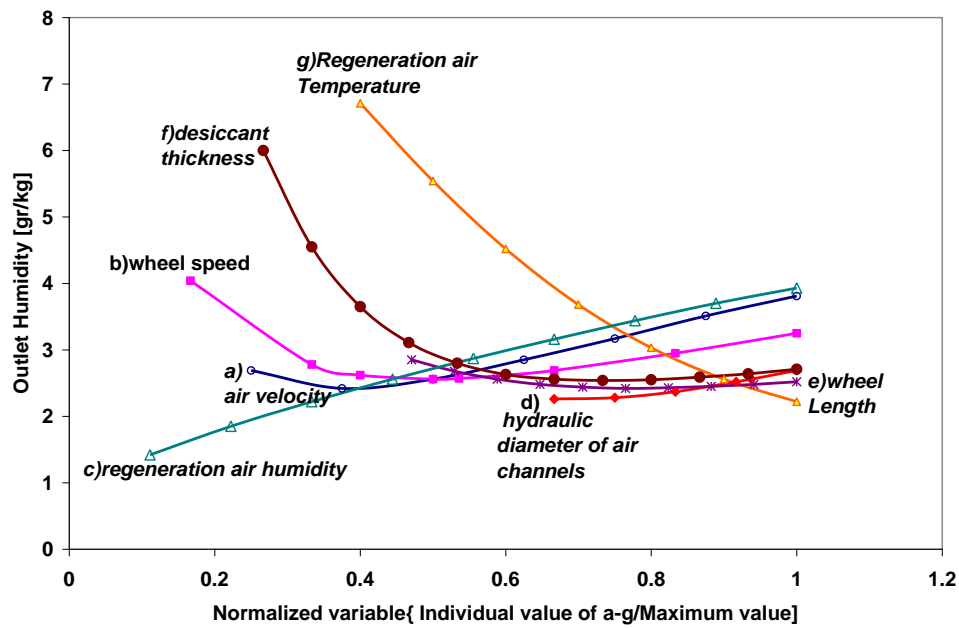


*Figure 4.35. Comparison of the effect of different parameters by normalized variables for outlet air humidity*

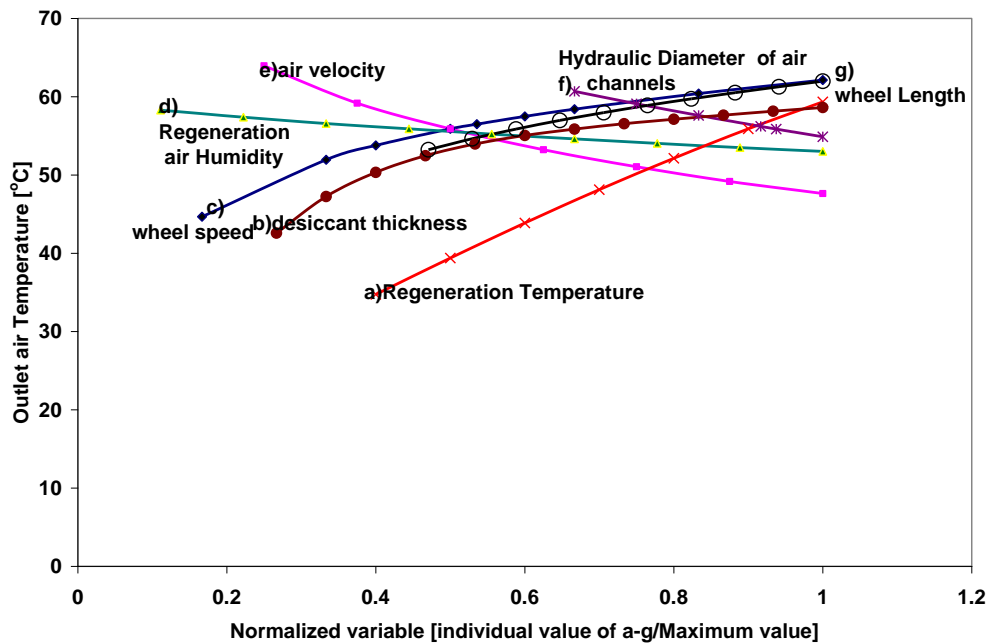


*Figure 4.36. Comparison of the effect of different variables by normalized variables (value of variable divided by maximum value) for outlet air temperature*

The outlet air conditions can be well approximated as a linear function of the regeneration temperature. In other words, the process gain factor or the derivative of this profile for the temperature decrease is considerable and almost constant. Therefore, it is an appropriate variable for control purposes. As it can be seen in these figures optimal values for characteristic of desiccant matrix are desiccant thickness and the air passages sizes. The increase of these parameters does not have a significant influence on outlet air conditions. The characteristics of sorption matrixes as designed by the manufactures are usually in the optimum value shown in these figures.

## 4.6. Analytical approach

The correlations derived in this chapter can be used only in the limited range of air conditions given by equations (4.54) through (4.58). Even in the boundaries of the limited range the error can be significant. Therefore, an analytical approach which can be derived from simplification assumptions was carried out and will be presented in this part.

### 4.6.1. The basic equations of heat and mass transfer

The basic equations of heat and mass transfer for air and the air in saturated layer in desiccant material were derived in this chapter as:

$$\rho C A dx \frac{\partial T}{\partial t} = \rho C u A (T - (T + \frac{\partial T}{\partial x} \partial x)) + h A' (T_m - T) \quad (4.63)$$

$$\frac{\partial T}{\partial t} = u(-\frac{\partial T}{\partial x}) + \frac{h A'}{\rho C A dx} (T_m - T) \quad (4.64)$$

In the steadystate conditions for air heat transfer equation will be as:

$$\frac{dT}{dx} = \frac{h A'}{u \rho A C dx} (T_m - T) \quad (4.65)$$

$$\frac{dT}{dx} = \frac{4h}{u \rho d_e C} (T_m - T) \quad (4.66)$$

In a similar way for mass transfer equation for air:

$$\frac{dX}{dx} = \frac{4h}{u C d_e \rho} (X_m - X) \quad (4.67)$$

$$\frac{dX}{dx} = \frac{4h}{u C d_e \rho} (X_m - X) \quad (4.68)$$

$$Le = 1, \frac{A'}{A dx} = \frac{4}{d_e}, \frac{A'}{A dx} = \frac{1}{\delta}$$



$X_m$  : air humidity in the saturated layer of Desiccant. Heat transfer equation for desiccant layer can be written as:

$$\rho_d C_d A_t dx \frac{\partial T_d}{\partial t} = h A' (T - T_m) + q A_t \rho_d dx \frac{\partial W}{\partial t} \quad (4.69)$$

$A_t$  = Total cross section surface of desiccant and Aluminum layer

$A'$  = Heat and mass transfer surface

$$A_t = \pi((R + \delta)^2 - R^2) \approx 2\pi R \delta = d_e \delta \pi \quad (4.70)$$

$\delta$  is half of the coating layer thickness . Therefore:

$$\rho_d C_d A_t dx \frac{\partial T_d}{\partial t} = h_m q A' (X - X_m) + h A' (T - T_m) \quad (4.71)$$

$$\frac{dT_d}{dt} = \frac{dT_m}{dt} = \frac{h q}{\rho_d C_d \delta C} (X - X_m) + \frac{h}{\rho_d C_d \delta} (T - T_m) \quad (4.72)$$

Mass transfer equation for solid layer will be as:

$$\frac{\partial W}{\partial t} \rho_d A_t dx = h_m A' (X - X_m) \quad (4.73)$$

Since the information about adsorbed amount of water vapor is given according to relative humidity of air it can be written as:

$$\frac{\partial W}{\partial t} = \frac{\partial W}{\partial \phi} \frac{\partial \phi}{\partial X_m} \frac{\partial X_m}{\partial t} + \frac{\partial W}{\partial \phi} \frac{\partial \phi}{\partial T_m} \frac{\partial T_m}{\partial t} = S_1 \frac{\partial X_m}{\partial t} + S_2 \frac{\partial T_m}{\partial t} \quad (4.74)$$

For example for a typical sorption curve as:

$$W = 0.348 \phi^{1/1.5} \quad (4.75)$$

it can be written as:

$$\phi = 10^{-6} \exp\left(\frac{5294}{T_m + 273.2}\right) \times \frac{X_m}{(1 + 1.61 X_m)} \quad (4.76)$$

$$S_1 = 0.23 \phi^{-0.33} \exp\left(\frac{5294}{T_m + 273.2}\right) \times \frac{10^{-6}}{(1 + 1.61 X_m)^2} \quad (4.77)$$

$$S_2 = 0.23 \phi^{0.4} \frac{-5294}{(273.2 + T_m)^2} \quad (4.78)$$

Therefore in general it can be written according to  $S_1$  and  $S_2$  as:

$$S_1 \frac{dX_m}{dt} + S_2 \frac{dT_m}{dt} = \frac{h_m A'}{\rho_d A_t dx C_d} (X - X_m) \quad (4.79)$$

$$S_1 \frac{dX_m}{dt} = \frac{h_m A'}{\rho_d A_t dx C_d} (X - X_m) - S_2 \left( \frac{h q}{\rho_d C_d \delta C} (X - X_m) + \frac{h}{\rho_d C_d \delta} (T - T_m) \right)$$

$$\frac{dX_m}{dt} = (X - X_m) \left( \frac{h}{S_1 C_d \rho_d \delta C} - \frac{h S_2 q}{\rho_d C_d \delta C S_1} \right) - \frac{h S_2}{\rho_d S_1 C_d \delta} (T - T_m) \quad (4.80)$$

$$(4.81)$$

Therefore the coupled and nonlinear heat and mass transfer equations for air and solid are derived as:

$$\frac{dT}{dx} = \alpha(T_m - T) \quad (4.82)$$

$$\frac{dX}{dx} = \alpha(X_m - X) \quad (4.83)$$

$$\frac{dX_m}{dt} = \beta_0(X - X_m) + \beta_1(T - T_m) \quad (4.84)$$

$$\frac{dT_m}{dt} = \lambda(X - X_m) + k(T - T_m) \quad (4.85)$$

Where:

$$\alpha = \frac{4h}{u \rho_d C} \quad (4.86)$$

$$\beta_0(T_m, X_m) = \frac{h - h S_2 q}{S_1 \rho_d C_d \delta C} \quad (4.87)$$

$$\beta_1(T_m, X_m) = -\frac{h S_2}{\rho_d S_1 C_d \delta} \quad (4.88)$$

$$\lambda = \frac{h q}{\rho_d C_d \delta C} \quad (4.89)$$

$$k = \frac{h}{\rho_d C_d \delta} \quad (4.90)$$

#### 4.6.2. The approach and solutions

It can be assumed that the saturated air temperature in the small length of wheel is constant, and only varies with time or  $\bar{T}_m(t)$ . In other words, the lumped model can be applied for saturated air temperature and humidity so:

$$\frac{\partial \bar{T}_m}{\partial x} \approx 0 \quad (4.91)$$

$$\frac{dT}{dx} - \frac{d\bar{T}_m}{dx} = \alpha(\bar{T}_m - T) \quad (4.92)$$

$$\frac{d(\bar{T}_m - T)}{(\bar{T}_m - T)} = -\alpha dx \quad (4.93)$$

After integrating in the length of the wheel L:

$$Ln \frac{(\bar{T}_m - T_{out})}{(\bar{T}_m - T_{in})} = -\alpha L \quad (4.94)$$

$$\exp(-\alpha L) = \frac{\bar{T}_m - T_{out}}{\bar{T}_m - T_{in}} \quad (4.95)$$

$$T_{OUT} = e^{-\alpha L} (T_i - \bar{T}_m) + \bar{T}_m \quad (4.96)$$

$$\bar{T}_m = \frac{T_{OUT} - e^{-\alpha L} T_i}{(1 - e^{-\alpha L})} \quad (4.97)$$

Similarly:

$$X_{OUT} = e^{-\alpha L} (X_i - \bar{X}_m) + \bar{X}_m \quad (4.98)$$

$$\bar{X}_m = \frac{X_{OUT} - e^{-\alpha L} X_i}{(1 - e^{-\alpha L})} \quad (4.99)$$

The integrating of the equations heat and mass transfer for solid layer may result in useful parameters of average of outlet air humidity and temperature:

$$\int_0^{t_0} \frac{dT_m}{dt} = \int_0^{t_0} \lambda (X - X_m) + \int_0^{t_0} k (T - T_m) \quad (4.100)$$

$t_0$  is the time for a revolution that is related to wheel speed  $N$  as:

$$t_0 = \frac{3600}{2N} \quad (4.101)$$

$$T_m(t_0) - T_m(0) = \lambda t_0 (\bar{X}_{out} - \bar{X}_m) + k t_0 (\bar{T}_{out} - \bar{T}_m) \quad (4.102)$$

$$T_m(0) \approx T_i \quad (4.103)$$

$$T_m(t_0) \approx \frac{\bar{T}_{out} - e^{-\alpha L} T_i}{(1 - e^{-\alpha L})} \quad (4.104)$$

It can be assumed that at the optimum Speed:  $T_{out}(t_0) \approx \bar{T}_{out}$ , therefore:

$$\begin{aligned} 0 &= \lambda t_0 \left(1 - \frac{1}{1 - e^{-\alpha L}}\right) \bar{X}_{out} + \left(k t_0 \left(1 - \frac{1}{1 - e^{-\alpha L}}\right) - \frac{1}{1 - e^{-\alpha L}}\right) \bar{T}_{out} \\ &+ \frac{e^{-\alpha L} k t_0 T_i}{1 - e^{-\alpha L}} + \frac{e^{-\alpha L} \lambda t_0 X_i}{1 - e^{-\alpha L}} - \frac{-e^{-\alpha L} T_i}{1 - e^{-\alpha L}} + \bar{T}_i \end{aligned} \quad (4.105)$$

Also, for mass transfer equation the similar integrating can be done:

$$\int_0^{t_0} \frac{dX_m}{dt} dt = \int_0^{t_0} \beta_0 (X - X_m) dt + \int_0^{t_0} \beta_1 (T - T_m) dt \quad (4.106)$$

It is desirable to simplify this integral with some assumptions to calculate the average of outlet air conditions:

$$X_m(t_0) - X_m(0) \approx \bar{\beta}_0 t_0 (\bar{X}_{out} - \bar{X}_m) + \bar{\beta}_1 t_0 (\bar{T}_{out} - \bar{T}_m) \quad (4.107)$$

$$X_m(0) \approx X_0, X_m(t_0) \approx \frac{X_{out}(t_0) - e^{-\alpha L} X_i}{(1 - e^{-\alpha L})}, \text{in optimum Speed: } X_{out}(t_0) = \bar{X}_{out}$$

$$\frac{X_{out}(t_0) - e^{-\alpha L} X_i}{(1 - e^{-\alpha L})} = \bar{\beta}_0 t_0 (\bar{X}_{out} - \bar{X}_m) + \bar{\beta}_1 t_0 (\bar{T}_{out} - \bar{T}_m) \quad (4.108)$$

$$0 = \bar{X}_{out} (1 + \bar{\beta}_0 t_0 - \frac{\bar{\beta}_0 t_0}{1 - e^{-\alpha L}} - \frac{1}{1 - e^{-\alpha L}}) + \bar{T}_{out} (\bar{\beta}_1 t_0 - \frac{\bar{\beta}_1 t_0}{1 - e^{-\alpha L}}) + \frac{\bar{\beta}_0 t_0 e^{-\alpha L} X_i}{1 - e^{-\alpha L}} + \frac{e^{-\alpha L} X_i}{1 - e^{-\alpha L}} + \frac{\bar{\beta}_1 t_0 e^{-\alpha L} T_i}{1 - e^{-\alpha L}} \quad (4.109)$$

$$a \bar{X}_{out} + b \bar{T}_{out} = c \quad (4.110)$$

$$d \bar{X}_{out} + e \bar{T}_{out} = f \quad (4.111)$$

So:

$$\begin{aligned} a &= \lambda t_0 (1 - \frac{1}{1 - e^{-\alpha L}}) \\ b &= (k t_0 (1 - \frac{1}{1 - e^{-\alpha L}}) - \frac{1}{1 - e^{-\alpha L}}) \\ c &= -\frac{e^{-\alpha L} k t_0 T_i}{1 - e^{-\alpha L}} - \frac{e^{-\alpha L} \lambda t_0 X_i}{1 - e^{-\alpha L}} + \frac{e^{-\alpha L} T_i}{1 - e^{-\alpha L}} - T_i \\ d &= (1 + \bar{\beta}_0 t_0 - \frac{\bar{\beta}_0 t_0}{1 - e^{-\alpha L}} - \frac{1}{1 - e^{-\alpha L}}) \\ e &= (\bar{\beta}_1 t_0 - \frac{\bar{\beta}_1 t_0}{1 - e^{-\alpha L}}) \\ f &= \frac{-e^{-\alpha L} (X_i (\bar{\beta}_0 t_0 + 1) + \bar{\beta}_1 t_0 T_i)}{1 - e^{-\alpha L}} \end{aligned} \quad (4.112)$$

#### 4.6.3. The investigation of the simplified assumptions

The equation of mass transfer or equation (4.84) is nonlinear according to the coefficients of  $\beta_0(T_m, X_m)$  and  $\beta_1(T_m, X_m)$ . Integrating of the equation (4.106) was done with a very simplified assumption that it needs to be studied.

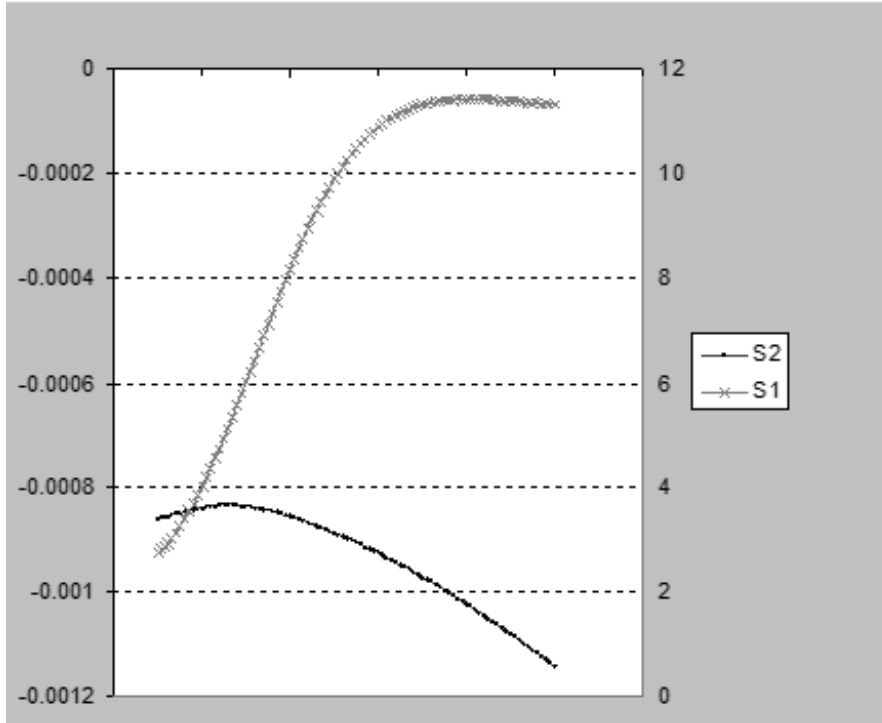


**Figure 4.37.** The functions of  $S_1(T_m, X_m)$  and  $S_2(T_m, X_m)$  according to time for a revolution or after  $t_0$  seconds

Figure 4.37 shows the functions of  $S_1(T_m, X_m)$  and  $S_2(T_m, X_m)$  change with respect to time for a revolution or after  $t_0$  seconds.

Figure 4.38 shows the behavior of  $\beta_1(T_m, X_m)$  and  $\beta_0(T_m, X_m)$  during a revolution as they are defined as functions of  $T_m, X_m$  through equations (4.87) and (4.88). Figure 4.39 represents the term of integration given by model as:

$$\int_0^{t_0} \beta_0(X - X_m) dt \quad (4.112)$$

The blue line (real values using model), presented as real in figure 4.39, represents the integration described in equation (4.113), and calculated by model. In this figure it has been named and shown as real values.

The red line (simplified with assumptions) is the result of the approximation given by assumption made in equation (4.107).

The same analogy can be carried out for the integration of:

$$\int_0^{t_0} \beta_1(T - T_m) dt \quad (4.113)$$

As it can be observed in figure 4.40 the difference in real result of the integrating term of (4.114) with the approximation value given by (4.107) illustrates the effectiveness of this assumption implemented by this approach.

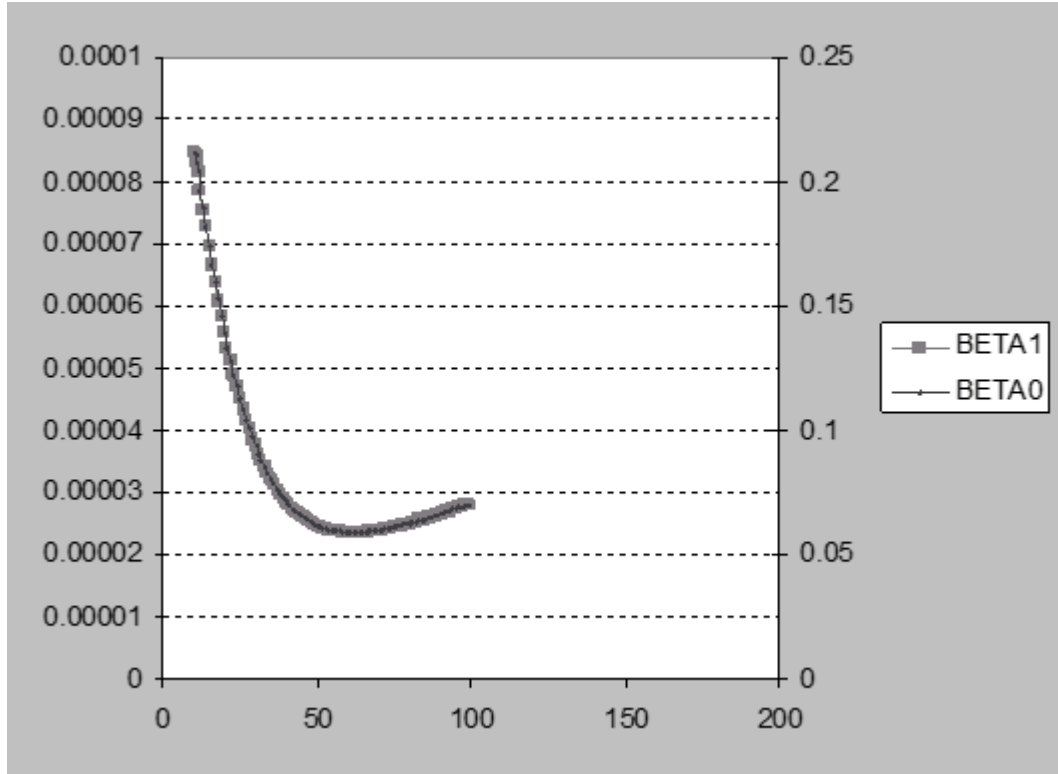


**Figure 4.38.** The behavior of  $\beta_1(T_m, X_m)$  and  $\beta_0(T_m, X_m)$  during a revolution as they are defined by equations (4.87) and (4.88)

#### 4.6.4. Example

A Simulink model has been made to calculate the outlet air conditions of a desiccant wheel from this approach. This model can easily be connected to the other building models for any long term simulation of different air conditioning cycles. In this part one example has been presented to clearly show how this approach works. The air conditions for both air streams as well as the other characteristics of wheel and air have been given by:

$$\begin{aligned}
 T_{in} &= 30^\circ\text{C}, \quad X_i = 8 \text{ gr/kg}, \quad N = 15 \text{ Rph}, \quad u = 2 \text{ m/s}, \quad \delta = 0.1 \text{ mm}, \quad d_e = 2.25 \text{ mm}, \quad L = 0.2 \text{ m}, \\
 T_R &= 80^\circ\text{C}, \quad X_R = 8 \text{ gr/kg}, \\
 h &= 46.7 \text{ W/K.m}^2, \quad \rho_d = 1400 \text{ kg/m}^3, \quad C_d = 1200 \text{ J/kgK}, \quad C = 1000 \text{ J/kgK}, \quad q = 2500000 \text{ J/m}^2
 \end{aligned}$$

The solutions can be obtained based on trial and error method as:

Initial guess:  $T_o = \frac{T_i + T_R}{2} = 55, X_o = \frac{X_i + X_R}{2} = .004$

$$\bar{S}_1 = S_1(\bar{T}_{mo}, \bar{X}_{mo})$$

$$\bar{S}_2 = 0.3 \times S_2(\bar{T}_{mo}, \bar{X}_{mo})$$

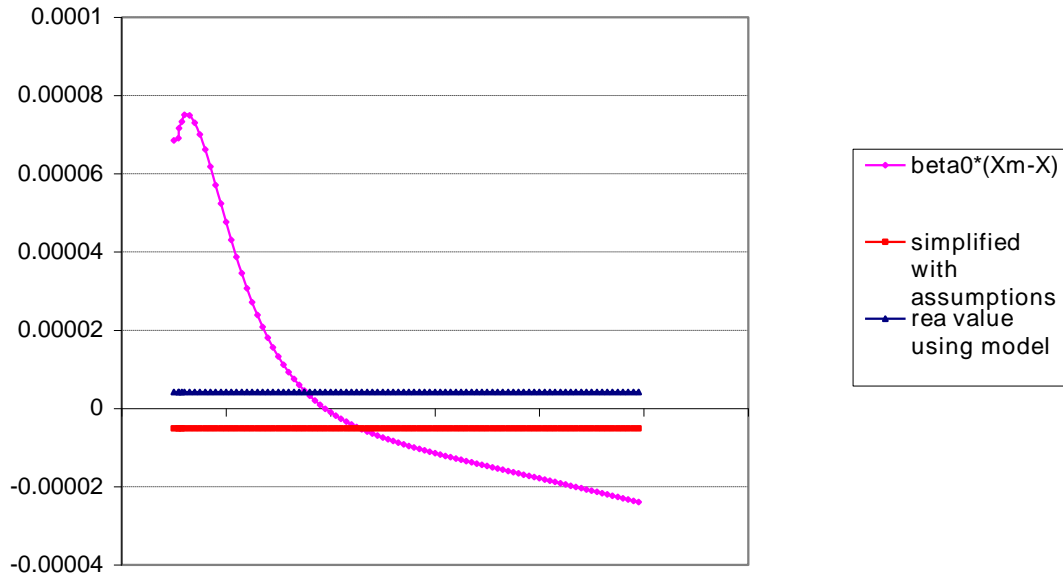


**Figure 4.39.** The comparison between integrating term given by equation (4.107) and calculated by model, with simplified term of (4.113)

$$\alpha = 34.6$$

$$\bar{\beta}_0 = 7.66\text{E-}02$$

$$\bar{\beta}_1 = 3.06\text{E-}05$$

$$\lambda = 695, k = 0.28$$

$$a = -8.26\text{E+}01$$

$$b = -1.03402299$$

$$c = -51.68134404$$

$$d = -1.01\text{E+}00$$

$$e = -3.64\text{E-}06$$

$$f = -0.003189976$$

$$-8.26\text{E+}01\bar{X}_o + -1.03402299\bar{T}_o = -51.68134404$$

$$-1.01\text{E+}00\bar{X}_o + -3.64\text{E-}06\bar{T}_o = -0.003189976$$

$$T_o = 50\text{C}, X_o = 3\text{gr/kg}$$

The trial and error calculations should be continued and completed until the following two conditions are met:

- 1 -  $T_o$  and  $X_o$  are close to  $T_o$  and  $X_o$  from the previous step.
- 2- for  $N_{\text{initial guess}}$  we need to get minimum  $X_o$ .

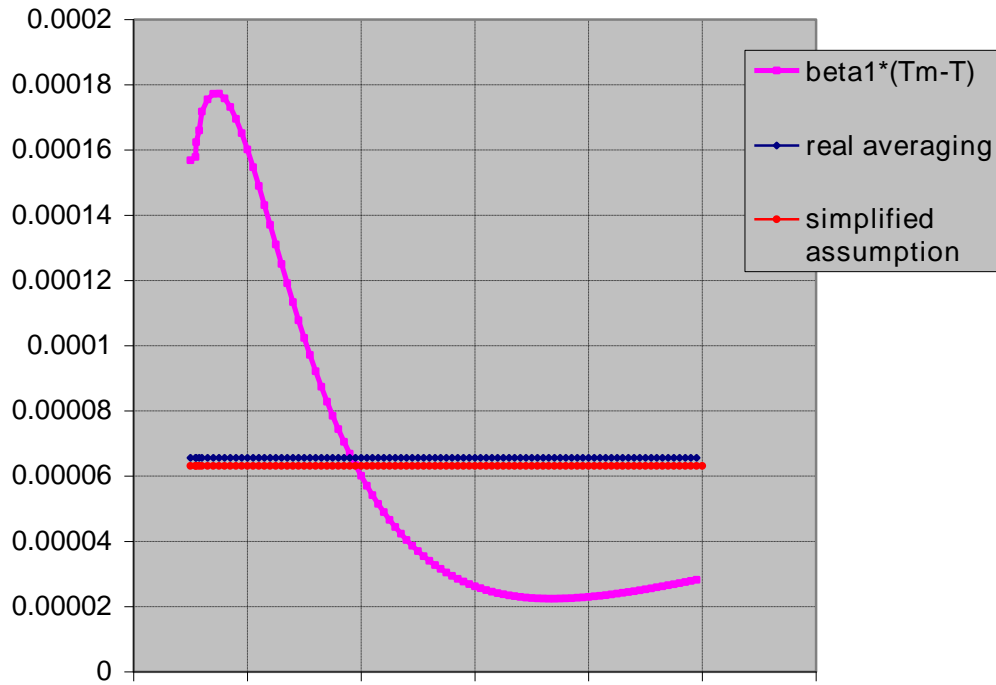


**Figure 4.40.** The difference in real result of the integrating term of (4.107) and approximation value given by (4.114)

## 4.7. Dimensionless groups

The correlation given by (4.59) and (4.60) are based on typical characteristics of commercial desiccant wheels from 3000 data produced by Simulink model and for a typical wheel with given information for desiccant matrix by industries<sup>1</sup>. Therefore, the developments of a correlation based on dimensionless groups that are not limited to a typical matrix are needed to be made. These correlations have been derived using optimization routine in Matlab and using dimensionless groups.

New variables are defined as:

$$T^* = \frac{T}{T_R - T_i} \quad (4.114)$$

$$x^* = \frac{x}{L} \quad (4.115)$$

---

<sup>1</sup> Hoval and DRI wheels



$h$  : heat transfer coefficient

$d_e$  : hydraulic diameter

$u$  : air velocity

$T_m$  : air temperature in the saturated layer of Desiccant

$A'$  : heat transfer surface

$A$  : air flow cross section surface

Therefore the heat transfer equation for air can be written according to new non dimension variables as:

$$\frac{dT^*}{dx^*} \frac{T_R - T_i}{L} = \frac{4h}{u\rho d_e C} (T_R - T_i)(T_m^* - T^*) \quad (4.116)$$

Therefore the dimensionless group of  $C_1$  can be resulted as:

$$\Rightarrow C_1 = \frac{4Lh}{u\rho d_e C} \quad (4.117)$$

New parameter of time can be introduced as:

$$t^* = t \times N \quad (4.118)$$

And for air humidity:

$$X^* = \frac{2X}{(X_i + X_R)} \quad (4.119)$$

The heat and mass transfer equations for solid matrix will be derived as:

$$\frac{\partial T_d}{\partial t} = \frac{2h}{\rho_d C_d \delta} (T - T_m) + \frac{q}{C_d} \frac{\partial W}{\partial t} \quad (4.120)$$

$$\frac{\partial W}{\partial t} = \frac{2h_m}{\rho_d \delta} (X - X_m) \quad (4.121)$$

$$N \times (T_R - T_i) \frac{\partial T_d^*}{\partial t^*} = \frac{2h}{\rho_d C_d \delta} (T_R - T_i)(T^* - T_m^*) + \frac{q}{C_d} \frac{4h_m}{\rho_d \delta} (X_R + X_i)(X^* - X_m^*) \quad (4.122)$$

Therefore, dimensionless groups are:

$$C_1 = \frac{4Lh}{u\rho d_e C} \quad (4.123)$$

$$C_2 = \frac{2h}{\rho_d C_d \delta N} \quad (4.124)$$

$$C_3 = \frac{q}{C_d} \frac{4h_m}{\rho_d \delta N} \frac{(X_R + X_i)}{(T_R - T_i)} \quad (4.125)$$

The selected functions to make correlations are:

$$\frac{T_{out} - T_{in}}{T_R + T_{in}} \quad (4.126)$$

$$\frac{X_{in} - X_{out}}{X_{in} + X_R} \quad (4.127)$$

Using same optimization routine and with data from Simulink model these correlations have been made according to the dimensionless groups:

$$\frac{T_{out} - T_i}{T_i + T_R} = 0.036 \times C_1 + 0.426 \times C_2 + 0.226 \times C_3 \quad (4.128)$$

$$\frac{X_{in} - X_{out}}{X_{in} + X_R} = 0.0329 \times C_1 + 5.29 \times C_2 - 1.8541 \times C_3 \quad (4.129)$$

Figures 4.41 and 4.42 show how the outlet air conditions of humidity and temperature calculated by the correlations in (4.129) and (4.130) can be compared with the results of simulation for a number of data produced in different air and wheel conditions.

The correlations given by equations (4.59) and (4.60) are based on physical parameters and are more accurate although they have the disadvantage that are applicable only for a typical characteristic of wheel given by manufactures. However, since they have been chosen according to physical facts governing adsorption phenomena they possess the physical properties of adsorption in the solid material and provide additional information for mathematical functions. The correlations made for dimensionless groups, although are independent of the wheel characteristics and can be used for all different matrixes, are less accurate since they lack physical information and are pure mathematical functions designed to fit a number of data. Considering this point and the fact that typical characteristics of wheel provided by the industries represent the optimum and practical values the correlations of (4.59) and (4.60) have been chosen for year-round simulation of desiccant cooling systems, in chapter 6 of this thesis. Figures 4.35 and 4.36 compare the effect of different variables and show the typical design parameters according to the information provided by the manufactures about the characteristics of the matrixes in the optimum area. Table 4.3 shows a comparison between different approaches.

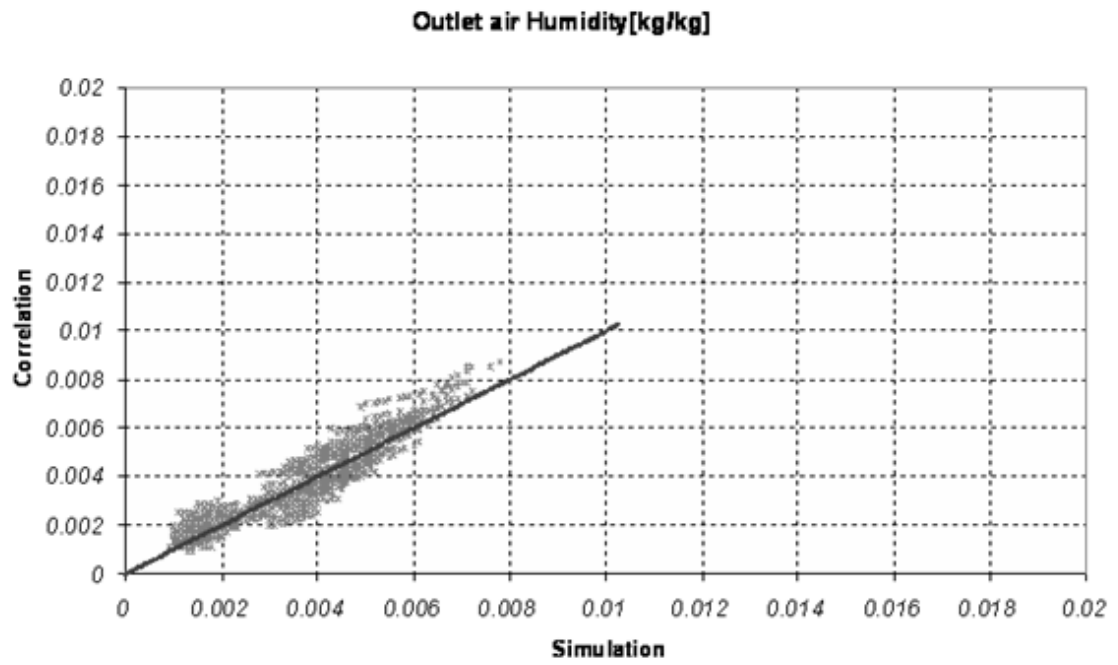


**Figure 4.41.** The comparison of simulation results with the results calculated by the correlation given by (4.130)

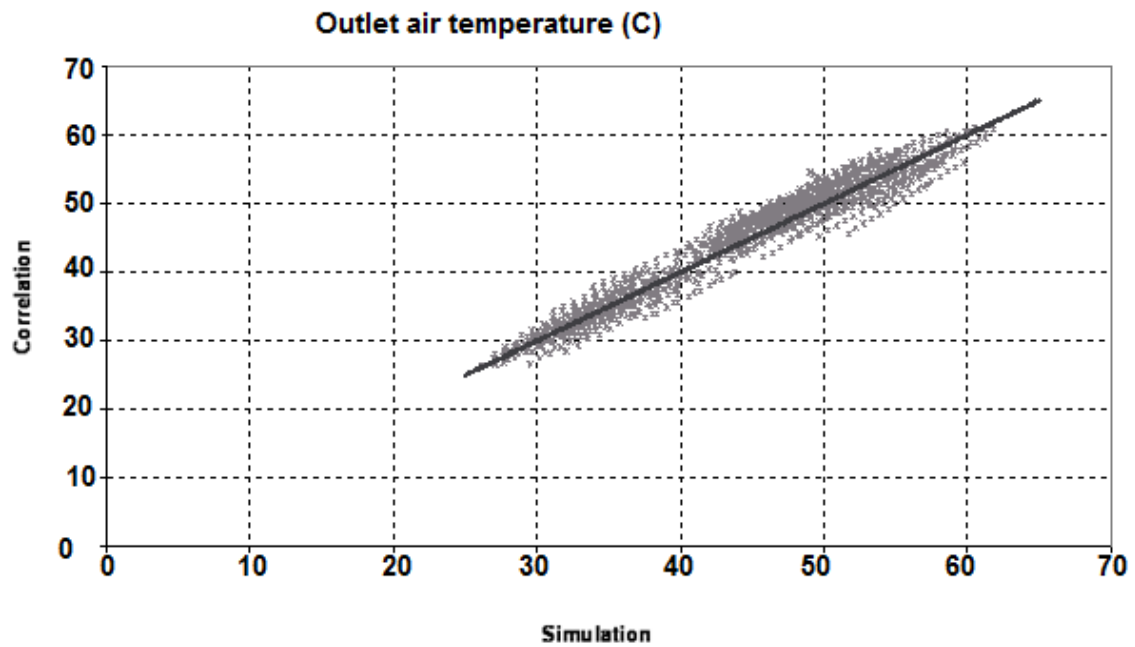


**Figure 4.42.** The comparison of simulation results with the results calculated by the correlation given by (4.129)

*Table 4.3. A comparison between different approaches.*

Inlet Conditions		Physical model	Correlations	Analytical model	Correlations Non dimension
$T_i$ °C	$X_i$ g/kgi	$T_{out}$ °C $X_{out}$ g/kgi	$T_{out}$ °C $X_{out}$ g/kgi	$T_{out}$ °C $X_{out}$ g/kgi	$T_{out}$ °C $X_{out}$ g/kgi
30	8	52.14 3.03	50.7 3.48	54.57 2.38	51.28 2.98
25	6	46.28 2.07	45.8 1.76	51.9 1.58	47.65 1.20

## 4.8. Summary and conclusions

- The basic concepts of this area of study such as the most important numerical and experimental studies of desiccant wheels have been reviewed and presented in this chapter. A survey of the literature dealing with this subject was also discussed.
- The Simulink model of heat and mass transfer for desiccant wheels was developed and improvised to produce results in shorter computer times. It can also more efficiently be connected to other building models. However, because of the limitation of computer memory and long calculation time, it was necessary to use simplified models in the application of year round simulation of desiccant cooling cycles.
- Desiccant wheels with a thick layer of solid desiccant are used in dehumidification applications at low speeds of 10-20 Rph. However, the results of the simulation show that the same desiccant wheel can easily operate as heat and moisture or enthalpy exchanger at higher speeds of 10-20 Rpm. Therefore, a desiccant wheel with a typical thick solid layer, which is common for dehumidification applications, is able to operate for both winter and summer applications just by changing the rotation speed. For summer applications the wheel works at lower speeds and for winter applications the speed needs to be higher. But, a desiccant wheel with the typical thickness of solid layer for enthalpy wheel is not able to provide the necessary dehumidification needed for air drying.
- The sensitivity study revealed the most important parameters or control variables. In addition, the behavior of model solutions for wheel efficiency at different speeds was compared with the published experimental data. In addition, results of the theoretical papers were recreated.
- Having studied the behavior of the system at different conditions and sensitivity studies, two physical parameters have been chosen to make simplified models or correlations.

- Using 1500 input data of model solutions, two correlations have been developed by an optimization routine program in Matlab. These equations correlate outlet air conditions with input air conditions, air streams, wheel rotation speeds and air speeds.
- The correlations are limited since they can only be used in the given range of air conditions and wheel speeds. However, this range is useful since it covers the practical situation that includes the actual weather of Europe according to weather data (Figure 4.30).
- The maximum error to calculate outlet air humidity by these correlations is  $\pm 8.5\%$ , and  $\pm 2.5\%$  for air temperatures.
- The error increases in the regions near the boundaries within the valid range. In other words, for air temperature, humidity and velocity at the minimum or maximum borders in the valid ranges larger errors are produced.
- The change in air conditions in the Mollier diagram show that the error in simulating the desired supply air temperature decreases the error of the desiccant cooling wheel by a factor of 3. Therefore, even in ranges of low accuracy the correlations are useful.
- These simplified equations will be used in programs such as Enerk and VABI.
- The correlations presented in this chapter are based on typical information for wheels prepared by manufactures. For wheels with other characteristics, the equations would need to be modified.
- The dimensionless groups were derived and new correlations were presented according to the functions of these groups. Although they have the advantage that they are not restricted to the typical wheels, they have less accuracy than the correlations for typical wheels. The simplified equations based on the dimension groups are more accurate, because they have been selected based on physical phenomena. In addition, the information used for a typical wheel are optimum and for a practical mater the different characteristics of different wheels are not as important as the control variables.
- Although the accuracy of correlations is acceptable within a margin of error for typical European data weather, they are not accurate for different climates, especially when all the variables are in the boundaries of ranges. Therefore, an analytical approach using physical simplified assumptions have been introduced and presented in this chapter. This analytical approach has been compared with other approaches. In addition, an example was presented in this chapter showing how to calculate outlet air conditions using this analytical approach.

## NOMENCLATURE

A	Adsorption Potential ( $kJ/kmol$ )
$A_c$	Interface area in a channel ( $m^2$ )
$A_d$	Cross section area for desiccant layer in a channel ( $m^2$ )
$A_g$	Cross section area for air flow ( $m^2$ )
C	Isobaric specific heat ( $J kg^{-1} K^{-1}$ )
$d_t$	Thickness of the desiccant coating ( $m$ )
$D_h$	Hydraulic diameter of a channel ( $m$ )
$E_0$	Characteristic energy of adsorption ( $kJ kmol^{-1}$ )
h	Heat transfer coefficient ( $W m^{-2} K^{-1}$ )
$h_m$	Mass transfer coefficient ( $kg m^{-2} s^{-1}$ )
H	Enthalpy ( $kJ kg^{-1}$ )
$k_F$	A constant in Freunlich equation
L	Depth of the rotor ( $m$ )
Le	Lewis number
$\dot{m}$	Air flow rate ( $kg s^{-1}$ )
$n_F$	A constant in Freunlich equation
N	Wheel Speed
Nu	Nusselt Number
P	Pressure (Pa)
q	Adsorption heat ( $J kg^{-1}$ )
R	Gas constant ( $J kg^{-1} K^{-1}$ )
t	Time (seconds)
$t_0$	Time for one wheel revolution (seconds)
T	Temperature ( $^{\circ}C$ )
$T_m$	Air temperature in saturated layer ( $^{\circ}C$ )
u	Control variable
U	Velocity ( $m/s$ )
V	Velocity ( $m/s$ )
W	Water content of the desiccant material ( $kg kg^{-1}$ )
x	Distance ( $m$ )
X	Air humidity ( $gr kg^{-1}$ )
$X_m$	Air humidity in saturated layer ( $gr kg^{-1}$ )

### Greek letters

$\delta$	Typical thickness ( $mm$ )
$\varepsilon$	Efficiency
$\rho$	Density ( $kg m^{-3}$ )
$\varphi$	Relative humidity
$\omega$	Humidity ratio ( $kg kg^{-1}$ )
$\omega_s$	Humidity ratio of air in equilibrium with the desiccant ( $kg kg^{-1}$ )

**Subscripts**

d	desiccant
e	enthalpy
g	gas
i	inlet
l	latent
m	moisture
min	the least value of process and exhaust mass flows to calculation of efficiency
o	outlet
s	saturation
st	sensible
v	water vapor

**Acronyms**

Rph	Revolutions per hour
Rpm	Revolutions per minute

## References

1. Chauch Y.K, P.Norton,F. Kreith, Transient Mass Transfer in Parallel Passage Dehumidifiers with & without Solid Side Resistance, ASME Journal of Heat Transfer ,V. 111, 1038-1044 , 1989.
2. Steich G., Performance of Rotary Enthalpy Exchangers, M.S. Thesis in Mechanical Engineering, University of Wisconsin-Madison, 1994.
3. ASHRAE, Handbook of Fundamentals, American Society of Heating, Refrigerating and Air-Condition Engineers, Atlanta, GA, 1993.
4. ASHRAE, Standard 62-1989, American Society of Heating, Refrigerating and Air-Conditioning Engineers, Atlanta, GA, 1989.
5. Hausen, H., Wärmeübergang im Gegenstrom, Gleichstrom und Kreuzstrom, Springer Verlag, 1. Auflage, Berlin, 1950.
6. Hoval, Hoval Rotary Heat Exchanger for Heat Recovery in Ventilation Systems, Handbook for Design, Installation and Operation, Doc.No.Hw60aE1-11/2002, [www.hoval.com](http://www.hoval.com)., Hovalwerk AG,Liechtenstein, 2002.
7. W. Zheng, W.M. Worek, D. Novolsel, Effect of operating conditions on optimal performance of rotary dehumidifiers, ASME Journal of Energy Resources Technology 117 (1995) 62–66, 1995.
8. A. Kodama, M. Goto, T. Hirose, T. Kuma, Experimental study of optimal operation for a honeycomb adsorber operated with thermal swing, Journal of Chemical Engineering of Japan 26 ,530–535, 1993.
9. R. Tauscher, U. Dingleiter, B. Durst, F. Mayinger, Transport processes in narrow channels with application to rotary exchangers, Heat and Mass Transfer 35 , 123–131, 1999.
10. Larry R.Rowland,Gopal S. Shiddapur , How to Accurately Analyze feasibility of Desiccant Dehumidification Applications, Energy Engineering: Journal of the Association of Energy Engineering , V. 96, N. 3, Fairmont Press Inc, Lilburn, GA, USA, 39-57, 1999.
11. E.Van den Bulck, J.W Mitchell, S.A.Klein, The Use of Dehumidifiers in Desiccant Cooling and Dehumidification Systems, ASME J. of Heat Transfer, V. 108, 684-693, 1989.
12. W. Zheng, W.M. Worek, Numerical simulation of combined heat and mass transfer processes in a rotary dehumidifier, Numerical Heat Transfer, part A: Applications 23 , 211–232 , 1993.
13. S. Neti, E.I. Wolfe, Measurements of effectiveness in a silica gel rotary exchanger, Applied Thermal Engineering Vol. 20 pp 309-322, 2000.
14. J.Y. San, S.C. Hsiau, Effect of axial solid heat conduction and mass diffusion in a rotary heat and mass regenerator, International Journal of Heat and Mass Transfer 36 , 2051–2059, 1993.
15. C.J. Simonson, R.W. Besant, Heat and moisture transfer in energy wheels during sorption, condensation, and frosting conditions, ASME Journal of Heat and Transfer 120 , 699–708, 1998.
16. C.J. Simonson, R.W. Besant, Energy wheel effectiveness: part I—development of dimensionless groups, International Journal of Heat and Mass Transfer 42 , 2161–2170, 1999.



17. Jae-Weon Jeong, Stanley A. Mumma, Practical thermal performance correlations for molecular sieve and silica gel loaded enthalpy wheels, *Applied Thermal Engineering* Vol. 25 pp 719–740, 2005.
18. H.Klein, S.A.Klein and J.W.Mitchel, Analysis of regenerative enthalpy exchangers, *Int. J. Heat Mass Transfer*. V.33, N.4, 735-744, 1990.
19. Ahmad A. Pesaran, Terry R. Penney, and Al W. Czanderna., Desiccant Cooling and Dehumidification Bibliography -Section 1, 2, <http://www.nrel.gov/desiccantcool/index.html>
20. [www.energycodes.gov/news/2003\\_workshop/pdfs/Case.pdf](http://www.energycodes.gov/news/2003_workshop/pdfs/Case.pdf)
21. Lew Hariman Design Guide, Humidity Control Design Guide for Commercial Buildings. Mason-Grant Consulting Proposal, 1999.
22. Handbook humidity guide, 2002.
23. D.G.Waugaman, A.Kini, C.F.Kettleborough, A Review of Desiccant Cooling Systems, *J.of Energy Resources Technology*, 115, 1-8, 1993.
24. Encyclopedia of Chemical Technology, John Wiley & sons, 1998.
25. CRC Hand book of Tables for Applied Engineering Science, second edition, CRC press, Boca Raton, 1972.
26. Perry's Chemical Engineers Handbook, McGraw-Hill Book Company, 1984.
27. Ahmad A. Pesaran and Anthony F. Mills, Moisture transport in silica gel packed beds- II Experimental study, *Int. J. Heat Mass Transfer*. Vol. 30, N. 6, pp. 1051-1060, 1987.
28. Andrea Bearzotti, Johnny Mio Bertolo, Plinio Innocenz, Paolo Falcaro, Enrico Traversa, Humidity sensors based on mesoporous silica thin films synthesized by block copolymers, *Journal of the European Ceramic Society* Vol. , 24 pp 1969–1972, 2004.
29. J Cheng-Chin Ni, Jung-Yang San, Measurement of apparent solid-side mass diffusivity of a water vapor–silica gel system, *International Journal of Heat and Mass Transfer* Vol. 45 pp 1839–1847, 2002.
30. Devrim Balkose, Sevgi Ulutan, Fehime Cakicioglu Ozkan, Sedat Celebi, Semra Ulku, Dynamics of water vapor adsorption on humidity-indicating silica-gel, *Applied Surface Science* Vol., 134 pp .39–46, 1998.
31. George W. Scherer, Effect of drying on properties of silica gel”, *Journal of Non-Crystalline Solids* Vol. 215, pp 155-168, 1997.
32. H. Hoffmann, M. Meyer, I. Zeitler, Control of morphology inside the mesoporous gel structure in silica-gels, *Colloids and Surfaces A: Physicochem. Eng. Aspects*, 2006.
33. P.J.Banks, Coupled equilibrium heat and single adsorbate transfer in fluid flow through a porous medium-1: characteristic potentials and specific capacity ratios, *Chemical Engineering Science*, V.27, 1143-1155, 1972.
34. Jin Sun, Robert W. Besant, Heat and mass transfer during silica gel–moisture interactions, *International Journal of Heat and Mass Transfer* Vol., 48 pp 4953–4962, 2005.
35. Kuei-Sen Chang, Hui-Chun Wang, Tsair-Wang Chung, Effect of regeneration conditions on the adsorption dehumidification process in packed silica gel beds, *Applied Thermal Engineering* Vol. 24 pp 735–742, 2004.

36. G. Limousin, J.-P. Gaudet, L. Charlet, S. Szenknect, V. Barthe`s, M. Krimissa, Sorption isotherms: A review on physical bases, modeling and measurement” *Applied Geochemistry* 22 (2007) 249–275, 2006.
37. Mihajlo N. Golubovic and William M. Worek , Influence of elevated pressure on sorption in desiccant wheels , *Numerical Heat Transfer, Part A*, 45: 869–886, 2004.
38. Mohamed E. Mahmoud, Sawsan S. Haggag, Abdelrahman H. Hegazi, Synthesis, characterization, and sorption properties of silica gel-immobilized pyrimidine derivative , *Journal of Colloid and Interface Science* Vol. 300 pp 94–99, 2006.
39. X. J. Zhang, K. Sumathy , Y. J. Dai<sup>3</sup> and R. Z. Wang, Parametric study on the silica gel–calcium chloride composite desiccant rotary wheel employing fractal BET adsorption isotherm”, *International Journal of energy research* Vol. 29, pp 37-51, 2005.
40. Xin Li, Zhong Li, Qibin Xia, Hongxia Xi, Effects of pore sizes of porous silica gels on desorption activation energy of water vapor , *Applied Thermal Engineering* Vol. 27 pp 869–876, 2007.
41. Polanyi, M., Section III. - Theory of the Adsorption of Gases. A General Survey and some Additional Remarks., *Trans. Far. Soc.*, Vol. 28, pp. 316-333, 1932.
42. Dubinin, M. M., Physical Adsorption of Gases and Vapors in Micropores, *Prog. Surf. Membrane Sci.*, Vol. 9, pp. 1-70, 1975.
43. Tsair-Wang Chung, Tien-Sheng Yeh, Thomas C.-K. Yang, Influence of manufacturing variables on surface properties and dynamic adsorption properties of silica gel, *Journal of Non-Crystalline Solids* Vol. 279, pp 145-153, 2001.
44. Motoyuki Suzuki, *Adsorption Engineering*, Elsevier, Kodansha, Tokyo, 1990.
45. Barry Crittenden, W John Thomas, *Adsorption Technology & Design*, Butterworth-Heinemann, 1998.
46. Sing, K. S. W., Reporting Physisorption Data for Gas/Solid Systems, *Pure and Applied Chemistry*, Vol. 54, No. 11, pp. 2201-2218, 1982.
47. Van den Bulck, E., Analysis of Solid Desiccant Rotary Dehumidifiers, M.S. Thesis in Mechanical Engineering, University of Wisconsin-Madison, 1983.
48. T.S. Kang, I.L. Maclain – cross, High Performance Solid Desiccant Cooling Cycles, *Transactions of ASME*, V. 111, 1989, 176-183, 1989.
49. P.J.Banks, Coupled equilibrium heat and single adsorbate transfer in fluid flow through a porous medium-1: characteristic potentials and specific capacity ratios, *Chemical Engineering Science*, 1972, V.27, 1143-1155, 1972.
50. P.J.Banks, Coupled equilibrium heat and single adsorbate transfer in fluid flow through a porous medium-2: predictions for a silica-gel air drier using characteristic charts, *Chemical Engineering Science*, 1972, V.27, 1157-1169, 1972.
51. McLain-Cross I.L., Banks D.J., Coupled heat and mass transfer in regenerators – prediction using an analogy with heat transfers, *Int. J. Heat Mass Tran.* 15, 1225-1242, 1972.
52. P.J.Banks, Prediction of Heat and Mass Regenerator Performance Using Nonlinear Analogy Method; Part 1-Basis, *ASME J. of Heat Transfer*, 107, 222-229, 1985.

53. B. P.J.Banks, Prediction of Heat and Mass Regenerator Performance Using Nonlinear Analogy Method; Part 2-Comparison of Methods, ASME J. of Heat Transfer, 107, 230-247, 1985.
54. Maclaine-cross, A Theory of Combined Heat and Mass Transfer in Regenerators, Ph.D. Thesis in Mechanical Engineering, Monash University, Australia, 1974.
55. W.Zheng, W.M.Worek, Numerical simulation of combined heat and mass transfer processes in a rotary dehumidifier, Numerical Heat Transfer, Part A, 23, (1993), 211-232, 1993.
56. Zheng W., Worek W.M., Novesel D., performance optimization of rotary operating conditions on optimal performance of rotary dehumidifiers, ASME J. Solar Energy Engng.117, 62-66, 1995.
57. Van den Bulck, E.Mitchell, J.W., and Klein, S.A., Design Theory for Rotary Heat and Mass Exchangers, Int.J.Heat Mass Transfer, Vol28, 1575-1586, 1985.
58. Van den Bulck, E.Mitchell, J.W., and Klein, S.A., Design Theory for Rotary Heat and Mass Exchangers Part 2-Effectiveness-number of transfer unit's method for rotary heat and mass exchangers, Int. J. Heat Mass Transfer, Vol. 28, 1587-1595, 1985.
59. K.J.Schultz, J.W.Mitchell, Comparison of DESSIM Model with a Finite difference Solution for Rotary Desiccant Dehumidifier, ASME J.of Heat Transfer, V.111, 286-291, 1989.
60. C.J.Simonson, R.W.Besant, Energy wheel effectiveness. Part 2: correlations, International Journal of Heat and mass Transfer, 42, 2171-2185, 1999.
61. Popescu. M, Ghosh. T.K, Dehumidification and simultaneous removal of selected pollutants from indoor air by a desiccant wheel using a 1M type desiccant, Journal of solar energy engineering, Transactions of the ASME, Vol. 121, N. 1, pp 1-13, 1999.
62. H.Klein,S.A.Klein and J.W.Mitchel, Analysis of regenerative enthalpy exchangers, Int. J. Heat Mass Transfer. V.33, N.4, 735-744, 1990.
63. M.Epstein, M.Gromles, K.Davidson, D.Kosar, Desiccant Cooling System Performance: A Simple Approach, Journal of Solar Energy Engineering, V.107, 21-28, 1985.
64. E.Van den Bulck, J.W Mitchell, S.A.Klein, The Use of Dehumidifiers in Desiccant Cooling and Dehumidification Systems, ASME J. of Heat Transfer, V. 108, 684-693, 1986.
65. J.J.Jurinak, J.W.Mitchell, W.A.Beckman, Open-Cycle Desiccant Air Conditioning as an Alternative to Vapor Compression Cooling in Residential Applications, ASME J. of Heat Transfer,V.106, 252-262, 1984.
66. Larry R.Rowland,Gopal S. Shiddapur, How to Accurately Analyze feasibility of Desiccant Dehumidification Applications, Energy Engineering: Journal of the Association of Energy Engineering, V. 96, N. 3, Fairmont Press Inc, Lilburn, GA, USA, 39-57, 1999.
67. L.Z.Zhang, J.L.Niu, Performance comparisons of desiccant wheels for air dehumidification and enthalpy recovery, Applied Thermal Engineering 22, 2002, 1347-1367, 2002.
68. Bejan Adrian, Convection Heat Transfer, John Wiley and Sons, New York, NY, 1984.

69. Zheng W., Worek W.M., Novesel D., performance optimization of rotary operating conditions on optimal performance of rotary dehumidifiers, ASME J. Solar Energy Engineering. 117, 62-66, 1995.
70. W.Zheng, W.M.Worek , Numerical simulation of combined heat and mass transfer processes in a rotary dehumidifier, Numerical Heat Transfer, Part A, 23, 211-232, 1993.
71. Y.J. Dai, R.Z. Wang, H.F. Zhang, Parameter analysis to improve rotary desiccant dehumidification using a mathematical model, Int. J. Thermal. Science. 40, 400–408, 2001.

# 5. MODEL VALIDATION

## Introduction

The purpose of this chapter is to set forth a concise description of the validation of the model described in Chapter 4. The test data and information prepared and supplied by Carrier HH is used as well as some experimental measurements for two different wheels<sup>1</sup>, an enthalpy (sorption) wheel and a desiccant wheel.

In the laboratory of TUDelft, two test facilities were set up for the wheels and an experimental study was carried out to compare model results with actual measurements. In addition, the sorption potential under different air humidities with a definite temperature was studied for the wheels.

The first part of the test data was derived from a report prepared by University of Luzern<sup>[1]</sup> and comparison was carried out only for enthalpy wheels and not dehumidifier wheels. The test report did not contain any information about the test of the dehumidifier wheels. In addition, the temperature efficiency and humidity efficiency of an enthalpy wheel for different air conditions and wheel speeds were observed and shown in this part.

In the second part, the experimental measurements collected by the test facilities in TUDelft laboratory were studied and compared with model results.

## 5.1. Model validation by available test results for an enthalpy wheel

### 5.1.1. The principle information

According to the information provided by Carrier HH, the enthalpy wheel investigated in this chapter has the following configuration listed in Table 5.1. The information given in table 5.1 has been calculated by using the following method:

The channels have a triangular shape and the air way height= 1.9 mm.  
Therefore, the edge of air channel cross section= 2.24 mm.

$$\text{Hydraulic Diameter} = \frac{4 \times 2.24 \times 1.9}{2 \times 3 \times 2.24} = 1.27 \text{ mm}$$

---

<sup>1</sup> Hoval and DRI wheels

**Table 5.1** The characteristics of one of Hoval wheels

Desiccant Layer Thickness	10 $\mu\text{m}$
Hydraulic Diameter of Air Channels	1.27mm
Aluminum Thickness	60 $\mu\text{m}$
Wheel depth	200mm
Wheel diameter	950mm
Matrix diameter	600 mm

In addition, according to Carrier HH, 1 m<sup>2</sup> of the sheet surface has 10 gram of silica gel. The certainty of this value is in question.

The density of silica gel is 500 kg/m<sup>3</sup> given by Carrier HH. A coating of a varnish plus Silica gel is applied on it before rolling the wheel. Density of silica gel may vary because of the varnish carrying the Silica gel. Weight of Silica gel of 0.01 kg/m<sup>2</sup> is from the manufacturer and was not checked.

Therefore:

$$(1) \text{ m}^2 (2.8) (500) \text{ kg m}^{-3} = (0.01) \text{ kg} \\ \delta = 10 \mu\text{m}$$

According to Carrier HH, the prediction of the thickness of the layer is highly uncertain. The value of  $\delta = 10 \mu\text{m}$  used in the model gave the best fit with the measured data. Because of the uncertainties this is supposed to be a useful value involving all kind of uncertainties. So it may not be the real one, but appropriate to be used in the model as a calculation parameter compensating for all kind of not observed errors.

### 5.1.2. The Experimental Measurements in Different Air Conditions and Wheel Speeds and Comparison with the Model Solutions

The test information in the report from carrier HH <sup>[3]</sup> is given in table 5.2. The measurements have been carried out at different wheel speeds as given in the same table ranging from 4 to 12 revolutions per minute (Rpm).

The description of the nomenclature in Luzern University report for the temperature and humidity of inlet fresh air and supply and exhaust airs according to the wheel configuration has been shown in figure 5.1. These measured values ( $t_{22}$ ,  $X_{22}$ ) in that report are compared with that of the physical model of the enthalpy wheel as described in chapter 4.

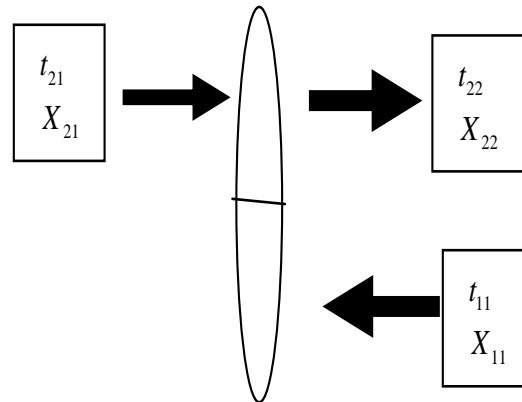


**Figure 5.1.** The description of the indices in Table 5.2 for air streams, as  
 $21 \equiv$  inlet fresh air;  $22 \equiv$  supply fresh air;  $11 \equiv$  exhaust air

### 5.1.3. Adsorption Isotherm Curve

The definition of isotherm curves and their importance have been described in the chapter 4 of this thesis. The model solutions have been calculated by using an adsorption isotherm curve for silica gel given by literature <sup>[2]</sup> with some correction as:

$$W = 0.348\phi^{1/1.5} \quad (5.1)$$

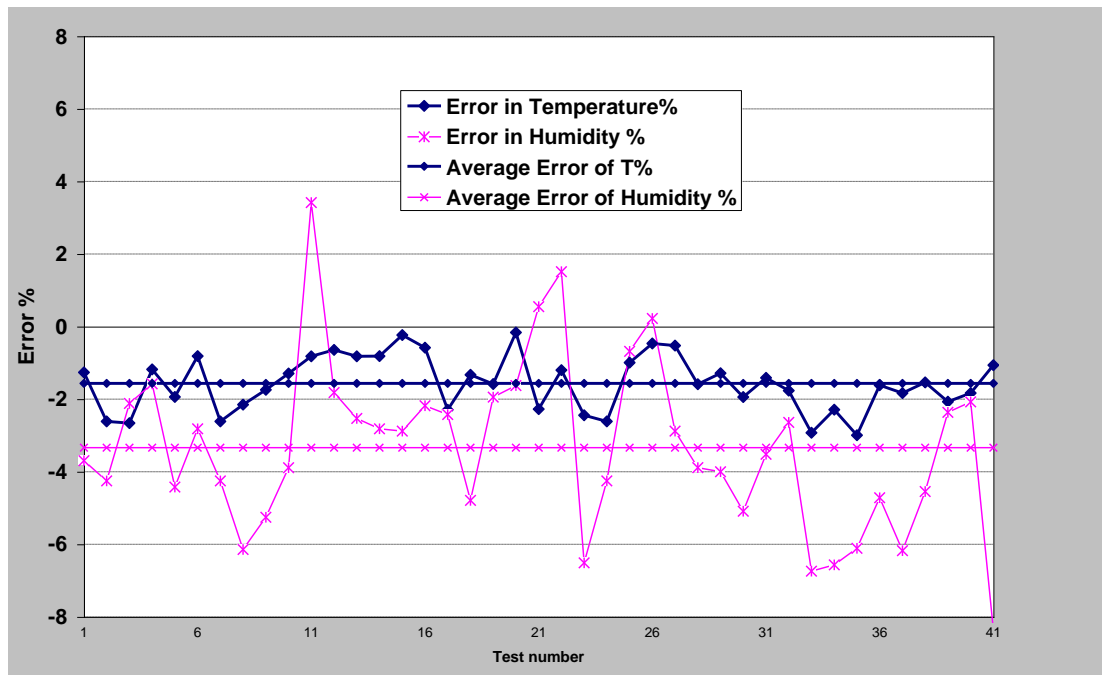


**Figure 5.2.** The distribution of relative errors for air temperature and air humidity from the tests results and model solutions given in table 5.2 with the adsorption curve given by equation (5.1)

**Table 5.2.** The air conditions in different tests as well as model solutions in those conditions for the wheel with characteristics given in this thesis in different speeds.

Air Conditions					Measurements		Wheel Speed	Simulation		Errors: <i>Simulation-measurements</i> Average value $\times 100$	
Test Nu.	T11 °C	X11 g/kg	T21 °C	X21 g/kg	T22 °C	X22 g/kg	n Rpm	T22 °C	X22 g/kg	Temperature %	Humidity %
1	25.2	10.3	10.4	7.5	21.4	9.2	12	21.67	9.54	1.26	3.7
2	25.2	10.4	5.1	5.3	19.9	8.7	12	20.42	9.07	2.61	4.25
3	25.1	10.4	0.6	3.7	18.8	8.5	12	19.3	8.68	2.66	2.12
4	22	6	5	5.3	17.8	5.7	12	18.01	5.79	1.18	1.58
5	22	6.1	-0.1	3.5	16.5	5.2	12	16.82	5.43	1.94	4.42
6	21.1	8	5.2	5.3	17.2	7.1	12	17.34	7.3	0.814	2.82
7	25.2	10.4	5.1	5.3	19.9	8.7	12	20.42	9.07	2.61	4.25
8	25.2	8.2	5	5.3	20	7	12	20.43	7.43	-2.15	6.14
9	25.2	6.6	5	5.2	20.1	5.9	12	20.45	6.21	1.74	5.25
10	25.1	5.8	4.9	5.2	20.1	5.4	12	20.36	5.61	1.29	3.89
11	21.1	13.4	5.1	5.3	17.1	11.7	12	17.24	11.3	0.82	3.42
12	21.1	10.1	5	5.3	17.1	8.8	12	17.21	8.96	0.64	1.82
13	21.1	9.1	5	5.2	17.1	7.9	12	17.24	8.1	0.82	2.53
14	21.1	8	5.2	5.3	17.2	7.1	12	17.34	7.3	0.81	2.82
15	21.1	6.4	4.9	5.2	17.2	5.9	12	17.24	6.07	0.23	2.88
16	21.1	5.8	4.9	5.2	17.2	5.5	12	17.3	5.62	0.58	2.18
17	21.1	7.9	-0.3	3.4	15.7	6.6	12	16.06	6.76	2.29	2.42
18	21	5.6	-0.3	3.4	15.8	4.8	12	16.01	5.03	1.33	4.79
19	21	3.8	-0.2	3.4	15.8	3.6	12	16.05	3.67	1.58	1.94
20	21.2	8.5	9.1	7.2	18.3	8	12	18.33	8.13	0.16	-1.62
21	21	9	-5.3	2.1	14.5	7.3	12	14.83	7.26	2.2	0.55
22	21	10.5	-3.7	2.5	15	8.6	12	15.18	8.47	-1.28	1.51
23	28.1	10.5	5.1	5.4	22.1	8.6	12	22.64	9.16	2.44	6.51
24	25.2	10.4	5.1	5.3	19.9	8.7	12	20.42	9.07	2.61	4.25
25	21.1	10.1	5	5.3	17.1	8.8	12	17.27	8.86	0.99	0.68
26	18.2	10.2	5.1	5.4	15	9	12	15.07	8.98	0.47	0.22
27	21.1	6.4	4.9	5.2	17.2	5.9	12	17.29	6.07	0.52	2.88
28	21.1	9	5.3	5.4	17	7.72	10	17.27	8.02	1.59	3.89
29	21.1	8	5.4	5.4	17.1	7	10	17.32	7.28	1.29	-4
30	21.2	6.3	5	5.2	17	5.7	10	17.33	5.99	1.94	-5.09
31	21.1	5.8	4.9	5.2	17	5.4	10	17.24	5.59	1.41	3.52
32	21.1	5.6	5.1	5.2	17	5.3	10	17.3	5.44	1.77	2.64
33	21.2	9	5.3	5.4	16.4	7.27	6	16.88	7.76	2.93	6.74
34	21.1	8.1	5.4	5.4	16.6	6.7	6	16.98	7.14	2.29	6.57
36	21.2	6.2	5	5.1	16.7	5.4	6	17.2	5.73	2.99	6.11
37	21.1	5.9	5	5.2	16.7	5.3	6	16.97	5.55	1.62	4.72
38	21.1	8	5.5	5.4	16.9	6.8	8	17.21	7.22	1.83	6.18
39	21.1	6.1	5	5.1	16.9	5.5	8	17.16	5.75	1.54	4.55
40	21.2	5.9	5	5.2	16.9	5.5	8	17.25	5.63	2.07	2.36
41	21.1	5.6	5.1	5.2	16.9	5.3	8	17.21	5.41	1.83	-2.08

There are two different sorption functions in literature. They are <sup>[2]</sup>:

$$W = 0.24\phi^{1/1.5}$$



And the other is <sup>[14]</sup>:

$$W = 0.106 \exp \left[ -\left( \frac{A}{8590} \right)^2 \right] + 0.242 \exp \left[ -\left( \frac{A}{3140} \right)^2 \right]$$

It should be explained that the model solutions observed for different coefficients in the adsorption curve equation, and the coefficient of 0.348 was chosen in equation (5.1) because they produced minimum errors as shown in figure 5.2. The errors for other coefficients are larger and have not shown here.

As it can easily be seen the result of accurate simulation model and the experimental data <sup>[1]</sup> are agreeable within the acceptable margin of error. Although the equation to describe the sorption curve has been chosen from literature, since it was not available for this experimental data, this comparison can well validate the model. In chapter 4 it was concluded that a large error in the outlet of the desiccant wheel results in a 3 times smaller error in the supply temperature. Consequently, the error in the models describing the performance of the desiccant wheel is less sensitive for the end result (supply air temperature).

#### 5.1.4. Dependency of Efficiency curves on the speed of rotation in different air conditions

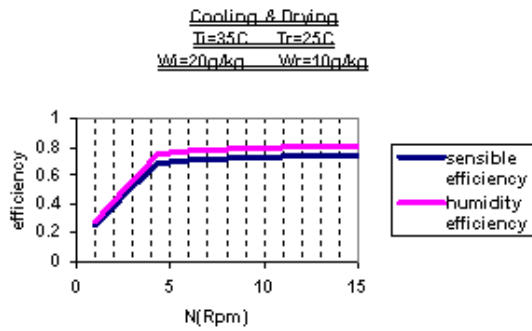
One of the important points observed through the results and charts by manufactures manuals <sup>[3]</sup> was that efficiency of enthalpy wheel seemed independent of inlet air conditions. In figures 5.3 through 5.6 the dependency of relative efficiency on the speed of rotation has been demonstrated. The results strongly depend on the air conditions and sorption properties of the desiccant.

Figure 5.3 is related to the application of air cooling and drying for sorption curve as given by equation (5.1), while figures 5.4 through 5.6 are related to the application of wheel for air heating and moisturizing.

The main idea is that adsorption heat depends on the amount of dehumidification can affect the heat exchange or temperature efficiency. But the degrees of changes are strongly dependent on the air conditions.

These following observations were made from the review and comparison of the measurements and model solutions:

The Adsorption Isotherm curve is the most significant characteristic and has considerable effect on the results and the range of accuracy of temperature and humidity. So for different coefficients in the semi-experimental equation of isotherm (such as equation (5.1)) different values of errors have been observed, and can be tuned according to an appropriate selection of the coefficient in the equations for adsorption isotherm curve. Therefore it is very important to conduct more experimental measurements in order to obtain the right adsorption curve for the test results of the wheel for validating the model and for testing the Isothermal curve as found here by tuning model outputs with measured values.



**Figure 5.3.** The dependency of relative efficiencies for fresh air conditions of  $35^\circ\text{C}$  and  $20\text{ gr/kg}$  and exhaust air with  $20^\circ\text{C}$  temperature and  $10\text{ gr/kg}$  humidity in different wheel rotation speeds. The adsorption curve given by equation (5.1)

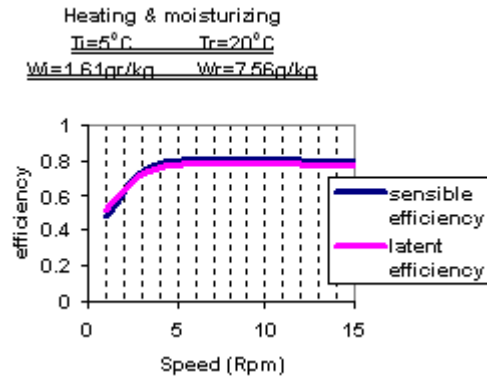


**Figure 5.4.** The dependency of relative efficiencies for fresh air conditions of  $5^\circ\text{C}$  and  $7.56\text{ gr/kg}$  humidity in different wheel rotation speeds. The adsorption curve given by equation (5.1)

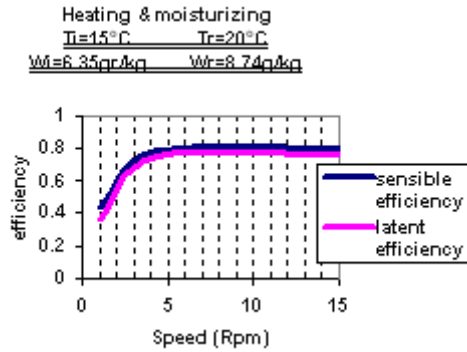


**Figure 5.5.** The dependency of relative efficiencies for fresh air conditions of  $15^\circ\text{C}$  and  $6.35\text{ gr/kg}$  and exhaust air with  $20^\circ\text{C}$  temperature and  $8.74\text{ gr/kg}$  humidity in different wheel rotation speeds. The adsorption curve has given by equation (5.1)

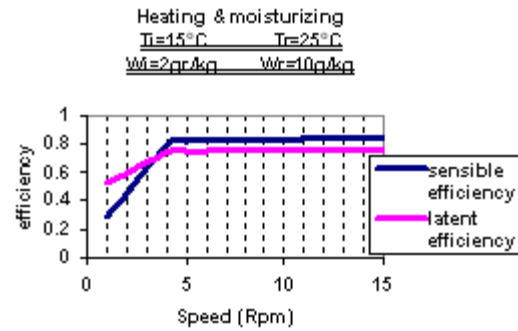


**Figure 5.6.** The dependency of relative efficiencies for fresh air conditions of  $15^\circ\text{C}$  and  $2\text{ gr/kg}$  and exhaust air with  $25^\circ\text{C}$  temperature and  $10\text{ gr/kg}$  humidity in different wheel rotation speeds. These air conditions rarely happens in the Netherlands and has been chosen according to the published experimental data<sup>[14]</sup>

## 5.2. Experimental studies for dehumidifier wheel DRI

### 5.2.1. Objective

The main purpose of these experiments is to measure the capacity of adsorption of silica gel in the different conditions of temperature and humidity through the dehumidification process in a desiccant wheel, and to validate the Simulink model.

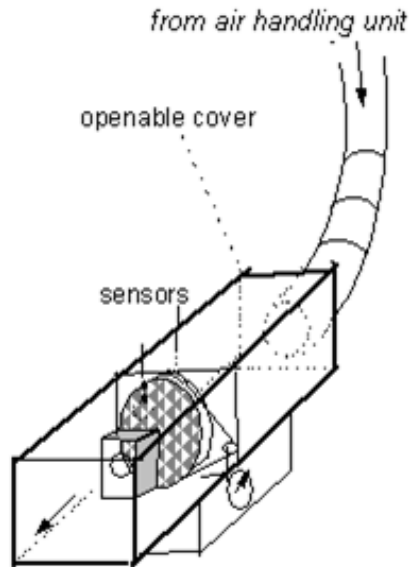


**Figure 5.7a.** A schematic outline of experimental set up

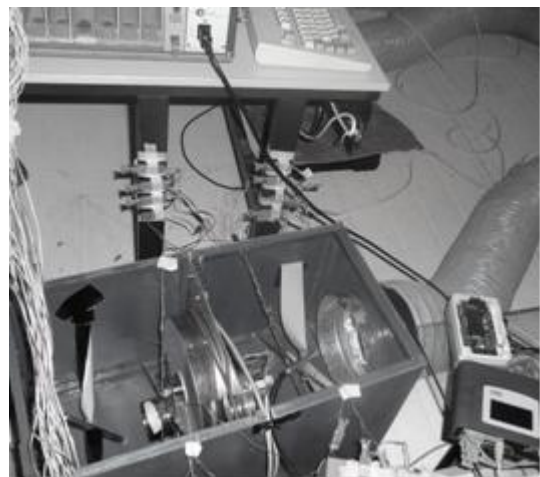


**Figure 5.7b.** The first test bed in the climate room for study and measurements of adsorption for DRI wheel

These values must lead to an equilibrium adsorption curve which is the most vital parameter to study the behavior of this type of systems and the improvement of their performance. Therefore, the results of the experimental measurements need to be represented by a mathematical model. In this chapter the set up and the important points to produce different air conditions with available air handling unit in TUDelft laboratory have been described. A comparison between the model results and these actual measurements has been presented.

### 5.2.2. Test Set Up to study Dehumidifier Wheel

In figures 5.7a and b the experimental set up in the climate room and a simple outline schematic of it at the TUDelft are shown. An isolated place that allows controlling the values of temperature and relative humidity is necessary. Besides, it is important to design and set up an appropriate system to measure the adsorbed quantity of water vapor by silica gel.

The inlet air was prepared by air handling unit and controlled the climate room. The air had a certain temperature and humidity. It passed through simple flexible ducts and was

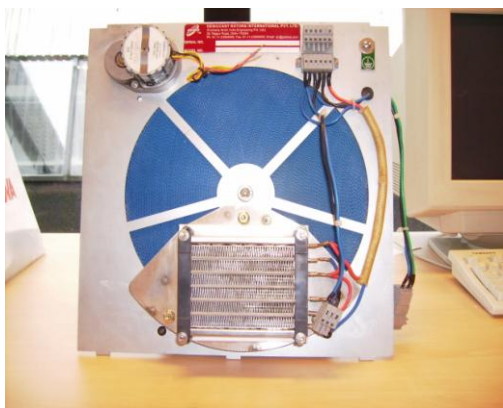


*Figure 5.8a. DRI wheel with heater and rotating motor*

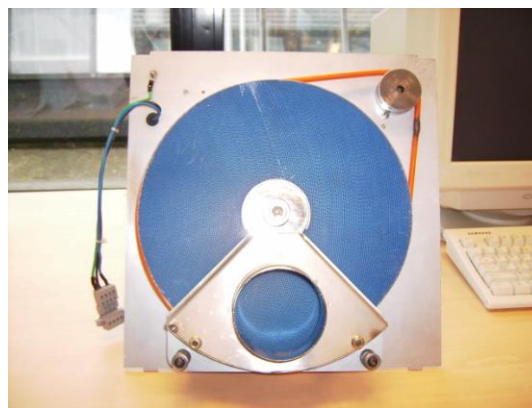


*Figure 5.8b. The other side or outlet side of the wheel*

conducted to the box with electric heater and wheel. The wheel, heater, and the rotor have been shown in figures 5.8a and 5.8b. The wheel with dimension  $260 \times 50$  mm was slowly rotating during both regeneration and adsorption processes.

The air after passing heater was heated up enough to regenerate the saturated wheel. The input air temperature and humidity were observed by sensors such as thermocouples and dew point meter before the wheel. The inlet humidity could be checked in this part only in the beginning of the experiments. The same sensors were used after the wheel to measure outlet air conditions. The thermocouples are connected to a data logger. Two metallic grids were prepared and put before and after the wheel for 17 thermocouples to record and save the temperatures in computer files. They are located as shown in figure 5.9.

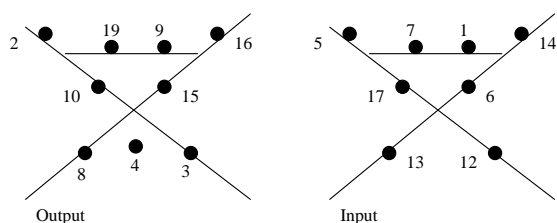


*Figure 5.9. The grids in input and output and the place of thermocouples*



*Figure 5.10. The aluminum piece covers the wheel, therefore only the hot air cross it*

During regeneration period the wheel was regenerated by hot air. A part of the wheel which was not crossed by hot air had to be covered by an aluminum disk as shown in figure 5.10. This covering was necessary to avoid adsorption.

There are two methods to measure the adsorbed amount of water vapor by silica gel. In the first method<sup>[4, 5, 6]</sup> the uptake amount of water vapor might be measured by measuring the air humidity after and before passing the wheel and by integration over a sufficiently long time. This method was not possible to be used for the first tests but it was prepared for the 2<sup>nd</sup> set up.



**Figure 5.11.** Air handling unit on the climate room roof

In the second method<sup>[7, 8, 9, 10, 11, 12, 13]</sup> the measurement of the adsorbed amount was carried out by observing and measuring the change in the weight of the desiccant. Both methods have restrictions regarding accuracy and practicality. They can be used to check mass balance (adsorbed water) measured by the difference in the inlet and outlet or by the scale. A scale with 1 gram accuracy was used to measure the weight. It is clear that the electrical heater was switched off during the adsorption processes.

On top of the climate room an air handling unit had been placed to deliver the air conditions for testing the wheel inside this room. The air handling unit on the roof of climate room has been shown in figure 5.11.

The air was supplied by an air handling unit in the climate room and each device was controlled by Building Control System installed inside the climate room.

The air flow through the wheel could be controlled with the Control System of the climate room. The desired set point needed to be selected and manipulated in such a way that the air passing the wheel had a velocity between 1 to 3 m/s. This velocity could be measured with two sensors placed at the end of the duct that conducted the air to the box containing the desiccant wheel.

### 5.2.3. Experiments

The procedure used to collect the data for this experiment was carried out in the following steps:

1. - All the machines were turned on and after steady conditions of flow, temperature and relative humidity were achieved the air velocity was measured at the entrance of the desiccant wheel box.

2. - Once desired values were achieved and remained steady the wheel was dried through the regeneration process. The steps for this process were:

a. - Placing the cover (metallic piece) for the wheel, so only hot air passed through the wheel

b. - Turning on the heater

c. Calibrating the scale of the balance

Then every five minutes the data of the loss of weight, outlet air relative humidity and temperature were collected. At the same time, the temperature of the heater needed to be measured.

When the value of the loss of weight remained constant the drying process was completed.

3. - After the regeneration of the wheel the adsorption process was initiated. The steps for the adsorption were:

a. - Taking off the cover

b. - Turning off the heater

c. - Calibrating the scale of the balance

Similar to the regeneration process, the weight, the air relative humidity, and temperature at the outlet were collected every five minutes.

The adsorption process was completed when the weight shown by the balance remained constant.

### 5.2.4. Experimental results

The measurements have been presented here by different profiles of the outlet air conditions and weight gain. Figure 5.12 shows the results of measurements during the **adsorption** process. It takes 50 minutes to reach the equilibrium conditions. It could be observed that when the adsorption process was finished the air relative humidity in the input and in the output were the same and about 70% (figure 5.13).

The amount of adsorbed water vapor was 167 grams and after 60 minutes the variation of the weight was negligible. In the beginning of the adsorption process (just after the calibration switching off the heater and taking away the covering disk) the matrix has the highest potential of adsorption but this could not be measured before calibrating the scale. The **regeneration** process at the beginning the outlet air relative humidity raised up to a value of 100%, and the desiccant matrix was losing the water vapor that had adsorbed before. After 20 minutes the outlet air relative humidity remained constant (Figure 5.13). The profile of losing weight with time as shown in figure 5.13 also indicates that after 20 minutes the weight was almost unchanged. The amount of desorbed water vapor in the regeneration process was about 155 grams. The difference of weight gained and weight

lost can be attributed to the hysteresis or regeneration temperature. It was observed that higher regeneration temperature can lead to a better adsorption process.

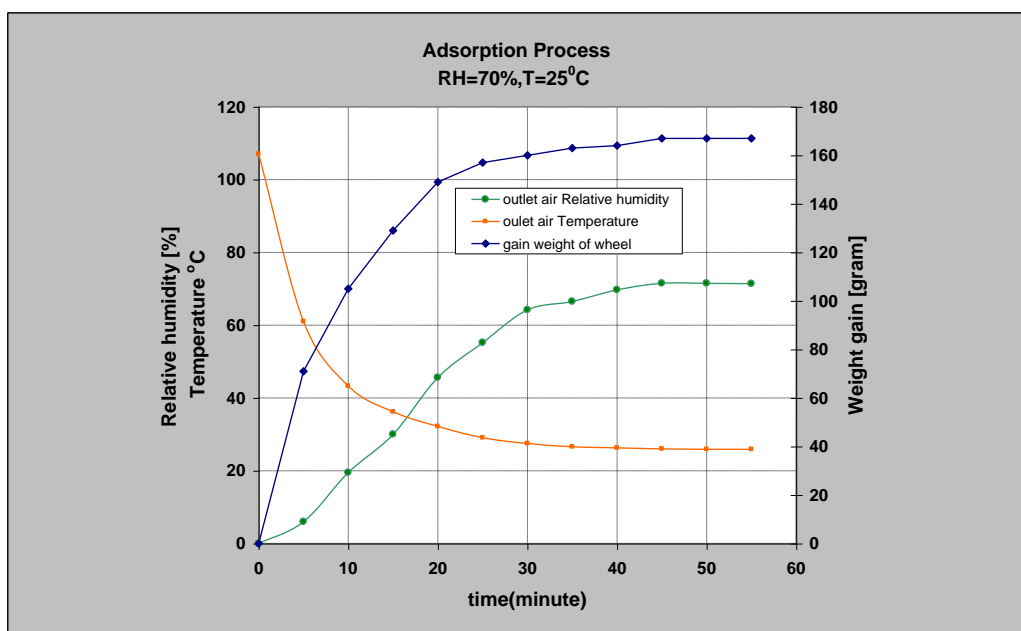


**Figure 5.12.** The profiles of outlet air relative humidity and temperature as well as the increase in the weight of silica gel matrix with given conditions in the figure

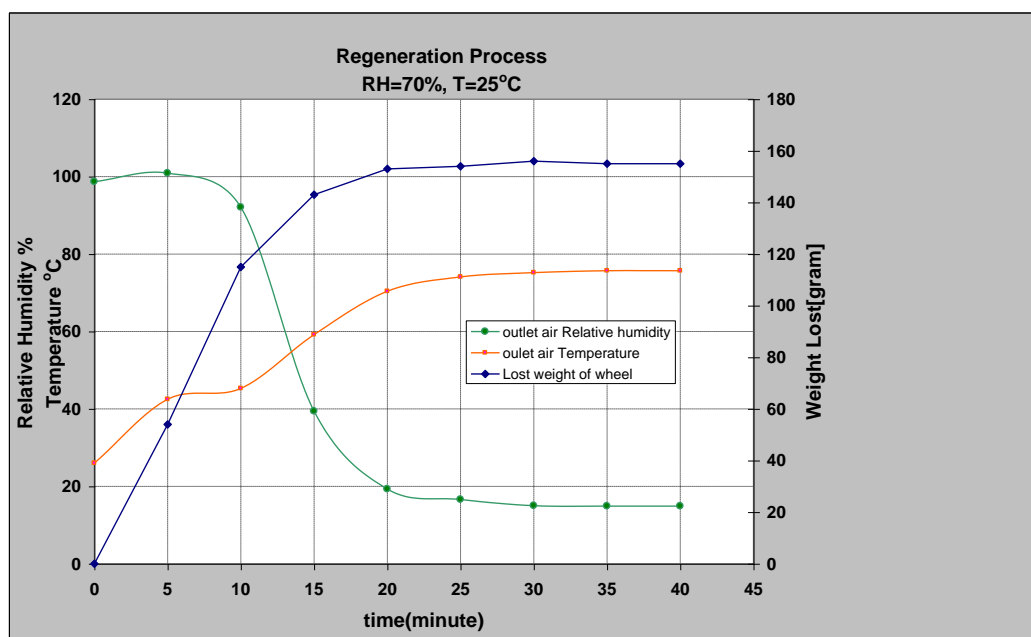


**Figure 5.13.** The profiles of weight losing and outlet air conditions during the regeneration process

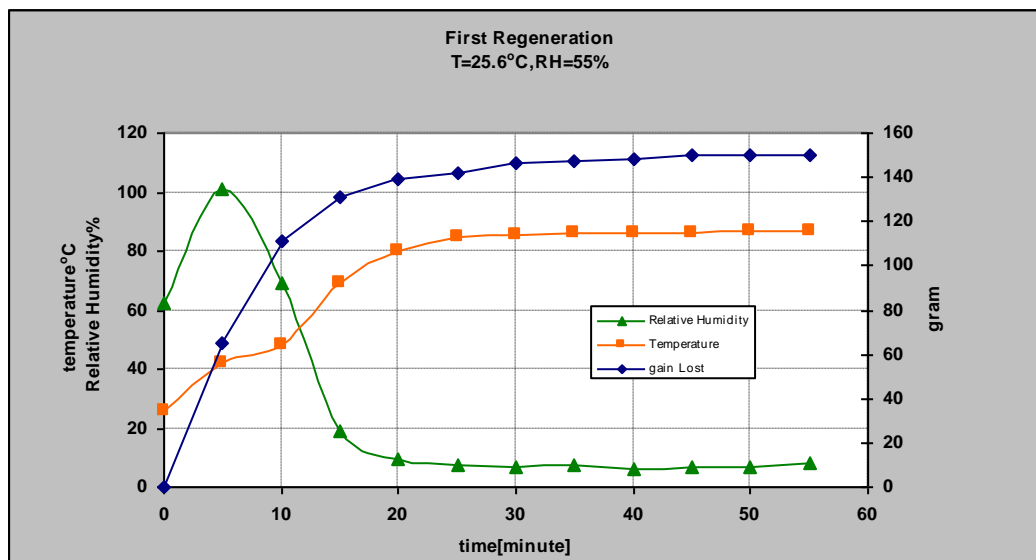


**Figure 5.14a.** The profiles of weight losing and outlet air conditions during the regeneration process for given conditions of inlet air

At the beginning the potential of adsorption is the highest, and the driest air can be observed. The adsorption potential of the desiccant layers will decrease with passing time. Therefore, at the end the wheel is saturated and can not adsorb any more moisture. Thus, the outlet air has the same relative humidity as the input air.

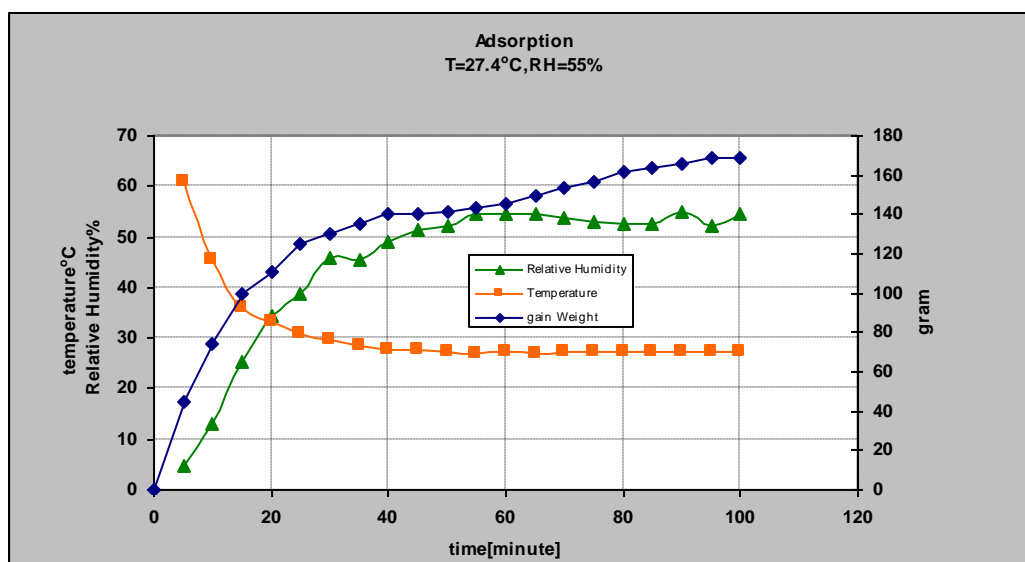
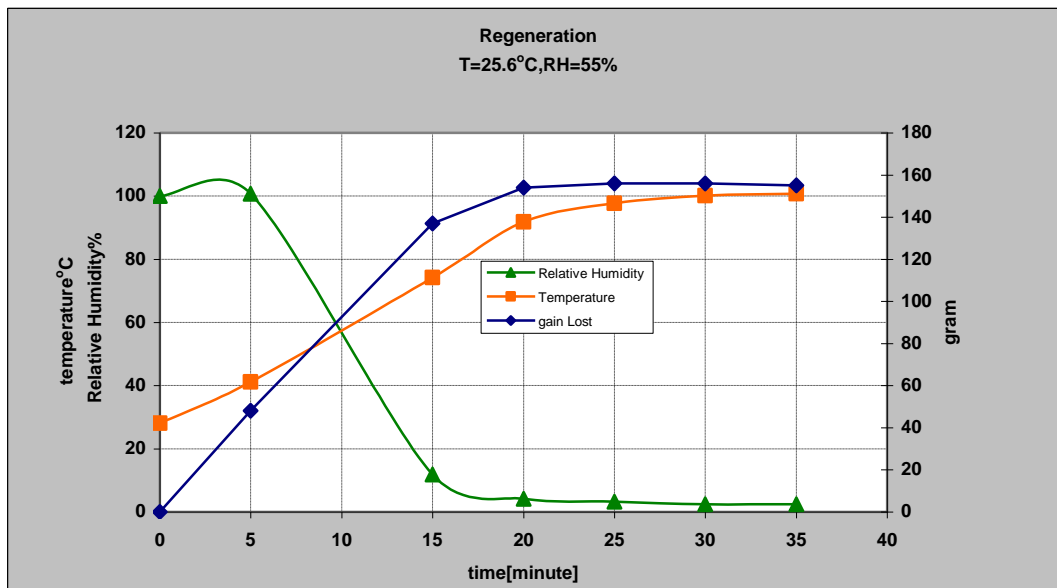


**Figure 5.14b.** The profiles of outlet air relative humidity and temperature as well as the increase in the weight of silica gel matrix with given conditions in the figure

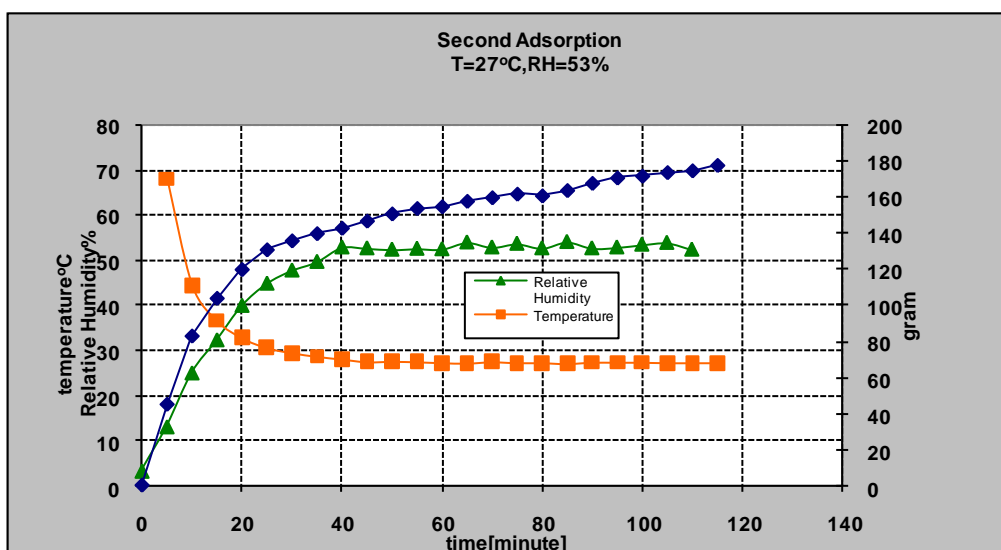
Regeneration air conditions are important variables and need to be selected under optimum conditions. The higher air regeneration temperature and lower humidity will



regenerate the matrix of silica gel more effectively, and increase the potential of the desiccant material to adsorb more humidity. This result can be observed in figures 5.14a, b , 5.15, and 5.16. Similar profiles for adsorption and desorption are measured but for different given air conditions as shown in these figures.



**Figure 5.15.** The profiles of outlet air relative humidity and temperature as well as the increase in the weight of silica gel matrix with given conditions in the figure



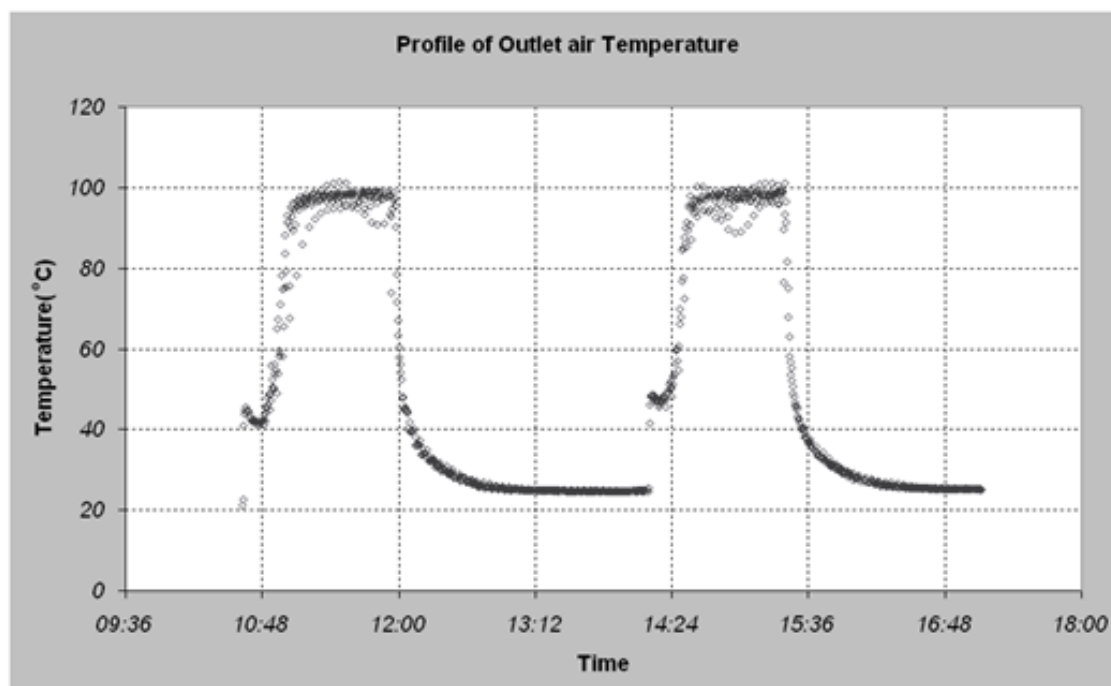
**Figure 5.16.** The profiles of outlet air relative humidity and temperature as well as the increase in the weight of silica gel matrix with given conditions in the figure

Figure 5.14b shows the adsorption of wheel with a regeneration air temperature of 86°C and a relative humidity of 8%. When the matrix has been regenerated with these air conditions the maximum adsorbed amount of humidity is 169 gram. In figure 5.16 the wheel has been regenerated with better air conditions of 100°C and 2% relative humidity, the weight gain is 178gram. The regeneration air conditions at 70% relative humidity was lower and did not have the same potential to regenerate the matrix of silica gel to adsorb its maximum potential of adsorption. Therefore, in measuring the adsorption by this method it is very important that wheel is regenerated with the same air conditions.

Figure 5.17 shows the profile of air temperature from one of the thermocouples in the outlet air. These results are for the thermocouple placed in outlet air and in the front of heater (T4 in figure 5.9).

As it can be seen in figure at 11.45AM the first regeneration process was completed and the heater was switched off. The adsorption process started at 11:50AM, and the same tests for the second time started at 14.05 for regeneration, and at 15:20 for adsorption processes in the same day.

Figure 5.18 shows the outlet air temperature only for adsorption process for the second test in the same day. The temperature decreased from 100 °C (which is prepared by the heater) and reached to the inlet air temperature of 25 °C after the wheel could no longer adsorb humidity. As it can be observed in this chart, the adsorption process takes almost 1 hour.



**Figure 5.17.** The outlet air temperature measured by one of the thermocouples (T4), Inlet air conditions are 25 °C and 60 % relative humidity

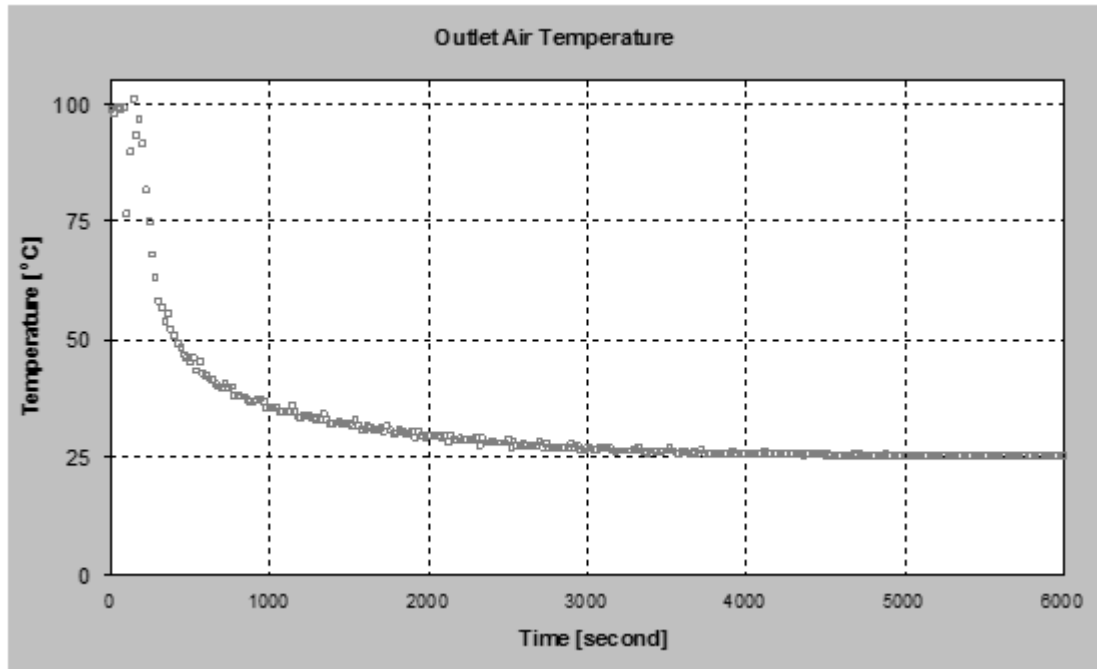


*Figure 5. 18. Outlet air temperature measured in adsorption process by thermocouple T4*

The number of the tests was not enough to calculate and present adsorption of silica gel with a mathematical equation. In addition, essential information such as the total mass of silica gel in the matrix, the silica gel layer thickness, and the hydraulic diameter of the air channels in the matrix of silica gel were not available. Considering a typical experimental model in the literatures <sup>[2, 14]</sup> the isotherm was chosen and used to obtain primary solutions from model.

Figure 5.19 shows how the model can be tuned by changing the input data to be comparable with the measured results. The input data are: 2.25 mm for hydraulic diameters of the air channels, 0.14mm thickness of silica gel layer, and 0.06 mm aluminum thickness. The air velocity was measured by different devices as different values. Therefore a typical value of 1.55 m/s was chosen to get these solutions from the model. The isotherm curve was chosen from the literature. <sup>[2]</sup>

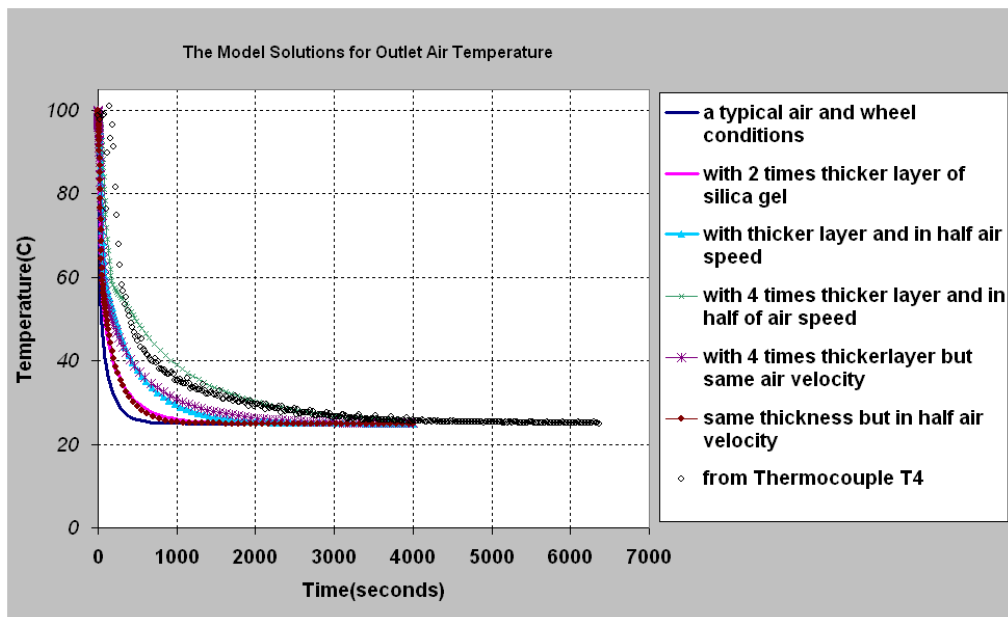


**Figure 5.19.** The model solutions for outlet air temperature in different conditions. The typical conditions for the input file of model

### 5.2.5. Test set up to study of Enthalpy Wheel

A test bed as shown in figure 5.20a and b was set up to study the enthalpy wheel of Hoval.

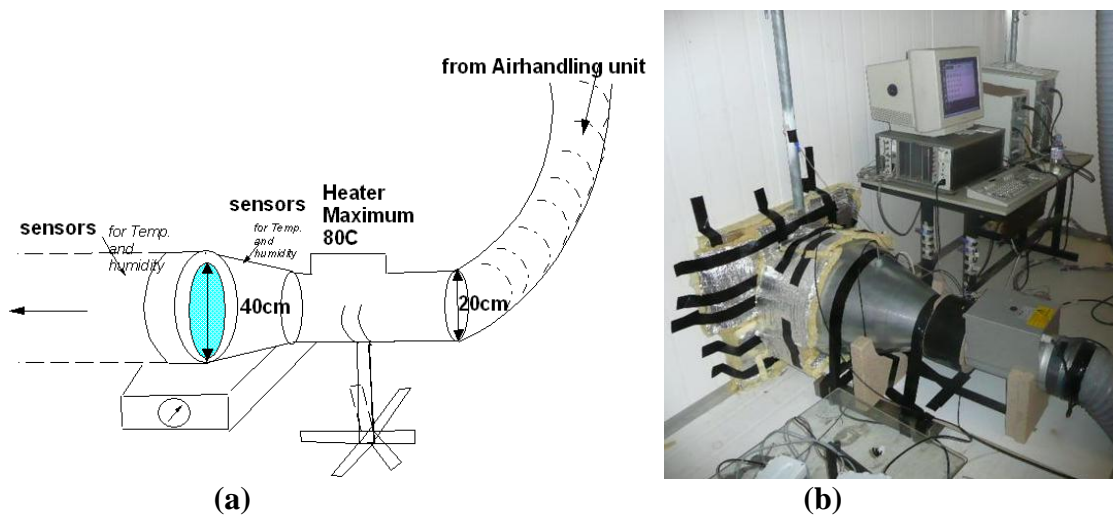


**Figure 5.20.** (a) Schematic and (b) the set up to study and test of Hoval that is an enthalpy wheel.

The limitations to prepare the necessary test facilities were the main reason for

postponing doing the measurements for this wheel. At first the tests were carried out with the dehumidifier wheel DRI, however, detailed information about this wheel was not available to conduct a comprehensive study.



**Figure 5.21.** Hoval wheel used to study and test an enthalpy wheel

The tests were helpful to organize the second test bed and solve the experienced problems in performing the measurements to produce and control stable air conditions. The wheel is shown in figure 5.21. The primary results presented in figure 5.22. The profiles of inlet air temperature and relative humidity for Hoval wheel as well as the outlet air conditions have been shown in this figure. Initially, the wheel was regenerated with air at about 75°C temperatures. The sensor measures the air temperature and humidity at a location close to wheel and center part of the wheel.

The fluctuations in input humidity are caused by a poor tuning of the controller and can be observed in the results. After turning off the heater adsorption process has been started. At the end of regeneration process inlet and outlet air conditions need to be equal, but the results show that still there is a large difference in temperatures of the inlet and outlet air. This difference indicates that the heater is off before the regeneration of the wheel is completed. The measurement of weight gain during adsorption has been shown in figure 5.23.

The maximum adsorption measured by scale was 55gram as seen in this figure. In addition, the measurements of inlet and outlet air conditions given in figure 5.22 the adsorption amount can be measured by:

$$\text{Adsorbed weight} = \rho VA \int (\omega_{in} - \omega_{out}) dt$$

The integral terms can be measured from the results of sensors shown in figure 5.22 during adsorption process as:

$$\int \omega_{in} dt - \int \omega_{out} dt = (32.77 - 32.36) = 0.41 \text{ kg kg}^{-1} \text{ sec}$$

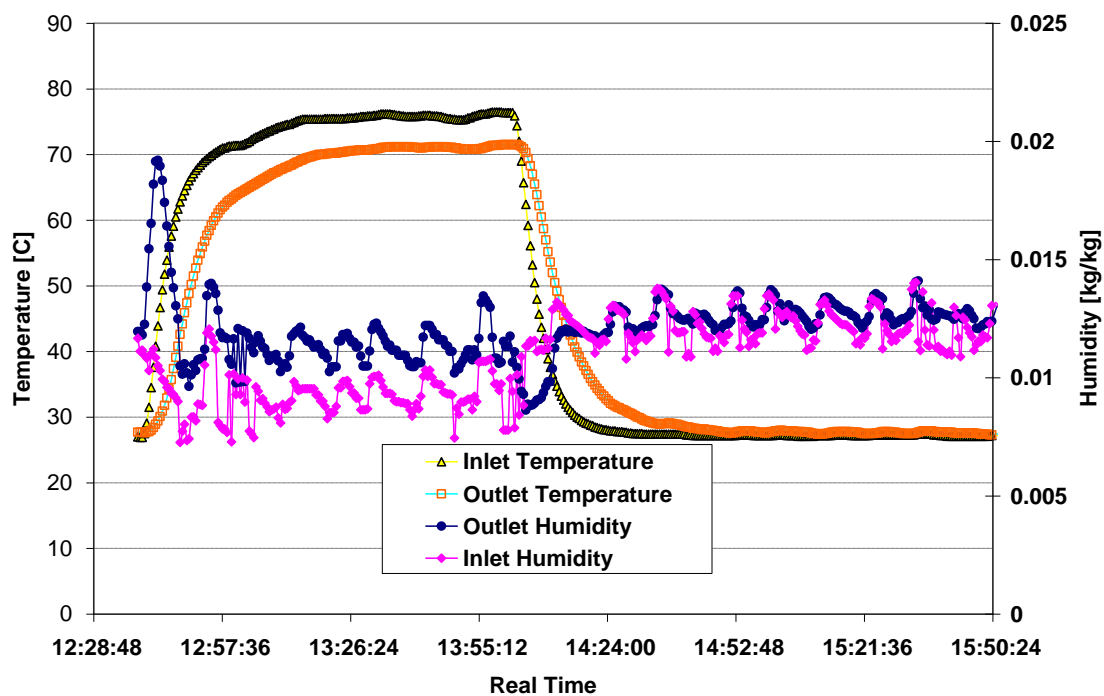


**Figure 5.22.** The profiles of inlet and outlet air conditions for Hoval wheel during the regeneration and adsorption of wheel. The desired inlet air conditions was set to 27°C temperature and 12 gr /kg humidity, but in practice has been measured by sensors as shown in this figure

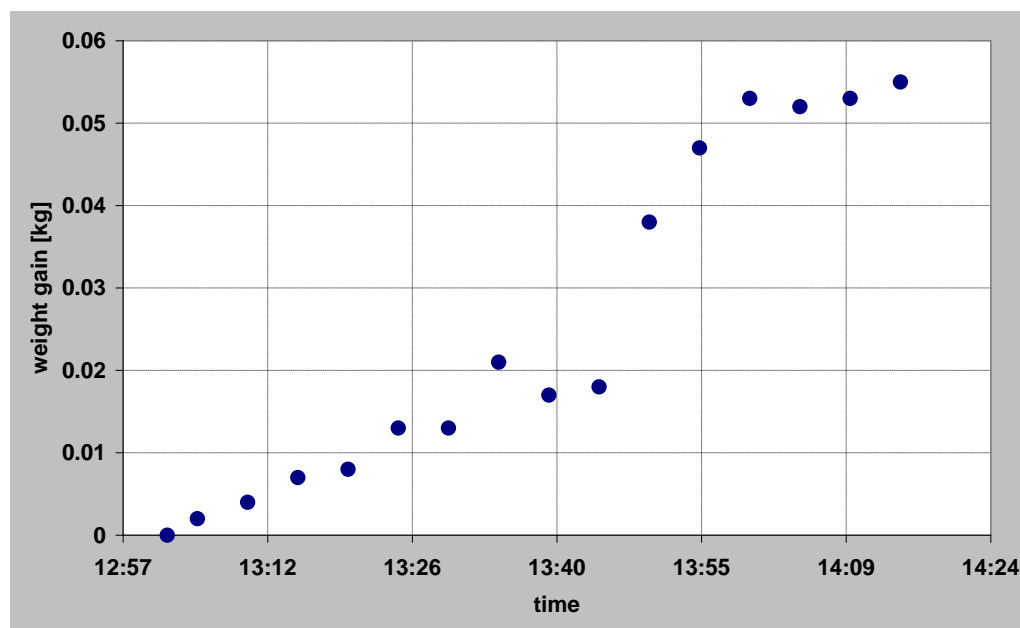


**Figure 5.23.** Adsorption process for Hoval wheel. Inlet air conditions were fluctuating around 27°C and 60% relative humidity

The number of air passages in the matrix, can be easily calculated (here 99200), and at air velocity of 1 m/s the adsorption can be measured by sensors as:

$$\begin{aligned} \text{Adsorbed weight} = \\ 1.2 \times 1 \times ((\pi \times 1.27^2 / 4) \times 10^{-6}) \times 99200 \times \int (\omega_{in} - \omega_{out}) dt = 0.062 \text{ kgr} \end{aligned}$$

Using the physical model the adsorption can also be calculated as:

$$\begin{aligned} \int (\omega_{in} - \omega_{out}) dt = (33 - 32.54) = 0.46 \text{ kg kg}^{-1} \text{ sec} \\ \text{Adsorbed weight} = \\ 1.2 \times 1 \times ((\pi \times 1.27^2 / 4) \times 10^{-6}) \times 99200 \times \int (\omega_{in} - \omega_{out}) dt = 0.069 \text{ kgr} \end{aligned}$$

As it can be seen, measurement by the scale yields a lower adsorption than the second method and the model. This difference is reasonably acceptable as in the second method all the air passages are assumed to be in the same conditions of air velocity and adsorption that is not realistic.

### 5.3. Summary and conclusion of experimental studies

- Data from measurements supplied by Carrier Holland Heating, compiled at Luzan University for an enthalpy wheel, with Simulink model solutions at the same conditions. The function for sorption of the material in the measurements was missing information but the solutions were calculated by one isotherm equation with some corrections in the literature.
- The agreement between the data and the Simulink model results was excellent and validated the model. The comparison between accurate simulation model and the experimental data <sup>[1]</sup> shows they agree within the acceptable margin of error. Having ignored the results for very low wheel speeds, since it is difficult to obtain accurate results for both model and experimental measurements, the errors are between  $\pm 2.5\%$  for air temperature and humidity.
- In chapter Four it was concluded that a large error in the outlet of the desiccant wheel results in 3 times a smaller error in the supply temperature. Consequently, a wide tolerance in validation can be accepted, therefore, even the larger amount of error in low speeds are negligible in modeling of an air conditioning cycle.
- Two different test beds were set up and the adsorption properties of two desiccant wheels (one dehumidifier DRI and the other enthalpy wheel Hoval), with the characteristics given in this chapter, were studied for different air conditions of temperature and humidity (20-27 °C and 35- 70%). The results of the second set up to test the Hoval wheel will be published in the papers since it could not be finished before publishing this thesis. Therefore, only the results of measurements from the first set up with DRI wheel have been discussed in this chapter.

- It was difficult to measure the adsorbed weight, especially in adsorption process. This is because in the beginning of the process the desiccant has the highest potential to adsorb humidity, so some changes had to be rearranged, such as removing the cover, the switching off the heater, and the re-calibration of the scale. All of these caused an error in the weight measurement.
- The profiles of the weight loss in the regeneration period and also the weight gain in the adsorption period, as well as outlet air humidity profiles, show well the symmetrical physical behavior of adsorption and desorption, and the time necessary for each process. It was observed that in general regeneration is a faster phenomenon than adsorption.
- The results show adsorption decreases with a rise in the air temperature. On the other hand, the increase in regeneration temperature and decrease of its humidity increases the adsorption. Therefore, for measuring maximum potential of adsorption in different air humidities, the matrix needs to be regenerated in the same air conditions.
- There was not enough information to compare the measurements and model solutions for the available dehumidifier wheel. Some primary information about the wheel such as the mass of silica gel matrix needs to be prepared. However, primary investigation shows the model can be tuned and calibrated with these experimental data. The model and the measurements are in agreement in the calculation the weight of adsorbed water vapor for typical inlet air conditions. Some corrections in the variations in inlet air humidity and the errors in weight measuring were added and considered for the comparison.



## References

1. Prof. R. Furter, P.Keller, Temperatur-und Feuchteübertragungsverhalten von Warmerückgewinnern im Teillastbetrieb, HTA Luzern, Dezember 2000.
2. A.Kodama, T.Hirayama, Maggot, T.Hirose, R.E.Critoph, The use of psychometric charts for the optimization of a thermal swing desiccant wheel, *Applied Thermal Engineering*. 21, 1657-1674, 2001.
3. Hoval Rotary Heat Exchanger for Heat Recovery in Ventilation Systems, Handbook for Design, Installation and Operation, Doc.No.Hw60aE1-11/2002, www.hoval.com.,Hovalwerk AG,Liechtenstein, 2002.
4. Chauch Y.K, P.Norton, F. Kreith, Transient Mass Transfer in Parallel Passage Dehumidifiers with & without Solid Side Resistance, *ASME Journal of Heat Transfer*, V. 111, 1038-1044, 1989.
5. Ahmad A. Pessaran and Anthony F. Mills, Moisture transport in silica gel packed beds- II Experimental study, *Int. J. Heat Mass Transfer*. Vol. 30, N. 6, pp. 1051-1060, 1987.
6. Popescu. M, Ghosh. T.K, Dehumidification and simultaneous removal of selected pollutants from indoor air by a desiccant wheel using a 1M type desiccant, *Journal of solar energy engineering*, Transactions of the ASME, Vol. 121, N. 1, pp 1-13, 1999.
7. C.X. Jia, Y.J. Dai \*, J.Y. Wu, R.Z. Wang, Experimental comparison of two honeycombed desiccant wheels fabricated with silica gel and composite desiccant material, *Energy Conversion and Management* 47, 2523–2534, 2006.
8. Ahmed M. Hamed, Experimental investigation on the adsorption/desorption processes using solid desiccant in an inclined-fluidized bed, *Renewable Energy* 30, 1913–1921, 2005.
9. Frank H. Dickey, The preparation of specific adsorbents, proceedings of the national academy of sciences, Volume 35, Number 5, May 15, 1949.
10. Yuri I. Aristov , Mikhail M. Tokarev , Angelo Freni b, Ivan S. Glaznev , Giovanni Restuccia, Kinetics of water adsorption on silica Fuji Davison RD, *Microporous and Mesoporous Materials* 96 , 65–71, 2006.
11. J. Cheng-Chin Ni, Jung-Yang San, Measurement of apparent solid-side mass diffusivity of a water vapor–silica gel system, *International Journal of Heat and Mass Transfer* Vol. 45, pp 1839–1847, 2002.
12. Devrim Balkose, Sevgi Ulutan, Fehime Cakıcıoglu Ozkan, Sedat Celebi, Semra Ulku, Dynamics of water vapor adsorption on humidity-indicating silica-gel , *Applied Surface Science* Vol. 134 pp .39–46, 1998.
13. George W. Scherer, Effect of drying on properties of silica gel, *Journal of Non-Crystalline Solids* Vol. 215, pp 155-168, 1997.
14. Steich G., Performance of Rotary Enthalpy Exchangers, M.S. Thesis in Mechanical Engineering, University of Wisconsin-Madison, 1994.



# 6. DESICCANT COOLING SYSTEMS

“Reprinted with permission from the American Institute of Aeronautics and Astronautics, AIAA”

## Introduction

In desiccant cooling processes fresh air is dehumidified, and then sensibly cooled by evaporation before being sent to the conditioned space. Since this technique works without conventional refrigerants, such as fluorocarbons and it allows the use of low-temperature heat (low temperature industrial waste heat or solar energy) to drive the cooling cycle, it attracted increased attention especially in America, Japan and Europe. <sup>[1]</sup> Desiccants remove moisture from the surrounding air until they reach equilibrium with it. This moisture can be removed from the desiccant by heating it to temperatures around 60-90°C (depending on air conditions) and exposing it to a regenerative air stream. The desiccant is then cooled so that it can adsorb moisture again, and cool down the supply air stream by humidification. Desiccant cooling cycles are particularly useful if they are used in humid regions.

The major advantage of desiccant cooling is its significant potential for energy savings and reduced consumption of fossil fuels. The electrical energy requirement can be very low compared with conventional refrigeration systems. Advantages of using desiccant cooling systems include the following: (1) very small electrical energy is consumed and the sources for the regenerating thermal energy can be diverse; (2) a desiccant system is likely to eliminate or reduce the use of ozone depleting CFCs (depending on whether desiccant cooling is used in conjunction with evaporative coolers or vapor compression systems, respectively); (3) better humidity control can be achieved when compared to those cases employing vapor compression systems, since sensible and latent cooling occur separately; (4) improvement in indoor air quality is likely to occur due to the normally high ventilation and fresh air flow rates being employed; and (5) desiccant systems have the capability of removing airborne pollutants. <sup>[2-4]</sup>

Having low coefficient of performance (COP) can be considered as the main disadvantage for desiccant cooling systems. COP values of 0.8-1 are commonly predicted for this cycle. COP or coefficient of performance is defined as the space cooling load divided by thermal energy required to regenerate the desiccant. Some investigators use the heat removed from the processes air stream divided by the thermal energy required to regenerate the desiccant.

Kang and Maclain-Cross <sup>[5]</sup> showed that the dehumidifier is the key component of a desiccant cooling system and the cooling COP can be significantly improved by improving the performance of this component. Due to the advantages of desiccant

cooling systems, they have been introduced as attractive alternatives to conventional vapor compression systems and a great number of studies have been done on different aspects of this technology. <sup>[6-12]</sup>

The typical adsorptive desiccant cooling system consists of desiccant wheel, heat exchanger, evaporative coolers and several configurations for desiccant cooling systems such as ventilation mode and recirculation mode have been proposed for the total system as has been reviewed and reported. <sup>[13]</sup> The sensitivity analysis shows a significant potential for an increase in the coefficient of performance (COP) by improving the performance of the dehumidifier. <sup>[14]</sup> Two methods for improving COP of these systems: the addition of inert heat capacity to the desiccant matrix, and staging of the regeneration air stream has been reported by Collier, et. al. <sup>[15]</sup> Since there are rarely published experimental works in this subject, the cooling efficiency studies with many assumptions have not been confirmed by the actual system of desiccant cooling. <sup>[16]</sup>

Although there have been a considerable number of efforts, there are still many unknowns surrounding the performance of a desiccant cooling system due to a variety of system designs and the number of variables effecting the operation of the system.

The objective of this chapter is to connect the heat and mass transfer model of a desiccant wheel described earlier in this thesis to the other models for components of different desiccant cooling cycles. In addition, a control strategy based on sensitivity analysis has been presented. This requires simple and fast correlation functions to limit the computing time to an acceptable level. These functions can be used for the year round simulation of the cycle. The results of year round simulation of a desiccant cooling cycle with the control strategy resulting from a sensitivity analysis have been presented in this chapter. All desiccant cooling systems employ three main components in varying quantities and positions: desiccant wheel, evaporative cooler, heat exchanger.

## 6.1. Modeling of desiccant cooling systems

To study cooling systems with evaporation and adsorption technology the performance of four different air-conditioning cycles has been considered. The schematics of the four cycles have been shown in figures 6.1 a-d.

The first cycle, and probably the most studied desiccant cooling cycle that is named ventilation cycle, has been shown in figure 6.1a. It takes ambient air into a rotating desiccant dehumidifier where moisture is adsorbed and the temperature increases. The air then is sensibly and evaporatively cooled, and introduced into the conditioned space. The air leaving the room is first evaporatively cooled, then passed through the sensible heat exchanger where it recovers heat of adsorption from the supply air. Next it is heated with low grade thermal energy and the hot air is used to regenerate the desiccant.

A variation of this cycle is the recirculation cycle shown in figure 6.1b. The difference is that the air from the conditioned space is partially (50%) recirculated through the dehumidifier and other components. Ambient air is used for regeneration, and then

exhausted to the atmosphere. This cycle with 100% recirculation is useful as dryer in greenhouses. There is no ventilation or 100% return air from greenhouse in order to keep  $\text{CO}_2$  that is supplied as fertilizer in the greenhouse.

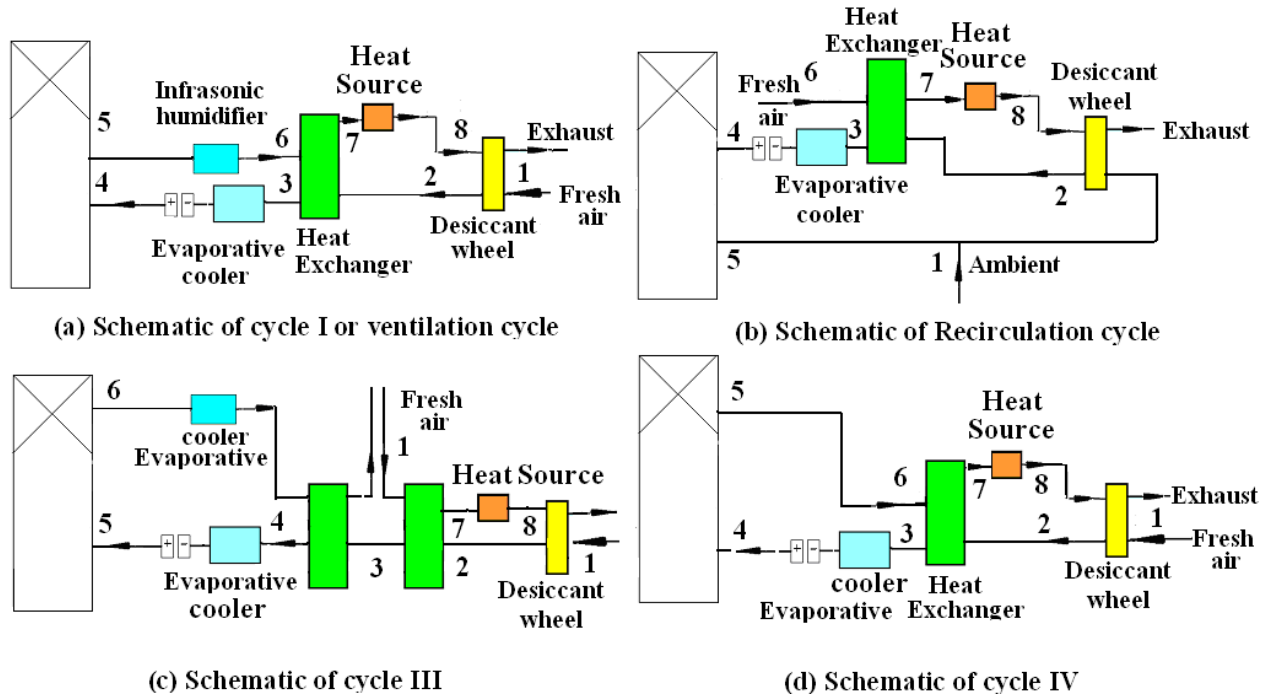


**Figure 6.1.** Four different desiccant cooling cycles; their performances have been studied by Simulink models with results presented in this chapter

Figure 6.1c shows a modification of these two cycles. Now the dry heat exchanger has been used for regeneration of the desiccant wheel and the other heat exchanger by using the infrasonic humidifier which has been partly wetted to cool down the supply air flow by indirect evaporative cooling.

The other modification has been shown in figure 6.1d. In this cycle the humidifier is not applied in the return air flow.

The simulation of these four different cycles has been done to investigate the highest COP or the minimum regeneration heat according to the desired supply temperature of  $16^{\circ}\text{C}$ .

Heat exchangers here are recuperative air to air heat exchanger type with efficiency of 80%. Evaporative cooler here means a humidifier that can produce humid air of 80-95 % relative humidity. Infrasonic humidifier can produce oversaturated vapor so it can make the surfaces of heat exchanger wet. In other words, infrasonic humidifier cools the air to saturation and more so the heat exchanger is wetted on the exhaust air side.

### 6.1.1. Modeling for Desiccant Wheel

The heat and mass transfer model in Matlab Simulink has this adaptability to easily connect to the building models and other air-conditioning models. However, the simulation for long periods needs a lot of calculation time and requires significant amount of computing memory that is not acceptable. Having used the correlations of outlet humidity and temperature, derived in the chapter 4, the simulation of wheel in different air conditioning cycles has been carried out for one reference year. However, for design purposes, the simulation has been carried out by physical model.

### 6.1.2. Modeling of wet heat exchanger for heat recovery unit

The humidifier is infrasonic that means it produces infra humidification and makes the heat exchanger's surfaces next to it partly wet. Here the heat exchanger surfaces are assumed to be completely wet surfaces. Figure 6.2 shows the configuration used to model the thermal resistances of this component.

The heat flux  $q$  refers to a part  $\Delta A$  of the heat exchanger surface  $A$  where heat and mass transfer occur. This can be calculated with the Merkel formula and also a linear assumption for enthalpy over a small range of temperature as:

$$q = \frac{\alpha}{C_p} (h_s - h) \approx \frac{\alpha e}{C_p} (t_s - t) \quad (6.1)$$

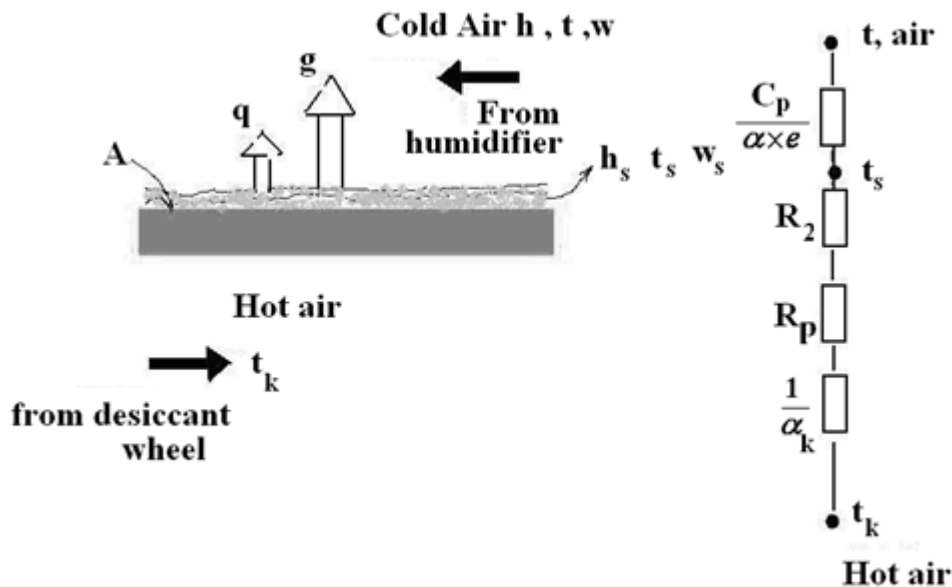


**Figure 6.2.** Scheme of the heat and mass transfers in the wet heat exchanger

The linearization factor “ $e$ ” can be calculated by considering two typical enthalpies of  $h_1$  and  $h_2$  at different temperatures  $t_1$  and  $t_2$ :

$$e = \frac{h_2 - h_1}{t_2 - t_1} \quad (6.2)$$

Therefore, the heat flux  $dq$  through a surface element  $dA$  is given by:

$$dq = \dot{m}_w dh = \dot{m}_w e dt \quad (6.3)$$

$$dq = K_t dA (t_k - t) \quad (6.4)$$

$$dq = -\dot{m}_k C_k dt_k \quad (6.5)$$

To obtain the total thermal resistance (due to the heat transfer between air and outside surface, conduction through the material of the surface, and the conductive heat transfer between two air streams inside the channels) these terms are combined into one resistance  $\frac{1}{K_t}$  as shown in figure 6.2:

$$\frac{1}{K_t} = \frac{C_p}{e\alpha} + R_2 + R_p + \frac{1}{\alpha_k} \quad (6.6)$$

Comparing with the procedure used to obtain temperature efficiencies for counter flow heat exchangers, the formulas for temperature efficiency of counter flow heat exchangers is derived as:

$$\varepsilon_w = \frac{1 - e^{-Ntu(1-C)}}{1 - Ce^{-Ntu(1-C)}} \quad (6.7)$$

With

$$Ntu = \frac{K_t A}{\dot{m}_k C_k} \quad (6.8)$$

And

$$C = \frac{\dot{m}_k C_k}{\dot{m}_w e} \quad (6.9)$$

It can be shown that the relation between the efficiency for the main and secondary air flow (  $\varepsilon_w, \varepsilon_k$  ) is given by:

$$\varepsilon_w = C \varepsilon_k = \frac{t_{wi} - t_{wo}}{t_{wi} - t_{ki}} \quad (6.10)$$

The outlet air humidity can be calculated using enthalpy balances for two air streams as follows:

$$h_{out,Cold} - h_{in,Cold} = h_{in,Hot} - h_{out,Hot} \quad (6.11)$$

The humidity of the air from desiccant wheel will not change. But the humidity of the air cooled by evaporation will be calculated by equation (6.11).

### 6.1.3. Computer Simulation

The simulations have been carried out using the Matlab Simulink environment shown in the block diagram in figure 6.3 due to adaptability with HVAC system and building simulation tool. In addition, the simulation parameters such as time steps, error tolerances, and solvers can be fitted to optimize both time and accuracy of the simulation. Output variables can be easily displayed with this modular tool. The psychrometric data are represented by the moist air properties equations following ASHRAE. [18] The desiccant wheel can be considered in optimum speed as the correlations used in the simulation are based on optimum speed of the wheel.

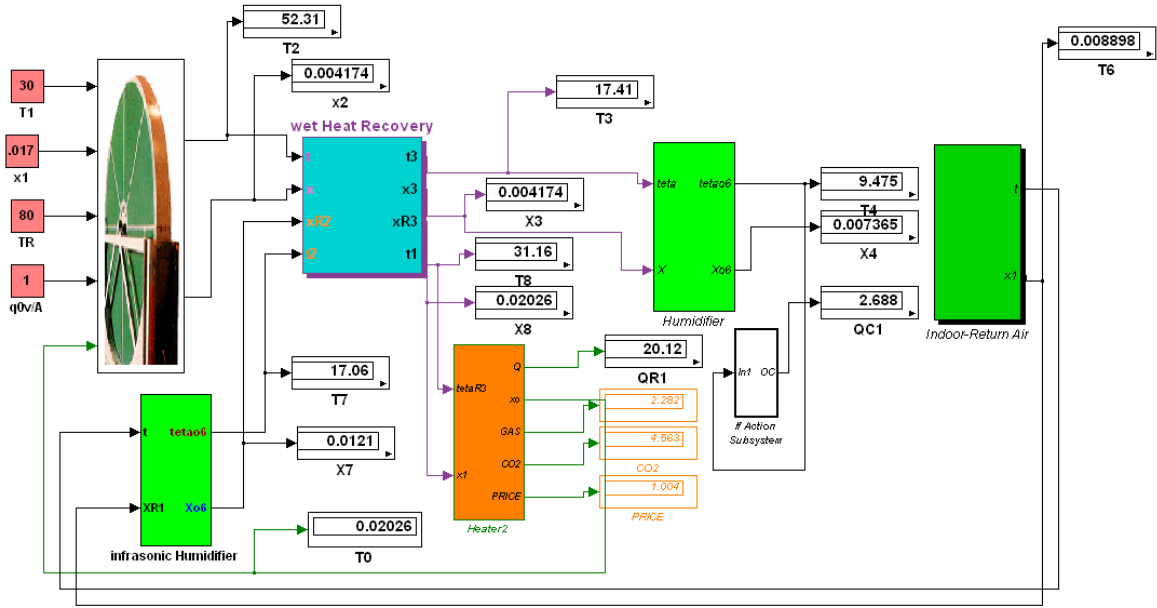


Figure 6.3. Simulink representation of the model, showing cycle I as a sample

### 6.1.4. Results of Simulation

The cooling capacity can be written as:

$$Q_{cool, cap} = c_p \dot{m} (T_{building} - T_{supply}) \quad (6.12)$$

Therefore, the heat rates can be calculated according to cooling capacity designed for the building. The COP or the coefficient of performance of the system can be calculated according to cooling load and the required energy as:

$$COP = \frac{\text{Cooling for air handling}}{\text{Required Energy}} = \frac{\dot{m} C_p (T_{\text{fresh air}} - T_{\text{Supply air}})}{(Q_R + Q_C + Q_H)} \quad (6.13)$$



The term  $Q_R$  refers to the energy needed for regeneration. The term  $Q_C$  to after cooling energy (needed when the supply air temperature is still higher than the set point). If the temperature is lower than desired supply temperature,  $Q_H$  is the energy needed to heat the supply air to the point of interest. Figures 6.4-6.7 show the change of air conditions. For the cycles shown in figures 6.1a-d, the ambient air conditions of 30°C temperature and 17 g/kg humidity are considered and the results are demonstrated for the optimum wheel speed.

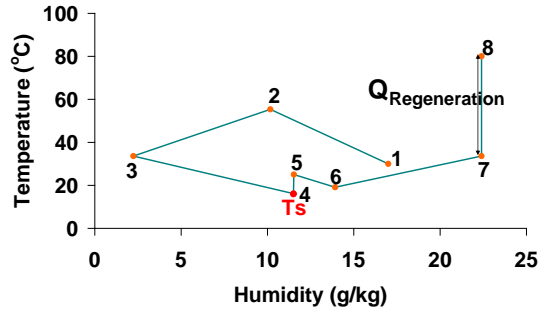


**Figure 6.4.** the Mollier chart of cycle I for ambient air of 30°C and 17gr/kg

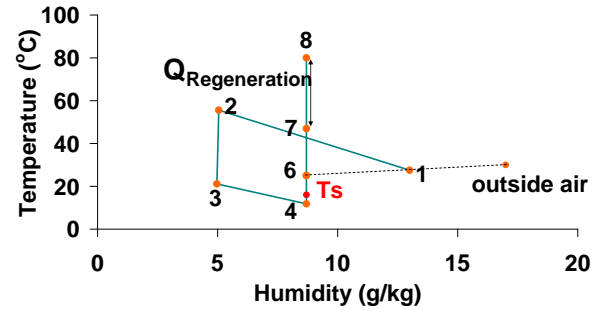


**Figure 6.5.** the Mollier chart of Recirculation cycle II for ambient air of 30°C and 17gr/kg

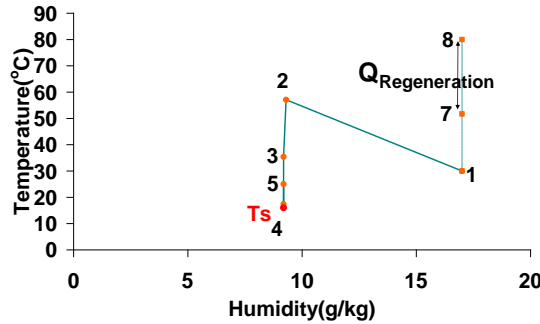


**Figure 6.6.** the Mollier chart of cycle III for ambient air of 30°C and 17gr/kg

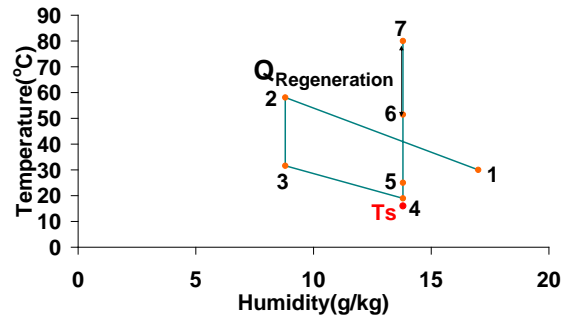


**Figure 6.7.** the Mollier chart of cycle IV for ambient air of 30°C and 17 gr/kg

The desired set point for the supply temperature has been chosen at 16°C (in saturation) for all four cycles. The results of simulation for coefficient of performance and supply temperature, energy needed for after cooling or after heating (depends on the temperature) and regeneration heat for all cycles have been given in table 6.1 two different conditions of outside air humidity and temperature. Calculations have performed using the physical model for desiccant wheel.

As it can easily be seen cycles III and IV have better values of coefficient of performance. In addition, the coefficient of performance of the system depends on the ambient air conditions so that it is higher for ambient air conditions of 40°C and 30g/kg

representing hot and humid climates. Table 6.2 shows the COP of the four cycles according to different outside conditions of humidity and temperature.

The effect of dry and wet heat exchangers has been evaluated for these cycles, as well. The surfaces are assumed to have been wetted by the infrasonic humidifier, using the model that was described in the previous section.

The choice of wet heat exchangers as provider of supply air has been based on the ability of delivering lower temperatures comparing with dry heat exchangers. Therefore the dry heat exchanger is an appropriate choice as a provider for pre-regeneration air since it can deliver the higher temperature before heating up the air for regeneration.

Therefore, an optimum performance can be predicted with the application of a regenerative evaporative cooler or Static cooler which was modeled in this study, and has been described in chapter 2 of this thesis. Proposing Static cooler as a heat exchanger, the incoming air is indirectly cooled by water. The water in turn is cooled by recirculation part of the supply air. The ratio of the recirculated air to the total incoming air is proposed to be 33%.

**Table 6.1.** The performance of the desiccant cycles 6.1a-d according to COP for different air conditions and regeneration heat.

	Ambient air		Ambient air	
	Temperature 30C	Humidity 17g/kg	Temperature 40C	Humidity 30gr/kg
Cycle I	QR(kw)	18.64	15.24	
	QC(kw)	-	1.46	
	QH(kw)	0.016	-	
	COP	0.3	0.57	
Cycle II	QR(kw)	12	10.89	
	QC(kw)	0.47	1.22	
	QH(kw)	-	-	
	COP	0.45	0.79	
Cycle III	QR(kw)	11.33	11.33	
	QC(kw)	1.21	0.16	
	QH(kw)	-	-	
	COP	0.45	0.84	
Cycle IV	QR(kw)	11.42	8.96	
	QC(kw)	0.39	1.5	
	QH(kw)	-	-	
	COP	0.47	0.91	

**Table 6.2.** The results of simulation for different outside air conditions of humidity and temperature. The regeneration air  $80^{\circ}\text{C}$  and set point for supply air of  $16^{\circ}\text{C}$  have been considered.

Out door conditions		Cycle I	Cycle II	Cycle III	Cycle IV
$^{\circ}\text{C}$	g/kg dry air				
30	15	0.29	0.3	0.48	0.47
30	25	0.31	0.42	0.49	0.49
40	25	0.56	0.8	1	0.91
40	35	0.58	0.79	0.98	0.91
40	45	0.6	0.77	0.99	0.89

### 6.1.5. Desiccant cooling system with three wheels

A new cycle using two heat exchanger wheels as shown in figure 6.8A' is suggested and, its performance is evaluated by simulation. Using the third wheel or a heat recovery wheel in figure 6.8A' for recovering the heat from the hot outlet regeneration air from the desiccant wheel will lead to an energy saving for pre-heating of regeneration air.

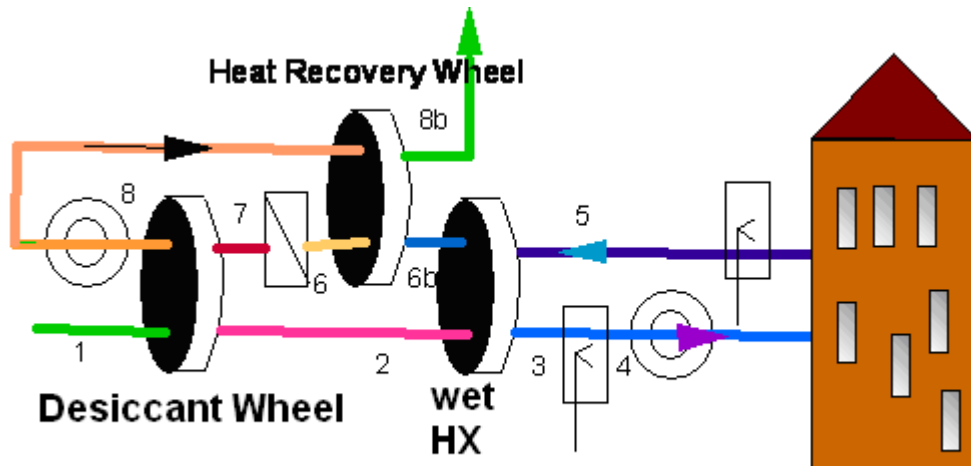


**Figure 6.8A'.** A special heat recovery wheel in the exhaust air flow saves about 20% energy required for the wheel regeneration

As shown in table 6.3, reductions of 25 % and 19 % in the regeneration heat requirement have been resulted. The efficiency of heat exchanger is 80%, and humidification efficiency is assumed to be 90%.

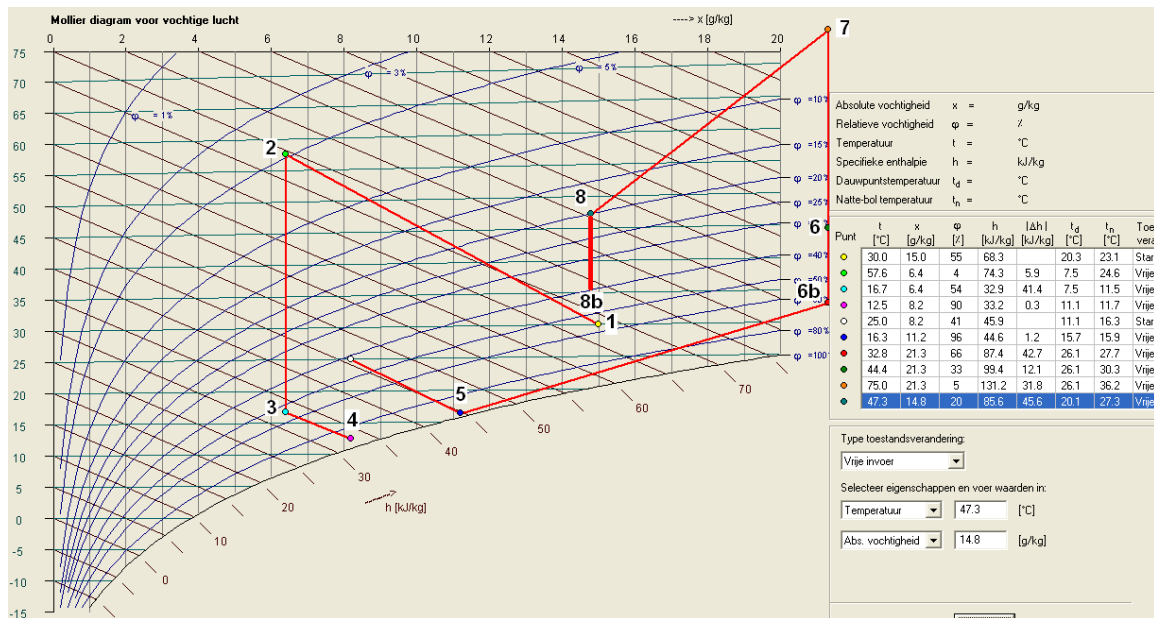


**Figure 6.8B':** The variations of air conditions in the Mollier diagram for the cycle shown in figure 6.8A'

**Table 6.3.** The improvement of about 25 % in the performance of desiccant cooling system using one additional wheel of heat exchanger.

	Outside Temperature °C	Outside Humidity gr/kg	Supply air Temperature °C	Regeneration Temperature °C	Regeneration Heat: kw	COP
Cycle I Without Additional heat exchanger	40	20	18	79	48.5	0.51
Cycle I with two heat exchangers	40	20	18	79	36.18	0.73
Cycle I Without additional heat exchanger	30	20	16	79.5	52	0.32
Cycle I with two heat exchangers	30	20	16	79.5	42.28	0.4

A typical situation has been chosen in Mollier diagram as shown in figure 6.8B'. It can be simply understood from this figure higher outlet temperature of desiccant wheel (point 8) can lead to more saving of heating energy rate. Therefore, COP is a function of the outlet air conditions from desiccant wheel and the efficiency of the heat recovery system. The regeneration temperature depends on the desiccant characteristics and the wheel speed and air conditions.

## 6.2. The sensitivity analysis for control strategy

A sensitivity analysis is carried out to study and optimize the performance of the air conditioning systems. Regarding the materials described in the previous chapters of this thesis, one of the important control variables is the regeneration air condition for desiccant wheel. Figures 6.8 and 6.9 show the result of simulation of a simple desiccant cooling system for different regeneration air temperatures; moderate, hot and humid climates respectively.

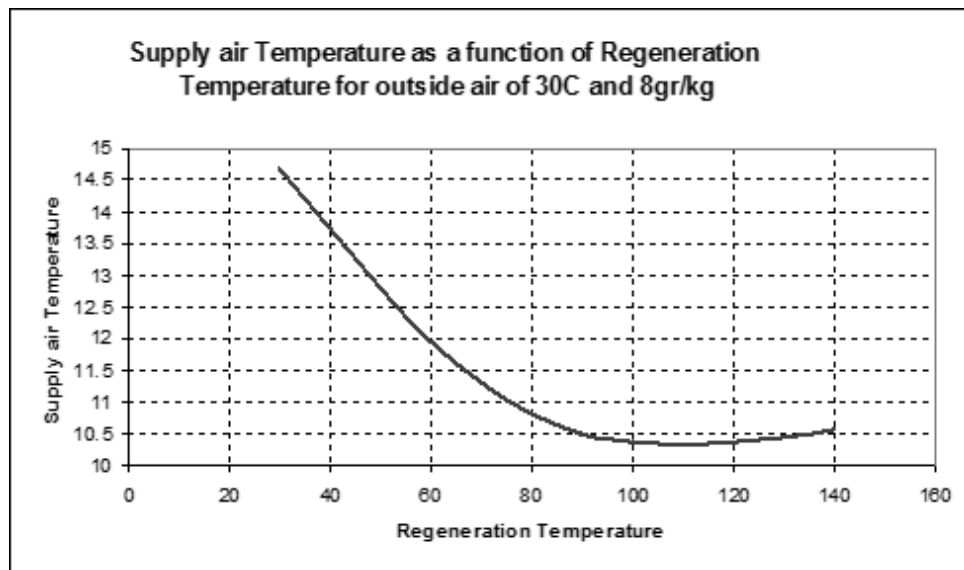


**Figure 6.8.** Increase in regeneration temperature result in decrease in supply air temperature

As it can be observed in figure 6.10, this profile also depends on the outside air conditions.

Figure 6.10 gives the results of simulation for supply air temperature in different wheel speeds for an extreme climate. It is clear the increase in wheel speed can reduce supply air temperature but after an optimum speed the increase of speed does not have effect and change the air conditions. The graphic for a moderate climate shows the same tendency.

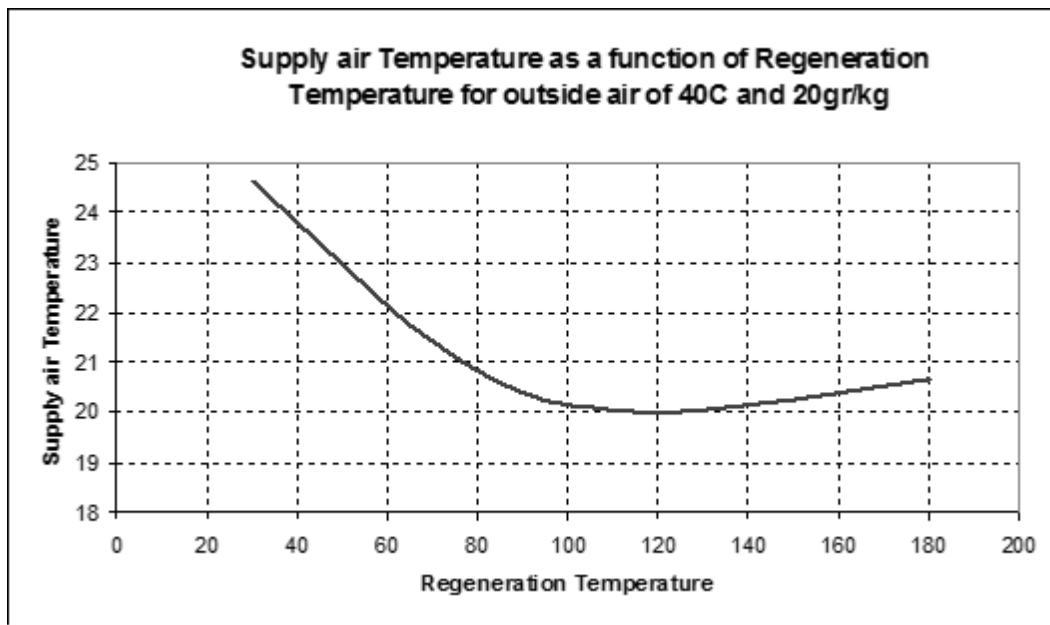


**Figure 6.9:** Increase in regeneration temperature results in decrease in supply temperature for more humid and hot air conditions

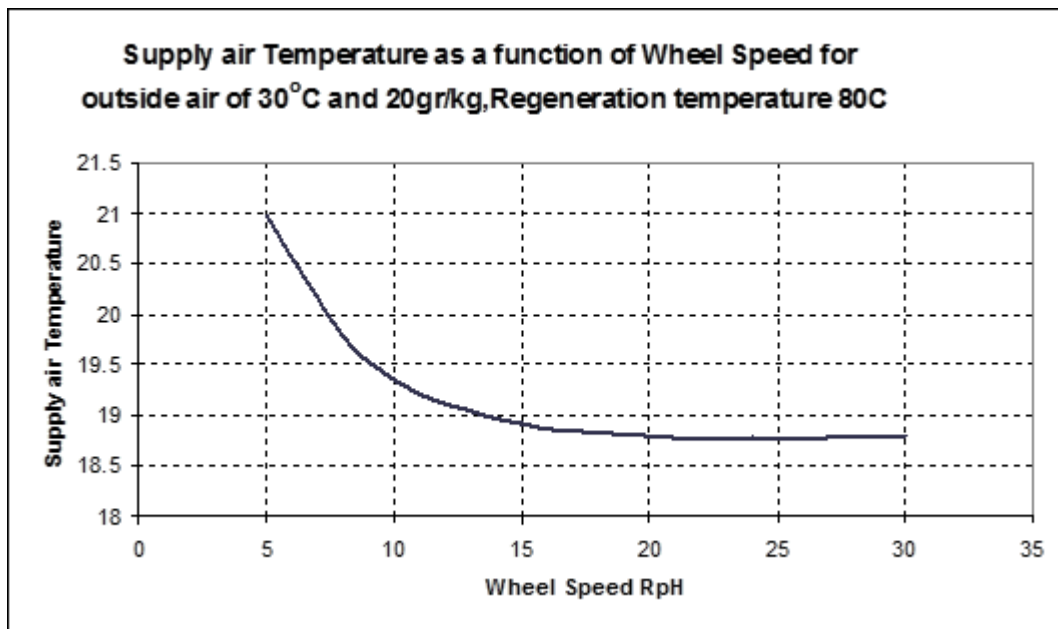


**Figure 6.10.** The increase in wheel speed results in decrease in the supply air temperature, but after an optimum speed the increase in speed does not change the air conditions

Using these results a strategy to control the performance of a typical desiccant air cooling system can be concluded. It seems the wheel needs to be rotated at the optimum speed but at a minimum temperature for regeneration air. The optimum value for regeneration air temperature depends on the outside air conditions and changes as a

variable. The increase in regeneration temperature has resulted in decrease in the supply air temperature as it is shown in these figures.

### 6.3. Year round simulation and control of a hybrid air-conditioning system

The cycle considered in this chapter for yearly simulation is a ventilation air-conditioning cycle shown in figure 6.11 due to simplicity and the fact that the supply air is 100% outside air. The fresh air is dehumidified through a desiccant wheel and then sensibly and evaporatively cooled before being sent to the conditioned space through a heat exchanger and a humidifier. The return air is cooled down through an infrasonic humidifier, which can produce over saturated air, and is heated by the air to air heat exchanger used for regeneration.

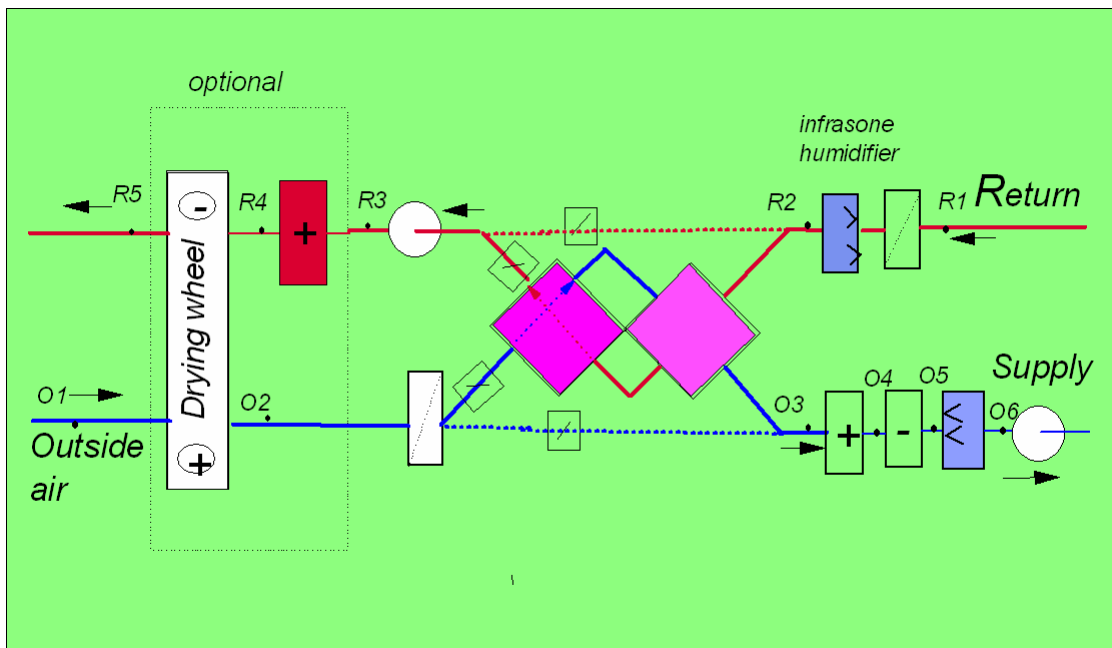


**Figure 6.11** Component elements of the desiccant cooling system

As shown in this chapter, desiccant coolers have very low coefficient of performance as a result of large amount of heating required for regeneration of the desiccant matrix. Therefore, a hybrid cooling system with desiccant wheel, as an auxiliary system, has been chosen for year-round simulation. Its performance has been simulated and compared with that of the conventional chillers. Based on a control strategy, the system uses a wheel as a dehumidifier only at extreme outside air conditions.

Four different systems are considered to be compared according to their performances. They are:

1. Hybrid desiccant cooling system: a desiccant cooling system that desiccant wheel is active only when the cycle of indirect evaporative cooler is unable to prepare supply air in set point temperature. If the system is still unable to supply air at the desired set point, then an auxiliary system using cold water from a conventional chiller is considered in the year- round simulations.
2. Conventional cooling system: a chiller with air cooler and heat recovery system.
3. Hybrid desiccant cooling using waste heat or solar thermal systems: the regeneration heat is delivered fully by a free source of thermal energy.
4. Evaporative cooling system using a heat exchanger with wet surfaces and conventional chillers as auxiliary system.

The simulations have been carried out using the Matlab Simulink environment due to its adaptability with HVAC system and building simulation. Matlab Simulink tool is well adapted to easily link the HVAC components with each other and eventually with the building models. Output variables can be easily displayed in this modular tool. The psychrometric data are represented by the equations for moist air properties following the ASHRAE. <sup>[18]</sup>

In these simulations the thermal behavior of the building is not considered. It is assumed that the air handling unit is used as a makeup unit for an air system with constant air conditions and the variations in the internal building cooling loads are not considered. The air handling unit delivers cold air  $T_{supply}$  for example 16°C. When the indoor temperature  $T_{building}$  is controlled at 24°C, the supply air with mass flow rate of  $\dot{m}$  delivers an amount of cooling to the building equal to:

$$Q_{cool, cap} = c_p \dot{m} (T_{building} - T_{supply})$$

The mass flow rates should be chosen so that the constant internal load of  $Q_{internal}$  given per m<sup>2</sup> floor area can be cooled away. The indoor temperature has been fixed at 24°C and the difference in absolute humidity between supply and return air due to high ventilation rates are neglected and the supply air is supposed to be saturated. The state for the outside temperatures lower than supply set point are switched off to zero, therefore the simulation results on the workspace are only considered for the outside temperatures higher than the set point for supply air temperature.

The performance of desiccant air-conditioning system has been studied for weather data of Beijing as an extreme climate as well as Netherlands as a typical moderate climate in reference years (winter 1964/ summer 1965). The set point temperature for supply air temperature has been considered equal to 16°C. In order to minimize regeneration heat the control strategy adjusts the minimum regeneration temperature according to the set point for supply air temperature to provide the required cooling capacity.



The regeneration temperature would be in maximum value if and only if the supply temperature is equal or more than set point according to this control strategy. For the states with supply temperatures higher than set point after cooling is required and have been considered using a conventional chiller in these simulations.

Heat recovery systems or heat exchangers with wet surfaces, which has been modeled as described in section 6.1.2, give lower supply air temperatures comparing with the heat exchangers with dry surfaces. Figure 6.12 shows how using heat recovery system with a wet surface in the return airflow stream reduces air temperature of supply air as well as the air temperature before heating or regeneration.

Although the heat exchanger with wet surfaces is capable of supplying air 2-4°K colder, the reduction in air temperature before the heater for regeneration is 8-16°K due to using wet heat recovery system. Consequently, it is not advantageous to use a heat recovery with wet surfaces when desiccant wheel is active and thermal energy for regeneration is not free.

However, the heat exchangers with wet surfaces are applied in the system when the desiccant wheel is not active or when the regeneration heat is prepared from the waste heat or solar energy. In addition, the efficiency of humidification has a considerable effect on the results, and has been described in the next section.

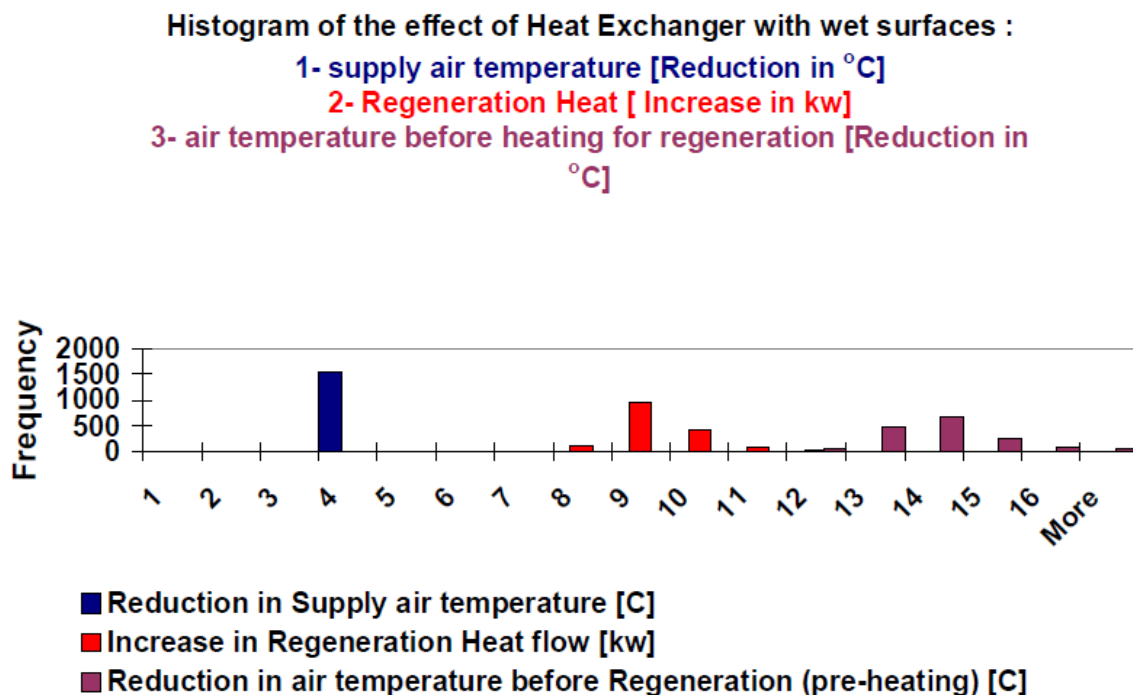


**Figure 6.12.** The reduction of supply air temperature and the air temperature before heating for regeneration due to use of wet heat exchanger during a reference year for the Netherlands

## 6.4. Results of yearly simulation

The cooling capacity is defined as the cooling or removing the surplus heat per  $\text{m}^2$  of the floor area, and can be described as:

$$Q_{cc} / A = \dot{m} C_p (T_{\text{set,indoor}} - T_{\text{set,supply}}) / A$$

Consequently, an air handling installation has to deliver this amount of cooling to the airflow. The COP or the coefficient of performance of the system can be calculated according to cooling load and the required energy.

The performance of desiccant air conditioning systems depend on the operating parameters of desiccant wheel. This study has been performed according to year-round simulation for variable cooling load; according to a selective supply air temperature and variable fresh air temperatures and humidities; so the required regeneration heat may be minimized by selecting proper values of regeneration temperature for a hybrid cooling system.

At the same time the control strategies influence system performance through optimum speed of wheel. This analysis presents a method for choosing optimal values. The optimal control strategy will allow the regeneration temperature to vary in proportion to the cooling load. The wheel rotational speed may be kept constant according to optimum speed and fine tuning of this speed is not important. The control strategy has been described in figure 6.13.

It can be observed that how a hybrid desiccant cooling system using desiccant wheel only in a part of summer, as shown in the tables, leads to saving energy and reduction in CO<sub>2</sub> emissions with different ratios for different climates.

Tables 6.4 and 6.5 show CO<sub>2</sub> emissions and energy costs at two different climates for different cooling systems.

The first system is related to a reference system or the conventional air cooler, studied in chapter 3, with a cooling factor equal to 3. The simulation results demonstrate that an auxiliary evaporative cooling system, using two humidifiers and a heat exchanger with wet surfaces, results in considerable reduction in energy costs and the emissions.

Use of evaporative cooling system suffices in the Netherland for 40% of summer time while this ratio is 25% for Beijing climate. In the next row, the results of simulation for a hybrid desiccant cooling system have been given. A combination of adsorption and evaporation cooling leads to the given results for the emissions and the energy costs. The advantage of desiccant technology, for the situations using waste heat or a free heat source such as solar energy is demonstrated in the last row. The energy necessary for fans

and pumps are not considered, since this factor would have been the same for each and every scenario described in table 6.4.

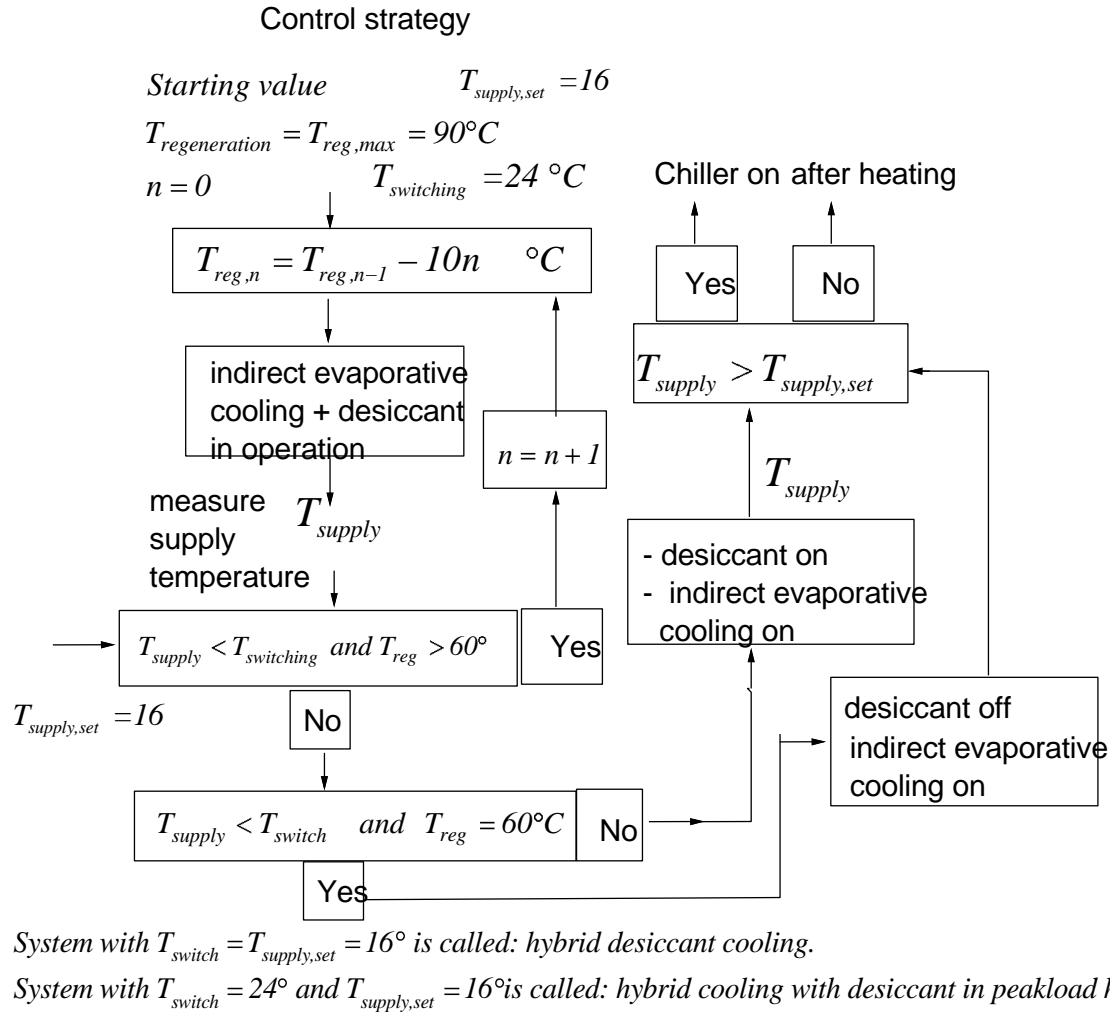


**Figure 6.13.** A graphical representation of the control strategy implemented in the year-round simulation of hybrid cooling system

These results are shown using different figures in this chapter. Figures 6.14 and 6.15 show the energy costs according to the given set point temperature  $16^{\circ}C$  for supply air and cooling capacity of  $30 \text{ W/m}^2$  for both climates. The comparison for conventional chillers with cold factor 3 and solar hybrid desiccant cooler is observed in these figures. As mentioned before, the desiccant wheel has been implemented as an auxiliary system for a hybrid system that is a combination of evaporative coolers and also heat exchanger. A conventional chiller is used to reach the desired set point for the situations that the system of adsorption and evaporative cooler is not able to achieve supply air at the desired set point.

This means that the desiccant system has been used only for peak load hours and for the rest of a year the hybrid system using heat recovery unit and two evaporative coolers is considered.

**Table 6.4.** Yearly CO<sub>2</sub> emissions and energy costs for the Netherlands using different cooling systems: The humidification and heat exchanger efficiency of 80% have been considered for all systems. The model of wet heat exchanger is given and discussed in this thesis. The effects of fans and pumps are the same for different systems and are not considered in these calculations.

	CO <sub>2</sub> emission kg/m <sup>2</sup>	Energy costs euro/m <sup>2</sup>	
Conventional Air Cooler	4.3	1.1	
(Wet HX+ Evaporative Cooler= system A )40%+ (system A+ Conventional Air Cooler as auxiliary system) 60%	1.16	0.29	60% of year evaporation is not enough then a conventional chiller is used as auxiliary system
(Dry HX+ Evaporative Cooler + Desiccant Wheel =system B + Conventional Air Cooler) 60%+ system A 40%	2.47	0.58	60% of year desiccant is used the rest evaporation cooling is enough
(Wet HX+ Evaporative Cooler + Desiccant Wheel=systemC) 60%+ (System A) 40%	0	0	Free heat(solar thermal system or waste heat is used for regeneration heat)

The results show that using desiccant wheel can result in some savings in the energy and reducing environmental impacts comparing with conventional chillers, for the Netherlands. However, when regeneration heat is prepared by free thermal source, the indirect evaporative cooling system and adsorption will suffice (without using conventional chillers) by themselves. For Beijing the reduction in the costs and emissions are 90% as it can be seen in the figures and the results of the tables.

Figures 6.16 and 6.17 show the comparison of CO<sub>2</sub> emissions for different coolings systems according to supply set point temperature. The efficiency of 90% for boiler has been assumed to calculate of gas consumption for regeneration heat.

The energy consumption needed for after cooling requirement has been calculated using a cold factor of 3 for conventional chillers and 40% efficiency of power plants. It is assumed that the after cooling requirement is calculated without considering the dehumidification for the conventional air cooler.

Considering that each cubic meter of gas can produce 9.8 kWh of thermal energy, then the yearly gas consumption for hybrid desiccant air conditioning system can be calculated as:

$$\text{Primary Required Energy} = \sum \frac{Q_{\text{Regeneration}}}{0.9} + \sum \frac{Q_{\text{after-cooling}}}{0.4 \times 3} \quad [\text{kwh}] \quad (6.14)$$

**Table 6.5.** Yearly CO<sub>2</sub> emissions and energy costs for Beijing and different cooling systems: The humidification and heat exchanger efficiency of 80% have been considered. The effects of fans and pumps are the same for different systems and are not considered in these calculations.

	CO <sub>2</sub> emission kg/m <sup>2</sup>	Energy costs euro/m <sup>2</sup>	
Conventional Air Cooler	4.3	1.1	
(Wet HX+ Evaporative Cooler= system A )40%+ (system A+ Conventional Air Cooler as auxiliary system) 60%	1.16	0.29	60% of year evaporation is not enough then a conventional chiller is used as auxiliary system
(Dry HX+ Evaporative Cooler + Desiccant Wheel =system B + Conventional Air Cooler) 60%+ system A 40%	2.47	0.58	60% of year desiccant is used the rest evaporation cooling is enough
(Wet HX+ Evaporative Cooler + Desiccant Wheel=systemC) 60%+ (System A) 40%	0	0	Free heat(solar thermal system or waste heat is used for regeneration heat)

$$\text{gas Consumption} = \frac{\sum \frac{Q_{\text{Regeneration}}}{0.9} + \sum \frac{Q_{\text{after-cooling}}}{0.4 \times 3}}{9.8} [m^3] \quad (6.15)$$

Using a cost of 0.44 Euro for each cubic meter of gas and 0.13 Euro for each kWh electricity, the energy costs have been calculated for hybrid desiccant system.

The system has been investigated for CO<sub>2</sub> emission in the given set point of supply air temperature and comparison has been made between hybrid desiccant system and conventional chillers.

It has been assumed that each cubic meter gas can produce 2kg of CO<sub>2</sub>. For conventional chillers the cold factor of 3 and power plant efficiency of 40% has been used to calculate the energy costs and CO<sub>2</sub> emission as:

$$\text{Thermal Energy Consumption} = \sum \frac{\text{Cooling Load}}{(3 \times 0.4)} = \sum \frac{\dot{m} C_p (T_{\text{outside air}} + 1 - T_{\text{supply}})}{(1.2)} [kWh] \quad (6.16)$$

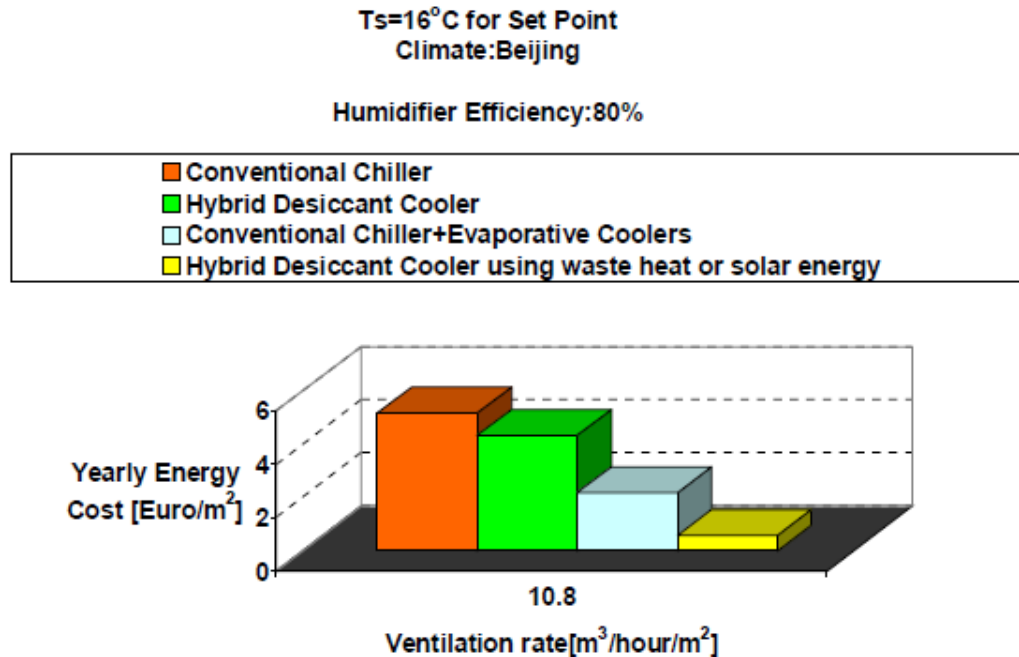


**Figure 6.14.** Comparison of energy costs for hybrid cooling system and conventional chiller with cold factor 3, and cooling capacity of  $30 \text{ W/m}^2$  for  $16^\circ\text{C}$  supply air temperature. Desiccant wheel is activated only in peak load hours. The simulation results show a proper combination of heat exchangers with wet surfaces, evaporative coolers and desiccant wheels can be energy efficient and show considerable emission reductions.

In the calculation of cooling load, one degree increase in the air temperature for the air heating by fans has been considered.

The effect of humidification efficiency of evaporative coolers on the performance of cooling system regarding energy costs and  $\text{CO}_2$  emissions have been shown in figures 6.19 and 6.20. It can be observed that how an increase in humidification efficiency improves the performance of hybrid desiccant cooling systems.

Desiccant cooling technology can be useful and practical when the latent load is large in comparison with the sensible load for the energy cost and  $\text{CO}_2$  emissions. Typical reductions of 10 and 55% in  $\text{CO}_2$  emission and energy costs can be obtained respectively. These figures increase to 90 and 100% reduction for the systems that use waste heat as regeneration heat. The thermal coefficient of performance (COP) is commonly used to compare the system performance. The definition of the thermal COP varies, and there are two definitions in the literatures. Some investigators use the space-cooling load divided by the thermal energy required to regenerate the desiccant. Others use the heat removed from the process air stream divided by the thermal energy required to regenerate the desiccant or equation (6.13). Figures 6.21 and 22 show the thermal coefficient of performance for year-round simulation of hybrid desiccant cooler respectively for the Netherlands and Beijing using this definition. The low values of COP are due to cooling system with desiccant wheel while the high values of COPs are due to the situations that

the required energy is only the energy needed for running fans. The COPs less than one are related to high values of the required regeneration energies.

In short, desiccant wheels have low coefficient of performance due to the high regeneration heat. According to the control strategy described here, the desiccant wheel has been used only in the peak load hours. Therefore, the desiccant wheel is an auxiliary system for a hybrid system including heat recovery and evaporative systems. In addition, desiccant cooling systems when the source of regeneration heat is waste heat or solar energy can save energy consumption and reduces CO<sub>2</sub> emission considerably as shown in the results of year-round simulation described in this chapter. It can be easily concluded that the desiccant technology is an attractive alternative for hot and humid climates.

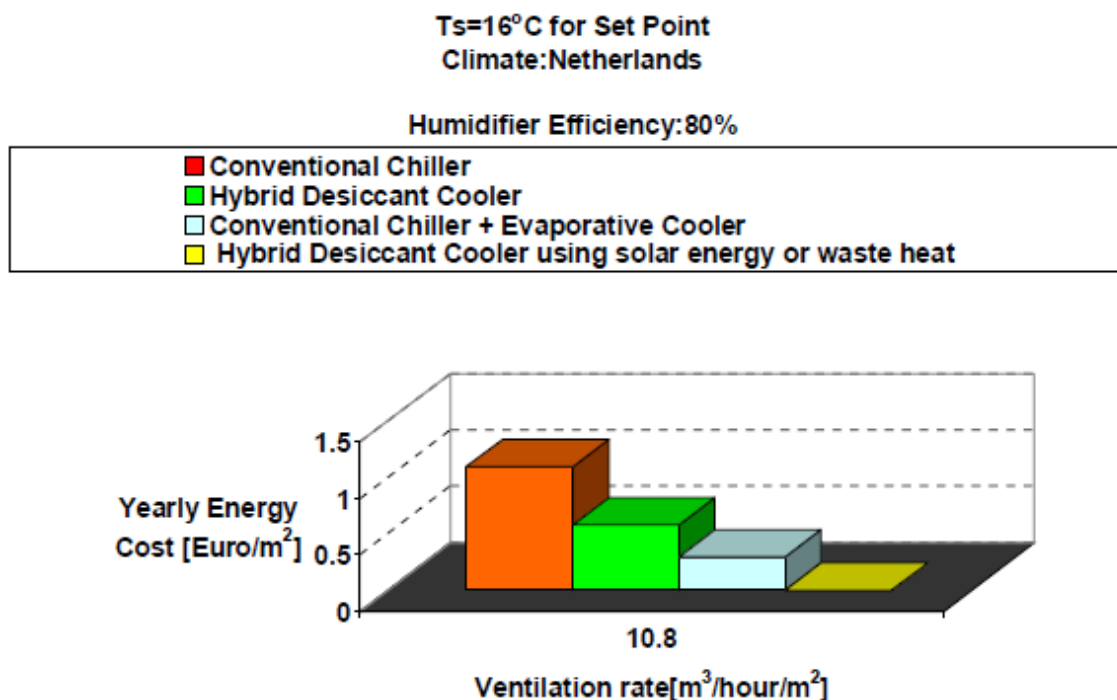


**Figure 6.15.** Comparison of energy costs for hybrid desiccant system and conventional chiller with cold factor 3, and cooling capacity of 30 W/m<sup>2</sup> for 16°C supply air temperature

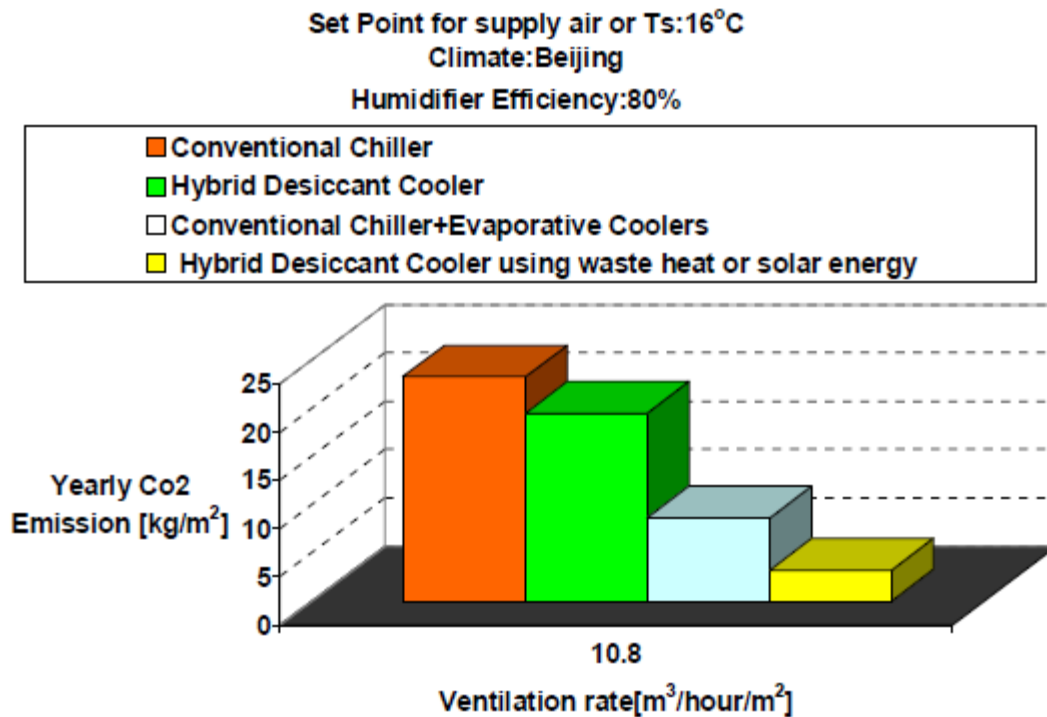


**Figure 6.16.** Comparison of CO<sub>2</sub> emissions for hybrid desiccant system and conventional chiller with cold factor 3, and cooling capacity of 30 W/m<sup>2</sup> for 16°C supply air temperature

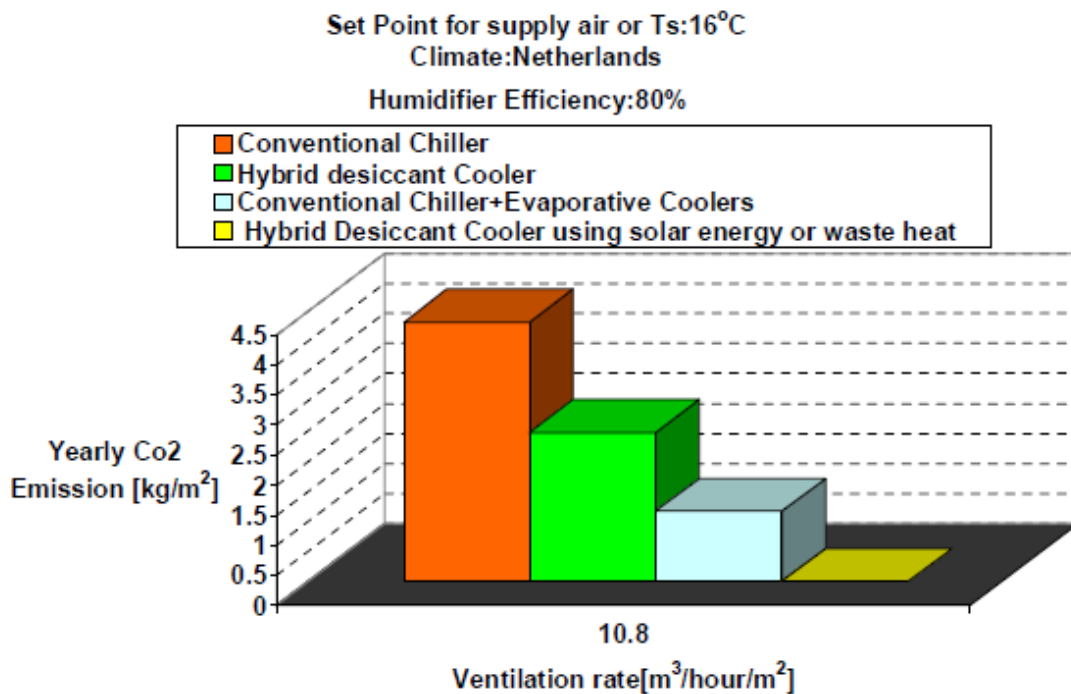


**Figure 6.17.** Comparison of CO<sub>2</sub> emissions for hybrid desiccant system and conventional chiller with cold factor 3, and cooling capacity of 30 W/m<sup>2</sup> for 16°C supply air temperature



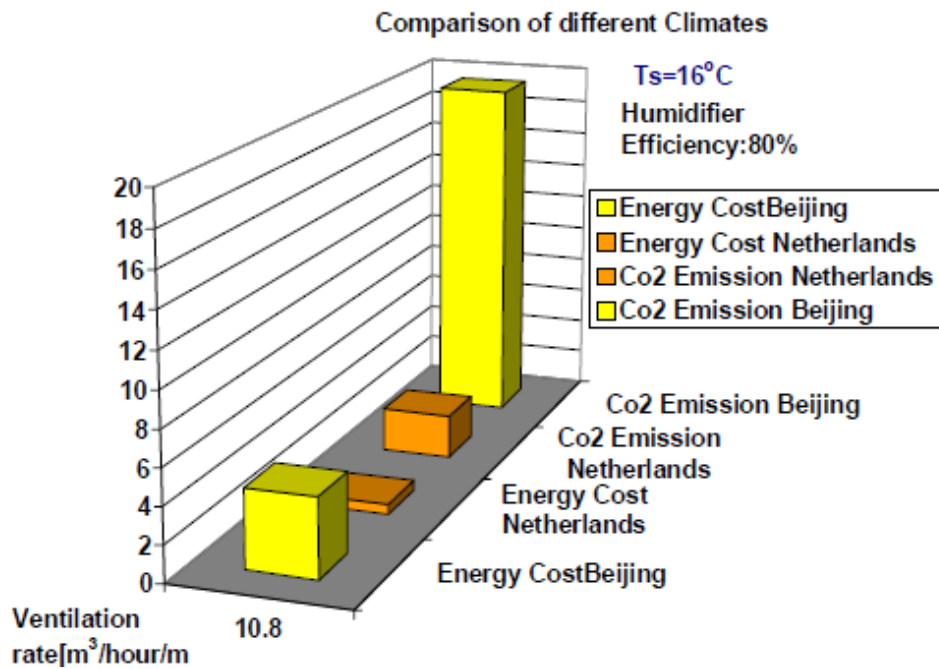


**Figure 6.18.** Comparison of different climates of Beijing and Netherlands on the energy costs and CO<sub>2</sub> emissions in the same set point of 16°C for supply air

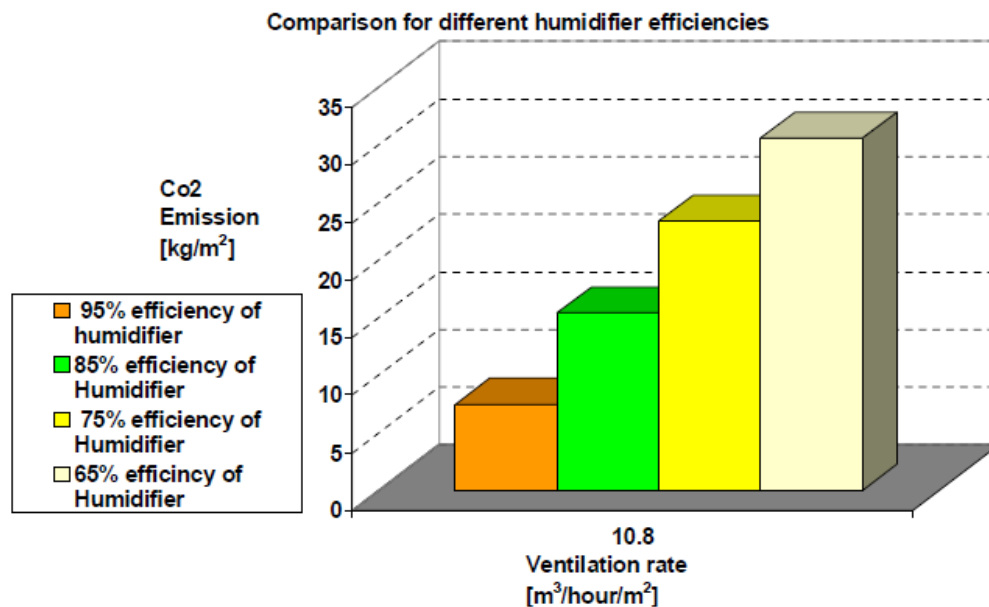


**Figure 6.19.** The effect of humidification on the results of CO<sub>2</sub> emissions for Beijing and supply air temperature set in 16 °C and cooling capacity of 30 W/m<sup>2</sup>

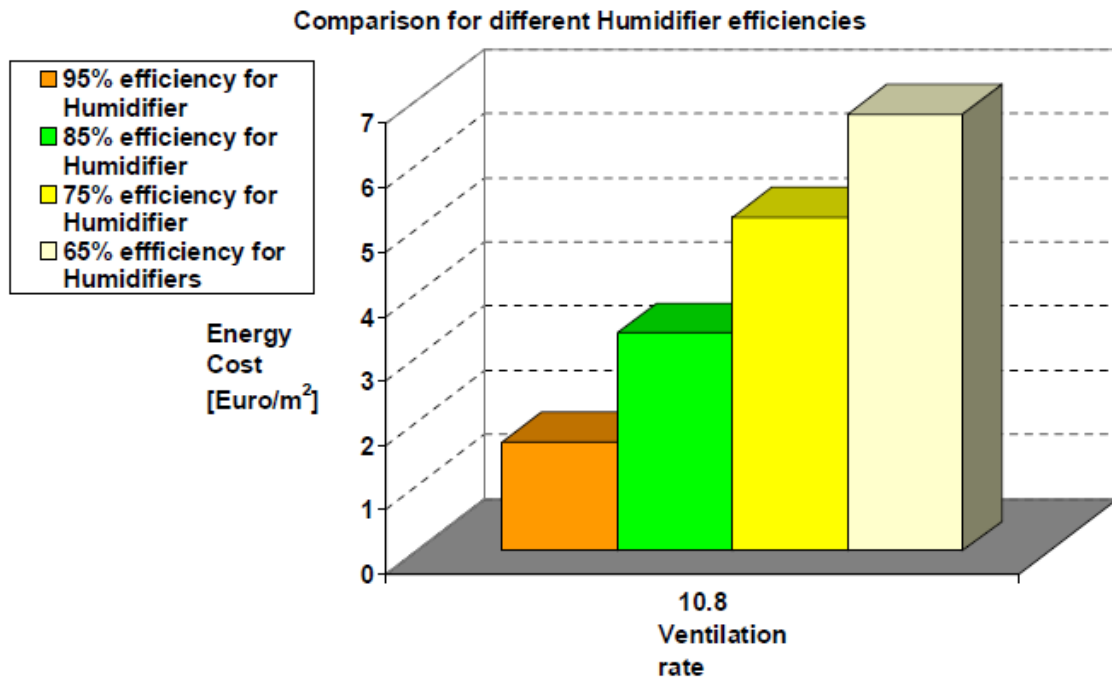


**Figure 6.20.** The effect of humidification on the results of the energy costs for Beijing and supply air temperature set in 16°C and cooling capacity of 30 W/m<sup>2</sup>

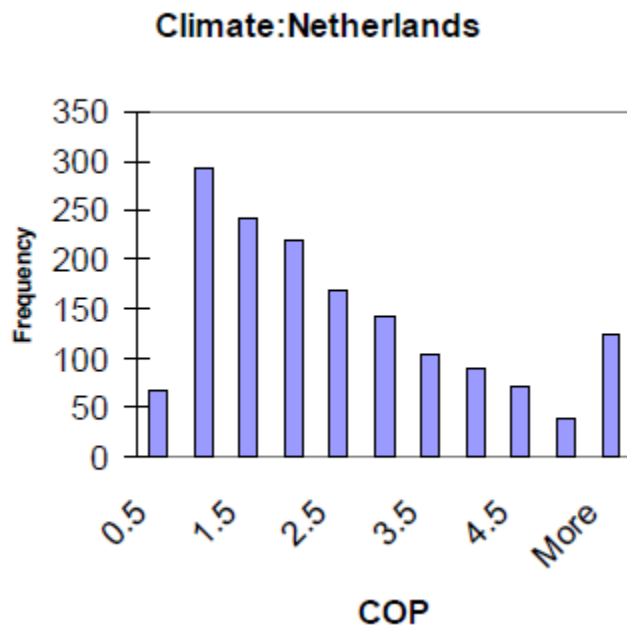


**Figure 6.21.** The thermal coefficient of performance for year-round simulation of hybrid desiccant cooler for the Netherlands using the definition according to the equation

(6.13). The high values of COP is related to the part of year that desiccant is not in operation and a simple evaporative cooling suffices the air cooling to the set point

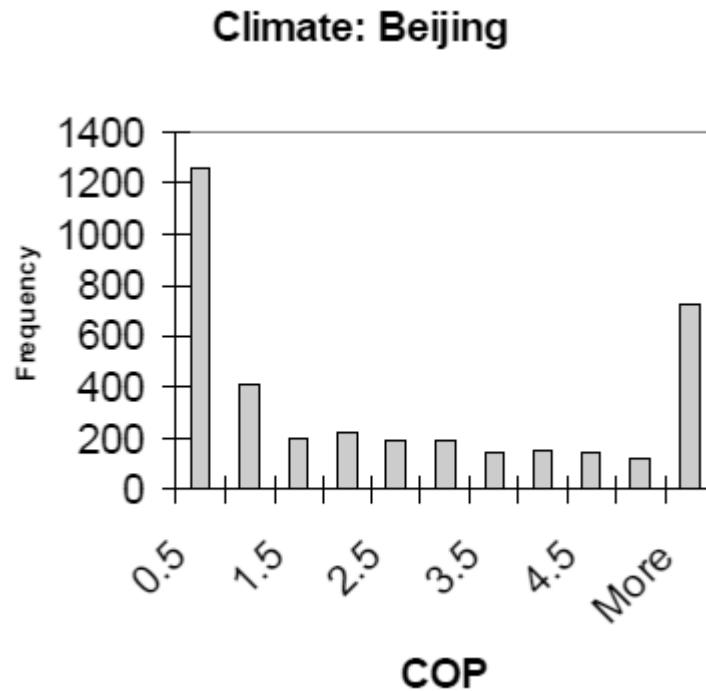


**Figure 6.22.** The thermal coefficient of performance for year-round simulation of hybrid desiccant cooler for Beijing using the definition according to equation (6.13)

## 6.5 Summary and conclusion

- The performance of four cycles for solid desiccant air conditioning systems has been predicted using the graphical computer tool of Simulink, it is a very simple and quick way to test different cycles.
- The results of this study show that the performances of these systems greatly depend on the operating parameters of the desiccant wheel with respect to the selection of optimum speed of the wheel and regeneration air temperature.
- The best application of the desiccant wheel for air conditioning has been suggested. The best choice of wet and dry heat exchangers is based on minimum regeneration heat and desired supply air temperature. The results can change considerably within different ranges of outside conditions.
- Desiccant air conditioning systems perform better when the latent load is higher than the sensible load. A significant improvement in the performance of the

desiccant cooling cycle has been predicted with the application of an evaporative cooler as applied in the cycles I, II, and IV.

- This study simulated a one-year time frame for variable cooling load, fixed supply temperature, and variable fresh air temperatures. The required regeneration heat was minimized by choosing proper values of regeneration temperature for a hybrid desiccant cooler. The desiccant control strategy was to maintain minimum regeneration heat. At the same time, desiccant control strategies influenced the system performance using wheel speed since only the optimum wheel speeds were used.
- This analysis presents a method for choosing optimal values. The optimal control strategy will let the regeneration temperature vary in proportion to the cooling load. The wheel rotation speed may be kept constant at optimum speed. Fine tuning of this speed is not important.
- The use of the graphical computer tool of Simulink is a promising way to test different control strategies. The key control parameters can easily and quickly be identified and modified for year round simulation.
- Using a heat recovery wheel to save exhaust heat from the desiccant wheel, as a preheating for regeneration of the desiccant matrix, can result in 20-25% energy saving.
- The results show desiccant cooling technology can be useful and practical, if it is in operation as an auxiliary system for an evaporation cooling system. The reduction of 10-55% in CO<sub>2</sub> emission and energy costs are observed from the year round simulation results. The reduction percentages will grow even larger if the source of thermal energy for regeneration can be prepared for free or inexpensively such as waste heat or solar energy. Of course the investment costs may be high and the energy saving may not compensate for it, but the reduction in CO<sub>2</sub> emission and the possibility to use waste heat and solar radiation may resolve these issues when applying these systems.
- The results of year round simulation show that conventional chillers can be replaced with hybrid desiccant air conditioning system, if desiccant wheels are active only for a limited time and the rest of year the evaporation cooling will suffice without desiccant in operation. In addition, the difficulties resulting from the overheating of cooling water for power plants, makes them attractive to be considered as a promising alternative that can be implemented within a short time.
- The results of performance of desiccant technology in air conditioning are strongly dependent on the climates.

## NOMENCLATURE

A	Heat Exchanger Surface ( $m^2$ )
C	Constant given by equation (5.7)
$C_k$	Hot fluid specific heat ( $J kg^{-1} K^{-1}$ )
$C_p$	Air specific heat ( $J kg^{-1} K^{-1}$ )
$C_w$	Water specific heat ( $J kg^{-1} K^{-1}$ )
COP	Coefficient of Performance defined in equation (5.13)
e	The linear coefficient of enthalpy
g	Mass flow ( $kg m^{-2}$ )
h	Enthalpy of humid air ( $kJ kg^{-1}$ )
$h_s$	Enthalpy of humid air in the boundary layer of the air ( $kJ kg^{-1}$ )
$K_t$	Total Heat transfer coefficient ( $W m^{-2} K^{-1}$ )
$\dot{m}$	Air flow rate ( $kg s^{-1}$ )
$\dot{m}_k$	Hot air flow rate ( $kg s^{-1}$ )
$\dot{m}_w$	Cold air flow rate ( $kg s^{-1}$ )
Ntu	Heat Transfer number
q	Heat flux related to a surface area of $\Delta A$ ( $W m^{-2}$ )
Q	Heat flow rate (W)
$Q_c$	After cooling load (W)
$Q_{cc}$	Cooling capacity (W)
$Q_{fan}$	The energy rate needed for two fans in the system (W)
$Q_R$	Regeneration heat rate (W)
$R_2$	Thermal conduction Resistance of water layer ( $W^{-1} K m^2$ )
$R_p$	Thermal conduction Resistance of heat exchanger Wall ( $W^{-1} K m^2$ )
$t_s$	Air temperature in saturated layer of wet surface ( $^{\circ}C$ )
$t_k$	Hot air temperature ( $^{\circ}C$ )
$t_w$	Cold air temperature ( $^{\circ}C$ )
$T_i$	Inlet air temperature to the desiccant wheel ( $^{\circ}C$ )
$T_R$	Regeneration air temperature ( $^{\circ}C$ )
$T_{out}$	Outlet air temperature from adsorption side of the wheel ( $^{\circ}C$ )
U	Velocity ( $m s^{-1}$ )

## Greek letters

$\alpha$	Convective Heat Transfer Coefficient ( $W m^{-2} K^{-1}$ )
$\alpha_k$	Convective Heat Transfer Coefficient for hot fluid side ( $W m^{-2} K^{-1}$ )
$\epsilon$	Humidity efficiency of the wheel
$\epsilon_k$	Temperature efficiency of hot fluid
$\epsilon_w$	Temperature efficiency of cold fluid
$\phi$	Relative Humidity%

- $\omega_t$       Input air humidity for the desiccant wheel (  $kg\ kg^{-1}$  )  
 $\omega_{out}$     Outlet air humidity for the desiccant wheel, the adsorption side (  $kg\ kg^{-1}$  )

## References

1. J. Jurinak, J.W. Mitchell, W.A. Beckman, Open-cycle desiccant air conditioning as an alternative to vapor compression cooling in residential applications, Transactions of the ASME 106 , 252–258, 1984.
2. D.G.Waugaman, A.Kini, C.F.Kettleborough , A Review of Desiccant Cooling Systems, J. of Energy Resources Technology, 115, 1-8, 1993.
3. Ahmad A. Pesaran, Terry R. Penney, and Al W. Czanderna., Desiccant Cooling and Dehumidification Bibliography -Section 1,2, <http://www.nrel.gov/desiccantc>
4. Maclain-cross, I.L.High, Performance Adiabatic Desiccant Open-Cooling Cycles, ASME J. of Solar Energy Engineering, 107, P.102-104, 1985.
5. T.S. Kang, I.L. Maclain–Cross, High Performance Solid Desiccant Cooling Cycles, Transactions of ASME, V. 111, 176-183, 1989.
6. Dauo K., Wang R.Z., and Xia Z.Z., Desiccant Cooling air conditioning: a review, Renewable and sustainable energy reviews, 10, 55-77, 2006.
7. Bullock,C.E. Therelkeld, J.L., Dehumidification of Moist Air by Adiabatic Adsorption, ASHRAE Transactions, Vol.72, 301-312, 1996.
8. Nelson, J.S., Beckman, W.A., Mitchel, J. W., and Close D.J., Simulation of the performance of open Cycle Desiccant Systems Using Solar Energy, Solar Energy, Vol.21, P.273-278, 1973.
9. B. S. Davanagere, S. A. Sherif D. Y. Goswami, <sup>A</sup> feasibility study of a solar desiccant air-conditioning system - Part I: psychrometrics and analysis of the conditioned zone International Journal of Energy Research Volume 23, Issue 1, P. 7 – 21, 1999.
10. Nesreen Ghaddar, Kamel Ghali , Antoine Najm, Use of desiccant dehumidification to improve energy utilization in air-conditioning systems in Beirut, Vol. 27, 15 , P.1317 – 1338, 2003.
11. M. Beccali, F. Butera, R. Guanella, R.S. Adhikari, Simplified models for the performance evaluation of desiccant wheel dehumidification International Journal of Energy Research Vol.27, 1, P.:17-29, 2003.
12. M. Pons, A. Kodama Entropic analysis of adsorption open cycles for air conditioning. Part 1: first and second law analyses, International Journal of Energy Research. 24, 3, P.251-262, 2000.
13. Akio Kodama, Weili Jin, Motonobu Goto, Tsutomu Hirose, Michel Pons Entropic analysis of adsorption open cycles for air conditioning. Part 2: interpretation of experimental data, International Journal of Energy Research. 24, 3, P.251-26, 2000.
14. A. I. Alkhamis, S. A. Sherif, Feasibility study of a solar-assisted heating/cooling system for an aquatic centre in hot and humid climates, International Journal of Energy Research, 21, 9, P.823-839, 1997
15. Collier, R. K., Cohen B. M.,' An Analytical Examination of Methods for improving the Performance of Desiccant Cooling Systems, ASME J. of Solar Energy Engineering, 113,P. 157-163, 1991.

16. Jin W., Kodama A, Goto M., An Adsorptive Desiccant Cooling using Honeycomb Rotor Dehumidifier, J. of Chemical Engineering of Japan, 31, P. 706-713, 1998
17. F.Esfandiari nia, Dolf van Paassen, M.Saidi, Modeling and Simulation of Desiccant Wheel for air Conditioning, Int. J. of Energy and Buildings, *Volume 38, Issue 10, 2006*.
18. ASHRAE, Handbook of Fundamentals, American Society of Heating, Refrigerating and Air-Conditioning Engineers, Atlanta, GA, 1993.





# 7. CONCLUSIONS AND FUTURE WORK

## 7.1. Conclusions

Heat and mass transfer are modeled in different components of sustainable air handling systems based on adsorption and evaporation in this thesis. This research advances the scientific understanding of this technology for making different design tools. The scientific findings of this research are discussed in the various chapters:

- A numerical model for the simulation of heat and moisture transfer in an indirect evaporative cooling system (Static Cooler) is developed, and compared with experimental data prepared by different manufactures and centers in the Netherlands. (Chapter 2);
- A numerical model for the simulation of heat and moisture transfer in a chilled water air cooler is developed and validated. This validated model is used to develop a simplified model using the Mollier diagram. It is applied as a design tool to a yearly energy analysis of conventional air handling installations. One of the uses of this simplified model is as a reference in the comparison of different air conditioning systems. (Chapter 3);
- A numerical model for the simulation of heat and moisture transfer in desiccant wheels is developed. The model is used to study different applications of desiccant technology for both low and high speeds of the wheel. At low speeds within a range of 10-20 revolutions per hour, desiccant wheels operate as dehumidifier wheels. At high speeds of 10-20 revolutions per minute they operate as energy recovery wheels. A variety of practical questions are answered using the physical model. The simplified models are derived from the physical model to produce quick and easy formulas to calculate the change in the condition of the air after passing through the wheel. An analytical approach is introduced to calculate the average values of the outlet air condition in a steady state after air passes through the wheel. An analytical approach is introduced to calculate the average values of the outlet air condition in a steady state after the air passes through the wheel. (Chapter 4);
- The numerical model of desiccant wheels was validated with experimental data prepared by manufacturers. Also measurements were carried out with a specially designed test facility in a climate room at TU Delft. (Chapter 5);

- The validated physical models are used to simulate various air conditioning systems in order to analyze them with respect to capacity, energy consumption and environmental aspects. In addition, the simplified equations developed in this thesis for dehumidifier wheels are used to simulate a hybrid evaporative desiccant cooling system at a reference year for two different extreme and moderate climates. The energy costs and CO<sub>2</sub> emissions are calculated for the different systems in the different climates. (Chapter 6);
- The validated models of air cooler and desiccant wheels are implemented in the computer program Enerk. It can be used to analyze and to compare any desiccant system with traditional and conventional air handling units. (Appendix A);

The final conclusions and contributions of this thesis are presented below and in the next section entitled “future work” are recommended.

Having used the model for the advanced evaporative cooler, any type of improvement in the performance of the system can be easily and quickly studied for different simulations such as: the selection of appropriate dimension and configuration of the system; the characteristics of air flow rate; the appropriate selection of the process and primary air streams ratios. A unit of these coolers was analyzed and the simulation results confirmed that the plates were not wetted properly and uniformly during the test measurements. The results after analysis show that the present configuration of the dimension and characteristics of the unit is not able to deliver the dew point temperature. However, changes in design are possible to yield the desired temperature that is below the wet bulb temperature.

The experimental set up made for air coolers provided the measurements for 24 different input conditions of air and cold water. The results show the need to make correction for both the overall heat transfer coefficient and the Lewis number. This is necessary because of condensation. The correction factors compensate for the simplified assumptions regarding the wet surface of fins and the analogy between heat and mass transfer. Furthermore, the correction factors depend on the dehumidification quantity. The corrected model has been implemented in studies of the advanced evaporative air-conditioning systems, where it has been used to construct a graphical model based on the rules for transients in the Mollier diagram.

The user-friendly and flexible programming environment of the Simulink provides an excellent alternative to obtain solutions for modeling of desiccant wheels. The advantages of the modeling platform include: adaptability; the ability to generate accurate solutions that are very concise with minimum calculation time; and ease and usefulness in studying and modeling the total system. The Simulink model of heat and mass transfer for desiccant wheels is improved to produce the results in shorter computer times and also made more efficient so that it can be connected to the other building models. However, because of the limitation of computer memory and long calculation time, the physical model was not used; instead the simplified models were made and applied in the year-round simulation of the desiccant cooling cycles.

Two physical parameters have been chosen to make simplified models or correlations. They are based on the relevant physical principles of adsorption that is a phenomenon similar to evaporation with constant enthalpy. The correlations are made using an optimization routine in Matlab. These equations correlate the outlet air conditions to the input air conditions for air streams as well as the wheel and air speeds. The correlations are limited in scope and can only be used in a given range of air conditions and wheel speed.

However, the range encompasses the practical situations that usually occur based on the weather data. The maximum relative error when estimating the outlet air humidity by these correlations for almost 1500 data inputs is calculated. The errors range from  $\pm 8.5\%$  for air humidity to  $\pm 2.5\%$  for air temperatures. The error increases in the regions near the boundaries within the valid range. In other words, for air temperature, humidity and velocity at the minimum or maximum borders in the valid ranges, larger errors are produced. Furthermore, the change in air conditions in the Mollier diagram show that the error in simulating the desired supply air temperature decreases the error of the simulation of outlet air conditions of the desiccant wheel by a factor of 3. Therefore, even in ranges of low accuracy the correlations are still useful.

Although the accuracy of the correlations is acceptable within a margin of error for a typical European data weather, they are not usable for other climates. The error is larger when all the variables are outside the boundaries. Therefore, an analytical approach using physical simplified assumption was introduced. This approach is based on many simplified assumptions. Although they are not satisfied in most real conditions, they make it possible to produce a very simple but helpful model.

The results of simulation show that a desiccant wheel with thicker layer of solid desiccant, used in dehumidification applications at low speeds, can easily instead operate as a heat and moisture or enthalpy exchanger in higher speeds. Therefore, desiccant wheel with a typical thick solid layer, common for dehumidification applications, is able to operate for both winter and summer applications just by changing the speed. For summer applications, the wheel works within lower speeds and in winter applications the speed needs to be higher. But, when the desiccant wheel is an enthalpy wheel, with a thin layer, it is unable to provide the necessary dehumidification needed for air drying.

In addition, the sensitivity study shows the most important parameters or control variables. The regeneration temperature is the most important parameter, the wheel speed, as far as operating in a practical range, is not so significant.

Adsorption equilibrium isotherms are the most important parameters in the study of sorption. The experimental study of adsorption was carried out by different measurements for two different wheels. It was observed that, in general, regeneration is faster phenomenon than adsorption and adsorption is reduced by a rise in temperature.

In addition, the numerical model of the desiccant wheel as an enthalpy wheel is validated with the measurements provided by the manufactures that cover a wide range of airflows, temperatures and humidities. The numerical and experimental values show agreement especially for practical situations.

The performance of four cycles for solid desiccant air conditioning systems is predicted using the graphical computer tool of Simulink. The results of this study show that the performance of these systems highly depend on the operating parameters of desiccant wheel with respect to the selection of the optimum speed of the wheel and regeneration air temperature. The best application of a desiccant wheel for air conditioning has been suggested, depending on to the choice of the wet and dry heat exchangers. This decision is made based on the minimum regeneration heat and the desired supply air temperature. The results can vary considerably in different range of outside conditions.

In addition, use of a heat recovery wheel to save exhaust heat from the desiccant wheel, as a preheating for regeneration of the desiccant matrix, was studied and observed that it can result in 20-25% energy saving.

The use of the graphical computer tool Simulink is an interesting way to test various control strategies. The key control parameters can easily and quickly be modified for year-round simulation. The results show desiccant cooling technology can be useful and practical, if the source of thermal energy for regeneration can be generated for free or inexpensively such as waste heat or solar energy. Of course, the investment costs may be high and the energy saving may not compensate for it, but the reduction in CO<sub>2</sub> emission and the possibility to use the waste heat and solar radiation may solve this problem and make it more attractive to apply these systems. The results of year-long simulation show that conventional chillers can be replaced with hybrid desiccant air conditioning systems. It is important as they can reduce electricity usage demand by at least 25% for cooling during peak load hours of summer.

A contribution of this thesis is the development of design tools for desiccant wheel and air coolers in the computer program Enerk. The correlation model of desiccant cooling is used in the computer program Enerk. With this program the energy consumption for air handling installations can be defined. Only conventional systems based on cold water air cooler could be simulated. Using the results of this thesis (the validated models) desiccant systems can be analyzed and compared with traditional models.

## **7.2. Future Work**

The simplified equations that have been developed in this thesis for desiccant wheels as dehumidifiers are validated only for a limited range of air conditions. In the situations that the air conditions and the wheel speed are not within the boundaries of valid range, the errors are considerably high. Although the errors of these calculations for

air conditions in a practical cycle are reduced by a factor 3, the new simplified equations which cover a wider range of air and speed conditions need to be developed.

The analytical approach developed in this thesis for a dehumidifier wheel is based on many simplified assumptions which are not satisfied in most conditions. Therefore, the analytical model needs to be improved in order to reduce the assumptions to obtain more accurate solutions.

Another major area of future research is to apply the simplified functions developed in this thesis to optimize different air conditioning cycles for use in buildings and some special applications such as green houses. With these simplified equations the sustainable air conditioning systems with least life cycle costs and energy consumption and CO<sub>2</sub> emission can be designed for building in different climates with local energy prices. These optimized solutions together with appropriate design methods, will be attractive to industry for implementation of optimal designs.

There are many questions for HVAC engineers and manufactures concerning design and manufacturing of these systems that should be addressed by future research projects. The design tools made by these simplified equations can be used for this purpose.

Since the heat regeneration can be provided by inexpensive sources of thermal energy, such as solar energy and waste heat or cogeneration heat, one of the most attractive examples of research projects in this area are calculations of energy savings and reduction of CO<sub>2</sub> emission for these systems. The results from this thesis can easily be implemented when performing these calculations, and optimizing the performance of these systems.



# Appendix A: Practical Application of Results of This Thesis

“Reprinted with permission of the American Society of Mechanical Engineers, ASME”

## Model of desiccant cooling process applied in the simulation program Enerk<sup>1</sup>

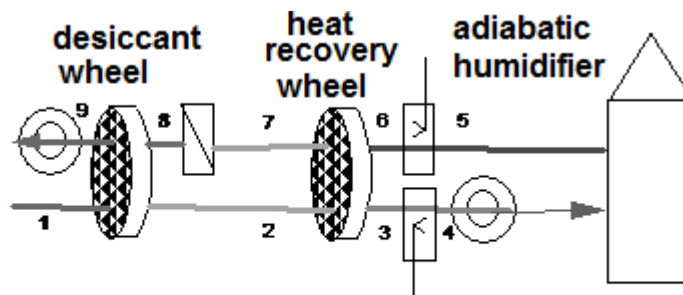


*Figure A1. Desiccant cooling system implemented in Enerk.*

In this chapter, it is shown how desiccant and evaporative cooling can be implemented in the computer program Enerk.

### A.1 Enerk in short

A computer program, ENERK, was developed at the TUDelft by van Paassen and van der Stelt to design heating, ventilating and air-conditioning systems for low energy buildings. It interacts with the designer of HVAC-systems by asking questions and by recommending appropriate control strategies for different systems to find the most energy efficient system.

This program is based on a new calculation method. It enables the designer to use rules of thumbs and cognitive strategies when deciding what to do during the design process. It shows much similarity with the design procedure that the user himself likes to follow.

The program offers a higher degree of flexibility in system design; a better understanding of the effects of energy savings, and the same accuracy as a computer program does based on an hour-by-hour calculation method.

---

<sup>1</sup> Reference for Enerk: Paassen, A.H.C. van , T.P. van der Stelt. Een interactief computerprogramma voor het ontwerpen van klimaatbeheersingsinstallaties ENERK. TVVL Magazine 30, november 2001.

Enerk is functioning in the following sequential steps:

- Based on the design data of a room with the window oriented in a specific direction the hour by hour response of the cooling and heating load is calculated.
- Then a bookkeeping type program counts the number of hours with outside conditions occurring in specific intervals of outdoor temperature and humidifiers. These intervals (indicated by i,j) are represented in sections in the Mollier diagram and for each section the average outdoor temperature and humidity and cooling and heating loads are defined. Thus, the time response is transferred in a probability function given per section the occurrence of the average outdoor temperature, humidity and heating and cooling load:

$$P_{ij}^{+}(Q_{ij,average}^{+}, \theta_{i,average}^{+}, X_{j,average}^{+}) \text{ and } P_{ij}^{-}(Q_{ij,average}^{-}, \theta_{i,average}^{-}, X_{j,average}^{-}) .$$

- For each section in the Mollier diagram the designer now select the sequence of air handling, and dictates the inlet and outlet condition belonging to each step of the air handling that eventually gives the required heating and cooling needed for that section. By means of a presentation of the psychometric chart on the monitor the air handling processes is shown and the designer can change the sequence or control strategy according his/her wishes.
- After the right sequence is defined the energy needed to realize this air handling per kg of air will automatically calculated. By summing up all the results per section the yearly energy consumption can be found automatically. Consequently, the designer can find the best air handling process and its control system by trial and error without the necessity of reprogramming, as is required for the more conventional computer programs.

## A.2 Desiccant cooling implemented in ENERK

The simulation models derived in this thesis is used to implement desiccant cooling in Enerk.

The fast correlation functions of Chapter 4 showed to be appropriate for this purpose.

In a similar way the curve of the change of air conditions due to desiccant cooling should be indicated in the Mollier diagram. In the menu of control strategy it is possible to choose between conventional (as it is now in Enerk), desiccant cooling and indirect evaporative cooling system (desiccant wheel not active). When desiccant cooling is selected the control strategies switch over to indirect evaporative cooling as soon as this can deliver the desired supply temperature. The reason is that evaporative cooling doesn't need regeneration heat.

The various options - ranging from conventional to desiccant cooling - can be selected using the screen "Installation data" as shown in figure A2.



*Figure A2. Installation data input of type of cooling and efficiencies*

## Model desiccant cooling in Enerk

The models of this thesis are used to simulate the desiccant cooling system as indicated in figure A1 in such a way it can be used in Enerk.

The cycle is as follows:

- Outside air with temperature  $T_1$  and humidity  $X_1$  is dried by the desiccant wheel to the condition  $T_2$  and humidity  $X_2$ .
- Then the recuperative air to air heat exchanger transfers the heat generated by adsorption to the exhaust air flow. Thus, the supply air flow is cooled down at point 3 to a lower temperature. Adiabatic humidification cools down this air flow further to the supply condition  $T_4$  and  $X_4$ .

The exhaust air flow conditions are changed as follows:

- The air leaving the building has a temperature close to that of the desired one (comfort temperature is  $24^\circ\text{C}$ . The humidity  $X_5$  is due to the moisture generated in the building by people slightly higher than that of the supply air ( $X_4 + 0.0005$ ).

- This air flow can be humidified to the wet bulb temperature  $T_6$ , and heated by the recuperative heat recovery wheel to  $T_7$ .
- To drive out the adsorbed moisture the temperature should be increased by an air heater to  $T_8$ . The more water should be driven out, the higher this temperature will be (60 to 90°C).

The model should be able to calculate the supply air conditions  $T_4, X_4$  for different input conditions  $T_1, X_1$  and control variables ( $T_8$ , wheel speed  $N$  and air speed  $V$ ).

The model shown in figure A3 is based on heat balances, correlation functions, and empirical data for the heat recovery efficiency.

The input air conditions are:

$T_1, X_1$  (outside air condition to be handled)

$T_5, X_5$  (building exhaust air condition)

Select:

Regeneration temperature:  $T_R = T_8$ ;

Wheel speed:  $N$ ;

Air flow:  $V$ ;

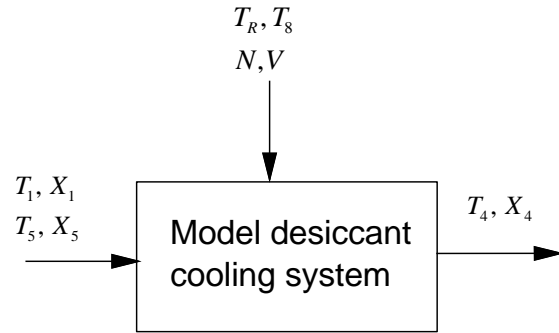


**Figure A3.** Set up model desiccant cooling system

Calculate

$T_6, X_R = X_6$  with following equations.

$$h_5 = c_p T_5 + r X_5 \quad (\text{sensible heat of water vapor is ignored})$$

$$h_6 = h_5$$

$$T_{wb,5} = 27.8 \ln \frac{h_5 + 36}{45.5}$$

$$T_6 = -\eta_{H1}(T_5 - T_{wetbulp,return}) + T_5$$

with  $\eta_{H1}$  efficiency of first adiabatic humidifier (5<->6)

$$X_6 = \frac{h_5 - T_6}{2.491}$$

$$X_R = X_6 = X_7 = X_8$$

The correlation study of the physical model results in the following characteristic variables:

$dT/dX$  and  $dT/T_R$ .

$$\frac{dT}{dX} = 0.0723N - 0.286V - 0.0401X_s - 0.178X_t + 3.7833$$

$$\frac{dT}{dX} = -0.0053T_1 - 0.0527V + 0.0041N - 0.003X_8 + 0.0127X_1 + 0.001T_8 + 0.3042$$

With constraints:

$$10Rph \leq N \leq 18Rph \quad 60 \leq T_R \leq 90$$

$$1.5 \frac{m}{s} \leq V \leq 3.5 \frac{m}{s} \quad 25 \leq T_i \leq 35$$

$$8 \frac{gr}{kg} \leq X_i \leq 16 \frac{gr}{kg}$$

$$8 \frac{gr}{kg} \leq X_R \leq 16 \frac{gr}{kg}$$

These 2 correlation equations are derived from a detailed physical model (chapter 4). With these equations and simple heat balances of the auxiliary components a straightforward set of equations could be obtained to calculate the curves in the Mollier diagram representing the change of air conditions during the air handling process and the heating energy needed to handle the drying and cooling process. With these equations the output of the desiccant wheel,  $X_2$  and  $T_2$  can be defined.

$$X_2 = X_1 - \frac{T_2 - T_1}{\frac{dT}{dX}}$$

$$T_2 = T_1 + T_8 \frac{dT}{T_8} \quad T_8 = T_R$$

Using temperature efficiency,  $\varepsilon_T$  of heat recovery unit or wheel gives  $T_7$ :

$$\varepsilon_T = \frac{T_7 - T_6}{T_2 - T_6} \text{ or}$$

$$T_7 = (1 - \varepsilon_T)T_6 + \varepsilon_T T_2$$

The heat balance over heat recovery wheel gives:

$$T_3 = T_2 - (T_7 - T_6)$$

$$h_4 = h_3 = c_p T_3 + 2.412 \cdot X_3 \quad \text{and} \quad X_3 = X_2$$

$$T_{wb,4} = 27.8 \ln \frac{h_4 + 36}{45.5}$$

$$\eta_{H2} = \frac{T_3 - T_4}{T_3 - T_{wb,4}} \text{ efficiency adiabatic humidifier (2th) gives: } T_4 = T_3 - \eta_{H2}(T_3 - T_{wb,4})$$

$$X_4 = \frac{h_4 - T_4}{2.491}$$

Heat needed for regeneration is:

$$Q_{Reg} = c_p (T_R - T_7)$$

### A.2. Mode of operation (control)

- Desiccant mode. The strategy is as follows. The maximum capacity is put in operation by controlling the regeneration temperature  $T_R$  to 90 °C. Also, the rotation speed of the desiccant wheel is set at maximum value (although its effect is less than that of  $T_R$ ), and both adiabatic humidifiers are on.  $T_R$  values are now controlled back to get the desired value of the supply air ( $T_4=T_{4,set}$ ). See figure A4.
- Indirect evaporative cooling. When the minimum value of 60 °C is reached the air heater for regeneration is switched off, and the desiccant wheel is stopped and, bypassed. Because humidifiers don't need energy the following mode is made active directly.
- Indirect and direct evaporative cooling. Now both humidifiers are switched on.
- Conventional mode. An air cooler is put in operation producing additional cooling. Of course, this requires electricity to drive the cold water chiller.

For the situation considered (outside air conditions, cooling load and frequency) a conventional air handling installation can be put in operation and compared with the desiccant system to see if it is appropriate.

The Mollier diagram is divided into small sections. Section by section the selected air handling system is put in operation and the energy required for making the required supply conditions are calculated. Summing up of the energies yields the yearly total energy consumption.

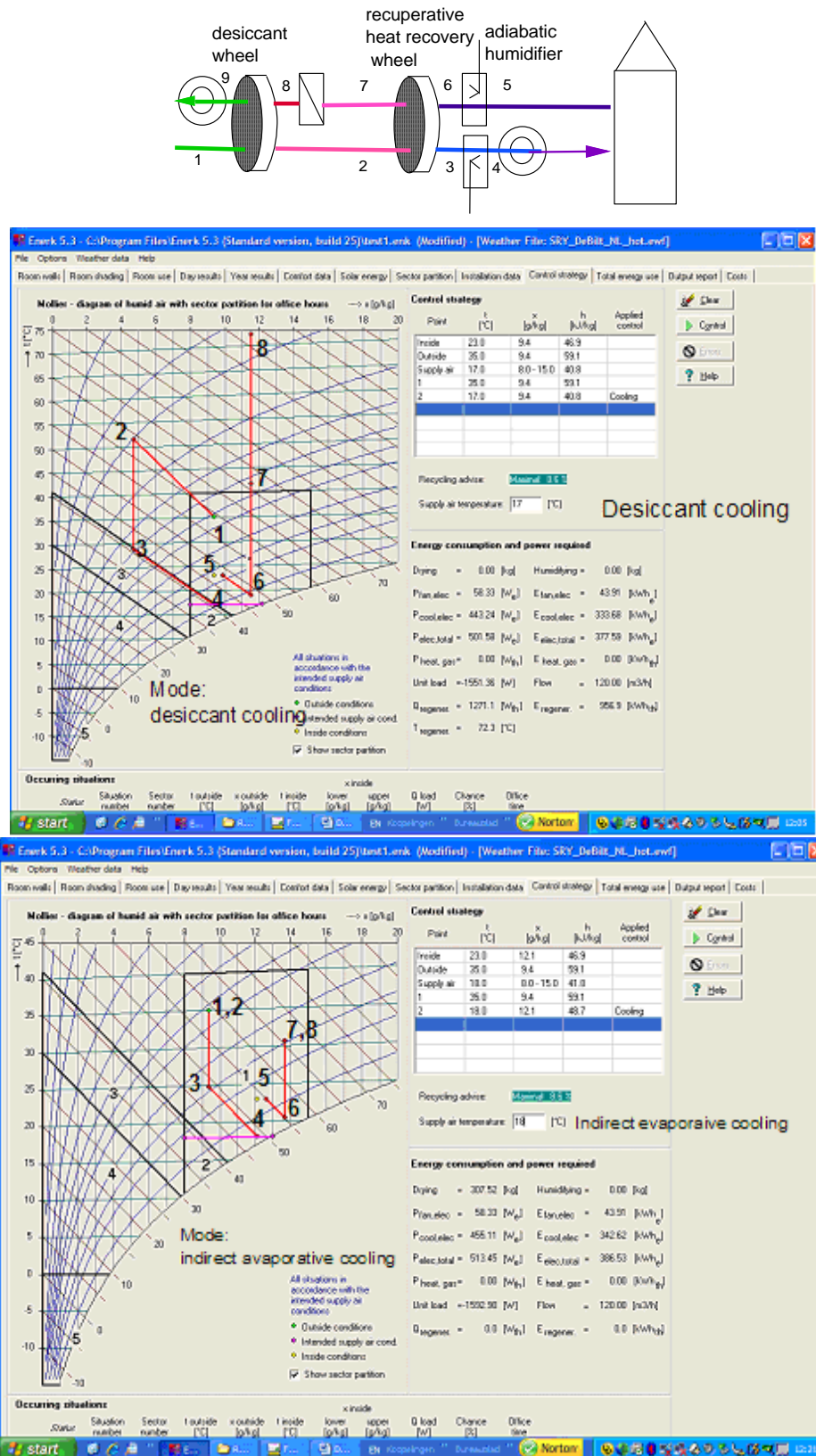


**Figure A4.** Depending on the required supply temperature one of the above graphs is shown. If the required set point can not be realized by indirect evaporative cooling then the graph on the top is shown (the desiccant cycle is placed in operation). The bold numbers of **1 to 8** are used to indicate the air conditions after each treatment, the smaller numbers of 1 to 5 are for indicating the sections with the same control strategy in the Mollier diagram.



## Appendix B: K-factors for One Row in Air Cooler

$$\begin{aligned}
 K_1 &= D_1 \cdot K_{02}, K_2 = D_2 \cdot K_{02}, K_3 = K_{01} \\
 K_4 &= -REF \cdot K_2, K_5 = KK_1 + KK_3 \cdot K_{06} \\
 K_6 &= KK_2 + KK_3 \cdot K_{07}, K_7 = KK_3 \cdot K_{02}, K_8 = KK_4 - KK_3 \cdot K_{08}, K_9 = KK_5 + KK_7 \cdot K_{06} \\
 K_{10} &= KK_6 + KK_7 \cdot K_{07}, \text{ If } K_{10} = 0.0 \text{ then } K_{10} = 1.0 \\
 K_{11} &= KK_7 \cdot K_{02}, K_{12} = KK_8 - KK_7 \cdot K_{08} \\
 K_{13} &= (D_1 + K_{03} \cdot K_{06}) / B_1, K_{14} = (D_2 + K_{03} \cdot K_{07}) / B_1 \\
 K_{15} &= K_{03} \cdot K_{02} / B_1, K_{16} = (-D_2 \cdot REF - K_{03} \cdot K_{08}) / B_1 \\
 B_1 &= \frac{4LH_F}{\rho_F C_F D_i V_F}, B_2 = \frac{H_A A_0 K_{opp}}{C_{C,tot} V_F}, A_0 = \pi D_0 L \\
 H_A &= \sigma H_{A,wet} + (1 - \sigma) H_{A,dry}, \sigma = 1, T_c < T_{dew} \\
 B_3 &= \frac{LD_i \pi H_F}{C_{C,tot} V_F}, B_4 = \frac{H_A}{\rho_A C_A V_A Y_A} \pi D_0 K_{opp} \\
 B_5 &= \frac{2LV_A}{D_0 V_F}, B_7 = \frac{\sigma H_m A_0 K_{opp}}{C_{C,tot} V_F} (R_0 - h_F); \\
 B_6 &= \frac{\sigma H_m \pi L K_{opp}}{V_F Y_A \rho_A}, H_F = C_{water} T_{dropples}
 \end{aligned}$$

Other symbols:

$$\begin{aligned}
 B_{04} &= \frac{2B_4}{(B_4 + 2)B_1}, B_{05} = \sigma \cdot \frac{2B_6 \cdot TGR}{(B_5 + B_6)B_1} \quad \sigma = 0 \text{ dry; } \sigma = 1 \text{ wet} \\
 EE_2 &= \frac{2B_2}{B_4 + 2}, EE_1 = \sigma \cdot B_7 (TGR - 0.5B_{05}B_1) + B_3 + EE_2 \\
 EE_3 &= \sigma \cdot \frac{B_5 B_7}{B_5 + B_6}, \text{ If } TC_M > T_{dew} \text{ then } \sigma = 0 \text{ (dry)} \\
 B_6 &= 0, B_{05} = 0, EE_1 = B_3 + EE_2, EE_3 = 0, D_1 = B_1 \cdot EE_2 / EE_1 \\
 D_2 &= B_1 \cdot EE_3 / EE_1, D_4 = (1 - B_3 / EE_1) B_1 \\
 K_{01} &= e^{-D_4}, K_{02} = (1 - K_{01}) / D_4 \\
 K_{03} &= B_1 - D_4, K_{05} = (1 - K_{02}) / D_4 \\
 K_{06} &= K_{05} D_1, K_{07} = K_{05} D_2 \\
 K_{08} &= K_{07} \cdot REF, KK_1 = (2 - B_4) / (2 + B_4) + B_{04} D_1 \\
 KK_2 &= B_{04} D_2, KK_3 = B_{04} K_{03}, KK_4 = -REF \cdot KK_2 \\
 KK_5 &= B_{05} D_1, KK_6 = \frac{EE_3}{B_7} - \frac{B_6}{B_5 + B_6} + B_{05} D_2 \\
 KK_7 &= B_{05} K_{03}, KK_6 = \frac{EE_3}{B_7} - \frac{B_6}{B_5 + B_6} + B_{05} D_2 \\
 KK_8 &= \left\{ \frac{2B_6}{B_5 + B_6} - D_2 B_{05} \right\} \cdot REF
 \end{aligned}$$





## Acknowledgements

The writing of this dissertation has been a challenging, but a most rewarding experience. This would not have been possible without the support of many advisors, colleagues, and family. First and foremost, I would like to express my deepest gratitude to the late professor **Dolf Van Paassen** who accepted and gave me the chance and opportunity to study and work in TUDelft. For his valuable guidance and advice as the research and dissertation progressed. His suggestions enabled constant improvement and refinement of the dissertation. He supported me all the way through this dissertation. His much valued advice and patient assistance were highly instrumental in getting me to where I am today in this research. His encouragement helped me brave the rough times when things did not seem to go in the right direction. And when I needed a good friend, **Dolf** and his lovely wife, **Margriet** were there to provide me moral support and unforgettable times.

After losing sadly the late Dolf, the cooperation and support of professor **Bendiks Jan Boersma**, and professor **Adrian Verkooijen** made this work to be fulfilled successfully. For that I express my sincere thanks to them, and also to the chairman of the Process and Energy Department at TU Delft, professor **Westerweel**.

Financial support is acknowledged and appreciated from: the Netherlands Agency for Energy and the Environment (**SenterNovem**), Stichting Ontwikkeling koeltechniek **SOK**, Stichting **W.O.I.** and **VABI** (software development).

A number of European and Dutch companies' access to laboratories data and software tools made this research work more relevant. To name a few, **Carrier Holland Heating**, **SOK**, **Hoval** and **DRI** have been very supportive. A special thanks to **Kees van Haperen** for his valuable information and kind discussions during the meetings and also **Dirk Glerum** to his kind support in providing the experimental set up. I appreciate the assistance of the workshop especially **Johan Boender** for his technical assistant and support and also **Bert van der Velden**.

I am very grateful to **Marteen de Groot**, for his role in facilitating the financial aspects of the project.

My special thanks go to **Joris van dorp** for great and friendly help and support to solve the technical problems in the air handling unit during the measurements. And also thanks to **Carlos Infante Ferreira** for his patience to read my papers and give me his valuable comments and also his kind help to write the memoriam. Thanks to **Noela Vilar Vigue**, **Zhuang Xiaoye** and **Andrés Anca Couce** for undertaking the experimental studies that were necessary to validate my model. Also I would like to name **Wojtek Stec** for his great help during my first months of programming and support of his lovely wife **Ania**. I never forget my good friend **Francesco Di Mio** and appreciate his help and support upon my arrival to Holland. Also I would like to name **Rob Staal** for his kind assistance when there was a need.

Thanks to all the nice people in **Aero & HydroDynamics Lab** who were patient with the noises and inconveniences of our measurements. Also I would like to name all of my dear colleagues and fellows which delighted me to be in a good mood during all ups and downs of life and work far from home. To name a few of faculty and staff I can name **Theo Woudstra, Teus, Eveline van der Veer, Judith, Jan, Marie Therese, and Alberto**. And to name a few of fellows: **Ryan, Atif, Zoupen, Hans and Ali Mesbah** who I always had their kind reply to my questions.

My special thanks go to my dear friend **Behnaz Pour Ebrahimi** for her wonderful and friendly supports during theses years. I never could complete my defense process from long distance without her great help and friendly advices.

And last but not least, I would like to thank my dear family; my lovely husband Alan Shar, my dearest mother Maryam, my dear brother Saeed and his lovely wife, Marcelle specially for her great help to edit my English and my dear Farhad and Nargess. They all have been very understanding and supportive in many ways.

# Curriculum Vitae

## Education

➤ 2004 – 2009

PhD Study in Mechanical Engineering Department, Energy Section, Delft University of Technology, Delft, Netherlands

➤ 2000 – 2004

PhD degree in Mechanical Engineering, Sharif University of Technology, Tehran, 11365-8639, Iran

Thesis title: **Modeling of Heat and Moisture Transfer in Desiccant Wheels and Evaporative Air-conditioning Systems.**

➤ 1989 – 1992

Master of Science in Physics  
Sharif University of Technology, Tehran, Iran.

➤ 1983 – 1988

Bachelor of Science in Physics  
Sharif University of Technology, Tehran, Iran

## Areas of Research & Study

Sustainable Thermal Systems, HVAC systems, Environment-Friendly Technologies, Solar Thermal Engineering, Molecular Dynamic Simulations

## Work Experiences

➤ 2010- Present

The University of Texas at Dallas, Natural Science and Engineering Laboratory, Richardson, TX, USA

**Job Title:** Visiting Scholar, Part Time Lecturer

**Responsibilities / Achievements:** Modeling and Molecular Dynamic Simulation of Nanofluids using LAMMPS (Large-scale Atomic/Molecular Massively Parallel Simulator), teaching Heat Transfer course Mechanical Engineering department.

➤ 2009- 2010

Arizona State University, National Center of Excellence on SMART Innovations for Urban Climate and Energy, Tempe, AZ, USA

**Job Title:** Postdoctoral Research Associate

**Responsibilities / Achievements:** Computer Modeling and conducting research on liquid desiccant cooling systems.

➤ 2004-2008

TU Delft, the Netherlands

**Job Title:** PhD candidate

➤ 2000- 2004

Completing the PhD studies in Mechanical Engineering, Sharif University of Iran

➤ 1996-1997

University of Azad, Tehran, Iran

**Job Title:** Adjunct Faculty & Lecturer

➤ 1990-2000

Iranian Organization for Science and Technology, Tehran, Iran

**Job Title:** Solar Energy R&D Team Member.

➤ 1988-1990

Sharif University of Technology, Tehran, Iran

**Job Title:** Teaching Assistant

## **Publication list related to this thesis**

- F.Esfandiarinia, Dolf van Paassen “A simplified Graphical model of Air Cooler using Mollier Diagram and implementation in Design Tool Enerk” Conference Proceeding Series 2008 ASME 2<sup>nd</sup> International Conference On Energy Sustainability, August 10-14, Jacksonville, FL, 2008.
- F.Esfandiarinia, Dolf van Paassen “Modeling of Desiccant Cooling Systems using simplified equations” Conference Proceeding Series, 2008 ASME Fluids Engineering Division Conference, August 10-14, Jacksonville, FL, 2008.
- F.Esfandiarinia, Dolf van Paassen “Determination of heat and mass transfer coefficients by condensation in an air cooler” Conference Proceeding Series, 2007 ASME Fluids Engineering Summer Meeting and Exhibition, July 30-August 2, San Diego, California, 2007.
- F.Esfandiarinia, Dolf van Paassen “Application of Desiccant Adsorption for Air-conditioning Cycle” AIAA Conference Proceeding Series, 4th International Energy Conversion Engineering Conference and Exhibit (IECEC), San Diego, CA, 2006.
- F. Esfandiar Nia, D. van Paassen, and M. H. Saidi “Modeling and Simulation of Desiccant Wheel for Air Conditioning” Engineering Buildings, vol. 38, pp. 1230-1239, October 2006.
- Fatemeh Esfandiar Nia, Dolf van Paassen, Mohamad Hassan Saidi “Year Round Simulation and Control of a Hybrid Desiccant Air-Conditioning System” Energy and Buildings, in press.
- F.Esfandiarinia, Dolf van Paassen, M.H.Saidi “Comparison of a New Modeling Approach with the Experimental and Numerical Modeling for Enthalpy Wheel and Air Dehumidifier” Conference Proceeding Series, 2005 ASME Summer Heat Transfer Conference, July 17-22, San Francisco, CA, 2005.
- F.Esfandiarinia, Dolf van Paassen, M.H.Saidi “A New Approach of Heat and Mass Transfer in a Rotary Dehumidifier” Conference Proceeding Series, 2005 ASME Fluids Engineering Summer Meeting and Exhibition, June 19-23, Houston, TX, 2005.
- F. Esfandiar Nia, M.H. Saidi, and A.H.C. van Paassen “Methods for Study of the Sorption Characteristic Curve Effect on Sensible and Latent Efficiency of Regenerators” in Proceedings of the International Sorption Heat Pump Conference (ISHPC2005), no 0013-2005, pp.1-8, June 22-24, 2005.